

University of Pavia
Department of Earth and Environmental Sciences
PhD program in Earth and Environmental Sciences



The Middle Triassic of Sardinia
in the frame of the Western Tethys evolution

Tutors:

Prof. Ausonio Ronchi

Prof. Javier Martin-Chivelet

Dr. José López-Gómez

PhD candidate:

Lorenzo Stori

Academic Year 2021/2022

PhD XXXV° series

Universidad Complutense de Madrid
Facultad de Ciencias Geológicas
PhD program “Geology and Geological Engineering”



The Middle Triassic of Sardinia
in the frame of the Western Tethys evolution

Tutors:

Prof. Ausonio Ronchi

Prof. Javier Martin-Chivelet

Dr. José López-Gómez

PhD candidate:

Lorenzo Stori





University of Pavia

Department of Earth and Environmental Sciences



Complutense University of Madrid

Facultad de Ciencias Geológicas

The Middle Triassic of Sardinia in the frame of the Western Tethys evolution

Lorenzo Stori

Supervisors:

Ausonio Ronchi

Javier Martin-Chivelet

José López-Gómez

January 2023

Index

Acknowledgements	1
Abstract	2
Resumen	5
1. Introduction	8
1.1 Preface.....	8
1.2 Presentation of the work	8
1.3 Aims of the project	10
2. Geological setting of Sardinia	11
3. Materials and methods	13
4. Lithostratigraphy	15
4.1 Introduction.....	15
4.2 Sarcidano-Gerrei.....	18
Escalaplano Formation	18
Monte Maggiore Formation	19
4.3 Campumari (Iglesiente)	21
Riu is Corras Formation	21
Campumari Formation	22
4.4 Porto Pino (Sulcis)	23
Punta Tonnara Formation	23
4.5 Scivu - Is Arenas (Arburese).....	25
Punta S'Arridelli Formation	25
Punta su Nuraxi Formation	26
4.6 Nurra	27
Arenarie di Cala Viola Formation	27
Punta del Lavatoio Formation	28
4.7 Stratigraphic sections	33
Escalaplano SW (Sarcidano-Gerrei).....	34
Arcu is Fronestas (Sarcidano-Gerrei).....	35
Orroli (Sarcidano-Gerrei).....	36
Monte Maggiore (Sarcidano-Gerrei).....	37
Punta su Nuraxi (Arburese)	38
Campumari (Iglesiente).....	39

Punta Tonnara (Sulcis).....	40
Punta del Lavatoio (Nurra)	41
Cala Viola (Nurra)	42
Monte Fogheras (Nurra)	43
Cala Bona (Nurra)	44
Monte Santa Giusta (Nurra).....	45
5. Fossil Content	46
5.1 Introduction.....	46
5.2 Methodology	47
5.2.1 Methodology for palynological study	47
<i>Palynological analyses</i>	47
5.2.2 Methodology for ammonoids, bivalves and other fossils study	48
5.3 Palynological content	54
5.3.1 Revision of palynological content and previous works.....	54
5.3.2 New and revised palynological data	59
5.4 Ammonoids	67
5.5 Bivalves.....	68
5.6 Other fossils.....	70
5.7 Biostratigraphy.....	81
<i>Microfloristic associations</i>	81
<i>Ammonoids, bivalves and other fossils</i>	86
6. Sedimentology and Sequence Stratigraphy.....	89
6.1 Facies and sedimentary environments	89
6.1.1 Sabkha – muddy coastal plain	90
6.1.2 Carbonate tidal flats.....	92
6.1.3 Shallow subtidal low-energy environment (lagoon)	96
6.1.4 Shallow subtidal high-energy environment (calcarenitic shoals)	98
6.1.5 Middle ramp sedimentary environment.....	98
6.2 Sequence stratigraphy.....	102
6.3 Correlation with Western Peri-Tethys areas (Iberian Ranges and Minorca)	113
7. Geochemistry.....	115
7.1 Introduction.....	115
7.2 Materials and methods	115
7.3 C and O isotopes.....	116
7.4 C and O isotopes result	118
7.4.1 Punta del Lavatoio section	118

7.4.2 Monte Santa Giusta.....	120
7.4.3 Monte Maggiore - Orroli.....	122
7.4.4 Punta Tonnara.....	125
8. Palaeogeography.....	130
9. Conclusions.....	135
10. References.....	137
Appendix 1.....	152
Appendix 2.....	172

Acknowledgements

Firstly, I would like to thank my supervisors. These doctoral years have been very hectic and complex from many points of view. I am truly grateful to Prof. Ausonio Ronchi, Prof. Javier Martin-Chivelet and Dr. José López-Gómez for the continuous support, both moral and scientific, they have provided me. I think I have grown a lot since the beginning of the PhD and I owe a big part of this process to them, for which I will never stop thanking them.

I would also like to thank all the people I collaborated with on my PhD project for their time, interest, and valuable advice. I would like to thank Prof. Anna Gandin for sharing her knowledge and for the scientific material she provided to us. Prof. Antonio Goy of the University of Madrid, the research team of the University of Vigo, Prof. Bienvenido Diez, and the research team of the University of Valencia, Prof. Ana Márquez-Aliaga, Prof. Leopoldo Márquez, and Dr. Sonia Ros Franch. In general, I would also like to extend my thanks to all those people of the University of Pavia and of the UCM Department of Stratigraphy who have directly contributed to the advancement of my thesis both from a scientific and bureaucratic point of view.

Finally, I would like to thank my parents for providing me with their support during these years, their presence has been fundamental. Matteo and Maddalena for always being interested and supportive and available at any time. Giulio, for always being close to me and unconditionally present in all moments and for all the love and patience, and Ambra for always being so kind and helpful.

I would also like to thank all my friends and colleagues from the University of Pavia, Madrid, and in general all the people, both old and new friends, who have contributed to making these doctoral years even more precious.

Abstract

The present study has been focused on the Middle Triassic successions of Sardinian Island, Italy. This sedimentary record has been studied from the end of the 19th century as it has been long recognized as a key-stratigraphic succession in understanding the palaeogeographical evolution of the Tethys western sector, and the precise position of the Island. It therefore includes the possible regional and interregional correlations of this sedimentary record with the Central Europe sector (Germanic basin) and the western Mediterranean sector (Spain, France, and the Southern Alps), and consequently in understanding how the paleogeography of Western Tethys Sea realm evolved throughout this period.

The main aim of this PhD project is so to integrate the present knowledge of the Sardinian continental-transitional Lower-Middle (Buntsandstein) and marine Middle (Muschelkalk) Triassic successions by means of a multidisciplinary approach. To do so, new detailed stratigraphic, sedimentological, paleontological (pollen associations, ammonoids, bivalves and foraminifera), sequence stratigraphy and geochemical (C and O isotope) data have been provided, in order to better define the stratigraphic, chronostratigraphic, paleoenvironmental and paleogeographical context of the studied sedimentary succession.

Following a stratigraphic survey fieldwork, 12 sections have been studied and sampled in detail as representative of the different fms. The facies, facies associations and microfacies analysis made possible to distinguish four main broad sedimentary environments: 1) sabkha – muddy coastal plain, 2) carbonate tidal flat, 3) shallow low-energy subtidal, 4) calcarenitic shoals and 5) middle ramp environment. These data, integrated with the complete bibliographical revision, made possible to perform a detailed regional correlation.

The palynological associations analysis have been obtained from re-evaluating previous works while the new associations have been obtained from three stratigraphical sections: Su Passu Malu section (Campumari, SW Sardinia), Arcu is Fronestas section and Escalaplano section (Escalaplano, Central Sardinia). The integration of these data with the stratigraphic and sedimentological data made possible to understand with greater precision the paleogeographic evolution of the W Tethys domain during the late Anisian-early Ladinian. This knowledge has made it possible to establish a) the lack of paleontological evidence for the early Anisian in Muschelkalk facies in Sardinia (Italy) b) a Pelsonian age for the Escalaplano Formation, an Illyrian age for the Su Pasu Malu Member (Campumari Formation).

The study of the ammonites, bivalves and foraminifera together with the sedimentological data allowed to precise the progressive westward settling of the carbonate platforms, and consequently to better understand the development of new migration and irradiation routes for Sephardic faunas from the SE (Palaeotethys) and Alpine faunas (Neotethys) from the NE. Based on new findings and on the revision of palaeontological associations previously reported by different research groups, comparisons have been made with associations of adjacent paleogeographic domains (Balearic Islands, Levantine area of Spain). This allowed to refine their palaeoecological distribution to frame Sardinia as a key area in the palaeogeographic evolution of the W Tethys during the Ladinian.

The sequence sedimentology and stratigraphy studies reflect the broad carbonate ramp developed during a period of approximately 5-6 million years (late Illyrian to latest Longobardian) and records a major transgressive – regressive cycle, which can be assimilable to a 2nd order cycle in the sense of Vail et al (1991). This sequence is particularly well developed and continuous in the Nurra Region, especially in the Monte Santa Giusta area, although it has been found in complete stratigraphical continuity only in the subsurface (Cugiareddu Well). The sequence is constituted by the upper part of the Buntsanstein (Röt facies), the different formations that represent the Muschelkalk and the lower part of the Keuper.

Interregionally, this 2nd order depositional sequence of the Sardinian Muschelkalk finds its equivalence in different basins of Spain (Mega-Depositional Sequence-II of Escudero-Mozo, 2015 and equivalents). The large-scale transgressive-regressive pattern is well-defined in these basins. In the Iberian Range, the MSD-II has a variable thickness, increasing towards E, and can reach a maximum thickness of 120m in the Mediterranean and Levantine-Balearic domain. It is represented by the upper part of the Mas Fm., the Cañete Fm. and the first unit (Jarafuel Fm) of the Keuper facies. In the Catalan Coastal Ranges, it is represented by the upper part of the “Middle Muschelkalk” unit, the “Upper Muschelkalk” and the lower part of the Keuper facies, while in Minorca it is represented by the Röt facies, the Monte Toro Fm. and the Arenal d'en Castell Fm. It should be noted that, unlike the Iberian Range – Coastal Catalan range, Levantine balearic Domain and Menorca – Castellon areas, the outer ramp – distal middle ramp systems do not appear in Sardinia.

The paleogeographic analysis allowed to define a) with greater accuracy the Tethys Sea incursion towards its westernmost domains in Sardinia during the Middle Triassic and the different stages of the transgression during the late Anisian-early Ladinian; b) that Sardinia,

together with Minorca and the eastern area of Castellón (easternmost Iberia), constituted a topographical high area, acting as a barrier between the realms of the Paleotethys and Neotethys seas, until the middle-late Illyrian (late Anisian), when an important change in the configuration of the Western Tethys realm occurred. c) that from the late Illyrian to the early Fassanian, the new transgression of the Tethys Sea progressively covered Sardinia and later reached the neighbouring easternmost Iberia and Minorca areas. During this stage of the Tethys transgression, almost all the elevated areas of the Western Tethys domain were finally covered.

Resumen

El presente estudio se ha centrado en las sucesiones del Triásico Medio de la isla de Cerdeña, Italia. Este registro sedimentario ha sido estudiado desde finales del siglo XIX, cuando fue considerado como una sucesión estratigráfica clave para comprender la evolución paleogeográfica del sector occidental de Tethys y la posición precisa de la isla. Esto incluye las posibles correlaciones regionales e interregionales de este registro sedimentario con áreas de Europa Central (cuenca germánica) y el sector del Mediterráneo occidental (España, Francia y los Alpes del Sur) y, en consecuencia, la mejor comprensión de la evolución paleogeográfica del W Tethys durante este periodo.

El objetivo principal de este proyecto de tesis doctoral es integrar los datos nuevos ahora estudiados con los previamente conocidos de las sucesiones del Triásico Medio-Inferior (Buntsandstein) en facies continental-transicional y del Triásico Medio (Muschelkalk) en facies marinas. Este estudio se realiza mediante un enfoque multidisciplinar que incluye estratigrafía, sedimentología, paleontología (asociaciones de polen, amonites, bivalvos y foraminíferos), estratigrafía secuencial y geoquímica (isótopos de C y O) para determinar el contexto estratigráfico, cronoestratigráfico, paleoambiental y paleogeográfico de la sucesión sedimentaria estudiada.

En base a un trabajo en detalle, se han estudiado y muestreado en detalle 12 secciones representativas de las diferentes formaciones estudiadas. El análisis de facies, asociaciones de facies y microfacies permitió distinguir cuatro ambientes sedimentarios principales: 1) sabkha - llanura costera fangosa, 2) llanura de marea carbonatada, 3) submareal poco profundo de baja energía, 4) bajíos calcareníticos y 5) ambiente de rampa media. Estos datos, integrados con una revisión bibliográfica detallada, permitieron realizar una correlación regional precisa.

El análisis de asociaciones palinológicas se ha obtenido a partir de la reevaluación de asociaciones de trabajos anteriores y las nuevas obtenidas ahora en tres secciones estratigráficas: Su Passu Malu (Campumari, suroeste de Cerdeña), Arcu is Fronestas y Escalaplano (Escalaplano, Cerdeña central). Como resultado de la integración de estos datos con aquellos estratigráficos y sedimentológicos, ha sido posible determinar con mayor precisión la evolución paleogeográfica en el dominio del W Tethys durante el Anisiense final - comienzo del Ladiniense. Este conocimiento ha permitido establecer: a) la falta de evidencia

paleontológica de la presencia de un registro del Anisiense inferior en facies Muschelkalk en Cerdeña; este dato permite determinar que en algunas zonas se muestra, incluso, un largo periodo sin sedimentación que abarca desde las sucesiones desde el Pérmico Medio hasta el Triásico Inferior; b) una edad Pelsoniense para la Formación Escalaplano, y una edad Iliriense para el Miembro Su Pasu Malu (Formación Campumari).

El estudio de los ammonites, bivalvos y foraminíferos, junto con los datos sedimentológicos, permiten precisar la progresiva instalación hacia el oeste de las plataformas carbonatadas y, consecuentemente, el desarrollo de nuevas rutas de migración e irradiación para faunas sefardíes del SE (Palaeotethys) y faunas alpinas (Neotethys) del NE. A partir de nuevos hallazgos y de la revisión de asociaciones paleontológicas registradas previamente por diferentes grupos de investigación, se han podido realizar comparaciones con asociaciones de dominios paleogeográficos próximos (Islas Baleares y área levantina de España), precisando así su distribución paleoecológica y enmarcando a Cerdeña como un área clave en la evolución paleogeográfica del W Tethys durante el Ladiniense.

Los estudios de sedimentología y estratigrafía secuencial reflejan el desarrollo de una amplia rampa de carbonato acumulada durante un período de aproximadamente 5-6 millones de años (Iliriense superior a Longobardiense superior) que muestra un ciclo transgresivo-regresivo general que puede ser asimilable a un ciclo de segundo orden en el sentido de Vail et al (1991). Esta secuencia está particularmente bien desarrollada y es continua en el área de Nurra, especialmente en la zona de Monte Santa Giusta, aunque sólo se ha encontrado en continuidad estratigráfica completa en el subsuelo (sondeo Cugiarreddu). La secuencia está constituida por la parte superior de las unidades en facies Buntsanstein (facies de Röt), las diferentes formaciones que representan el Muschelkalk, y la parte inferior de las unidades en facies Keuper.

Interregionalmente, esta secuencia depositacional de segundo orden del Muschelkalk sardo encuentra su equivalencia en diferentes cuencas de España (Secuencia Megadeposicional-II de Escudero-Mozo, 2015 y equivalentes). El patrón transgresivo-regresivo a gran escala está bien definido en estas cuencas. En la Cordillera Ibérica, el MSD-II tiene un espesor variable, aumentando hacia el E, pudiendo alcanzar un espesor máximo de 120 m en el dominio Mediterráneo y Levantino-Balear. Está representada por la parte alta de la Formación Mas, la Formación Cañete y la primera unidad (Formación Jarafuel) de la facies Keuper. En la Cordillera Costero Catalana está representada por la parte superior de la unidad

“Middle Muschelkalk”, la “Upper Muschelkalk” y la parte inferior de la facies Keuper, mientras que en Menorca está representada por la facies Röt, la Formación Monte Toro, la Formación Arenal d'en Castell. Cabe señalar que, a diferencia de las áreas Cordillera Ibérica - Cordillera Costera Catalana, Dominio Levantino Balear y Menorca - Castellón, los sistemas de rampa exterior - rampa media distal no aparecen en Cerdeña.

El análisis paleogeográfico, nos ha permitido: a) definir una mayor precisión de la transgresión del Tethys hacia los dominios más occidentales durante el Triásico Medio, es decir, las diferentes etapas de la transgresión durante el Anisiense superior-Ladiniense inferior; b) determinar cómo Cerdeña, junto con Menorca y el área oriental de Castellón (extremo oriental de Iberia), constituyeron una zona topográficamente alta hasta el Iliriense medio – superior (Anisiense superior), cuando se produjo un cambio importante en la configuración en el W Tethys. Hasta ese momento, el bloque Cerdeña-Menorca había jugado un papel clave al actuar como barrera entre los dominios del Paleotethys y Neotethys; c) desde el Iliriense superior hasta el Fasaniense inferior, la nueva transgresión del Tethys cubrió progresivamente Cerdeña y alcanzando posteriormente las áreas vecinas más orientales de Iberia y Menorca. Durante esta etapa transgresiva, casi todas las áreas del dominio del W Tethys fueron definitivamente cubiertas.

1. Introduction

1.1 Preface

This PhD project has been carried out in an international cotutorship (“cotutela”) between two institutions, the University of Pavia, Italy, for which the supervisor has been the Prof. Ausonio Ronchi, and the Complutense University of Madrid, Spain, for which the supervisors have been Prof. Javier Martín Chivelet and Dr. José López Gómez. A total of 6 months was spent at the Complutense University of Madrid, shared between the Faculty of Geological Sciences and the Institute of Geosciences (CSIC-UCM). This period included a 2-month Erasmus+ Traineeship scholarship. Short stays have also been carried out in the University of Valencia (Spain), under the supervision of Prof. Ana Márquez. The fieldwork has been carried out mainly in Sardinia (Italy), in the different areas selected for the study, but also partially in Spain, in particular in the central and NW Iberian Range. The fundings were provided by the University of Pavia, the Complutense University of Madrid, the CSIC-IGEO and project PGC2018-098272-B-100 of the Spanish Ministry of Science, Innovation and Universities.

1.2 Presentation of the work

The present work finds its framework in a broader line of research that studies the Permo-Triassic sediments in different parts of Europe (Spain, Italy, France, Germany) and in particular it focuses on the Middle Triassic of Sardinia, Italy. In general, the Triassic successions of Sardinia have been recognized and studied since the 19th century and their Germanic-like facies tripartition (Buntsandstein-Muschelkalk-Keuper) is well assessed and documented. As more studies have been conducted, also in recent times (eg., Márquez-Alliaga et al., 2000; Costamagna and Barca, 2002; Posenato, 2002; Barca and Costamagna, 2003; Knaust and Costamagna, 2012, 2019), it became clearer that the Triassic successions of Sardinia play a fundamental role in both regional and interregional correlations between the Central Europe sector (Germanic basin) and the Western Mediterranean sector (Spain, France, and the Southern Alps), and consequently in understanding how the palaeogeography of western Tethys Sea realm evolved throughout the Triassic period.

The onset of the Triassic witnessed the devastating outcome of the end Permian biotic crisis (Erwin, 1996, 2001; McGhee et al., 2013; Benton and Newell, 2014). The general geodynamic conditions of instability that still prevailed during the Early Triassic, including the still active Siberian volcanism, provoked strong periodic perturbations in the atmosphere that lasted until the complete recovery of life in early Anisian times (Svensen et al., 2009; Bond and Wignall, 2014; Stordal et al., 2017; Algeo, 2019), when this was possible without interruptions

(Wei et al., 2015; Song et al., 2018; Liu et al., 2021).

Despite better conditions for life radiation, vast areas located around future divergent plate margins were witnesses of regional tensional stress regimes during the Middle Triassic, such as the Western Tethys domain. This area was represented by the westward propagating Tethys rift system, an important trough that linked other corridors connecting areas thousands of km apart, from the Polish Trough to the Algerian graben (Gianolla and Jacquin, 1988; Ziegler, 1990; Ziegler and Stampfli, 2001). These geodynamic conditions triggered large volcanic episodes and the northward displacement of blocks related to Cimmerian terrains (Stefani et al., 2010; Stampfli and Borel, 2004), but also the migration of Sephardic and Alpine faunas and connections between them (Gandin et al., 1982; Escudero-Mozo et al., 2015; Pérez-López et al., 2019).

The first Triassic incursion of the Tethys Sea reached its westernmost areas (e.g., Iberia) during the middle Anisian (Pelsonian) (Escudero-Mozo et al., 2015) yet some blocks still remained as elevated areas 3-4 m.y. ago (e.g., Minorca and Ebro blocks, and central-eastern Betic Basin) (López-Gómez et al., 1998; Pérez-López and Pérez-Valera, 2007; Escudero-Mozo et al., 2014). These blocks are key to understanding the complex geodynamic palaeoecological and palaeogeographical evolution of this area.

Although different and important studies have notably contributed to an accurate Triassic stratigraphy for the island (Damiani and Gandin, 1973c; Coccozza and Gandin, 1976; Carrillat et al., 1999; Costamagna and Barca, 2002, 2016; Costamagna et al., 2000; Cassinis and Ronchi, 2002; Cassinis et al., 2003; Citton et al., 2020; Stori et al., 2022 among others) there are still many unresolved and open questions, such as the precise age of the first Mesozoic marine incursion in the island, or the position and configuration of Sardinia in the Western Tethys realm. This latter topic is in fact still an object of debate, even though different and up to date studies are through Europe are adding important data that are helping to have a better and general understanding on the topic (e.g. Escudero-Mozo et al, 2014, 2015; Borrueal-Abadia et al., 2015, 2016).

The present PhD project fits into this context and arises from the need to provide new and updated data, as well as a critical review of the pre-existent bibliographic data. As mentioned, some aspects still lack understanding and an integrated, multidisciplinary study provides an important and fundamental piece to the general puzzle of knowledge of the Middle Triassic successions in W Europe.

1.3 Aims of the project

The main aim of this PhD project is to integrate the present knowledge of the Sardinian continental-transitional Lower-Middle (Buntsandstein) and marine Middle (Muschelkalk) Triassic successions by means of re-examination consisting of a multidisciplinary approach, to provide new detailed stratigraphic, sedimentological, palaeontological, geochemical (isotope) data and to clarify the chronostratigraphic and palaeoenvironmental context of this succession.

The main goals have been:

- a) to provide a lithostratigraphic and sedimentological revision of the Middle Triassic units and to perform a study of their depositional environments through detailed facies and microfacies association analysis;
- b) to review of the previous and the new obtained palaeontological content with focus on the main groups of palaeoecological and palaeobiogeographical interest (microflora, ammonoids, bivalves and other fossil groups);
- c) to develop a detailed sequence stratigraphy, based on the elaboration and integration of field and laboratory data;
- d) to perform a chemostratigraphic study based on stable isotopes of C and O, which has never been done for the Middle Triassic successions of Sardinia;
- e) to improve the chronostratigraphic knowledge on the basis of the fossil content and the new sequence stratigraphic frame;
- e) to provide a more precise relative position of the island in the context of the geodynamic and palaeogeographic evolution of the W Tethys.

2. Geological setting of Sardinia

Sardinia Island is located in the western Mediterranean Sea, and it is separated from the Italian mainland by two deep marine basins, the Tyrrhenian Sea and the Western Mediterranean Sea. The island shows an important structural complexity and a great geodiversity, as the result of intense Variscan and Alpine tectonic activity. Together with Corsica Island, Sardinia is often considered and referred as “Sardinia-Corsica block/microcontinent” (Sartori, 2001). Its nowadays position reflects the 30° counterclockwise large-scale movement (Sartori, 2001; Casula et al., 2001; Speranza et al., 2002; Advokaat et al., 2014; Edel et al. 2014) that took place in two different phases: first, the rifting phase that led to the opening of the of the Western Mediterranean Ligurian-Provençal basin in the Oligocene, and the Early Miocene Oceanic accretion during the Early Miocene - Ferrandini et al., 2000; Gattacceca et al., 2007; Advokaat et al., 2014.

A consistent part of the Sardinia-Corsica block is made of the Permo-Carboniferous Batolith that was affected by the Variscan collisional tectono-metamorphic imprint (Carosi et al., 2014). It also comprises an igneous sedimentary sequence whose degree of metamorphism increases from south to north. The basement shows a NW-SE trend (Carmignani et al., 1979; 1986; 1994, 2001) and it is divided in different structural zones (Fig. 2.1). The foreland thrust-and-folds belt external zone, outcropping in SW Sardinia, consisting of a metasedimentary sequence and characterized by a low-grade metamorphic imprint (Carosi et al., 2014). An Internal zone that consists of a Palaeozoic igneous-sedimentary succession with low-medium metamorphism (Central Sardinia). An “Inner” zone or “axial zone” (N Sardinia – Corsica) consisting of late-Variscan intrusion and a medium to high degree metamorphism (Carosi et al., 2014). From the Variscan cycle to the Miocene, Sardinia has represented a stable block, periodically subjected to marine transgressions and regressions, that led to the deposition of different units throughout the Mesozoic and the Cenozoic (Carmignani et al., 2001). The following post-Variscan late Palaeozoic-Mesozoic sequences can be identified following regional unconformities (Carmignani et al., 2001): I) A lower sedimentary volcanic complex, dated late Carboniferous – Permian? to Early Triassic that concludes the variscan sedimentary cycle and start the deposition of the “alpine” succession; II) transitional and marine Middle Triassic-Early Cretaceous, representing prevalently carbonate platform deposits of the southern passive European edge; III) marine, Late Cretaceous successions unconformably resting over the Middle Triassic-Early cretaceous deposits.

Regarding the Permian-Triassic time-interval, three main sedimentary sequences have been recognized (Cassinis and Ronchi, 2002; Cassinis et al., 2002, 2003):

- 1) The first post-Variscan deposits belong to the lower Permian, consisting mainly of detrital sediments of alluvial and lacustrine origin, associated with acid volcanites (Ronchi et al., 2008; Gaggero et al., 2017), which rest unconformably on the Variscan basement. These sediments represent a first sequence linked to initial dismantling of the Variscan chain.
- 2) A much thicker sequence unconformably overlies the preceding one (lower Permian to early-Middle Permian), and consists of a megacycle of alluvial deposits related to an initial phase of post-orogenic rifting (namely the “Nurra Group” in Ronchi et al., 2011).
- 3) A third sequence starts with a continental-transitional sequence in Buntsandstein facies (Lower to early Middle Triassic) and is followed by marine deposits of a carbonate platform in Muschelkalk facies (late Middle Triassic) in different parts of the W Tethys (Damiani and Gandin 1973c; Costamagna and Barca 2002; Bourquin et al., 2007; Durand, 2008; Borrueil-Abadia et al., 2019). This third sequence is related to the progressive opening of the NeoTethys basin and to the anticlockwise rotation of Cimmerian micro-terrains, which was followed by Upper Triassic deposits in Keuper facies, deposited in a phase of general marine regression (Costamagna and Barca, 2002).

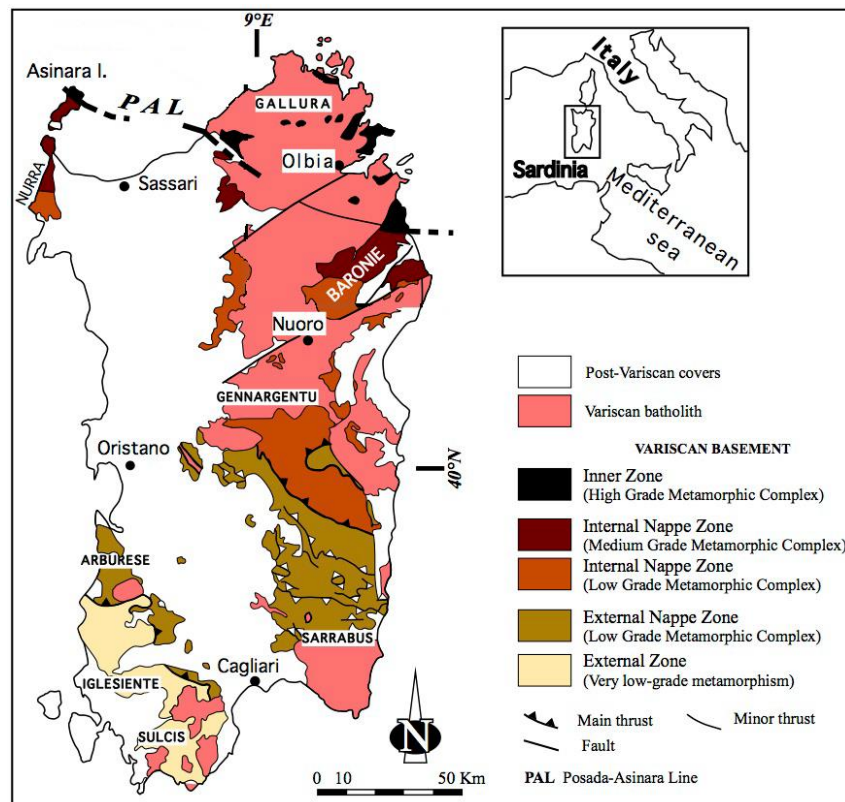


Fig. 2.1 - Tectonic sketch-map of the Variscan belt in Sardinia (modified from Carosi et al., 2005).

3. Materials and methods

This thesis work consists of a multidisciplinary analysis, hence for its accomplishment different methodologies have been used, these being the commonly used in field-based sedimentary basin analysis, including sedimentology, biostratigraphy, sequence stratigraphy, and sedimentary geochemistry. The work has been based on three main pillars (Fig. 3.1):

Bibliographic research

The first and essential part of the work has been the bibliographic research. The thesis work has a strong component of synthesis and revision; hence the research and analysis of previous studies has been a fundamental step. Moreover, the area of study consists of all the Sardinia region, and being the succession scattered all through the island, the bibliographic research has been crucial to locate the most significant outcrops to study and to plan the fieldwork.

Fieldwork

A total of 12 stratigraphic sections have been revised and studied in detail. The sections and surveyed areas are found mainly in 4 different areas (or regions), from N to S: 1) Nurra, 2) Sarcidano-Gerrei, 3) Arburese and 4) Sulcis-Iglesiente. The fieldwork consisted in: survey and recognizing the different lithostratigraphic units; description of the sedimentological characteristics; facies recognition and facies association interpretation; localization of the main unconformities or stratigraphic gaps; sampling of the succession for further laboratory studies.

Laboratory work

Petrography. The studied samples have been prepared at the University Complutense of Madrid. Each of the rock samples collected during the fieldwork was cut into sections, parallel to the orientation of the sample. Through this process, a tablet has been obtained, from which a thin section 30 µm thick has been cut, then polished and glued to a glass slide. A total of about 170 thin sections were made. All the thin sections were studied with a polarized light microscope (Nikon Eclipse E400POL) with a Nikon Coolpix 5000 digital camera attached. For the petrographic description, the classifications of carbonate rocks by Dunham (1962) and Embry and Klovan (1971) for microfacies, and by Folk (1965) and Friedman (1965) for dolomites have been followed.

Stable Isotope (C and O) geochemistry. For the study and analysis of C and O in carbonates, about 142 microsamples have been extracted. The methodology for this study is explained in further details in Chapter 7.

Biostratigraphic analysis and fossil associations. All the fossil samples of the studied rocks, both the new material collected during the fieldwork and from previous works, have been analysed and studied in detail, in collaboration with various specialists in the different fossil groups, as will be shown later. This study constitutes an essential part of the carried-out work, due to the importance of the new chronostratigraphic data obtained, as well as the new palaeoecological and palaeobiogeographic information provided by this material. Further details are explained in Chapter 5. Regarding the palynological analysis, the sediment samples (dark lutites) have been subjected to an extraction process to verify the presence of microfloristic associations. The preparation of these samples has been carried out in the Palynology Laboratory of the Department of Stratigraphy of the Complutense University of Madrid and Geosciences Institut (CSIC-UCM), following the method used by the palynology laboratory of the Louis Pasteur University of Strasbourg. The samples that provided palynological evidence were sent to Dr. Bienvenido Díez from the Department of Marine Geosciences and Territorial Planning of the University of Vigo, Spain. The methodology for this study is explained in further detail in Chapter 5.

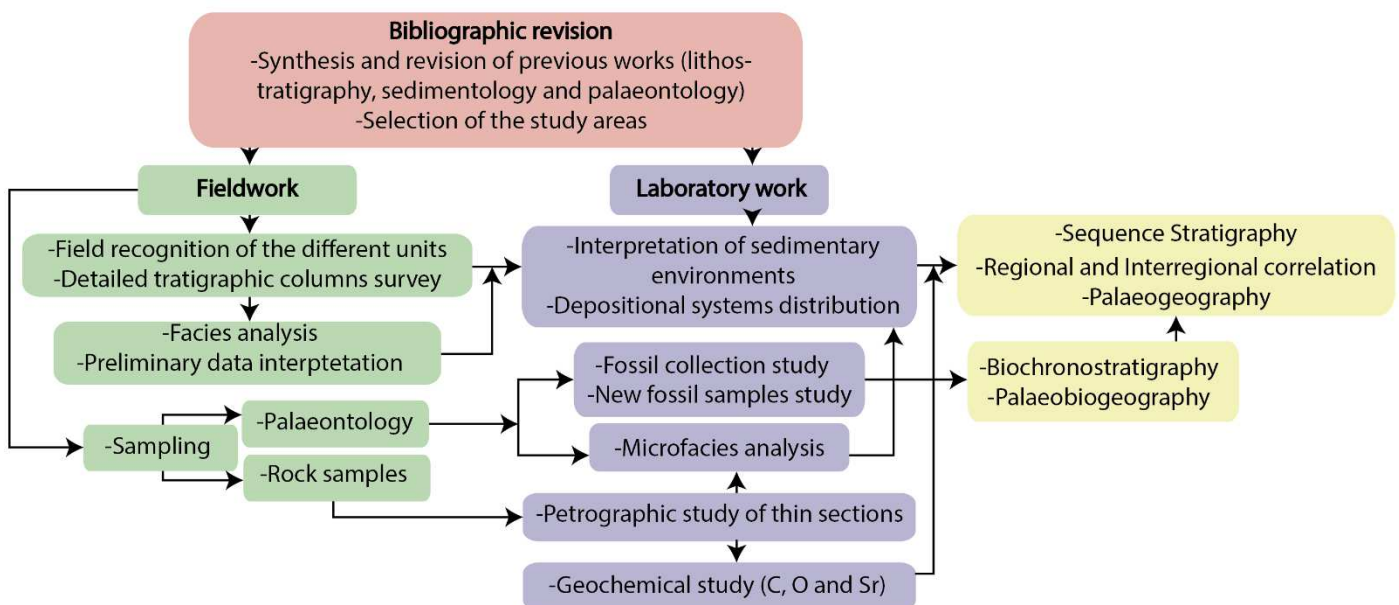


Fig. 3.1 Workflow diagram

4. Lithostratigraphy

4.1 Introduction

Since the 19th century, the Triassic of Sardinia has been classified and divided according to the classic tripartition of the Germanic Triassic: Buntsandstein, Muschelkalk and Keuper (Bornemann, 1881; Lovisato, 1884; Oosterbaan 1936; Vardabasso, 1956; Damiani and Gandin, 1973 a,b,c; Gandin, 1976; Costamagna and Barca, 2002). The Triassic basal clastic sequence can be difficult to separate from the Upper Permian facies, as for example, in the case of the Riu is Corras Fm. (Barca and Costamagna, 2003) (Fig. 4.1), outcropping in the Iglesiente (SW Sardinia) or the lower member of the Punta S'Arridelli Fm. (Arburese, SW Sardinia) (Barca et al., 1995b). In such cases, they can be mentioned in some previous works as generic "Permo-Triassic" age, and broadly attributed to Buntsandstein facies (Costamagna and Barca, 2002). Despite these difficulties, different works carried out in the last decades have allowed to better understand this stratigraphic succession. One of these works was carried out by Pecorini (1962) who ascribed to the Early Triassic the upper part of the "Permo-Triassic" siliciclastic succession of Nurra based on macrofloral remains (*Equisetum mougeotii*). Many authors also observed a sensible sedimentation change that took place during the Anisian, testified by the transition from a continental environment, mainly represented by the Riu is Corras Fm. (Sulcis-Iglesiente, SW Sardinia), Arenarie di Cala Viola Fm. (Nurra, NW Sardinia) and Punta S'Arridelli Fm. (Arburese, SW Sardinia) (Fig. 4.1), to a more transitional one, represented by the Escalaplano Fm. (Sarcidano-Gerrei, E Sardinia), the upper member of the Punta S'Arridelli Fm. and the lower member of the Campumari Fm. (Sulcis Iglesiente, SW Sardinia) (Fig. 4.1). In this latter unit, several microfloristic associations characteristic of the late Anisian have been found (Pittau and Del Rio, 1980, 2002; Pittau-Demelia and Flaviani 1982b; Costamagna et al. 2002; Stori et al., 2022).

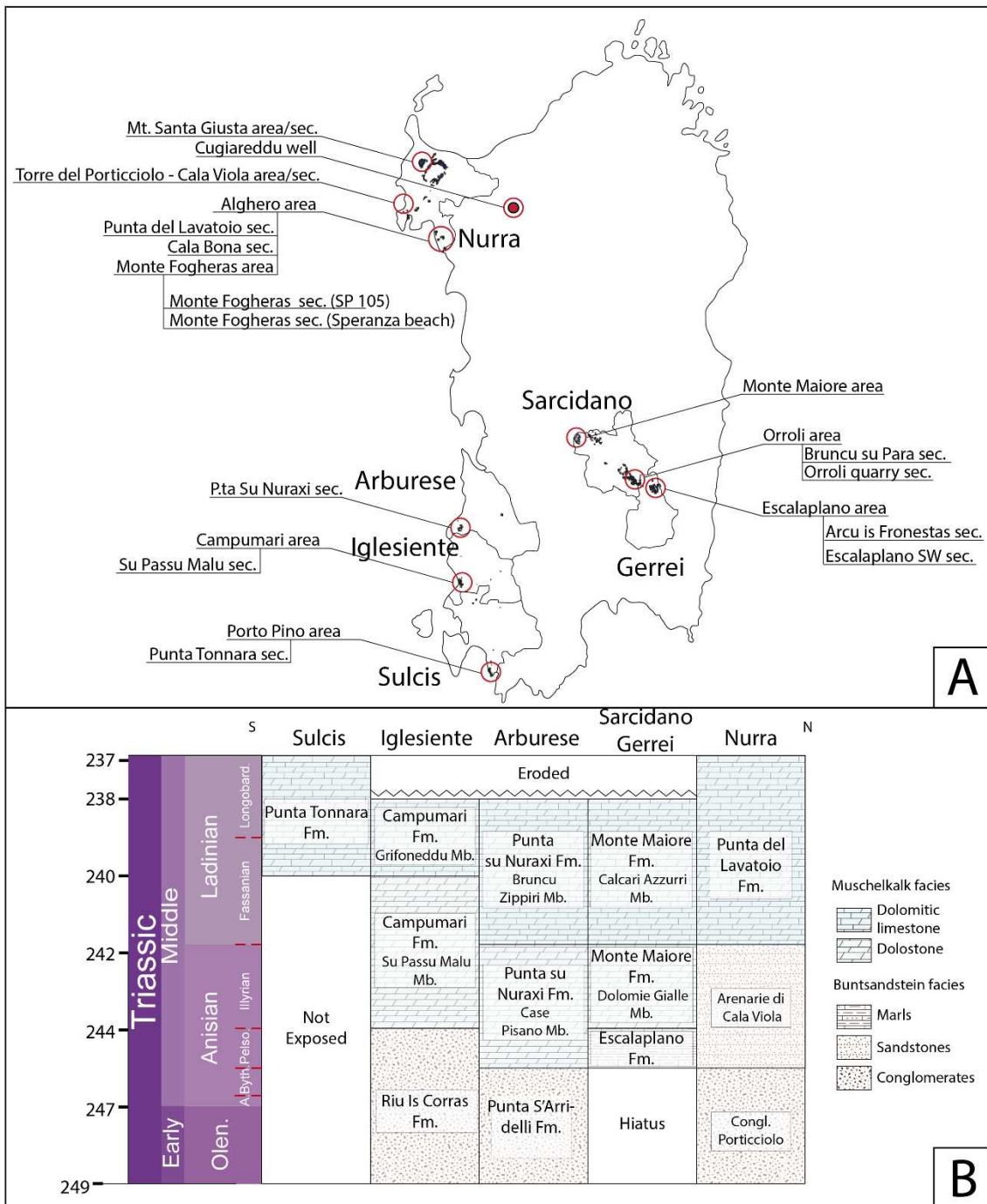


Fig. 4.1. A) Map showing the different regions, areas and outcrops presented B) Chronostratigraphic scheme with the Muschelkalk group Fms. and their sub-units.

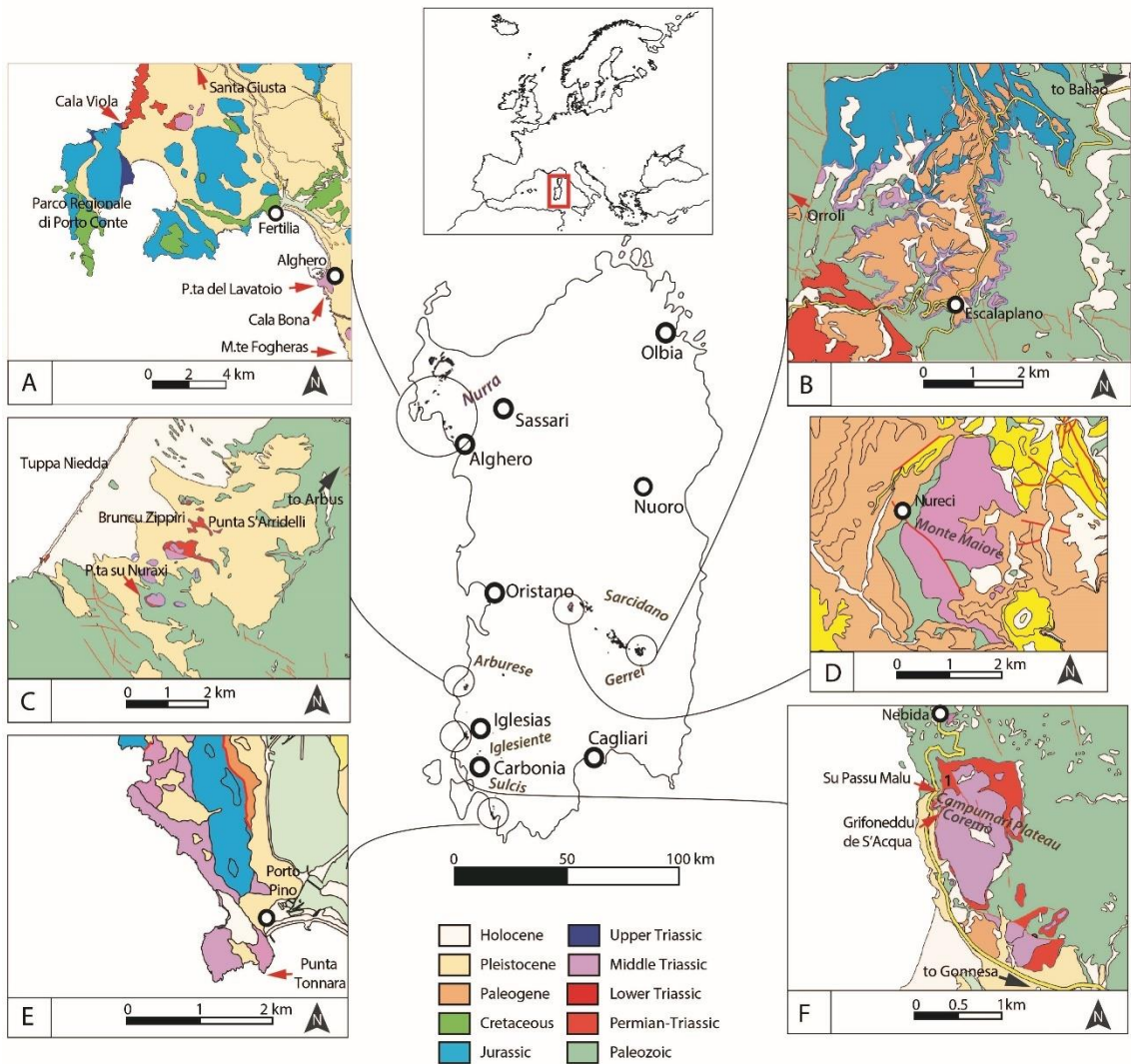


Fig. 4.2. Location and geological sketch maps of the Middle Triassic sequences of Sardinia discussed in the text. A Nurra ; B Escalaplano (Gerrei); C Scivu-I-Arenas Arburese ; D Monte Maiore (Sarcidano); E Porto Pino (Sulcis); F Campumari (Iglesiente)

4.2 Sarcidano-Gerrei

Close to the village of Escalaplano, to the SW of the study area (Fig. 4.2: B), the post-Variscan deposition is mainly represented by a lower Permian volcano-sedimentary sequence that fills a small (about 15 km²) intramontane basin (Fig. 4.2: B). On the whole, the extruded calc-alkaline magmatic products in this succession have an extrabasinal origin and largely exceed the strictly sedimentary units.

According to Pecorini (1974), Ronchi (1997) and Ronchi et al. (2008), the entire Permian sedimentary succession can be subdivided into two main parts, namely “Lower” and “Upper” volcanic and sedimentary successions: both begin with a coarse sedimentary unit, continue with reworked volcanoclastites, tuffites, lacustrine-to-palustrine deposits and end with, respectively, an acidic ignimbrite deposit and an andesitic lava flow. Nine lithostratigraphic units have been distinguished within the two cited volcano-sedimentary sequences by Ronchi et al. (2008), which seem to be separated by a paraconformity (?). The estimated average thickness is approximately 150 m, possibly reaching a maximum of almost 200 m in the basin's NW sector.

Conversely, all around the Escalaplano area (Fig. 4.2: B), Buntsandstein deposits directly overlie the Variscan basement (Pertusati et al., 2000a, b) or, very locally, the Permian sediments. Dorn (1940) assigned the succession outcropping at Escalaplano to the “Keuper” (Late Triassic), due to the presence of gypsiferous shale. Later, other authors working on this section suggested a Middle Triassic age for this succession and referred to a transitional “Buntsandstein” laid down before the subsequent Muschelkalk marine carbonate transgression (Fazzini et al., 1974; Pecorini, 1974; Damiani and Gandin, 1973a,b,c; Fontana et al., 1982). Later, Pittau (in Ronchi, 1997) studied in detail the palynological associations in the Middle Triassic sedimentary succession of this area.

Escalaplano Formation

The Anisian sedimentary record, included in the Buntsandstein facies (Damiani and Gandin 1973 a,b,c; Pecorini 1974; Barca et al. 1997; Costamagna et al., 2000), is here represented by the Escalaplano Fm. (Figs 4.1, 4.3) (Costamagna et al., 2000). This unit has been subdivided in 4 different lithofacies. At the bottom (Lithofacies 1), it is possible to observe para-conglomerates and sandstones filling erosive surfaces (channels) over the Variscan basement (Fontana et al., 1982; Cassinis et al., 1996a). Lithofacies 2 consists of dark to yellowish silty marls showing dessication features (mud cracks, halite casts etc.), bioturbation and caliches. Lithofacies 3 is composed of dark silty-clayey marls with lenses of

satin spar – microcrystalline gypsum. Finally, lithofacies 4 consists of thin reddish clays and yellowish-grey marls. Its maximum thickness is approximately 20m, and it has been dated through its palynofloristic associations (Costamagna et al., 2000; Stori et al., 2022).

Monte Maggiore Formation

The Muschelkalk in this area is represented by the Monte Maggiore Fm. (Figs. 4.1, 4.2: B, D) (Costamagna and Barca, 2000), previously described by Damiani and Gandin (1973a,b). The Monte Maggiore Fm. crops out in the Escalaplano area over the Escalaplano Fm., but it is on the Monte Maggiore hill that it reaches its greatest thickness of about 70 m. Here, the succession was subdivided into different members by Damiani and Gandin (1973a,b) and subsequently re-defined by Costamagna et al. (2000). In the Monte Maggiore area (Fig. 4.2: D), it is possible to observe the base of the succession directly overlaying the crystalline basement with a transgressive breccia (Damiani and Gandin, 1973a,b), while in the Escalaplano and Orroli areas (SE Gerrei), the succession unconformably rests on the Escalaplano Fm. which, as mentioned before, progressively thins towards Monte Maggiore (NW). The basal breccias are followed by a basal member (“Membro delle dolomie gialle”; Costamagna et al., 2000), which is mainly composed of yellow dolomitic limestones to dolostones that are badly stratified, with intra-formational breccia horizons often bearing pyrite crystals and evaporitic moulds. In the area of Orroli village, a rich dasycladacean algal assemblage (*Diplopora annulata*, *Kantia dolomitica*, *Macroporella beneckeii* and *Teutloporella nodosa*) has been recently discovered by Costamagna and Piros (2022), pointing to an Illyrian age for the bottom of the Monte Maggiore Fm.

Above this, another member (“Membro dei calcari azzurri”; Costamagna et al., 2000) is represented by an alternation of grey calcarenites to calcilutites and marls, arranged in shallowing upward sequences and showing tempestite events involving bioclast accumulations and bioturbation. Among the bioclasts recognized in the storm layers Damiani and Gandin (1973b), the bivalve *Costatoria goldfussi* Alberti is consistent with a Ladinian age of the Monte Maggiore Fm. (Costamagna et al., 2000). In this unit, several dasycladacean algae have been described by Damiani and Gandin (1973b): *Diplopora annulata*, *Diplopora annulate debilis*, *Macroporella cf. spectabili*, *Solenopora cf. simionescui*, *Teutloporella peniculiformis*, and *Teutloporella cf. nodosa*. The bioturbation was interpreted as *Chondrites* and *Thalassinoides* (Damiani and Gandin, 1973b). The upper part of this Member is slightly more dolomitic and bears chert nodules.

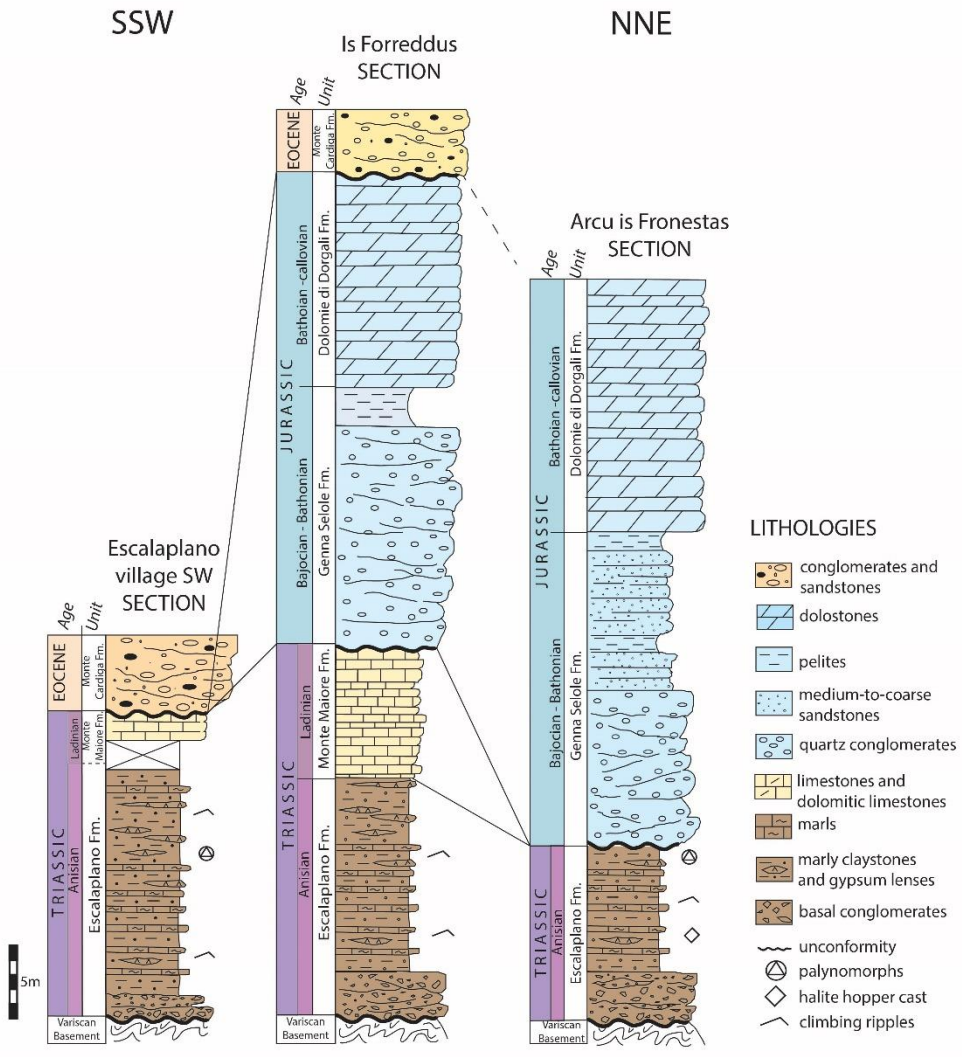


Fig. 4.3 Simplified sections to show the stratigraphic relationships and erosional surfaces in the Escalaplano area

4.3 Campumari (Iglesiente)

The Campumari-Coremò area (Fig. 4.4) is located along the SW coast of Sardinia, in the Iglesias area, and it consists of a series of small tabular reliefs with slightly different heights, forming a plateau with a maximum altitude of 219 m a.s.l. (Fig. 4.2: F).

The post-Variscan "Permo-Triassic" auctt. deposits vary from a minimum of 10 m in the "Case Miniera Panecconi" locality up to a maximum of 45 m in the Su Grifoneddu de S'Acqua area, and they lie in angular unconformity over the low metamorphic basement (Fig 4.2: F).

The Campumari plateau has been studied since the end of the 19th century (Lovisato, 1881; Tornquist, 1902; Novarese, 1914; Taricco, 1928) but there was never any unanimous opinion about the chronology of its sedimentary formations, which were attributed to very different ages (Permian, Triassic, Cretaceous and Eocene). It was not until the work of Coccozza and Gandin (1976) that the sequence was studied in detail; these authors recognized a stratigraphic gap between the true Eocene deposits and the underlying carbonate lithologies, and these latter deposits were finally attributed to the Triassic, based on facies analogies with the Triassic sediments of the Scivu-Is Arenas and Monte Maiore areas. Later, Pittau and Del Rio (1980) describe a palynological association from a discontinuous gray-blackish clay level located in the upper part of the "B interval" (Coccozza and Gandin, 1976), now formalized as "Su Passu Malu Member" (Barca and Costamagna, 2003). They therefore attributed at least the upper part of the clastic unit of the Campumari succession to the Middle Triassic or "Lower Muschelkalk". Subsequently, Barca and Costamagna (2003) performed another detailed sedimentological study of the Campumari sequence, identifying and formalizing two formations and their respective members, the Riu Is Corras Fm. and Campumari Fm. (Barca and Costamagna, 1997b) (Fig. 4.1).

Riu is Corras Formation

The "Riu Is Corras" Fm. (Costamagna and Barca, 2003) (Fig. 4.1) is transgressive and rests on angular unconformity over the Variscan basement. The formation consists of polygenic conglomerates, of grain with a sustained matrix with rare and fine horizons of siltstones and red sandstones, and frequent calicheified horizons, often showing a nodular or brecciated aspect. The clasts show heterogeneous composition. It is possible to find clasts with carbonate composition, as well as quartz clasts and fragments deriving from the metamorphic basement. The clasts sizes also heterogeneous, with a maximum diameter of 15 cm and shapes ranging from sub-rounded to subangular. The Riu Is Corras Fm. reaches a maximum thickness of 24 m on the W side of the Riu Is Corras valley. It is not possible to attribute a precise age to

the Fm., because of the lack of reliable biostratigraphic data. On the basis of sedimentological and stratigraphic considerations, up to now, it is only possible to attribute a generic “Permo?-Triassic” age to this formation and it has been interpreted as the product of a coastal plain depositional environment (distal fan) in a semi-arid hot climate (Cocozza and Gandin, 1976; Costamagna and Barca, 2002).

Campumari Formation

The Campumari Fm. (Fig. 4.1) was attributed to the Muschelkalk facies and sub-divided into two members by Costamagna and Barca (2002). The lower Su Passu Malu Member shows dark marly-clayey deposits in its lower part and consists mainly of thin-bedded yellow dolostones. In its uppermost part, formerly the “B interval”, different palynological associations were reported (Barca and Costamagna, 2003; Stori et al., 2022). The upper Grifoneddu de S’acqua Member, whose base is marked by a brecciated bed, is mostly comprised of a dolomite succession originally interpreted as a lagoon environment (Costamagna and Barca, 2002). The fossiliferous content of the Campumari Fm. is low, shows low diversity and it is difficult to interpret due to superimposed dolomitization processes that altered most of the original depositional structures and microfacies.

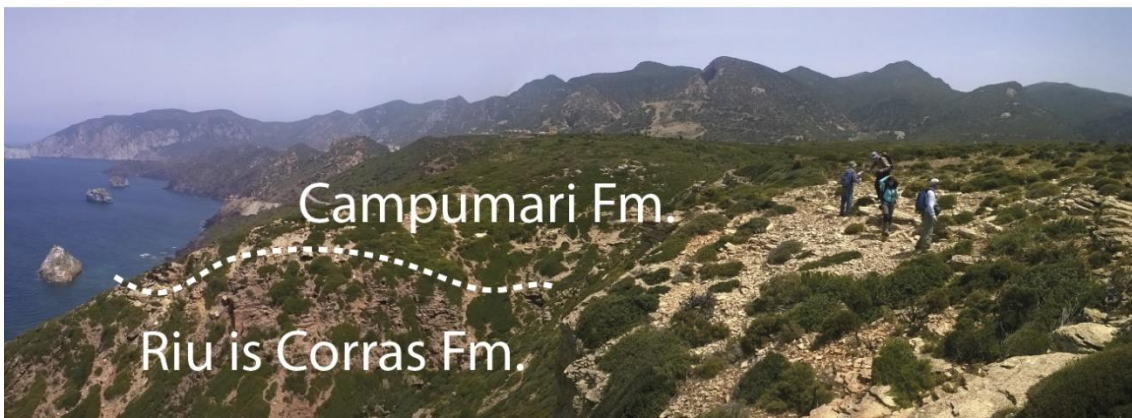


Fig. 4.4. The Campumari-Coremò plateau, showing the stratigraphic relationships between the Riu is Corras Fm. and the Campumari Fm.

4.4 Porto Pino (Sulcis)

The Porto Pino area is found on the SW coast of the Sulcis region (Fig. 4.2: E). Since the late 19th century, the Mesozoic sequence of this area was a focus of study for different authors (e.g., Lamarmora, 1826), but it was not until the second half of the 20th century that the sequence was characterized in detail and recognized as Triassic and attributed to Germanic facies (Fontanarosa, 1963; Baud et al., 1977; Gandin, 1978b). The Mesozoic sequence has been further investigated by Costamagna (1997a, 2000, 2002), who identified two different sequences corresponding to two different superimposed tectonic units: the “Cala Su Trigu” and the “Guardia Sa Perda” units. In both Mesozoic sequences of the Porto Pino area, it is difficult to locate the base of the Mesozoic sequences (represented in Buntsandstein facies) due to Alpine tectonism. The “Guardia Sa Perda” tectonic unit is about 300 m thick and comprises 4 units, ranging from the Middle Triassic to the upper Lias-lower Dogger: The formations of Punta Tonnara (Figs. 4.1, 4.5), Monte Zari, Guardia Sa Barracca and Medau Mereu (Costamagna, 2000).

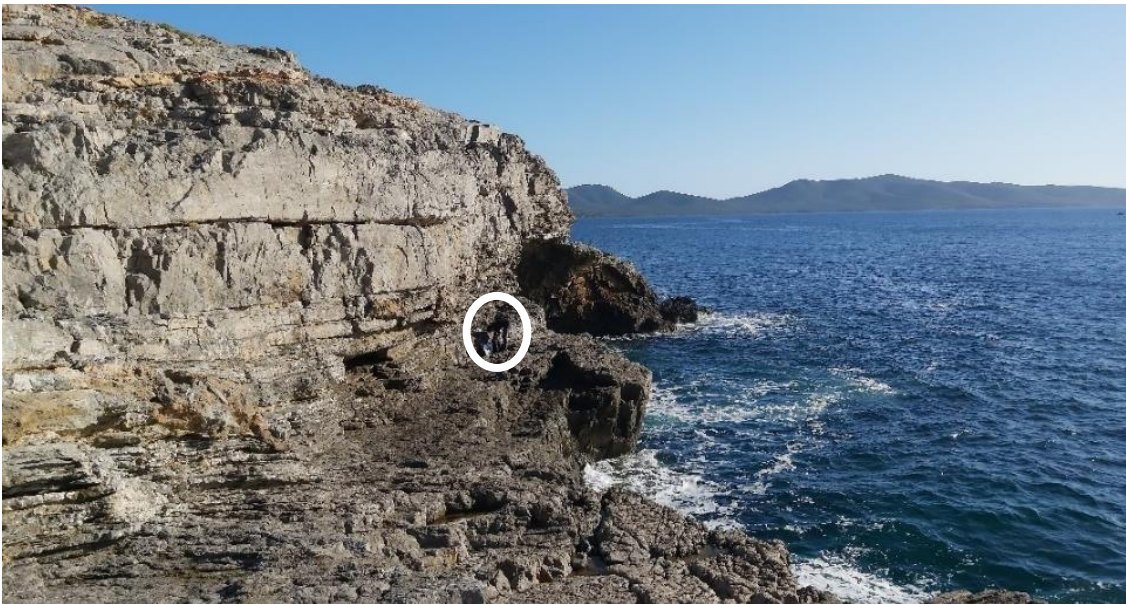


Fig. 4.5. The Punta Tonnara promontory, exposing a 20m thick section of the Punta Tonnara Fm. (White circle: person for scale)

Punta Tonnara Formation

The base of the sequence, comprising the 20-m thick Punta Tonnara Fm., has been attributed to the Muschelkalk facies (Costamagna, 2000) (Fig. 4.1). Its base is not exposed, yet shallowing upward features occur in the outcrop organized as follows: at the base they are represented mainly by grey to dark grey bioturbated limestones (lower intertidal-upper subtidal) with laminated marl intercalations, and these evolve upwards to more massive, grey limestones with less bioturbation and more microbial lamination, ripples and evaporitic pseudomorphs (intertidal) and finally to a reddish limestone with chert nodules, evaporitic

pseudomorphs and tepee structures (upper intertidal/sabkha) (Costamagna, 2000). The fossiliferous content of the Punta Tonnara Fm. is low (Martini et al. 1987), thus allowing for the succession's ascription only to a Middle Triassic to Late Triassic age. These latter authors highlighted, via a cathodoluminescence technique, the presence of a rich but monospecific foraminifera assemblage of *Agathammina? sp.*, belonging to the *Miliolina* suborder.

4.5 Scivu-Is Arenas (Arburese)

The Scivu-Is Arenas region runs along the SW coast of Sardinia, S of the Gulf of Oristano (Fig. 4. 2: C). The first systematic studies of the area were carried out by Bornemann (1881), who attributed the sedimentary succession of the area to the Triassic based on its fossil contents: *Myophora goldfussi* Von Alberti, *Gervilleia subglobosa* Credner, and *Rhynchocorallium jeneense* Zenker. Moreover, according to facies similarities, the author alluded to correlation with the Grès Bigarré of Provence. Later, Oosterban (1936) proposed correlation between the "Arenarie variegate" of the Nurra region and the base of the Triassic succession of Scivu-Is Arenas. Moreover, he attributed to the Muschelkalk facies, the limestone beds outcropping at the top of the succession in this area. Further studies were those of Damiani and Gandin (1973b), who proposed correlations with other Triassic outcrops of Sardinia, offering more detailed palaeoenvironmental reconstructions. This was followed by a detailed sedimentological and stratigraphical study of the Triassic succession by Barca et al. (1995b), who split the Triassic sedimentary succession into two units: the Punta S'Arridelli Fm. (Permian?-Triassic to late Anisian) and the Punta Su Nuraxi Fm. (late Anisian-Ladinian) (Fig. 4.1).

Punta S'Arridelli Formation.

The older Triassic unit, namely Punta S'Arridelli Fm. (Costamagna and Barca, 2002), lies nonconformably on top of the Palaeozoic basement (Figs. 4.2: C and 4.6) and consists of two subunits, the lower Su Ripostiggiu Member and the upper Bruncu Pilloni Member, representing the evolution from a continental braided fluvial system environment, to a more transitional, sabkha to shallow marine setting (Costamagna and Barca, 2002). The Su Ripostiggiu Member starts with thin reddish breccias continuing to coarse sandstones with angular-to-sub-rounded clasts coming from the eroded metamorphic basement and volcanic detritus, and it evolves upwards to purple-reddish paleosols and carbonate layers containing fragments of the basement and reddish sandstones. From base to top of this member, there is a decrease in the clast size and a variation in clast composition, which changes from almost totally volcanic to exclusively consisting of metamorphic basement fragments, marking an increase in erosive sub-aerial conditions (Barca et al., 1995). The Su Ripostiggiu Member (about 20m) passes upwards (or laterally to the S) to the Bruncu Pilloni Member, formed by dedolomitized, locally cavernous limestone, bearing siliceous pseudomorphs, levels of dissolution-collapse breccias and traces of calcitization processes in its upper part.

Punta Su Nuraxi Formation

The Punta Su Nuraxi Fm. (Costamagna and Barca, 2002) (Figs. 4.1 and 4.6) overlies Punta S'Arridelli Fm. with a slight angular unconformity and is divided into two different subunits: the lower, Case Pisano Member and the upper, Bruncu Zippiri Member (Costamagna and Barca, 2002). The Case Pisano Member locally starts with a dark, marly mudstone layer, yielding a microflora assemblage suggesting a late Anisian age, according to Barca et al. (1995b).

There following metric alternations consist of massive, cavernous, calcareous mudstones bearing siliceous pseudomorphs and evaporitic minerals, and whitish layered and cross laminated calcarenites-calcilutites. Salt tectonic structures (folds several metres in size) occur in this subunit, along with collapse-dissolution breccias and localized calcrete structures. The Case Pisano Member evolves upwards in the Bruncu Zippiri Member through a thick layer of dissolution-collapse breccias. The Bruncu Zippiri Member consists of two facies The first is represented by blue-gray limestone with reddish intercalation of bioclastic grainstones-packstones, locally presenting cross, wavy and planar lamination, fossil content (bivalves, foraminifera and algae) and rare evidence of storm beds eroding the substratum (Costamagna and Barca, 2002). The second facies is represented by massive calcarenite-calcilutite (packstones to wackestones) evolving upwards into gray-reddish, marly limestones (wackestones to mudstones), showing bioturbation structures classified as *Planolites* and *Paleophycus tubularis* (Moore 1962; Costamagna and Barca, 2002).



Fig. 4.6. Stratigraphic relationship between the Fms. of the Arburese region

4.6 Nurra

The post-Variscan succession of the Nurra region (NW Sardinia, Fig. 4.2: A) was unconformably deposited on the Variscan crystalline basement during the early Permian to Middle Triassic timespan; it is represented by a thick pile of continental sediments (about 700m thick), mainly Permian in age, and evolving into continental-to-shallow marine Triassic deposits with the classic Germanic facies (Buntsandstein, Muschelkalk and Keuper Auct.) (Fig. 4.1). The first and second sequences belong to the Permian and are represented by the stacking of different fluvial to lacustrine formations (e.g., Cassinis et al., 2003; Costamagna, 2019).

The third sequence (approx. 50 m thick) consists of two formations, named Conglomerato del Porticciolo Fm. and Arenarie di Cala Viola Fm. (Fig. 4.1), respectively, separated by a minor erosional surface. The former (up to 12 m thick) represents a gravelly braided fluvial system deposition, setting under conditions of persistent aridity, as suggested by the common occurrence of wind-worn clasts (Cassinis et al., 2003; Durand, 2008). Its base consists of the alternation between massive to cross-bedded ortho- and para-conglomerates (mainly polycrystalline quartz), presenting imbrication features and cross-laminated siltstones to sandstones. The top of the formation consists of a 4-5 m alternation of trough cross-bedded, medium-fine sandstones of fluvial and aeolian origin and coarser pebbly sandstones.

Arenarie di Cala Viola Formation

The Arenarie di Cala Viola Fm. (Fig. 4.1) is about 40 m thick and unconformably overlies the Conglomerato del Porticciolo Fm. Its base is mainly represented by dark red sandstones and siltstones of continental origin arranged in thin beds and presenting, pedogenic-origin beds, intraformational breccias, sets of climbing ripples evolving into horizontal-to-low-angle laminated or trough cross-bedding, and subordinate mudstones in the lower part. It is overlain by a few meters of gray-green, pink and reddish, medium- to coarse-grained sandstones, with the occurrence of lensoid geometries and trough cross-bedding. Further up, in the medium-upper part of the unit, there are thinly- to well-bedded, medium- to fine-grained, dark orange/red to purple sandstones and siltstones and, finally, the top of the unit consists mainly of whitish-green to grey siltstones and claystones. The Arenarie di Cala Viola Fm. marks a drastic change in the sedimentary and climatic conditions. In fact, while the Conglomerato di Porticciolo was probably deposited during the late Early Triassic (late Olenekian) sedimentary cycle, under arid to hyper-arid conditions (Durand, 2006, 2008; Bourquin et al., 2007, 2011; Borrueil-Abadia et al., 2019), similarly to the Poudingue de Port-Issol in Provence, the Arenarie

di Cala Viola Fm., with its finer grained facies, was deposited in a terminal fan setting under semi-arid conditions (Cassinis et al., 2003; Durand, 2006, 2008; Citton et al. 2020), as testified by the presence of pedogenetic carbonate concretions, mud cracks, tree-related bio-sedimentary structures and the presence of inundite sequences (*sensu* Seilacher, 1982). Some authors (i.e. Fontana et al., 2001; Costamagna, 2012) postulated a tidal influence during the sedimentation of the Arenarie di Cala Viola Fm. based on the sedimentology and the stratigraphic position of this unit, which shortly predates the widespread Middle Triassic marine transgression shown by the 'Muschelkalk'-type carbonates.

Punta del Lavatoio Formation

In this area, the Muschelkalk is represented by the Punta del Lavatoio Fm. (Fig. 4.1) which crops out not only at Monte Santa Giusta but also along the Alghero coast (Punta del Lavatoio, Monte Fogheras, Cala Bona) (Fig. 4.7). Overall, this unit is of a variable thickness from about 40 m at the Punta del Lavatoio outcrop (Alghero town S shoreline Fig. 4.7: C), overturned and intensely tectonized by the "Pyrenean phase" (Costamagna and Barca, 2002), to 251 m in the former hill (Carrillat, 1997; Carrillat et al., 1999a, b) and to some 80 m in the subsurface (Cugiareddu Well: Pomesano Cherchi, 1968).

The Punta del Lavatoio Fm. was divided in sub-units by previous authors. It starts with an "Upper Unit" (Gandin, 1978b) and was later subdivided by Costamagna (2002) into Lithofacies A or L1 and Lithofacies B or L2. The former consists of nodular limestones and marls containing reworked fossils (Gandin, 1978; Posenato, 2002; Urlich and Posenato, 2002) such as: *Encrinus liliformis*, *Hoernesia socialis* (Schlotheim), *Enantiostreon difforme* (Schlotheim), *Plagiostoma* = cf. *striatum* (Schlotheim), *Costatoria goldfussi* (Alberti), *Placunopsis plana* (Giebel), *Curionia gastrochaena* (Dunker), *Septifer eduliformis* (Schlotheim), *Bakevellia subcostata* (Goldfuss), *Costigervilia substriata* (Credner) and *Pleuronectites laevigatus* (Schlotheim) (Posenato, 2002). In addition to this rich fossil content, Tornquist (1904) reported the presence Lithofacies A of ammonoids (of alpine affinity) such as *Protrachyceras longobardicum* Mojsisovics, which he called "Upper Nodosus-Horizont" (see also Urlich and Posenato, 2002). Lithofacies A also shows a moderate degree of bioturbation harbouring *Protovirgularia* isp., *Planolites montanus* and *Balanoglossites triadicus* (Knaust and Costamagna, 2012). Lithofacies B is represented by grey limestones (locally dolomitized) organized in metre-thick strata, showing weak bioturbation (*B. triadicus* and *Protovirgularia* isp), lamination and accumulation of bioclasts, in particular dasycladacean algae (*Diplopore annulata*), indicating a very shallow high-energy marine environment (Gandin, 1978b; Posenato, 2002; Knaust and Costamagna, 2012). Lithofacies A/L1 and Lithofacies B/L2 have

been interpreted as the passage from a middle-outer ramp environment, characterized by moderate energy, to a higher-energy shoal environment (Knaust and Costamagna, 2012). The third unit, Lithofacies C/L3 (Costamagna and Barca, 2002), consists of well-stratified limestones and dolomitic limestones with marl intercalations arranged in shallowing upwards sequences. In this unit, a drop in taxonomic diversity has been observed and the most abundant species are *Costatoria Goldfussi* (Alberti), *Hoernesia socialis* (Schlotheim) and subordinately *Pleuromya musculoides* (Posenato, 2002). Ammonoids have been also reported in this unit called the Lower “Nodosus-Horizon” by Tornquist, (1904) (see also Urlichs and Posenato, 2002). This unit was most likely deposited in a lagoon environment featuring sporadic high-energy episodes, as testified by the presence of tempestite layers (Gandin, 1978; Posenato, 2002; Costamagna and Barca, 2002; Knaust and Costamagna, 2012). These latter authors reported the presence of the following ichnofossils: *Thalassinoides suevicus*, *Protovirgularia* isp. *Rhizocorallium commune*, *Lockeia siliquaria*, *L. Serialis* and *Planolites montanus*. The last unit or Lithofacies D or L4 (Costamagna and Barca, 2002), or Lower Unit according to Gandin (1978b), consists of dark brown dolostones with yellowish dolomitic marl intercalations, organized as decimetric banks. This last unit is referred to as the Keuper facies by Knaust and Costamagna (2012) and shows low and poorly-preserved bioturbation such as *Protovirgularia* isp., *P. montanus*, *Taenidium crissum*, *Thalassinoides suevicus* and *B. triadicus*.

At Monte Santa Giusta hill (4.7: B), the Muschelkalk sequence, about 251 m thick (Bartusch, 1985; Carrillat 1997, 1999; Knaust and Costamagna, 2012), has been divided into 4 units that lay between the sedimentary record related to the upper Buntsandstein (early-middle Anisian) (Knaust and Costamagna 2012; Stori et al., 2022) and the one related to the Keuper (Knaust and Costamagna 2012). The lower unit, or “Lower Dolomitic Unit” (Carillat, 1999 a, b; Posenato, 2002; Knaust and Costamagna, 2012), starts with 30 m of nodular marly dolostones and grey laminated dolostones beds, showing bioturbation and shell fragments (Knaust and Costamagna, 2012). Palynomorph associations suggest a Fassanian age (Cherchi, and Schroeder, 1985; Pittau, 1999). Above this unit lies conformably the “Lower Calcareous Unit”, which is about 40 m thick (Carillat 1999 a, b; Posenato, 2002; Knaust and Costamagna, 2012). This unit consists of few metres of marly limestones and dolostones and bioturbated fossiliferous limestones with clay intercalations (Carillat 1999 a, b; Knaust and Costamagna, 2012). Its top consists of: i) heavily bioturbated limestones with *Rhizocorallium commune* and *Balanoglossites triadicus* (Knaust and Costamagna, 2012), and ii) biocalcarenes and oolitic limestones, with a significant conodont content (Bagnoli et al., 1985 a, b). The following sequence is the “Upper Dolomitic Unit” (Carillat 1999 a, b; Posenato, 2002; Knaust and Costamagna, 2012), which is about 30 m thick and mainly consists of dolomitic marls and light

grey dolostones, with more levels rich in conodonts (Bartusch, 1985). The uppermost unit of the Monte Santa Giusta succession is the "Upper Calcareous Unit" (Carillat, 1999 a, b; Posenato, 2002; Knaust and Costamagna, 2012), whose thickness has been estimated about 100 m. It was subdivided by Bartusch (1985) into 3 different subunits: mo1, mo2 and mo3. The former, which consists of 40m thick succession of dolomitic limestones evolving to more massive and grey limestones towards the top, yields the conodonts *B. truempyi* and *B. hungaricus*. After the mo2 subunit, which consists of about 10 m of reddish barren dolostones beds, the mo3 subunit follows. This subunit, which is about 50 m thick, shows abundant yielding dasycladacean algae, various bivalve species (e.g., *Plagiostoma striatum* Schlotheim), brachiopods (*Coenothyris vulgaris* Schlotheim) and echinoderms (*Encrinus liliiformis* Schlotheim) (Tornquist, 1902; Posenato, 2002). The data providing an accurate age for the Muschelkalk units in the Nurra area is based on conodonts, ammonoids and microfloristic associations.

Regarding the ammonoids content, in the early decades of the last century, Tornquist (1901) identified the ammonoids *Ceratites* cf. *nodosus* Bruguière close to Monte Santa Giusta. In the same place, this author also *ex situ* described *C. ex aff. evolutus* which, according to Urlich and Posenato (2002) and Urlichs (2002), is likely a *Ceratites* (*Austrocerarites*) and whose stratigraphic distribution is late Fassanian - earliest Longobardian. Later, this author (Tornquist, 1904), showed the extra-Alpine character of the Triassic sedimentary record of Sardinia, pointing out its unquestionable resemblance to the Germanic Triassic. He also indicated that the levels containing "*Encrinus liliiformis*" from the Monte Santa Giusta section seem to be missing in the Punta del Lavatoio section. This author collected 6 ammonoid specimens south of Alghero that looked more like *C. munsteri* (Diener) than *C. nodosus* Bruguière, and also found a specimen of *Protrachiceras longobardicum* Mojsisovics associated with *C. munsteri*, which could indicate the first incursion of Alpine fauna, as described by Urlichs and Posenato (2002).

The first detailed work on conodonts was carried out by Pomesano Cherchi (1967) who sampled the Middle Triassic in Muschelkalk facies from Monte Fogheras and Monte Zirra outcrops and the Cugiareddu well (Pomesano Cherchi, 1968). This author found a rich assemblage of specimens belonging to 22 species, of which 16 are characteristic of Middle Triassic Germanic facies: *Gondolella* (3), *Hindeolella* (2), *Lonchodina* (2), *Apatognathus* (1), *Prioniodella* (1), *Ozarkodina* (1), *Spathognathodus* (1), and *Polygnathus* (1).

Later on, Bagnoli et al. (1985a, b) also described different conodont species from two fossiliferous horizons in the Punta del Lavatoio section: "F0" in Lithofacies A or L1 (later also

described by Costamagna, 2002) (former “oberer Nodosen Horizonti” of Tornquist, 1904) and another one located above the “dasycladacean banks” of Lithofacies B or L2 (later also described by Costamagna, 2002). The species found in these horizons belong to *Epigondolella truempyi* (Hirsch)”, a marker of a late Fassanian age. The genera “*Epigondolella*” were later revised (Kozur et al., 1994; Nicora and Brack, 1995) and the name changed to “*Burdovignathus*”. Its stratigraphic range has also shifted slightly and now corresponds to the early Longobardian. Some years later, Carrillat et al. (1999) identified the following species in the Muschelkalk of the Monte Santa Giusta section: *Gondolella constricta* (Mosher and Clark, 1965), originally described from the Humboldt Range in Nevada, USA, and later also found in the Alps, Carpato-Balkanik Range, Hellenids, Kokaeli Peninsula (Turkey), and Japan; *Carinella truempyi* (Hirsch, 1971), originally recorded from the Muschelkalk facies of Provence (France) and later also found in the Balaton Plateau (Hungary); *Carinella japonica* (Hayashi, 1968), originally described in the Adayama Fm. (Japan), and later also identified in Europe, Hellenids and Carpato-Balkanik Range. Based on the joint occurrence of *Carinella truempyi* and *Gondolella constricta*, the authors attributed a late Fassanian age to the lower-middle carbonate part of the Monte Santa Giusta section. *Carinella truempyi* is in fact a marker of the Tuempyi-range-Zone, corresponding to the upper Curionii-Zone of late Fassanian age (Kovacs and Kozur, 1980). *Gondolella constricta* has a slightly wider range: Illyrian-Fassanian (Vrielynck, 1987). The presence of *Carinella japonica*, a marker of the top of the Gredleri-Zone to the base of the Archelays-Zone (Krystyn, 1983), indicates an early Longobardian age, and dates the Monte Santa Giusta section as late Fassanian - early Longobardian.

According to pollen data, Pittau Demelia and Flaviani (1982) described a well-preserved microfloristic association in the calcareous Diplopora banks of Lithofacies C or L3 (later defined by Costamagna, 2002) at the Punta del Lavatoio outcrop. The association comprised the morphological group *Alisporites-Sulcatisporites-Cuneatisporites*, *Triadispora crassa*, *Aratrisporites* sp., *Aratrisporites paraspinosus*, *Camarozonosporites* cf. *rudis*, *Polypodiaceoisporites* sp. and *Verrucosisporites* sp. Based on this association and on correlations with similar assemblages found in the A2 zone of the Cugiareddu well, the basal part of the Punta del Lavatoio succession was ascribed a late Anisian age (Pomesano Cherchi, 1968). Subsequently, Bagnoli et al. (1985a, b) and Posenato (1995) examined the age of the Punta del Lavatoio sequence via macrofauna (bivalves and ammonites) and other microfauna (conodonts) and provided a more precise chronological resolution (late Fassanian - early Longobardian). The microfloristic association of Pittau-Demelia and Flaviani (1982) has been recently revised by Stori et al. (2022), ascribing it to a Pelsonian-Longobardian age, which is a

broader range for this association. Moreover, palynological assemblages were reported from similar facies at the base of the Monte Santa Giusta section by Carillat et al. (1999).

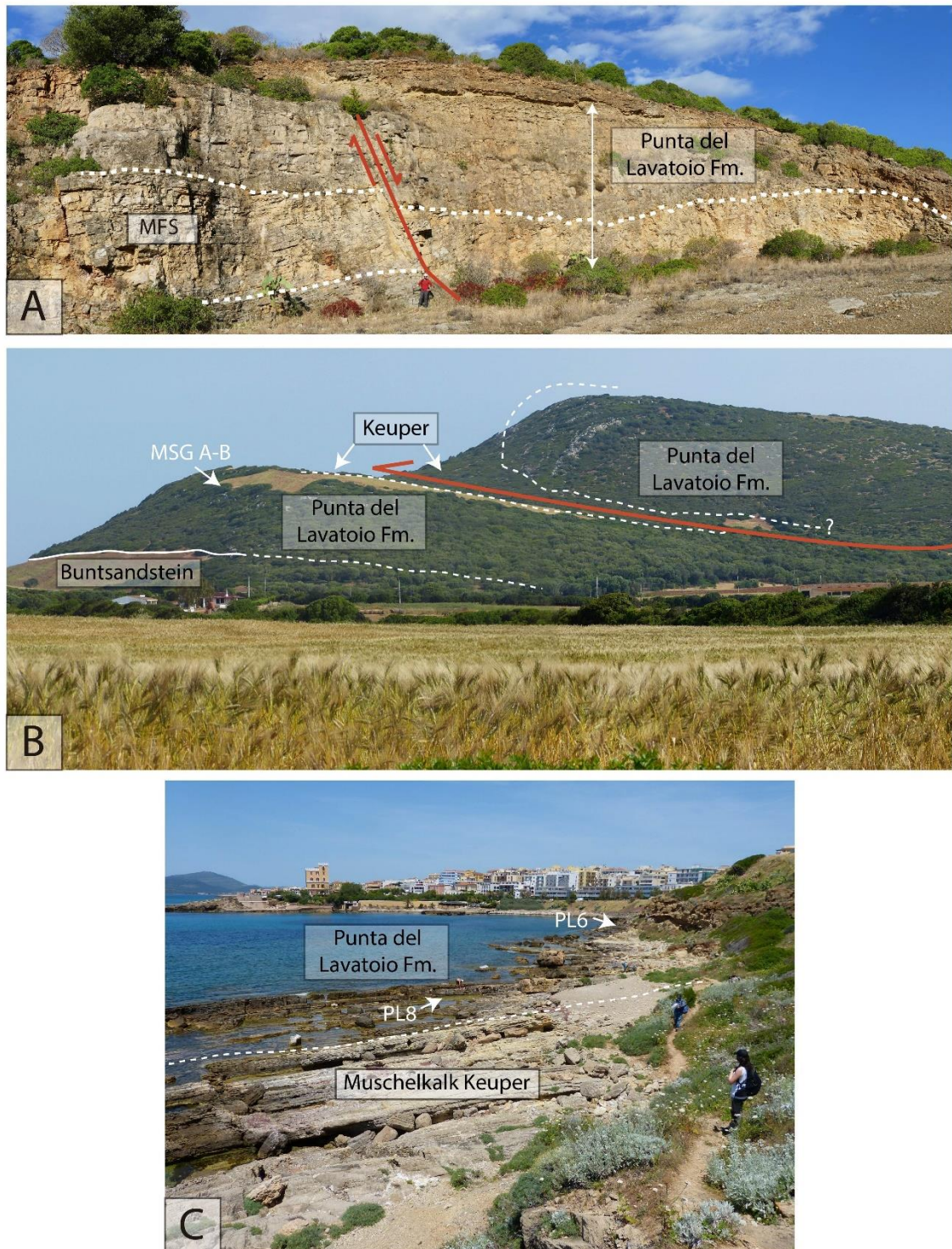


Fig. 4.7: Field pictures portraying the Nurra outcrops of a) Monte Fogheras b) Monte Santa Giusta c) Punta del Lavatoio, with indicated the position of the fossiliferous levels discussed in chapter 6. Respectively: MFS; MFSG A-B, PL6 and PL8.

4.7 Stratigraphic sections

Escalaplano SW (Sarcidano-Gerrei)

The Escalaplano stratigraphic section is about 20m thick and it is located in the SW of the Escalaplano village, along the SS 128 Ballao-Escalaplano road, just before the first buildings at the southern entrance to the village. It comprises the basal part of the Escalaplano Fm. and few m of the Monte Maggiore Fm.

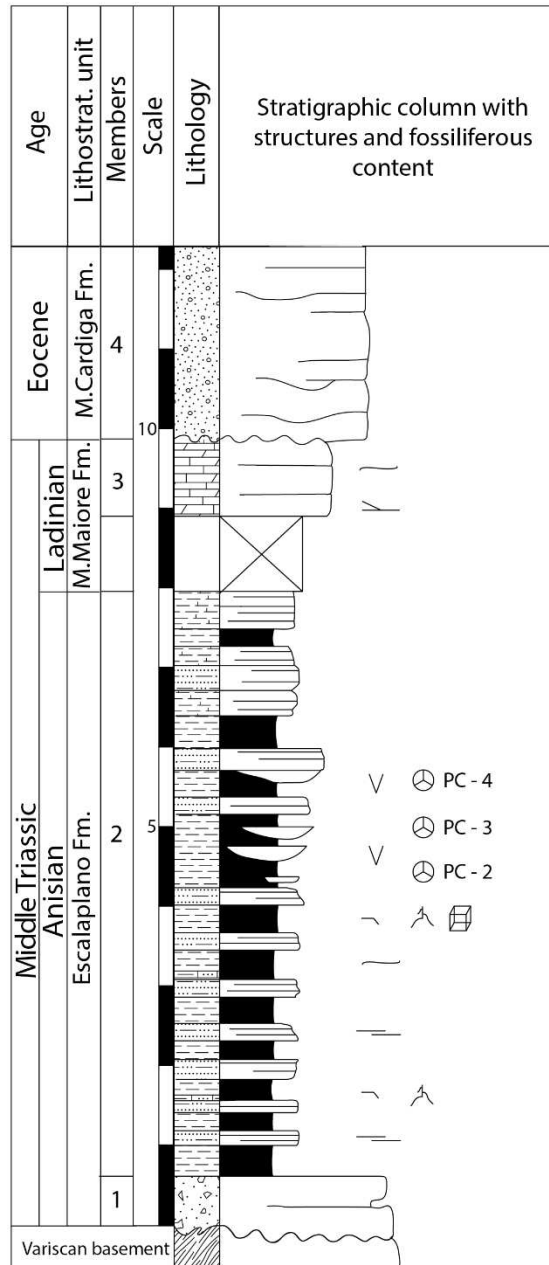


Fig. 4.8. Escalaplano SW stratigraphic section (see fig. 4.20 for legend).

Arcu is Fronestas (Sarcidano-Gerrei)

In the Arcu Is Fronestas locality, located about 3km to the NE of Escalaplano, on the road to Perdasdefogu, the Middle Triassic succession is about 20 m thick. It lies unconformably over the Variscan basement and is unconformably overlain by the Middle Jurassic quartz conglomerates of the Genna Selole Formation.

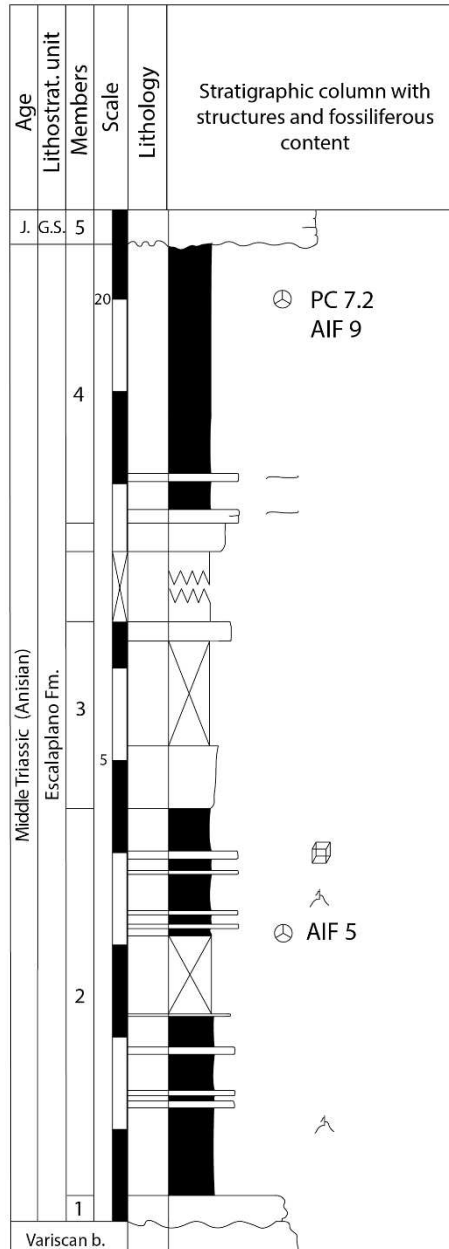


Fig. 4.9. Arcui s Fronestas stratigraphic section (see fig. 4.20 for legend).

Orroli (Sarcidano-Gerrei)

The Orroli stratigraphic section about 15m thick. It is a composite column, consisting of a few meters thick wall exposed along the SP65 street (Bruncu su Para), and a quarry wall about 200m E from the first outcrop. It comprises the lowest part of the Monte Maggiore Fm., and its lower part is in direct contact with the upper part of the Escalaplano Fm.

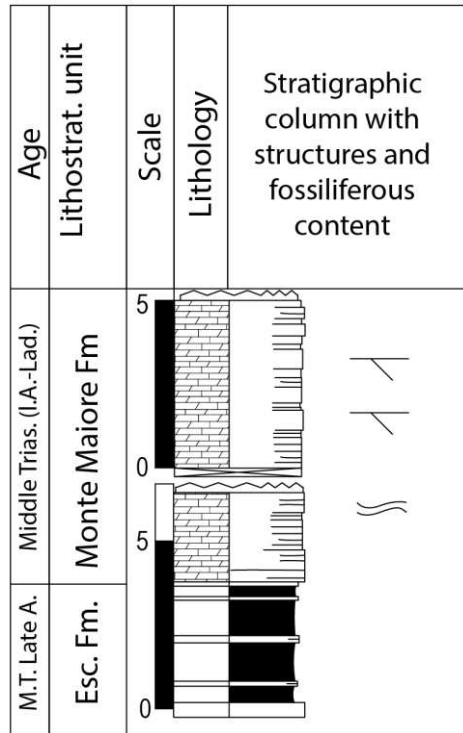


Fig. 4.10. Orroli stratigraphic section (see fig. 4.20 for legend).

Monte Maiore (Sarcidano-Gerrei)

The Monte Maiore outcrop comprises the entirety of the Monte Maiore Fm., and it is a composite of two outcrops. The first one is about 10m thick, and located at the base of a quarry located south of the Nureci village. This lower part comprises the base of the Monte Maiore Fm. lying directly on top of the basement. The top of the studied column is about 15m thick. This outcrop located at the top of the Monte Maiore hill, and it comprises the top part of the Fm.

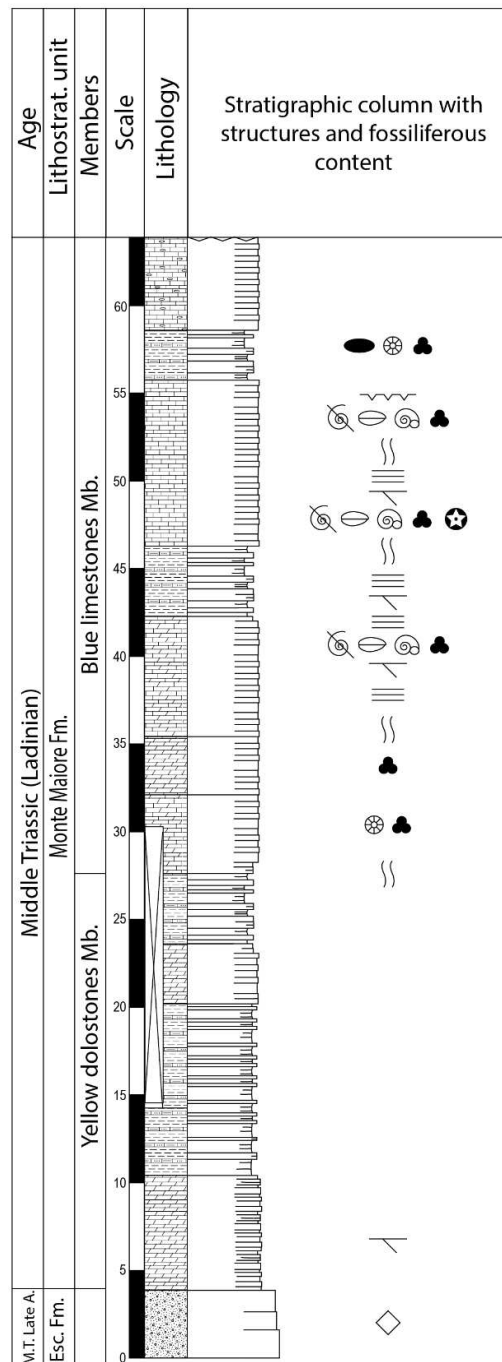


Fig. 4.11. Monte Maiore stratigraphic section (see fig. 4.20 for legend).

Punta su Nuraxi (Arburese)

In the Scivu-Is Arenas locality, located at about 10km W from Arbus village, it is possible to reach a small relief, located approximately at 39.482562, 8.433834. On the side of the hill the section of Punta su Nuraxi has been measured, and it is about 50m thick. It comprises the Variscan basement and the Fms. og Punta S'Arridelli e Punta su Nuraxi.

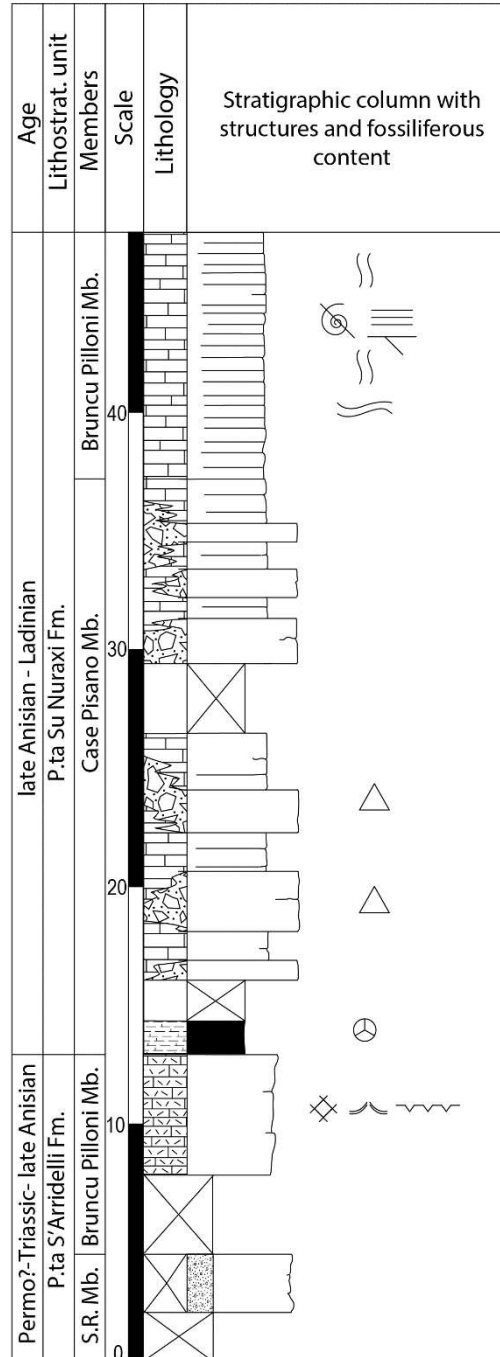


Fig. 4.12. Punta su Nuraxi stratigraphic section (see fig. 4.20 for legend).

Campumari (Iglesiente)

The Su Passu Malu stratigraphic section is about 45m thick and well exposed. It is located in the “Campumari” promontory, on the side of a small valley that dips towards the sea, intersecting the SP83 street. It is a well exposed section comprising the Variscan basement, the Riu Is Corras Fm. and the Campumari Fm.

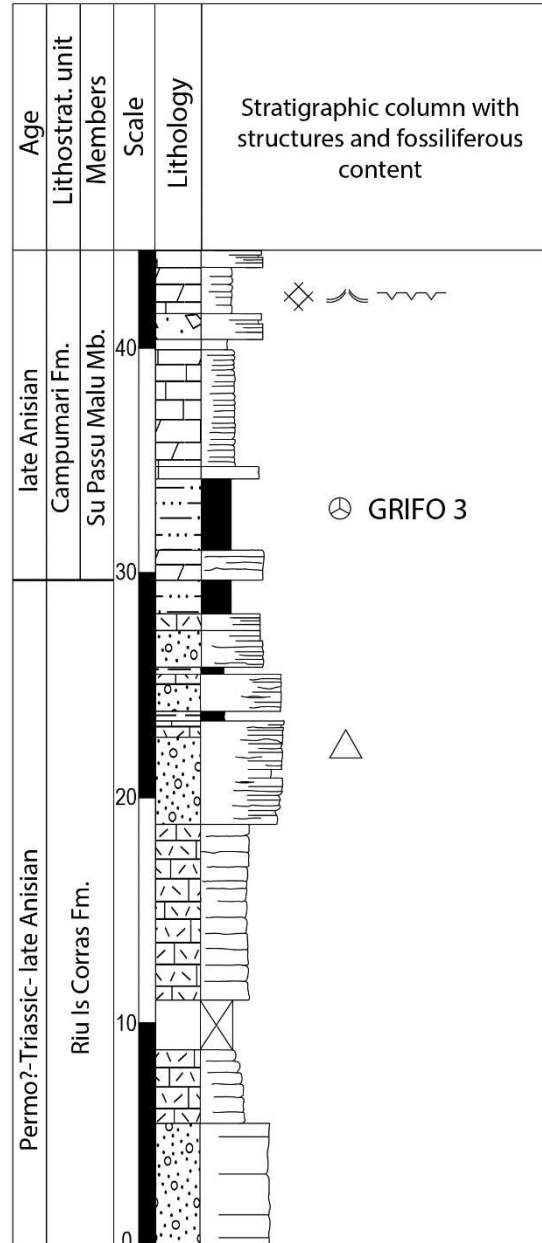


Fig. 4.13. Campumari stratigraphic section (see fig. 4.20 for legend).

Punta Tonnara (Sulcis)

The studied stratigraphic section is exposed at the rocky promontory of Punta Tonnara, SW of Porto Pino beach. It can be reached by taking the path directly connected to the car parks of the pier on the canal. The section is not very thick (about 15 meters from sea level) but well outcropping and complete and comprises the Punta Tonnara Fm. of the Muschelkalk Group of Sardinia.

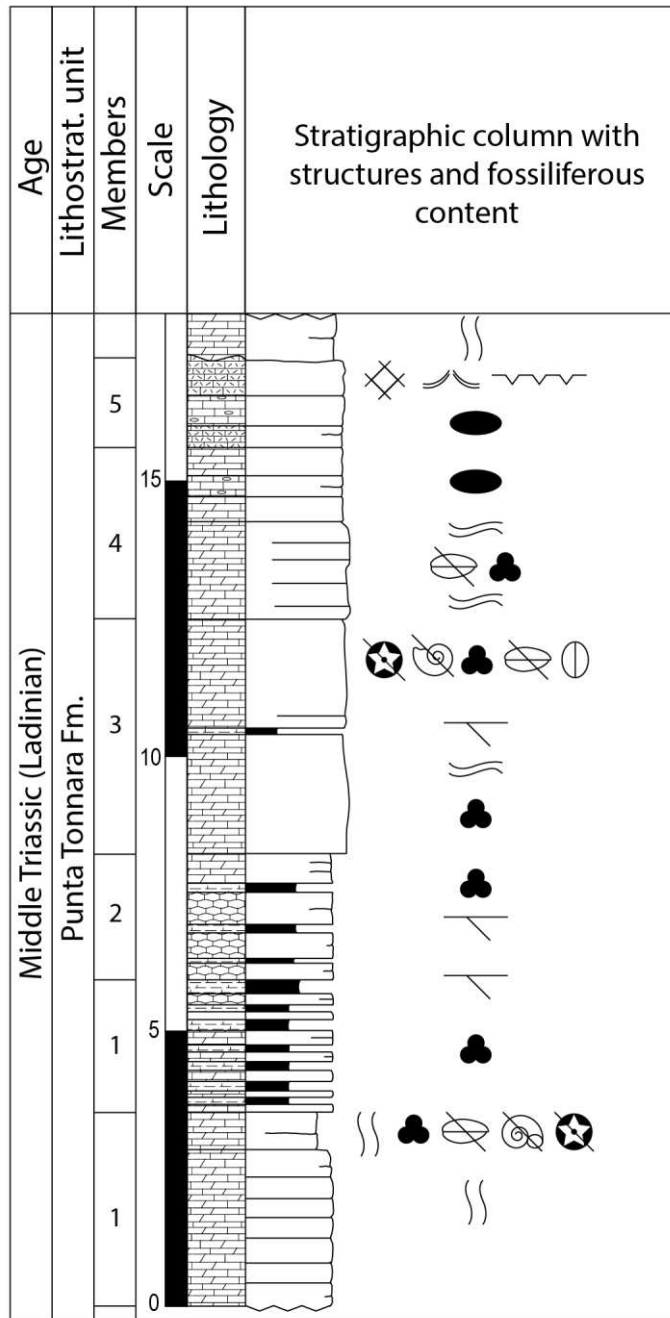


Fig. 4.14. Punta Tonnara stratigraphic section (see fig. 4.20 for legend).

Punta del Lavatoio (Nurra)

The Punta del Lavatoio section is the best exposed, accessible, and continuous section of the Punta del Lavatoio Fm. in the Nurra region. It is located at the city of Alghero, right at the end of the Alghero seafront. The measured overturned profile is about 40m thick and is bounded at the top and at the bottom by tectonic discontinuities.

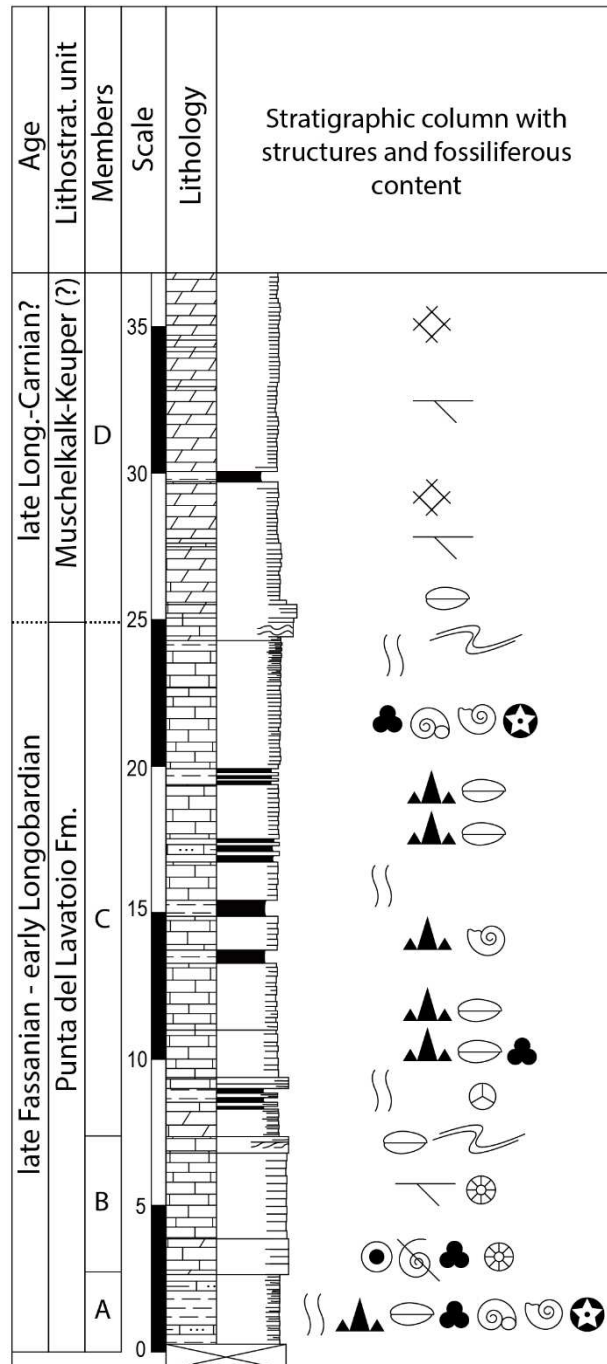


Fig. 4.15. Punta del Lavatoio stratigraphic section (see fig. 4.20 for legend).

Cala Viola (Nurra)

The Cala Viola-Torre del Porticciolo area is located approximately 20km NW of Alghero city. Here, the Lower-Middle Triassic succession crops out and it has been investigated and surveyed.

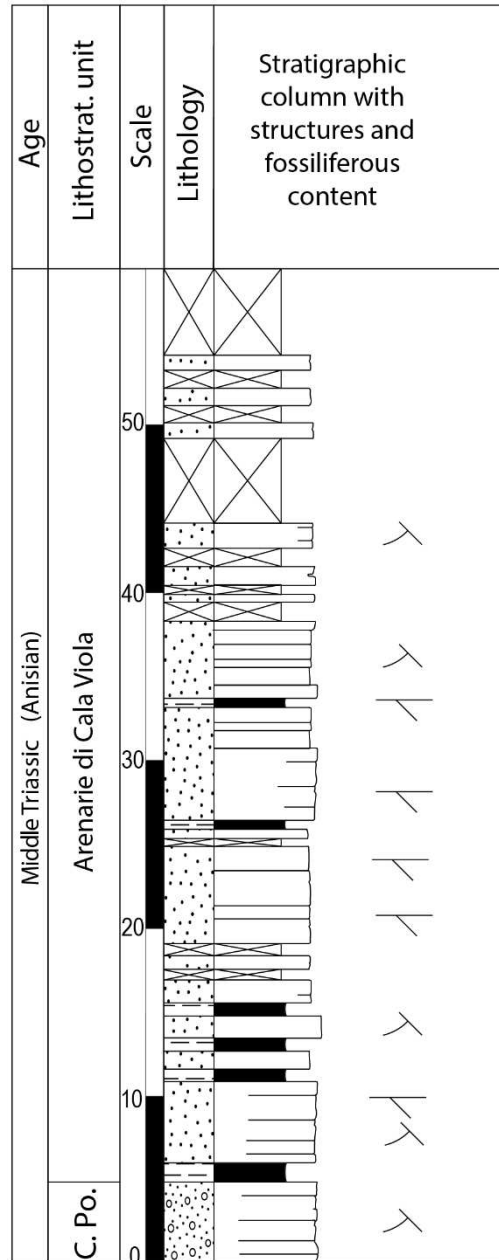


Fig. 4.16. Cala Viola stratigraphic section (see fig. 4.20 for legend).

Monte Fogheras (Nurra)

At the Monte Fogheras location, approximately 2km S of Alghero, there are two outcrops about 20m thick each, one located on the SP105 Alghero-Bosa and the other one on the rocky coast West to Spiaggia della Speranza. The complicated tectonic setting and the presence of folds and faults did not hamper a precise correlation between the two sections, which was performed based on association of facies and fossil content.

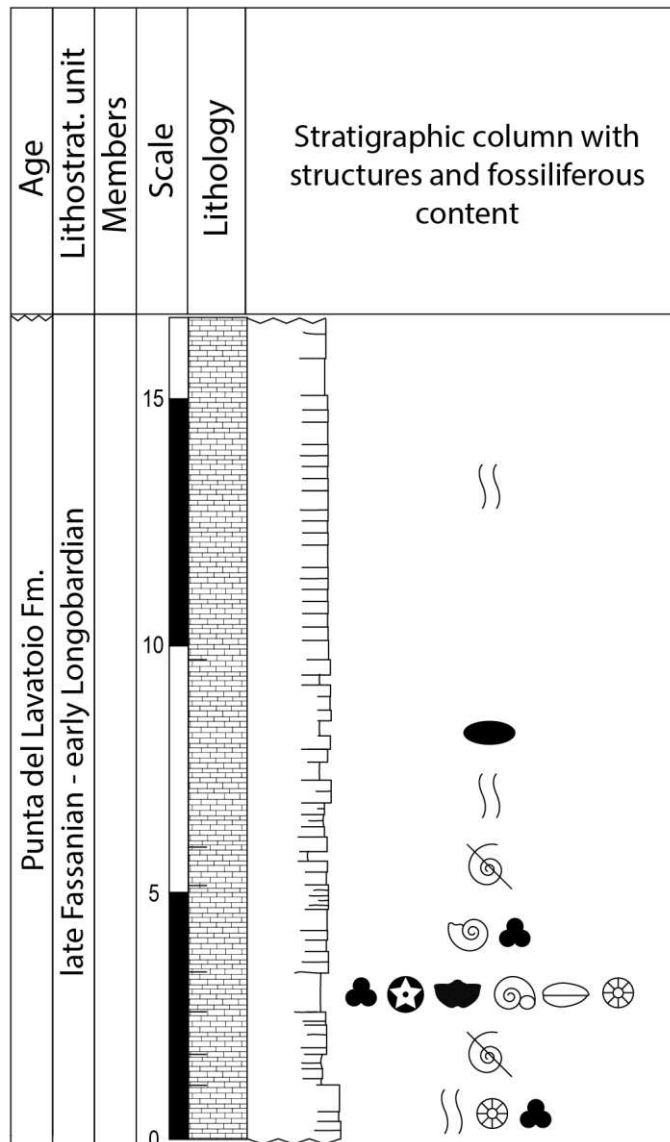


Fig. 4.17. Monte Fogheras stratigraphic section (see fig. 4.20 for legend).

Cala Bona (Nurra)

About 1km to the South, the succession of Cala Bona has been investigated. It crops out continuously for about 20m, ranging from the middle Permian p.p. to the Middle Triassic in facies Buntsandstein (Cala Viola Sandstones). The Middle Triassic in facies Muschelkalk (Punta del Lavatoio Fm.) crops out at the top, for a thickness of about 10m.

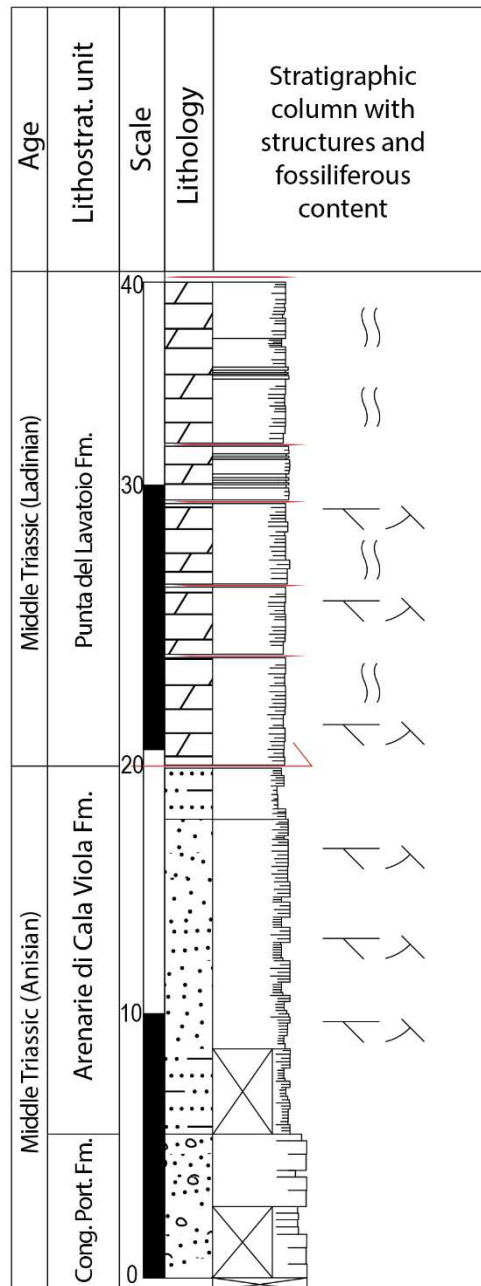


Fig. 4.18. Cala Bona stratigraphic section (see fig. 4.20 for legend).

Monte Santa Giusta (Nurra)

The Monte Santa Giusta hill is located about 25km N of Alghero, and it is approximately 250m high. At this location it is possible to observe the most complete Triassic succession of Sardinia, ranging from the Buntsandstein to the Keuper, which is interested by a NNE/SSW thrust that “doubles” the entire succession. A section of about 60m was here described.

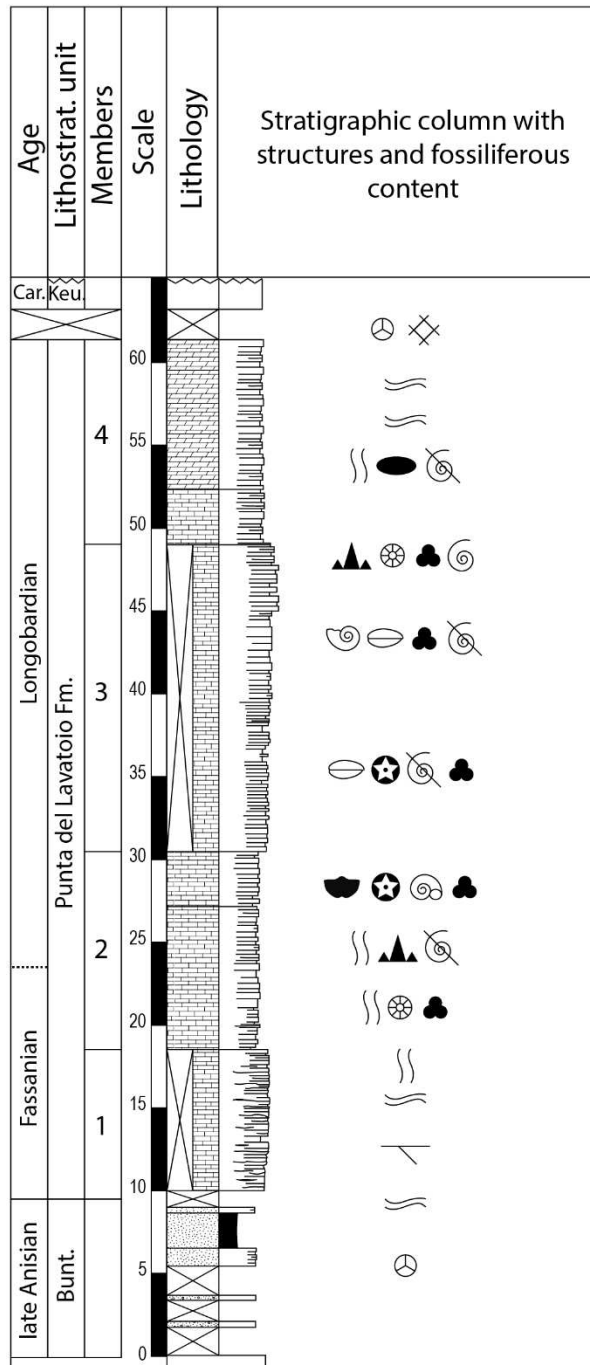


Fig. 4.19. Monte Santa Giusta stratigraphic section (see fig. 4.20 for legend).























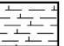
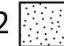
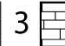












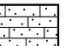

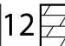
Structures and fossiliferous content					
	Pollens		Tepee structures		Halite
	Microbialites		Mudcracks		Rootlets
	Bivalves		Slumping		
	Gastropods		Lamination		
	Echinoderms		Evaporitic pseudomorphs		
	Calcareous algae		Singenic quartz		
	Foraminifera		Chert nodules		
	Brachiopods		Sparite veins		
	Conodonts		Planar lamination		
	Ammonoids		Collapse breccia		
Lithologies					
1		2		3	
4		5		6	
7		8		9	
10		11		12	
13		14		15	
16		17		18	

Fig. 4.20. Legend. Lithologies: 1) Marls 2) Sandstones 3) Limestones 4) crossbedded conglomerates, 5) Sandy limestone 6) Gypsum 7) Breccia, 8) Bedded sandstone 9) Dolomitic limestone 10) Interbedded sandstone and siltstone 11) Schist 12) Dolostone 13) Conglomerate 14) Crossbedded sandstone 15) Calcrete 16) Interbedded shale and silty limestone 17) Clay 18) Silty limestone.

5. Fossil content

5.1 Introduction

Different studies have been conducted throughout the years on the fossiliferous content of the Middle Triassic of Sardinia, and it is widely assessed and proved that it is overall scarce. As mentioned, Sardinia Triassic successions are scattered throughout the Island and are not exceptionally developed or well preserved, mainly due to the Alpine tectonics overprint. Nonetheless, the study of these fossil associations it is a powerful tool that can provide a precise age and palaeoenvironmental data for these successions. Furthermore, it can also provide insightful data to better understand the palaeogeographic evolution of the Island in the W Tethys domain during the Middle Triassic, which is nowadays a still debated matter.

In this chapter new and revised data are discussed, and the aim is to provide a better understanding and information about the biochronostratigraphy of these successions, as well as their palaeobiogeography and palaeoenvironment. To this end, the bibliography has been discussed and integrated with the new obtained data. Moreover, considerations on regional scale and to a broader interregional scale have been made with the neighbouring Iberian provinces.

The study and analysis have been conducted in collaboration with different specialists. For the microfloristic associations revision and analysis, Dr. Bienvenido Diez and Dr. Manuel Antonio Juncal Rosales, from the “Geociencias Marinas y Ordenación del Territorio” of the University of Vigo. For the ammonoids, Prof. Antonio Goy, from the Complutense University of Madrid, and for the bivalves and other microfossils Prof. Ana Marquez Aliaga, Prof. Sonia Ros Franch and Prof. Leopoldo Marquez from the University of Valencia. An important contribution consisting of different samples (thin sections, fossil specimen) and memories (field notes, personal notes), has been provided by Anna Gandin, retired Prof. from the University of Siena.

5.2 Methodology

5.2.1 Methodology for palynological study

A precise review of all the previous palynological publications on the Sardinian Anisian (Fig.5.1) was undertaken, and it was necessary to establish the validity of these data for our purposes.

The minimum conditions for considering the data valid were:

- 1) Correct figuration: lists of taxa without representation were not considered valid since there was no possibility of confirming or identifying the palynomorph.
- 2) Correct location: each palynomorph association must be referred to an exact position in the stratigraphic section in which it was sampled.

Using these premises, identifications from previous works that meet these requirements have been incorporated into the discussion, together with B. Diez's unpublished data and new obtained results.

Palynological analyses

In this study, have been included unpublished and revised results from Diez's PhD thesis (2000) collected in 1996 in the Escalaplano area: three samples (PC-2, PC-3 and PC-4) at the southern entrance to Escalaplano village (Escalaplano SW section, Figs. 5.1: 4 and 5.5) and another sample (PC-7.2) taken from the Arcu is Fronestas section, north of the same village (Figs. 5.1: 3 and 5.6). Three new samples (AIF-2, AIF-5, and AIF-9) were later collected in 2015 and 2016 fieldwork in the Arcu Is Fronestas section and another one (GRIFO 3) was collected from the Su Passu Malu section on the Campumari site (Campumari section, Figs. 5.1: 6 and 5.7).

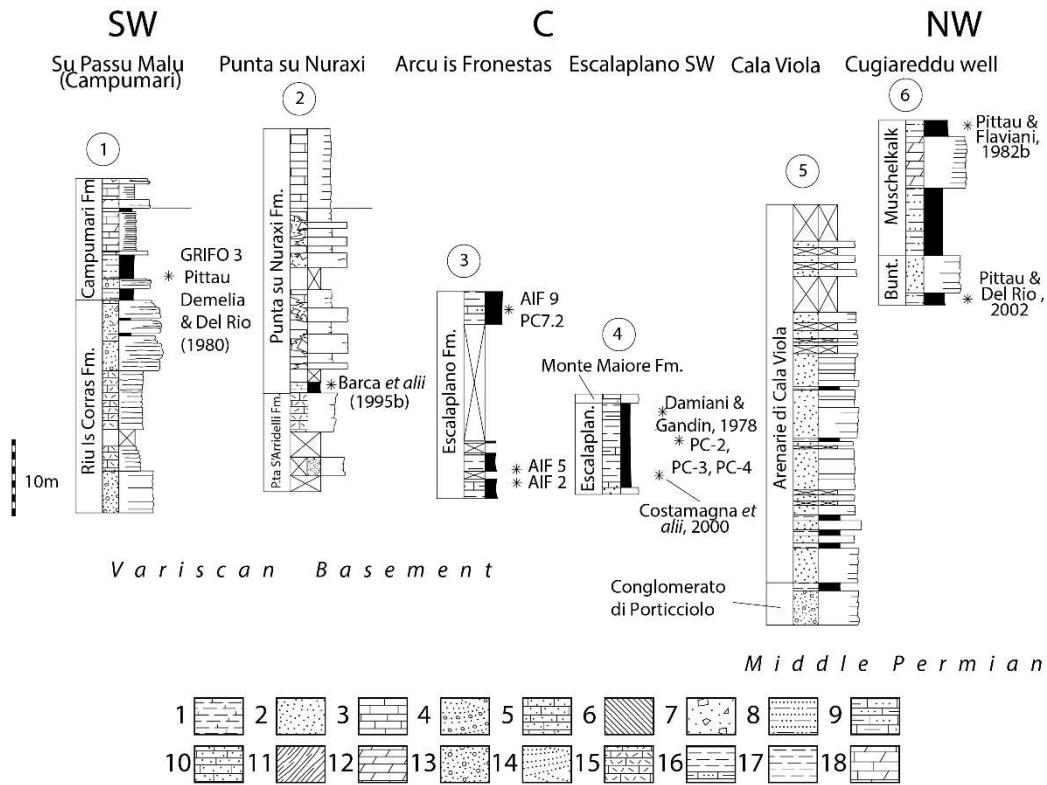


Fig. 5.1. Simplified sections, from SW to N, with * indicating the pollen samples dating the successions. Sections: 1) Su Passu Malu (Campumari, Iglesias), 2) Punta su Nuraxi (Arburese), 3) Arcu is Fronestas (Escalaplano), 4) Escalaplano SW (Escalaplano), 5) Cala Viola (Nurra), 6) Cugiareddu well (Nurra). Lithology: 1) Marls, 2) Sandstones, 3) Limestones, 4) crossbedded conglomerates, 5) Sandy limestone, 6) Gypsum, 7) Breccia, 8) Bedded sandstone, 9) Dolomitic limestone, 10) Interbedded sandstone and siltstone, 11) Schist, 12) Dolostone, 13) Conglomerate, 14) Crossbedded sandstone, 15) Calcrete, 16) Interbedded shale and silty limestone, 17) Clay, 18) Silty limestone. See Fig. 1 for locations.

Palynological samples were processed using HCl-HF-HCl classic attack techniques, as described by Wood et al. (1996), in the Geosciences Institute (CSIC-UCM), Madrid, and the Palynology Laboratory of the Department of Geosciences at the University of Vigo (AIF-2, AIF-5, AIF-9, GRIFO 3) and the Paleobotany Laboratory in the University Pierre et Marie Curie, Paris-6 (PC-2, PC-3, PC-4 and PC-7.2). A dispersing agent was added to facilitate filtering and sieving at 10µm. The palynological slides were studied under a Leica DM2000 LED, and the photomicrographs were taken with a Leica ICC50 W camera using x1000 magnification.

The slides are stored in the Palynology Laboratory in the Department of Geosciences at the University of Vigo.

5.2.2 Methodology for ammonoids, bivalves and other fossils

This study was based on a detailed review of available literature and palaeontological data from different collections of the Muschelkalk of Sardinia, but also on new unpublished palaeontological data. To support the biostratigraphic data a lithostratigraphic revision

completed with new data has been performed and shown in Figs. 5.2 and 5.3, where the main differentiated facies of the previously described Muschelkalk units of Sardinia have been compiled. A total of 9 field sections have been carried out (Fig. 5.4: 2-10). These sections show the main sedimentary characteristics recognized in the evolution of each of the lithostratigraphic units represented in them, and which are indicated by previously described facies.

Group	Fms and Sub-units			Symbol	Description	Fossil content	Interpretation	Location		
Sardinian Muschelkalk	Monte Maiore Fm Grey limestones Mb Punta su Nuraxi Fm Bruncu Zippiri Mb	Punta Tonnara Fm.	MCS7	reddish limestone bearing chert nodules, evaporitic pseudomorphs ^{3,4,7,9}	scarce: forams, bivalves, echinoderms 1,3,4,5,6,7,8,9,10,11	intertidal to supratidal	Porto Pino (Sulcis)			
			MCS6	grey limestones bearing chert nodules and lenses ^{1,5,6,7,8,9,10,11}						
			MCS5	well stratified limestones and dolomitic limestones with marl intercalations, bioturbations, arranged in shallowing upwards sequences ^{1,5,6,7,8,9,10,11}						
			MCS4	Blue-gray limestone, with reddish intercalation of bioclastic grainstones-packs-tones showing wavy and planar cross-lamination ^{1,5,6,7,8,10,11}				scarce: forams and bivalves 1,5,6,7,8,9,10,11	Middle ramp	Scivu-Is Arenas (Arburese) Monte Maiore (Sarcidano)
			MCS3	Thin layered, yellow dolostones, with collapse breccias and/or locally interested by halokinesis structures ^{1,2,5,6,7,8,10,11}						
			MCS2	massive grey dolostones with silicization processes ^{1,2,5,6,7,8,10,11,12}						
			MCS1	thin-bedded yellow dolostones with dark clays intercalations ^{1,2,5,6,7,8,10,11}				palynomorphs 1,2,5,6,7,8,10,11,12,14	Tidal flat	
	Bunt.	Escalaplano Fm.	Punta su Nuraxi Fm Case Pisano Mb Campumari Fm Grifoneddu Mb Campumari Fm Passu Malu Mb	BCS2	dark-reddish marls with clay intercalations or cavernous, calchified limestones ^{1,2,5,6,7,8,10,11}	palynomorphs 1,2,5,6,7,8,10,11,14	Intra-supra tidal (sabkha)	Scivu-Is Arenas (Arburese), Monte Maiore (Sarcidano), Campumari (Iglesiente)		
		Riu Is Corras Fm.		BCS1	Conglomerates and/or breccias that may evolve upwards to reddish sandstones with paleosols and caliches ^{1,2,5,6,7,8,10,11}	none	alluvial to transitional			
	References	Damiani & Gandin 1973 a,b,c (1); Coccozza & Gandin, 1976 (2); Martini et al. 1987 (3); Gandin et al. 1987 (4); Barca et al. 1997 (5); Barca et al. 1995b (6); Costamagna 1998 (7); Costamagna et al. 2000 (8); Costamagna, 1997a (9); Costamagna & Barca, 2000 (10); Barca & Costamagna, 2003 (11); Costamagna & Piros, 2022 (12); Stori et al., 2022 (13); Pittau & Del Rio, 1980 (14)								

Fig. 5.2. Facies association scheme for the Middle Triassic of the Central-Southern Sardinia Muschelkalk. Symbols for the facies associations: BSC1-2: Buntsandstein 1 and 2; MCS1-7: Muschelkalk of Central and Southern Sardinia 1 to 7.

Fm.	Sub-units					Symbol	Description	Fossil content	Interpretation	Location			
	1	3	18	18	8, 17 5								
Keuper		A	I1	L4	G4	Keuper	KN	dark brown dolostones with yellowish dolomitic marls intercalations and evaporitic pseudomorphs ^{2, 14, 18, 16}	low: forams, bivalves shell fragments ^{6, 9, 14, 17, 18}	Shallow lagoon - tidal flat - intertidal to supratidal	Cugiareddu well, Monte Santa Giusta, Alghero, Cala Viola		
		B					MN6	bioturbated grey limestones bearing chert nodules and lenses ^{3, 4, 9, 10, 11, 14, 15, 18, 20}			Monte Santa Giusta, Monte Fogheras		
Punta del Lavatoio Fm.	Gervilla bank					G3 U.C.S.	MN5	well stratified limestones and dolomitic limestones with marl intercalations, bioturbations, arranged in shallowing upwards sequences ^{3, 4, 9, 10, 11, 14, 15, 18, 20}	abundant: ammonoids, bivalves, echinoderms conodonts, forams ^{6, 9, 14, 17, 18}	Lagoon	Mid-outer ramp to inner ramp		
	Lower Nodosus Horizon	C	I2	L3									
	Rhizocorallium limestone	D											
	Massive Limestone	E		L2					MN4	grey limestones organized in metric thick strata, showing weak bioturbation, lamination and bioclasts ^{3, 4, 9, 10, 11, 14, 15, 18}		low: forams. bivalves and echinoderms ^{6, 9, 14, 17, 18}	Shoals
	Upper Nodosus Horizon	F	I3									abundant: ammonoids, bivalves, echinoderms conodonts, forams ^{6, 9, 14, 17, 18}	
	?Terebratulid bank	G		L1					MN3	nodular bioturbated limestones and marls containing reworked fossils ^{3, 4, 9, 10, 11, 14, 15, 18}			Mid-outer ramp
Bunt.						G2 U.C.I.	MN2	marly limestones and dolostones and bioturbated fossiliferous limestones with clays intercalations ^{3, 4, 5, 10, 11, 14, 15, 17, 18}	low: calcareous algae ^{10, 11, 14, 18}	Mid-outer ramp			
						G1 U.D.I.	MN1	nodular marly dolostones and grey, laminated dolostones ^{3, 4, 5, 10, 11, 14, 15, 17, 18}	low: palynomorphs ^{2, 4, 12, 19}	Intra-supra tidal (sabkha)			
						Bunt.	BN2	dark-reddish sandstones to claystones ^{5, 7, 10, 11, 13, 14, 16, 18, 21}	vertebrate and invertebrate tracks ²²	alluvial to transitional	Cugiareddu well, Monte Santa Giusta, Cala Bona, Cala Viola		
					Bunt.	BN1	Conglomerates and reddish sandstones ^{5, 7, 8, 10, 11, 13, 14, 16, 18, 21}	none					
References	Tornquist, 1904b, 1902 (1); Pomesano Cherchi, 1968 (2); Gandin, 1978b (3); Pittau & Flaviani, 1982a (4); Bartush, 1985 (5); Bagnoli et al. (1985a, b) (6); Gasperi & Gelmini, 1980 (7); Cherchi & Schroeder, 1985 (8); Posenato, 1995 (9); Carrillat, 1997 (10); Carrillat et al., 1999 (11); Pittau, 1999 (12); Costamagna & Barca, 2002 (13); Costamagna, 2002 (14); Posenato, 2002 (15); Cassinis et al., 2003 (16); Urlich & Posenato, 2002 (17); Knaust & Costamagna, 2012 (18); Stori et al., 2022 (19); Cuzzi, 1960 (20); Costamagna, 2012 (21); Citton et al., 2019 (22)												

Fig. 5.3. Facies association scheme for the Middle Triassic of Nurra, with main focus on the Punta del Lavatoio Fm facies association and sub-units. Symbols for the facies associations: BN1-2: Buntsandstein of Nurra 1 and 2; MN 1-6: Muschelkalk of Nurra 1 to 6; KN: Keuper Nurra

The reviewed most fossil-rich stratigraphic sections are mainly located in the Nurra and the Sarcidano-Gerrei regions, to the NW and E respectively (Fig. 5.4: 2, 4, 6). Three stratigraphic sections represent the Nurra region were revised and described according to a synthetic section: 1) Punta del Lavatoio, 2) Monte Fogheras, and 3) Monte Santa Giusta (Fig. 5.4: 2, 4, 6). For the latter area, the Cugiareddu well (Fig. 5.4: 1, Pomesano Cherchi, 1968) was

taken into consideration as a control due to its relevance for regional correlations. In the Sarcidano-Gerrei region, the Monte Maggiore stratigraphic section was reviewed and studied in detail.

The palaeontological data reviewed were mainly from Lovisato (1884); Tornquist (1901, 1902, 1904); Deninger (1907); Oosterbaan (1936); Gandin (1978, 1985, 1987); Damiani and Gandin (1973a, b, c); Bartusch (1985); Carrillat et al. (1999) Posenato (2002); Posenato et al. (2002); Urlichs and Posenato (2002) Knaust and Costamagna (2012), and Costamagna and Barca (2002). The collections are currently stored in the Departments of Botanic and Geology of the University of Valencia, and Department of Geodynamics, Stratigraphy and Paleontology of the Complutense University of Madrid. New data have also been obtained in recent fieldwork campaigns on the island (2016-2021).

The fossil cephalopods of NW Sardinia examined here (Figs. 5.11 and 5.12) come from: an outcrop on the road to Cala Bona (Capella della Esperanza, Level 4C) in the Monte Fogheras section (MF: 1 ammonoid) (Fig. 5.13); the Punta del Lavatoio section (PL) (Fig. 5.14) providing a total of 20 specimens (18 ammonoids and 2 nautiloids); the Monte Santa Giusta section (MSG) (Fig. 5.15) providing 3 specimens (2 ammonoids and 1 nautiloid). Almost all belong to the collections of the Dipartimento di Scienze della Terra, Siena University (Italy) and were collected by Prof. Anna Gandin.

The preservation quality of the specimens examined depend on the characteristics (dolomitization, tectonics...) of the studied section and has been especially important in the study of some ammonoids (Figs. 5.11 and 5.12). The ammonoid specimens found at the level of PL8 are relatively small, but presumably they are sub-adult or adult individuals. In these specimens, only part of the fragmocone and room chamber is preserved. In some cases, some of the internal whorls were not well filled with micritic sediment, possibly because of the existing fast sedimentation rate when they were buried.

Specimens from PL6 do not preserve the whole chamber, usually just part of it and the last partitions of the fragmocone at most, which seems to indicate that their burial was also rapid. In the Ceratiidae from MF, *Alloceratites* feature a well preserved fragmocone, up to 48 mm in size, while in the *Hungaritidae* from MSG, *Iberites* preserves part of the fragmocone. In specimen MSG619 (Fig. 11), probably from a ferruginous level with reworked elements, the fragmocone is preserved over a diameter of up to about 60 mm.

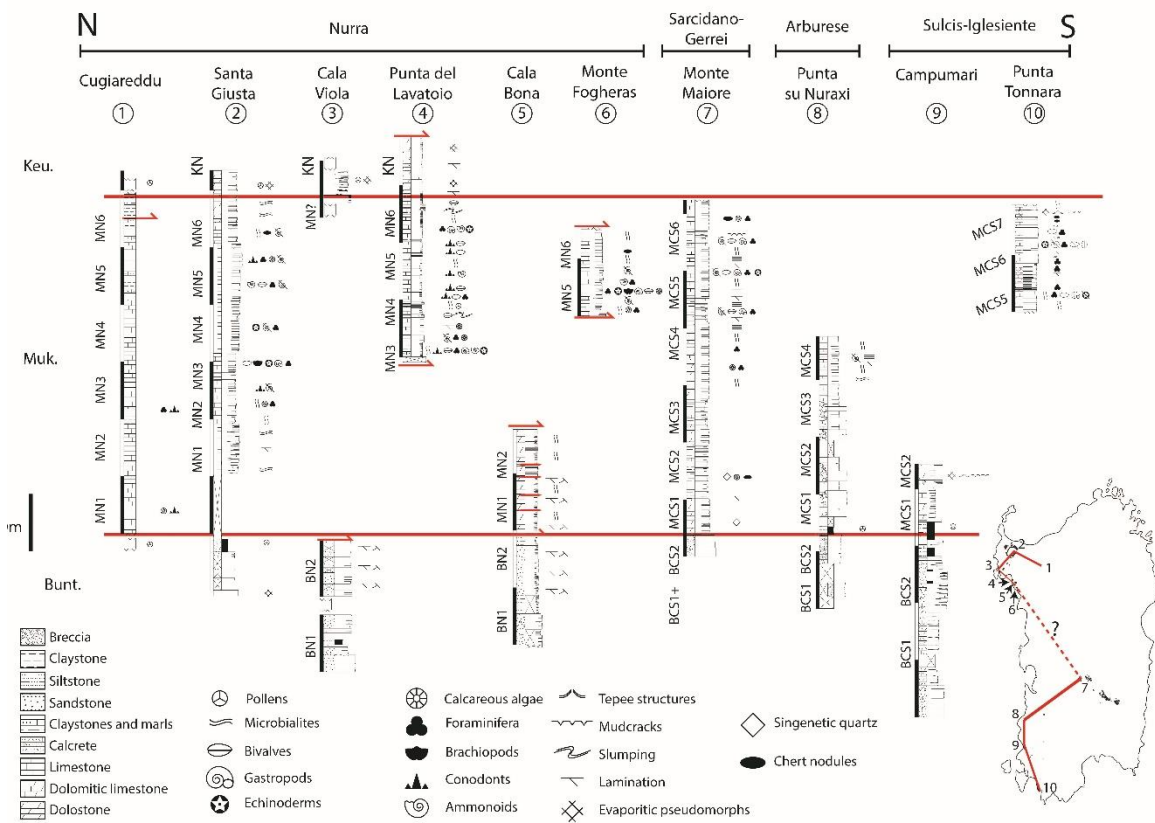


Fig. 5.4. Simplified key sections, from N to S, with their respective fossil content. 1) Cugiareddu well log, 2) Monte Santa Giusta, 3) Cala Viola, 4) Punta del Lavatoio, 5) Cala Bona, 6) Monte Fogheras, 7) Monte Maggiore, 8) Punta su Nuraxi, 9) Campumari, 10) Punta Tonnara. Red lines indicate the boundaries between Buntsandstein, Muschelkalk and Keuper facies.

5.3 Palynological content

5.3.1 Revision of palynological content and previous works

Various palynological studies have been previously analysed from different Anisian assemblages in Sardinia. Displaying the information in chronological order, a detailed review has been done for the following publications: Damiani and Gandin (1973c), Pittau Demelia and Del Rio (1980), Flaviani (1980), Pittau Demelia and Flaviani (1982 a, b), Frechengues et al. (1993), Barca et al. (1995b), Ronchi (1997), Costamagna et al. (2000) and Pittau and Del Rio (2002).

The first reference to the presence of a Middle Triassic pollen associations is found in Damiani and Gandin (1973c). These authors mentioned a productive sample collected in reddish marly layers just tens of metres southwest of the village of Escalaplano (level 2 of the section that corresponds to km 47.4 of the s.s. Nurri-Escalaplano, now SP10) (Fig. 5.5). At the time of the publication of Damiani and Gandin work, the palynological sample was being studied by Del Rio and, for this reason, the authors preliminarily only pointed out the presence of a continental floristic association of the Middle Triassic, represented mainly by gymnosperms.

The first formal palynostratigraphic study on the Anisian of Sardinia was done by Pittau Demelia and Del Rio (1980) for a sparse and poorly preserved palynological assemblage (see the complete list of taxa in Appendix 1) in the marly-clay levels of the upper part of member B (*sensu* Coccozza and Gandin, 1976) of the stratigraphic section of the Campumari outcrop, at km 1.7 between Funtanamare and Nebida (Fig. 5.7). These authors assigned to this sample a “lower Muschelkalk” age due to the presence of *Stellapollenites muelleri* (= *Hexasaccites muelleri*), *Minutosaccus crenulatus* and the genus *Triadispora*. Although the figures do not confirm all the taxonomic attributions, it is possible to suggest an Anisian *sensu lato* age through the correct identification of *Hexasaccites muelleri* (Visscher and Brugman, 1981; Brugman 1983, 1986; Diez 2000; Kürschner and Herengreen, 2010).

In Flaviani (1980), the palynostratigraphy from the subsurface of Nurra (Cugiareddu well, Fig.5.4: 6) was presented. This is an unpublished study which results were used at the time to make lithostratigraphic correlations between Triassic outcrops in Sardinia. In this work, new palynomorphs were described, and the authorship of these new species was attributed to P. Pittau in later papers (Pittau and Flaviani 1982; Pittau and Del Rio, 2002), and they were used only for Sardinian Triassic studies. Normally this type of publication should not be treated

in the context of a review as it is unpublished research, but due to its importance to the development of this thesis, it has been necessary to include it.

The samples used for palynostratigraphic studies in Flaviani's thesis were provided from a previous work by Pomesano Cherchi (1968) on the Cugiareddu well (Fig. 5.4: 6). These samples correspond to level 545 (sample 970 in Flaviani, 1980), ascribed to the Permian; levels 477 and 443 (samples 756 and 755 respectively, in Flaviani, 1980), which Pomesano Cherchi (1968) described as "Buntsandstein" but Flaviani attributed to the lower and middle Muschelkalk respectively; and, finally, level 429 (sample 754 in Flaviani, 1980) was described as lower Muschelkalk, and as upper Muschelkalk by Flaviani (1980).

From sample 970, Flaviani (1980) showed a poor assemblage (see the complete list of taxa in Appendix 1) and ascribed it to an inconclusive "Permian-Triassic" age through comparison with the Germanic Zechstein associations. However, the joint appearance of the guide taxa *Lueckisporites virkkiae*, typical of the middle and upper Permian, *Hexasaccites muelleri* that appears during the Anisian (Middle Triassic) and other Triassic taxa such as *Triadispora crassa*, *Enzonasporites leschikii* or *Illinites* sp., suggests an Anisian *sensu lato* age. The presence of a single specimen of *Lueckisporites virkkiae* would not be sufficient for any Permian affinity.

The next two associations of samples 756 and 755 (See the complete list of taxa in appendix 1), were included in "Zone A": this Zone would correspond to the lower and middle Muschelkalk interval (Anisian). It would be characterized by the high presence of *Hexasaccites muelleri* and *Triadispora crassa*, and the *Alisporites-Cuneatisporites-Sulcatisporites* bisaccate pollen morphogroup. Also, Flaviani differentiated two subzones: A1 (sample 756) and A2 (sample 755). Subzone A1 (lower Muschelkalk, Anisian) would be characterized by the presence of *Aratrisporites bulloides* (n. sp. in Flaviani, 1980), *Lunatisporites rhaeticus* and *Lunatisporites acutus*. Subzone A2 (middle Muschelkalk, Anisian) would be characterized by *Myriamsporites triassicus* (n. sp. in Flaviani, 1980) and *Aratrisporites distalirugulatus* (n. sp. in Flaviani, 1980), as well as *Krauselisporites cuspidus*, *Aratrisporites paraspinosus*, *Ellipsovelatisporites plicatus*, *Striatibieites aytugii* and *Angustisulcites klausii*. As it is explained in the next section, the presence of *Hexasaccites muelleri* would indicate an Anisian age for samples 756 and 755. Unfortunately, subdivisions A1 and A2 could not be justified using new species from levels that have not been geochronologically dated or correlated with other sources previously.

Flaviani (1980) assigned the fourth association (see the complete list of taxa in Appendix 1), referred to sample 754 (429 m.), to the upper Muschelkalk ("Zone B", Anisian-Ladinian transition), based on the absence of *Hexasaccites muelleri* and the presence of *Ovalopollis pseudoalatus*. However, following the adopted methodology, it is not possible to endorse this data, since it does not accept the absence criterion.

Pittau Demelia and Flaviani (1982b) included a partial publication of the study by Flaviani (1980) of the Cugiareddu well. However, the featured palynomorphs are not correctly referenced, and neither these authors show photos of all the listed taxa, nor any references to the studied samples. It can be deduced, solely from the wording of the text, that the specimens are the same, and the new species described in Flaviani (1980) already appear as Pittau in Flaviani, 1980. Therefore, the same considerations made for Flaviani (1980) can be applied to Pittau Demelia and Flaviani (1982b). Some photos of taxa are included, without mentioning what level they correspond to. In this case, it allows to confirm the existence of *Hexasaccites muelleri* and the possible classification of *Triadispora crassa* and *Prodiploxypinus gracilis*, which reaffirms the notion that nothing can be said about those levels containing *H. muelleri* that does not correspond to the Anisian *sensu lato*.

Subsequently, new palynological data (see the complete list of taxa in Appendix 1) were described from the Punta del Lavatoio section (Fig. 1A) by Pittau Demelia and Flaviani (1982a). The authors sampled different dark clay layers located in the "Lithofacies C" (Costamagna, 2002). Due to the presence of the morphological group *Alisporites-Sulcatisporites-Cuneatisporites*, *Triadispora crassa*, *Aratrisporites* sp., *Aratrisporites paraspinosus*, *Camarozonosporites cf. rudis*, *Polypodiaceoisporites* sp. and *Verrucosisporites* sp, in sample 1275, coming from one of these levels, it was possible to correlate it with subzone A2 of the Cugiareddu well (Flaviani 1980; Pittau and Flaviani 1982). With this correlation, the authors pointed out that, as in the A2 subzone defined in the Cugiareddu well (not in Punta del Lavatoio), *Stellapollenites muelleri* (= *Hexasaccites muelleri*) occurs, and so this level can be ascribed to the late Anisian, and the upper part to the early Ladinian due to the presence of *Diplopora*. This reasoning is not viable under our methodology because photos of only seven taxa are presented (*Aratrisporites* sp., *Chordasporites singulicorda*, *Concavisporites* sp., *Polypodiaceoisporites* sp., *Striatoabieites* sp., *Triadispora plicata* and *T. suspecta*). Furthermore, the determination is based on a taxon that would not even have been present in the sample.

Subsequently, Fréchenes et al. (1993) described palynological results for a sample (see the complete list of taxa in Appendix 1) in a Muschelkalk dark clay level, indirectly included in the Escalaplano section, which is also comparable to those mentioned above by Damiani and Gandin (1973a) (Fig. 5.4: 4). The authors suggested a Ladinian age to this sample due to the presence of a large amount of *Triadispora* spp., numerous *Alisporites*, *Pityosporites neomundanus* and *Cycadopites*, the absence of *Ovalipollis* and Circumpolles and the low quantity of spores, except for *Aratrisporites saturni* and *A. fisheri*. In the same work, the authors compared this assemblage with similar ones in the Pyrenean ranges and with the association described in Pittau Demelia and Flaviani (1982a) for the section of Punta del Lavatoio. Of all the taxa referenced, only the photo of *Heliosaccus dimorphus* is published. This does not allow to conclude that the classification is correct and, because of the lack of characterization of the forms presented in that work, it was preferred not to attribute these levels to the Ladinian.

In Barca et al. (1995b), a well-preserved association (see the complete list of taxa in Appendix 1) is yielded by the basal marly levels of the carbonate Case Pisano Member (Punta Su Nuraxi Formation, Costamagna and Barca, 2002) in the Scivu-Is Arenas section (Fig. 5.4: 2). The authors reported a very diverse palynomorph content with fifty-three different taxa, but photos of only twenty-six of these are shown. Due to the presence of *Triadispora crassa*, together with *Illinites chitonoides*, *Angustisulcites klausii*, *Microcachrydites fastidioides*, *Stellapollenites thiergartii* (= *Hexasaccites muelleri*), *Perotriletes minor* and *Cristianisporites triangulatus*, they consider that the association would be Pelsonian-Illyrian in age and would be correlated with the “phase Mu-1” of Dockter et al. (1980). Opportunely, Barca et al. (1995b) illustrates some taxa, but not all, to evaluate the identifications presented. We would change, according to our interpretation of the original diagnoses, some of the published identifications, including *Aratrisporites* sp. for *Cerebropollenites mesozoicus* Nilsson 1958, *Chordasporites singulichorda* Klaus 1964 for *Microcachrydites doubingeri* Klaus 1964, *Cuneatisporites radialis* Leschik 1955 for *Angustisulcites* sp., *Giggiospora escalaplanoi* Pittau Demelia 1980 for *Enzonalsporites* sp., *Myriamsporites triassicus* Pittau Demelia in Flaviani 1980 for *Paleospongisporis europaeus* Schulz 1965, *Perotriletes minor* (Mädler) Antonescu & Taugourdeau Lantz 1973 for *Perotriletes* sp., *Stellapollenites muelleri* (Reinhardt & Schmitz) Pittau Demelia 1983 (= *Hexasaccites muelleri*), *Striatoabieites aytugii* Visscher 1966 for *Strotersporites richteri* (Klaus) Wilson 1962, *Triadispora maxivestita* Pittau Demelia in Flaviani 1980 for *Triadispora* sp., *Varirugosisporites roeticus* (Schulz) Pittau Demelia in Flaviani 1980 for *Verrucosisporites* sp., *Verrucatosporites cugiarreddu* Pittau Demelia in Flaviani 1980 for

Verrucosisporites thuringiacus Mädlér 1964. This new interpretation of the data has allowed to specify the previous dating.

In Ronchi (1997), two palynological associations (see the complete list of taxa in Appendix 1), from samples collected in levels known as the “Buntsandstein of the Triassic basin of Escalaplano”, were studied by Pittau. The ARPE-02 sample was obtained at the northeast of the basin (Arcu Is Fronestas) along the Escalaplano-Perdasdefogu road and the ARPE-04 sample at the southern entrance to Escalaplano village (Fig. 5.4: 4). Both levels were attributed to the Anisian by Pittau (A. Ronchi *Pers. Com.*), as the presence of *Stellapollenites thiergartii* is referable to Anisian. Unfortunately, it is not possible to make any assessment as the work does not present any photos of the taxa mentioned.

In order to formalize the Escalaplano Fm., Costamagna et al. (2000) described three levels with palynomorphs (see the complete list of taxa in Appendix 1) of two different sections of the “lithofacies B”: two levels in a section (nowadays covered by a road wall) not far to the southern entrance of the village of Escalaplano, along the Escalaplano-Orroli road, 2 and 4 m from the underlying contact on the Palaeozoic basement, and the third level along a cut of the Escalaplano-Perdasdefogu road in the locality of Arcu Is Fronestas. Based on the presence of *Stellapollenites muelleri*, *Cristianisporites triangulatus* and *Dyupetalum vicentinense*, these levels were considered late Anisian (Pelsonian), correlating with the “vicentinense-muelleri” phase, according to Brugman (1986), Visscher and Brugman (1981) and Van Der Eem (1983), and the Escalaplano Fm is thus upper Anisian-basal Ladinian.

Observation of the photographs allows to verify the referenced taxa and propose a new attribution for some of them, as appropriate. Among others (see Appendix 1), for us, the form attributed to *Dyupetalum vicentinense* can also be *Cristianisporites triangulatus*. According to the authors, the coexistence of these taxa would justify a late Anisian (Pelsonian-Illyrian interval) to early Ladinian attribution. Unfortunately, it is impossible to know the stratigraphic relationship between the studied samples and their relative position, since these authors do not provide separate lists and do not attribute their published photos to specific sampled levels.

The last published reference would be Pittau and Del Rio (2002), in which the authors publish a compilation of all the previous palynostratigraphic works of the Permo-Triassic sequences of Sardinia. For the Scythian to early Anisian interval, the authors refer to a listed association (with only three photos, however) consisting of *Enzonasporites leschikii* Mädlér 1964, *Microcachrydites fastidiosus* Jansonius 1962, *Sulcatisporites splendens* Leschik 1955,

Triadispora crassa Klaus 1964, cf. *Stellapollenites muelleri* (Reinardt & Schmitz) Pittau Demelia 1993 and *Voltziaceosporites heteromorpha* Klaus 1964. This is the same association first described by Flaviani (1980) and related to the Permian in Pittau Demelia and Flaviani (1982b) for level 545 (sample 970). In this work, the authors reevaluate this pollen association and consider a possible Olenekian (late Scythian) or, more probably, early Anisian due to the impossibility of affirming the identification of *Stellapollentes muelleri* (= *Hexasaccites muelleri*). However, *Voltziaceasporites heteromorpha* made its first appearance in the late Olenekian, according to Brugman (1986). This deduction based on the criterion of absence is not acceptable, and therefore the attribution of this level to the Scythian is similarly unacceptable. The following section of this compilation is dedicated to the Anisian and it repeats the arguments presented in Pittau and Flaviani, (1980), Barca et al., (1995b), Pittau et al., (2000) and Costamagna et al. (2000).

5.3.2 New and revised palynological data

The original palynological slices analyzed in Diez (2000) have been revised and re-photographed with better image capture systems, offering a slightly more comprehensive taxa list. These slices correspond to samples PC-2, PC-3, PC-4 (“Escalaplano SW”, Fig. 5.5) and PC-7.2 (“Arco is Fronestas” section, Fig. 5.6).

Palynological analyses from different Sardinian outcrops, including the Escalaplano section, have recently been performed. New productive samples (AIF-2, AIF-5 and AIF-9) were obtained in the “Arco is Fronestas” section (Fig. 5.6) to complete the information of Diez (2000). Moreover, a new sample was obtained in Su Passu Malu (Campumari) (Grifo 3, Fig. 5.7).

Synthetic plates of all the samples studied are presented (Plate 5.1 and Plate 5.2).

Escalaplano SW

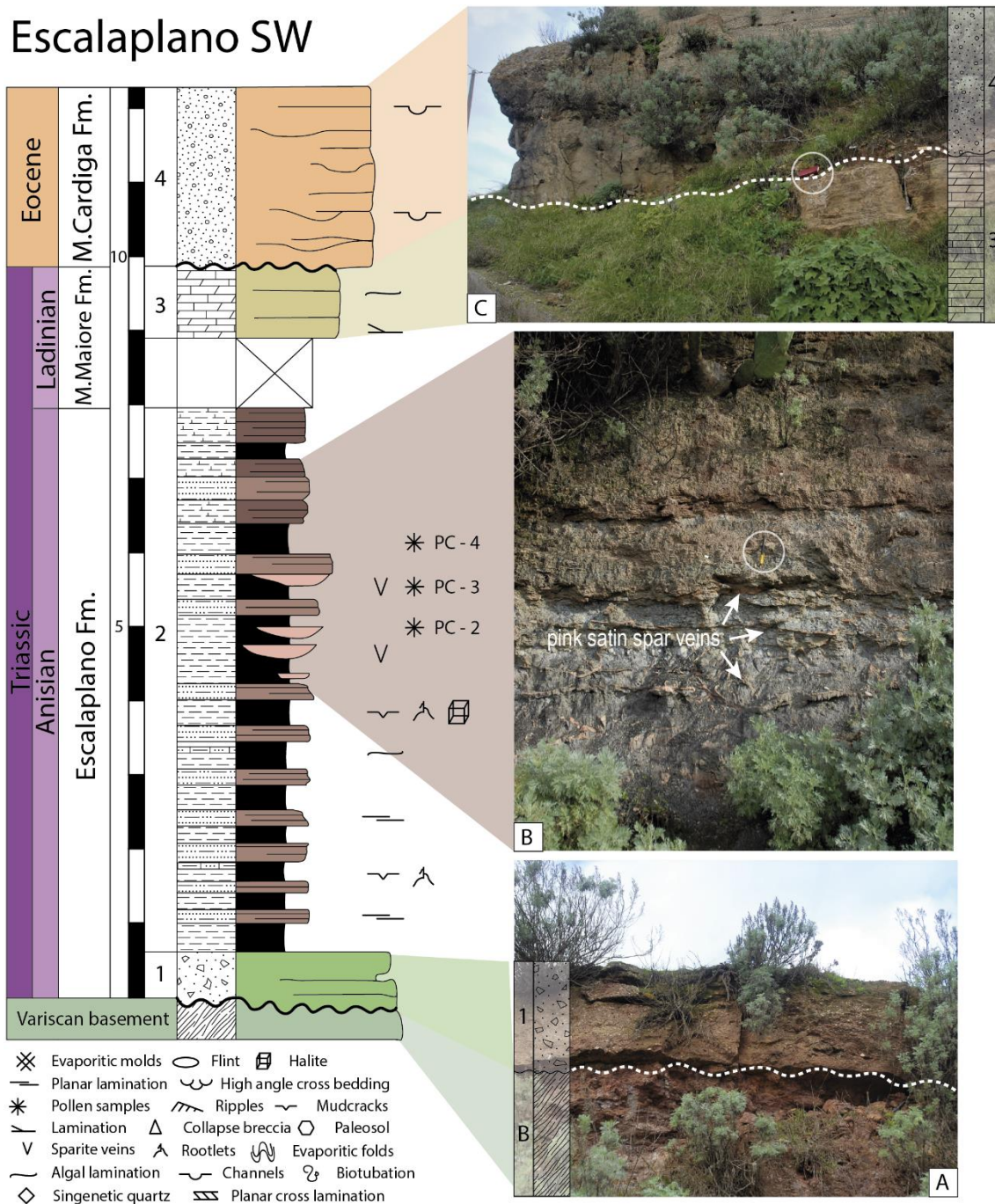


Fig. 5.5. Stratigraphic section of the outcrop located at the Escalaplano SW entrance. A) Basal reddish conglomerates lying over the Variscan basement; B) Anisian satin spar-bearing marly argillites with pollen sample site (asterisk); C) contact between the Muschelkalk and the Eocene conglomerates. See also Figure 2 to complete the legend.

Arco Is Fronestas (Escalaplano)

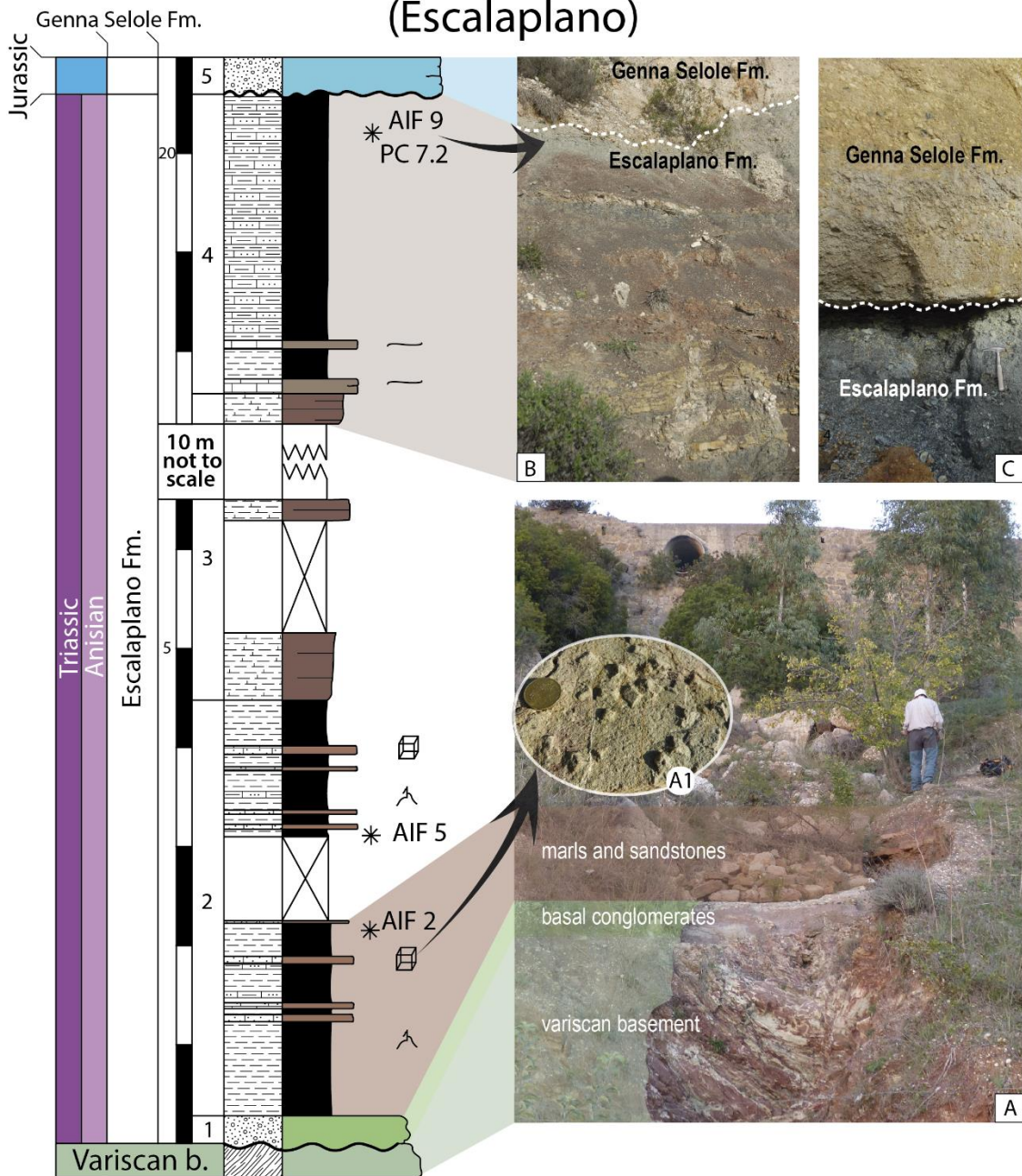


Fig. 5.6. Arco Is Fronestas section. A) basal reddish conglomerate lying over the Variscan basement's schists; A1) halite casts; B) dark gray claystones and marly sandstones C) black claystones to yellowish marly claystones. See also Figure 2 and 4 to complete the legend.

Su Passu Malu (Campumari, SW Sardinia)

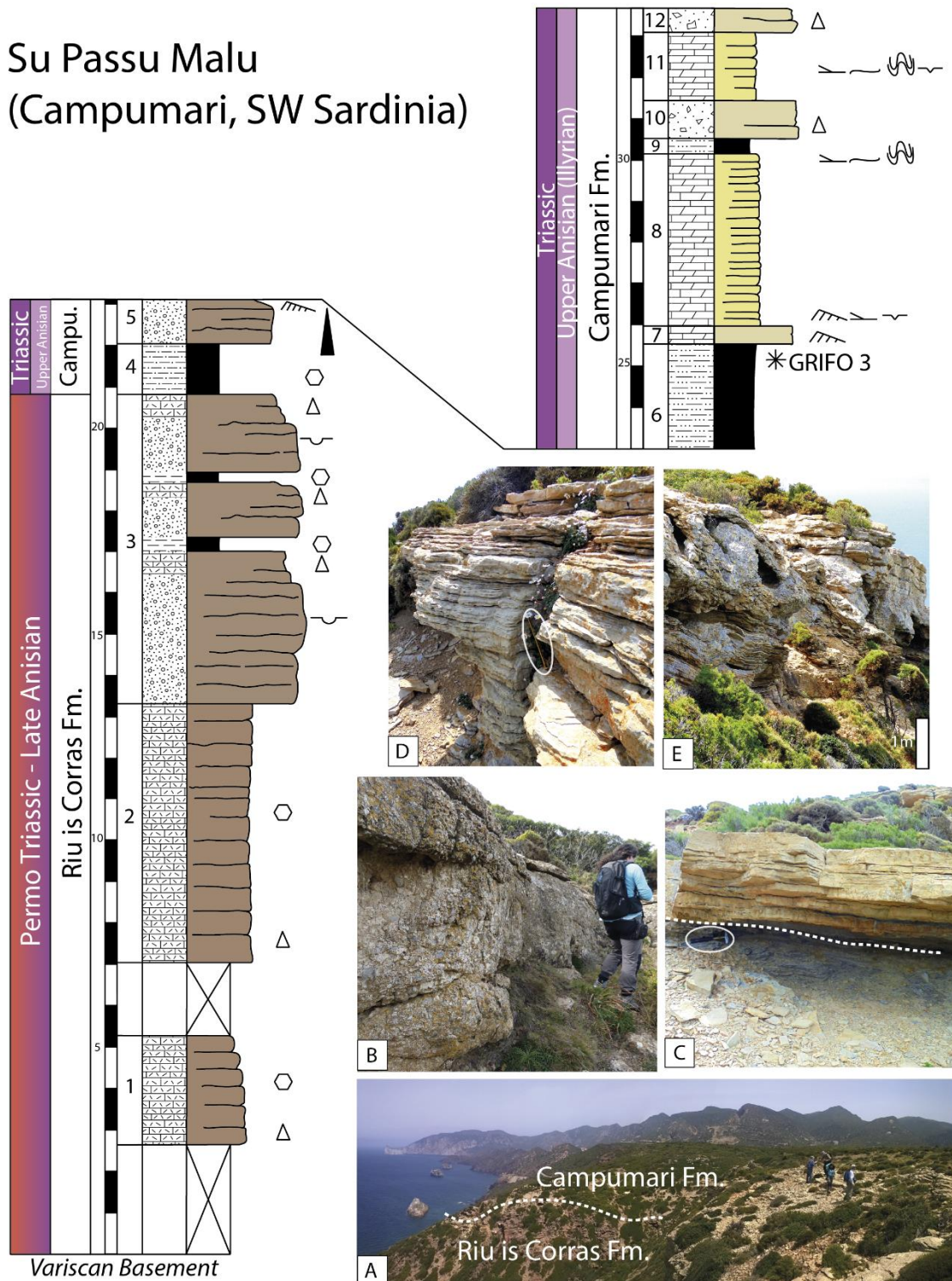


Fig. 5.7. Campumari section. A) Panoramic view of the Campumari - Coremò plateau; B) conglomerates of the Riu Is Corras Formation; C) detail of the dark gray mudstones overlain by the yellow, laminated dolostones; D) detail of the yellow, laminated dolostones; E) alternation of breccias and dolostones from the upper part of the Grifoneddu Member. See also Figure 2 and 4 to complete the legend.

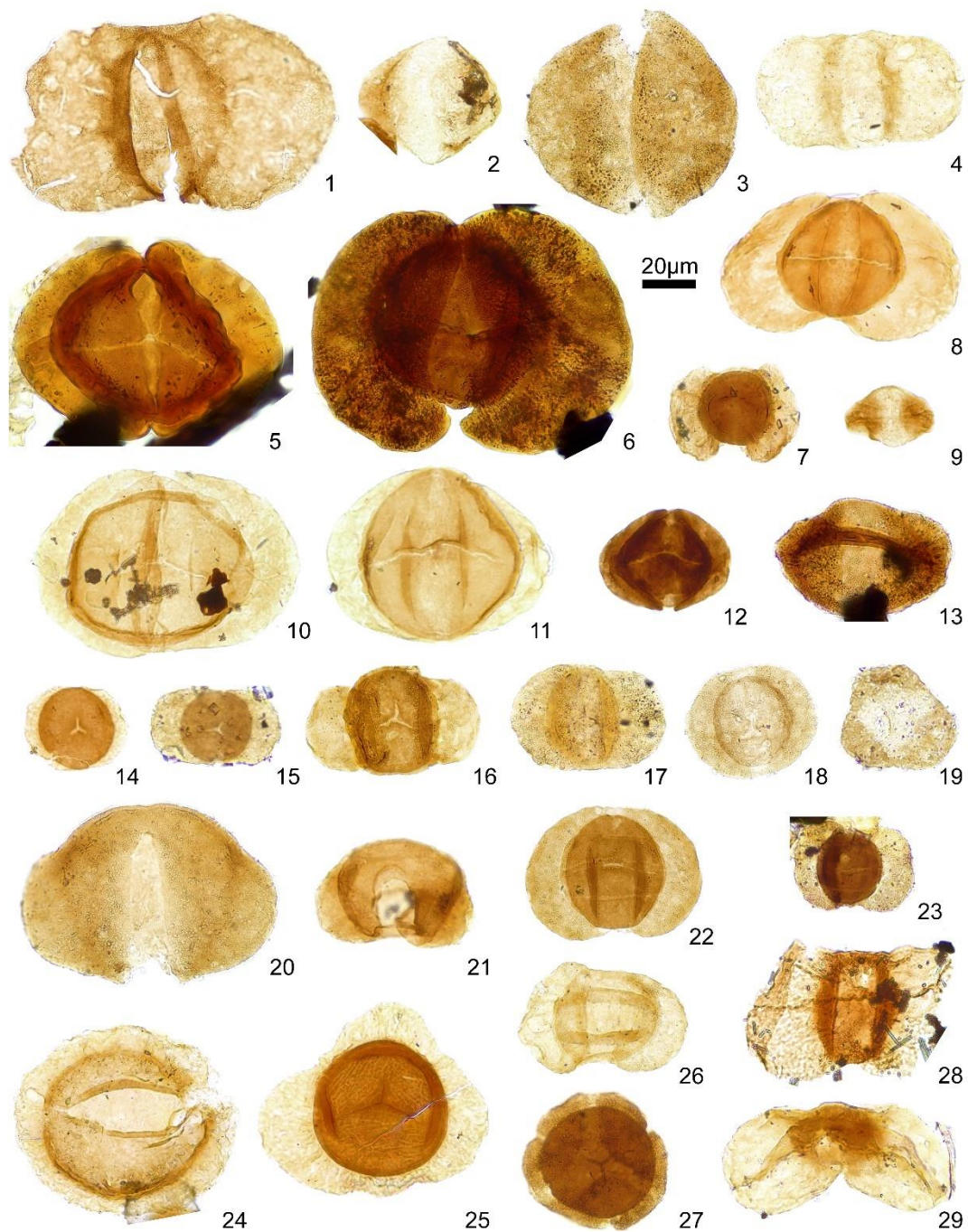


Plate 5.1. Synthesis of the palynomorphs found in the Sardinian sections. Scale bar: 20 μm . The acronym indicates section-sample_number slide_England Finder slide coordinates. **1.** *Alisporites magnus* Jain 1968. PC-3_B_03_K234. **2.** *Alisporites grauvogeli* Klaus, 1964. AIF-5_04_N151. **3.** *Alisporites opii* Daugherty, 1941. PC7.2_01_U424. **4.** *Alisporites* sp. PC-4_B_03_K380. **5.** *Angustisulcites klausii* (Freudenthal) Visscher, 1966. PC-4_B_01_M324, **6.** *Angustisulcites grandis* (Freudenthal) Visscher, 1966. PC-2_B_01_V350. **7.** *Angustisulcites* sp. GRIFO3_01_J052. **8.** *Angustisulcites gorpji* Visscher, 1966. AIF-5_02_H193. **9.** *Vitreisporites* sp. AIF-5_04_M040. **10.** *Illinites chitonoides* Klaus, 1964. AIF-5_04_L211. **11.** *Illinites kosankei* Klaus, 1964. AIF-5_01_R370, **12.** *Illinites* sp. AIF-5_01_N221. **13.** *Chordasporites singulichorda* Klaus, 1960. PC-2_B_01_H402. **14.** *Triadispora plicata* Klaus, 1964. AIF-5_02_L363. **15.** *Triadispora crassa* Klaus, 1964. PC-3_02_O414. **16.** *Triadispora falcata* Klaus, 1964. PC-04_B_03_O400. **17.** *Triadispora staplinii* (Jansonius) Klaus, 1964. PC7.2_02_F360. **18.** *Triadispora suspecta* Scheuring, 1970. PC-3_B_01_D274. **19.** *Triadispora* sp. (Three-saccated anomalous form) PC-3_01_U434. **20.** *Klausipollenites schaubergeri* (Potonié and Klaus) Jansonius, 1962, **21.** *Klausipollenites* sp. AIF-5_01_M480. **22.** *Lunatisporites acutus* Leschik, 1955. PC-4_B_03_X480. **23.** *Lunatisporites* cf. *puntii* Visscher, 1966. PC-3_01_O313, **24.** *Heliosaccus* cf. *dimorphus*. Mädlér, 1964. PC-4_B_02_Q411. **25.** *Cristianisporites triangulatus* Antonescu, 1969. AIF-5_02_R500. **26.** *Lunatisporites noviaulensis* (Leschik) de Jersey, 1979. **27.** *Hexasaccites muelleri* (Reinhardt and Schmitz) Adloff and Doubinger, 1969 (= *Stellapollenites thiergartii* (Mädlér) Clement-Westerhof et al. 1974). PC-2_B_04_W351. **28.** *Platysaccus leschikii* Hart, 1960. AIF-2_01_S273, **29.** *Platysaccus papilionis* Potonié and Klaus, 1954. PC-3_B_03_M352.

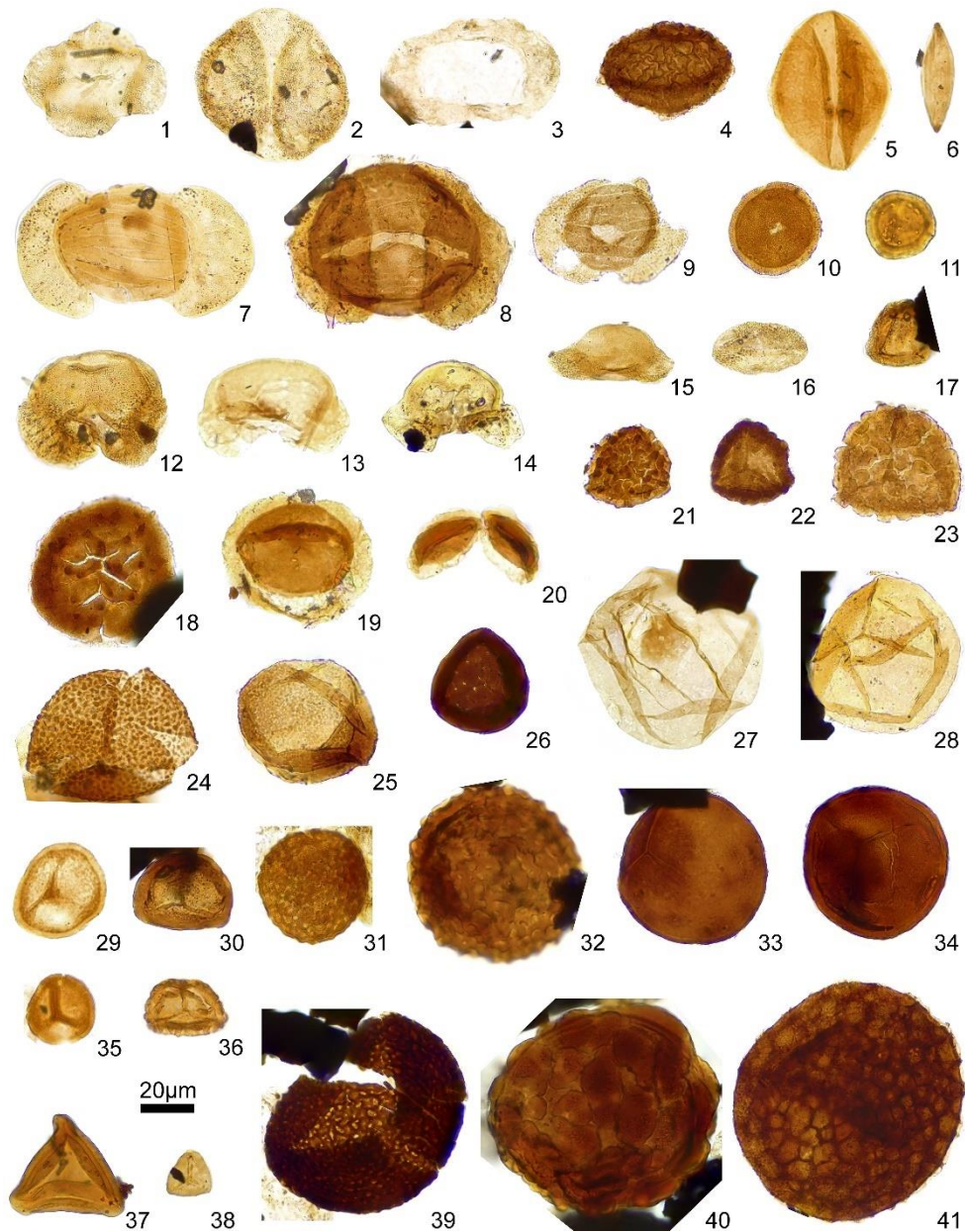


Plate 5.2. Synthesis of the palynomorphs found in the Sardinian sections. Scale bar: 20 µm. The acronym indicates section-sample_number slide_England Finder slide coordinates. **1.** *Bascanisporites* sp. GRIFO3_02_E154. **2.** *Brachisaccus neomundanus* (Leschik) Mädler, 1964. **3.** Cf. *Cordaitina* sp. GRIFO3_02_F123. **4.** *Cerebropollenites mesozoicus* Nilsson, 1958. PC-3_B_02_H310. **5.** *Chasmatosporites* sp. AIF-5_03_H401. **6.** *Cycadopites* sp. AIF-5_01_M443. **7.** *Striatoabieites aytugii* (Visscher) Scheuring, 1978. GRIFO3_01_L411. **8.** *Strotersporites jansonii* Klaus, 1963. PC-3_B_02_T340. **9.** *Striatopodocarpidites cancellatus* (Balme & Hennelly) Hart, 1963. PC-3_B_01_U232. **10.** *Enzonalaspores vigens* Leschik, 1955. PC-3_B_03_N404. **11.** *Paracirculina* sp. AIF-9_04_C173. **12.** *Microcachrydites doubingeri* Klaus, 1964. GRIFO3_03_N163. **13.** *Microcachrydites fastidioides* (Jansonius) Klaus, 1964. AIF-5_01_S192. **14.** *Microcachrydites sittleri* Klaus, 1964. PC7.2_01_X352. **15.** *Microcachrydites* sp.1. GRIFO3_01_R180. **16.** *Ovalipollis ovalis* (Krutzsch) Scheuring, 1970. GRIFO3_01_E052. **17.** *Duplicisporites granulatus* (Leschik) Scheuring, 1970. GRIFO3_04_K353. **18.** *Kraeuselisporites* sp. PC-3_B_03_K294. **19.** *Aratrisporites* cf. *granulatus* (Klaus) Playford and Dettmann, 1965. AIF-5_02_O301. **20.** *Aratrisporites* sp. AIF-5_01_O094. **21.** *Uvaesporites* sp. PC-3_B_03_L291. **22.** *Rewanispora vermiculata* Antonescu and Taugourdeau-Lantz, 1973. PC-2_B_04_W343. **23.** *Rewanispora* sp. PC-3_B_01_T342. **24.** *Cyclotriletes granulatus* Mädler, 1964. PC-3_B_03_R452. **25.** *Cyclotriletes oligoanifer* Mädler, 1964. PC-3_B_02_H270. **26.** *Limbosporites* sp. PC-2_B_03_Q274. **27.** *Calamospora tener* (Leschik) Mädler, 1964. PC-4_B_02_E343. **28.** *Calamospora* sp. PC-2_B_01_M520. **29.** *Densoisporites neiburgii* (Schulz) Balme, 1970. AIF-5_03_C430. **30.** *Densoisporites* sp. PC7.2_01_W391. **31.** *Microreticulatisporites gallii* Adloff and Doubinger, 1969. PC-4_B_02_K250. **32.** *Reticulatisporites* sp. PC7.2_01_R410. **33.** *Punctatisporites fungosus* Balme, 1963. PC-3_B_01_P414. **34.** *Punctatisporites triassicus* Schulz, 1964. PC-3_B_03_N281. **35.** *Camarozonosporites* sp. AIF-5_04_J353. **36.** *Annulispora* sp. GRIFO3_02_J401. **37.** *Dictyophyllidites mortonii* (de Jersey) Playford and Dettmann, 1965. GRIFO3_01_M420. **38.** *Deltoidospora* sp. GRIFO3_01_K262. **39.** Unidentified spore PC-4_B_01_Q292. **40.** *Verrucosisporites thuringiacus* Mädler, 1964. PC7.2_02_U432. **41.** *Paleospongisporis europaeus* Schulz, 1965. PC-2_B_01_E472.

The complete palynological assemblages are shown in Appendix 1 (Table 1 and Figs. S1 to S8). Based on the taxonomic similarity of the palynomorph assemblages found and their stratigraphic location, these assemblages have been grouped into several synthetic associations indicating the same age.

The synthetic association obtained in the southern entrance to the Escalaplano village, or "Escalaplano SW Section" (Fig. 5.5), corresponding to the C-2, PC-3 and PC-4 samples is composed of: *Alisporites grauvogeli* Klaus, 1964, *Alisporites magnus* Jain 1968, *Alisporites opii* Daugherty, 1941, *Alisporites* sp., *Angustisulcites grandis* (Freudenthal) Visscher, 1966, *Angustisulcites klausii* (Freudenthal) Visscher, 1966, *Aratrisporites* sp., *Calamospora tener* (Leschik) Mädlar, 1964, *Calamospora* sp., *Chasmatosporites* sp., *Cerebropollenites mesozoicus* Nilsson, 1958, *Chordasporites singulichorda* Klaus, 1960, *Cyclotriletes oligogranifer* Mädlar, 1964, *Cyclotriletes granulatus* Mädlar, 1964, *Enzonalasporites vigens* Leschik, 1955, *Heliosaccus* cf. *dimorphus*. Mädlar, 1964, *Hexasaccites muelleri* (Reinhardt & Schmitz) Adloff & Doubinger, 1969, *Illinites kosankei* Klaus, 1964, *Illinites chitonoides* Klaus, 1964, *Klausipollenites schaubergeri* (Potonié and Klaus) Jansonius, 1962, *Kraeuselisporites* sp., *Limbosporites* sp., *Lunatisporites acutus* Leschik, 1955, *Lunatisporites noviaulensis* (Leschik) de Jersey, 1979, *Lunatisporites* cf. *puntii* Visscher, 1966, *Microcachryidites doubingeri* Klaus, 1964, *Microcachryidites fastidioides* (Jansonius) Klaus, 1964, *Microreticulatisporites gallii* Adloff & Doubinger, 1969, *Paleospongisporis europaeus* Schulz, 1965, *Platysaccus papilionis* Potonié and Klaus, 1954, *Platysaccus* sp., *Punctatisporites fungosus* Balme, 1963, *Punctatisporites triassicus* Schulz, 1964, *Rewanispora vermiculata* Antonescu and Taugourdeau-Lantz, 1973, *Rewanispora* sp., *Striatoabieites aytugii* (Visscher) Scheuring, 1978., *Striatopodocarpidites cancellatus* (Balme & Hennelly) Hart, 1963, *Strotersporites jansonii* Klaus, 1963, *Triadispora crassa* Klaus, 1964, *Triadispora falcata* Klaus, 1964, *Triadispora plicata* Klaus, 1964, *Triadispora staplinii* (Jansonius) Klaus, 1964, *Triadispora suspecta* Scheuring, 1970, *Triadispora* sp.1., *Uvaesporites* sp., *Verrucosisporites* sp.1. and two unidentified spores.

The samples from the "Arcu Is Fronestas" section can be grouped into two synthetic associations. The first corresponds to the AIF-2 and AIF-5 samples collected in the lower part of the section (Fig. 5.6) and is composed of: *Alisporites grauvogeli* Klaus, 1964, *Alisporites magnus* Jain 1968, *Alisporites opii* Daugherty, 1941, *Alisporites* sp., *Angustisulcites gorpilii* Visscher, 1966, *Angustisulcites klausii* (Freudenthal) Visscher, 1966, *Angustisulcites* sp., *Aratrisporites* cf. *granulatus* (Klaus) Playford & Dettmann, 1965, *Aratrisporites* sp., *Brachisaccus neomundanus* (Leschik) Mädlar, 1964, *Camazonosporites* sp., *Chasmatosporites* sp., *Chordasporites singulichorda* Klaus, 1960, *Cristianisporites triangulatus* Antonescu, 1969, *Cycadopites* sp.,

Densoisporites nejburgii (Schulz) Balme, 1970, *Enzonasporites vigens* Leschik, 1955, *Hexasaccites muelleri* (Reinhardt & Schmitz) Adloff & Doubinger, 1969, *Illinites chitonoides* Klaus, 1964, *Illinites kosankei* Klaus, 1964, *Illinites* sp., *Klausipollenites* sp., *Kraeuselisporites* sp., *Lunatisporites noviaulensis* (Leschik 1956) DE Jersey, 1979, *Microcachrydites doubingeri* Klaus, 1964, *Microcachrydites fastidioides* (Jansonius) Klaus, 1964, *Microcachrydites* sp., *Paracirculina* sp., *Platysaccus leschikii* Hart, 1960., *Platysaccus* sp., *Punctatisporites fungosus* Balme, 1963, *Rewanispora vermiculata* Antonescu & Taugourdeau-Lantz, 1973, *Triadispora crassa* Klaus, 1964, *Triadispora plicata* Klaus, 1964, *Triadispora staplinii* (Jansonius) Klaus, 1964, *Triadispora suspecta* Scheuring, 1970, *Triadispora* sp., *Uvaesporites* sp., *Vitreisporites* sp. and one unidentified spore.

The second synthetic association of the section "Arcu Is Fonestas" corresponds to the samples AIF-9 and PC-7.2 and was obtained from the upper part of the Buntsandstein facies, just under the unconformity separating this section from the Jurassic quartz-conglomerates (Fig. 5.6). They are represented by: *Alisporites grauvogeli* Klaus, 1964, *Alisporites opii* Daugherty, 1941, *Alisporites* sp., *Angustisulcites klausii* (Freudenthal) Visscher, 1966, *Angustisulcites* sp., *Calamospora tener* (Leschik) Mädler, 1964, *Calamospora* sp., *Cerebropollenites mesozoicus* Nilsson, 1958, *Chordasporites singulichorda* Klaus, 1960, *Cristianisporites triangulatus* Antonescu, 1969, *Cycadopites* sp., *Cyclotriletes oligogranifer* Mädler, 1964, *Cyclogranisporites* sp., *Densosporites* sp., *Enzonasporites vigens* Leschik, 1955, *Hexasaccites muelleri* (Reinhardt & Schmitz) Adloff & Doubinger, 1969, *Illinites chitonoides* Klaus, 1964, *Illinites kosankei* Klaus, 1964., *Kraeuselisporites* sp., *Lunatisporites acutus* Leschik, 1955, *Lunatisporites* sp., *Microcachrydites doubingeri* Klaus, 1964, *Microcachrydites fastidioides* (Jansonius) Klaus, 1964, *Microcachrydites sittleri* Klaus, 1964, *Microcachrydites* sp.1., *Paracirculina* sp., *Platysaccus papilionis* Potonié & Klaus, 1954, *Punctatisporites triassicus* Schulz, 1964, *Rewanispora vermiculata* Antonescu & Taugourdeau-Lantz, 1973, *Reticulatisporites* sp., *Striatoabieites aytugii* (Visscher) Scheuring, 1978, *Striatoabieites* sp., *Strotersporites jansonii* Klaus, 1963, *Triadispora crassa* Klaus, 1964, *Triadispora falcata* Klaus, 1964, *Triadispora plicata* Klaus, 1964, *Triadispora staplinii* (Jansonius) Klaus, 1964, *Triadispora suspecta* Scheuring, 1970, *Triadispora* sp., *Uvaesporites* sp., and *Verrucosisporites thuringiacus* Mädler, 1964.

The last association, which corresponds to the Grifo-3 sample from the Su Passu Malu section (Figs. 5.7), is composed of: *Alisporites grauvogeli* Klaus, 1964, *Alisporites opii* Daugherty, 1941, *Angustisulcites gorpilii* Visscher, 1966, *Angustisulcites* sp., *Annulispora* sp., *Aratrisporites* cf. *granulatus* (Klaus) Playford and Dettmann 1965, *Bascanisporites* sp.,

Brachisaccus neomundanus (Leschik) Mädlar, 1964, *Calamospora tener* (Leschik) Mädlar, 1964, *Calamospora* sp., *Chasmatosporites* sp., *Cerebropollenites mesozoicus* Nilsson, 1958, *Chordasporites singulichorda* Klaus, 1960, Cf. *Cordaitina* sp., *Cristianisporites triangulatus* Antonescu, 1969, *Cyclogranisporites granulatus* Mädlar, 1964, *Deltoidospora* sp., *Dictyophyllidites mortonii* (De Jersey) Playford & Dettmann, 1965, *Duplicisporites granulatus* (Leschik) Scheuring, 1970, *Enzonalaspores vigenis* Leschik, 1955, *Hexasaccites muelleri* (Reinhardt & Schmitz) Adloff & Doubinger, 1969, *Illinites chitonoides* Klaus, 1964, *Kraeuselisporites* sp., *Lunatisporites noviaulensis* (Leschik) De Jersey, 1979, *Lunatisporites* sp., *Microcachryidites doubingeri* Klaus, 1964, *Microcachryidites fastidioides* (Jansonius) Klaus, 1964, *Microcachryidites* sp.1., *Ovalipollis ovalis* (Krutzsch) Scheuring, 1970, *Paleospongisporis europaeus* Schulz, 1965, *Paracirculina* sp., *Rewanispora vermiculata* Antonescu & Taugourdeau-Lantz, 1973, *Rewanispora* sp., *Striatoabieites aytugii* (Visscher) Scheuring, 1978, *Triadispora crassa* Klaus, 1964, *Triadispora falcata* Klaus, 1964, *Triadispora plicata*. Klaus, 1964, *Triadispora staplinii* (Jansonius) Klaus, 1964, *Triadispora suspecta* Scheuring, 1970, *Triadispora* sp., *Uvaesporites* sp., *Verrucosisporites thuringiacus* Mädlar, 1964, and *Verrucosisporites* sp.

5.4 Ammonoids

At the Punta del Lavatoio (Alghero) section (Fig. 5.8), two levels containing ammonoids (PL6 and PL8) (Figs. 5.11 and 5.12) can be differentiated:

- PL6: *Mojsvaroceras haasi* Parnes, 1986 (PL6_589, PL6_591); *Allocceratites toulonensis* (PL6-594, PL6-595, PL6-596, PL6-597 and 599), *Allocceratites* sp. (PL6-594, PL6-598, PL6-602).
- PL8: *Ceratites (Opheoceratite?)* sp. (PL8-570); *Gevanites awadi* Parnes, 1975, with two varieties: armed variety (var. *armata*) (PL8-571, PL8-572, PL8-577, PL8-579, PL8-580), and expanded variety (var. *expansa*) (PL8-578, PL581); *Gevanites* sp. (PL8-573, PL8-575); and *Falsanolcites* gr. *Recubariense* (PL8-574).

The Monte Santa Giusta section contains (Fig. 5.9):

- One *Nautiloidea* specimen, probably *Germanonautilus* sp. (MSG-May 2016), and two *Hungaritidae*, close to *Iberites (I. pradoi)* (MSG-618, MSG-6019). The *Ceratites* cf. *nodosus* Bruguière, possibly corresponding to an *Allocceratites* specimen (Tornquist, 1901) can be added to the findings in this section.

The Monte Fogheras section contains Fig. (5.10):

An almost complete fragmocone (found in 1988 on the Cala Bona Road, at 4C level of the Cappella della Speranza section – A. Gandin, pers Comm.) was initially considered as *Ceratites (Doloceratites) muensteri* Philippi by Márquez-Aliaga et al. (2000), and

later was described by Urlichs (2016) to be close to *Alloceratites tornquisti* (Philippi, 1901).

Tornquist (1904) cited 6 specimens in an outcrop south of Alghero, but unfortunately these are likely missing today. They resemble *C. muensteri* more than *C. nodosus* (as would be the case if they were *Gevanites* of an equivalent level to PL8). This same author also described *Protrachyceras longobardicum* Mojsisovics, 1882 which should have come from more recent levels (lower Longobardian). However, when specimens are not well preserved, it is not easy to separate this species from other *Trachyceratidae* in the *Curionii* Zone.

The best-preserved specimens of PL8, subadults or adults, only conserve part of the fragmacone and the living chamber. It is not easy to know what type of association they correspond to in the classification system of Fernández-López (1985, 2014). There are almost no juvenile shells; these are abundant or frequent in Association 1. Thus, the associations are most likely Association 2 or 3, as juvenile shells are scarce or absent, and adult or sub-adult shells are frequent or dominant. Therefore, they could be occasional immigrants and even come from distant areas after experiencing a notable necro-planktonic drift in their shells. However, the PL6 bis specimens only conserve the chamber (usually a part) and the last partitions of the fragmacone, and at least some of them show evidence of being reworked. Associations are of type 3 or 2, as juvenile shells are absent.

5.5 Bivalves

In the Nurra region, the Punta del Lavatoio section harbours the most complete and diverse bivalves' association. Three fossiliferous levels have been recorded: Sectors 1, 2 and 3. The position of these levels can be attributed to the lower, middle, and upper part of the Punta del Lavatoio section (Figs. 5.8 and 5.14). The following are their contents:

- Sector 1: *Costatoria goldfussi* (Alberti), *Hoernesia socialis* (Schlotheim), *Limea costata* (Münster), *Pleuromya* cf. *mactroides* Schlotheim and *Pseudoplacunopsis ostracina* (Schlotheim).
- Sector 2: *Bakevella subcostata* (Goldfuss), *Bakevella crispata* (Goldfuss), *Costatoria goldfussi* (Alberti), *Hoernesia socialis* (Schlotheim), *Limea costata* (Münster), *Myophoria vulgaris* (Schlotheim), *Neoschizodus laevigatus* (Ziethen), *Pseudocorbula gregaria* (Münster), *Pleuromya* cf. *mactroides* (Schlotheim), *Pleuronectites laevigatus* (Schlotheim), *Pseudoplacunopsis ostracina* (Schlotheim)
- Sector 3: *Bakevella subcostata* (Goldfuss), *Bakevella crispata* (Goldfuss), *Costatoria goldfussi* (Alberti), *Hoernesia socialis* (Schlotheim), *Limea costata* (Münster), *Elegantinia elegans* (Dunker), *Myophoria vulgaris* (Schlotheim), *Neoschizodus*

laevigatus (Ziethen), *Pleuromya* cf. *mactroides* (Schlotheim), *Pleuronectites laevigatus* (Schlotheim), *Pseudoplacunopsis ostracina* (Schlotheim).

In the Monte Fogheras area (Figs. 5.10 and 5.13), located south of Alghero city, two fossiliferous levels have been recognized: MFS and MFS2A. At the time of the fossil collection (80s), level MFS was situated on an outcrop on the side of the SP 104 Alghero-Bosa. Nowadays, the precise position of this level is hard to tell because of road renovation and maintenance work, but it is likely to be at about 40°29'53.8"N 8°22'04.7". MFS2A is situated on a seaside outcrop found some 200 m W of the Poglina beach. The contents (Fig. 5.13) of these levels are:

- MFS: *Bakevella crispata* (Goldfuss), *Costatoria goldfussi* (Alberti), *Hoernesia socialis* (Schlotheim), *Limea costata* (Münster), *Pleuromya* cf. *mactroides* (Schlotheim), *Pseudoplacunopsis ostracina* (Schlotheim).
- MF2A: *Bakevella crispata* (Goldfuss), *Costatoria goldfussi* (Alberti), *Hoernesia socialis* (Schlotheim), *Limea costata* (Münster), *Elegantinia elegans* (Dunker), *Myophoria vulgaris* (Schlotheim), *Neoschizodus laevigatus* (Ziethen), *Pleuromya* cf. *mactroides* (Schlotheim), *Pseudoplacunopsis ostracina* (Schlotheim), *Umbostrea cristadiformis* (Schlotheim).

In the Monte Santa Giusta outcrop (Fig. 5.9), one rich fossiliferous level MSG A-B has been surveyed, which roughly corresponds to sub-unit mo3 of the "Upper calcareous unit" (Carrillat 1999 a, b; Posenato, 2002; Knaust and Costamagna, 2012) (Fig. 5.3). Its contents are:

- Level MSG A-B: *Costatoria goldfussi* (Alberti), *Hoernesia socialis* (Schlotheim), *Limea costata* (Münster), *Pleuromya* cf. *mactroides* (Schlotheim).

To the S of the region (Fig. 5.4), the Monte Maggiore outcrop presents two fossiliferous levels: level H and level I, both occupying the middle-upper part of the "Calcari Azzurri" member (Costamagna et al., 2000). Their contents (Fig. 5.15) are:

- Level H: *Costatoria goldfussi* (Alberti) and *Pleuromya* cf. *mactroides* Schlotheim
- Level I: *Bakevella crispata* (Goldfuss), *Costatoria goldfussi* (Alberti), *Pseudocorbula gregaria* (Münster) and *Pleuromya* cf. *mactroides* (Schlotheim).

The SW-most surveyed outcrop at Punta Tonnara (Fig. 5.4) features a scarce fossil content. The assemblage consists of: *Limea costata* (Münster) and *Pseudocorbula gregaria*

5.6 Other fossils

It has been possible to recognize different species of foraminifera through the study of thin sections from the following key sections of the island: Monte Maggiore, Monte Santa Giusta, Punta del Lavatoio, and Porto Pino (Fig. 5.4: 2, 3, 7, 10). Our study was mainly carried out on mudstone and wackestone facies, where the better-preserved fossils were found in a microsparitic matrix. These facies often show bioturbation, pressure-dissolution features, recrystallization (sparite patches) and dolomitization. Occasionally, the dolomitization is high and pervasive, and no fossils (or only ghosts) or sedimentary structures can be recognized.

Foraminifera are commonly associated to other fossils of such as bivalves, gastropods, echinoids, and calcareous algae (Fig. 5.16).

Monte Santa Giusta

MSG0: *Trochammina* cf. *alpina* (Kristan-Tollmann); *Tolypammina gregaria* (Wendt).
MSG2A: *Aulotortus pragsoides* (Oberhauser); *Glomospirella* (?); *Planiinvoluta carinata* (Leischner), *Planiinvoluta* cf. *carinata* (Leischner), MSG20C: *Endothyranella wirtzi* (Koehn-Zaninetti), *Glomospira* (?), *Endothyranella robusta* Salaj, *Trochammina* cf. *alpina* (Kristan-Tollmann).

Monte Maggiore

MM59217: *Endothyra kueperi* (Oberhauser), *Glomospirella vulgaris* (Ho), *Endothyranella wirtzi* (Koehn-Zaninetti), *Nodosaria* ? sp., *Nodosaria ordinata* (Trifonova), *Hoyenella sinensis* (Ho), *Earlandia tintinniformis* (Mišík), *Endotriada tyrrhenica* (Vachard, Martini, Rettori and Zaninetti).

Punta Tonnara

Nodosaria ordinata (Trifonova), *Nodosaria shablensis* (Trifonova), *Earlandia tintinniformis* (Mišík).

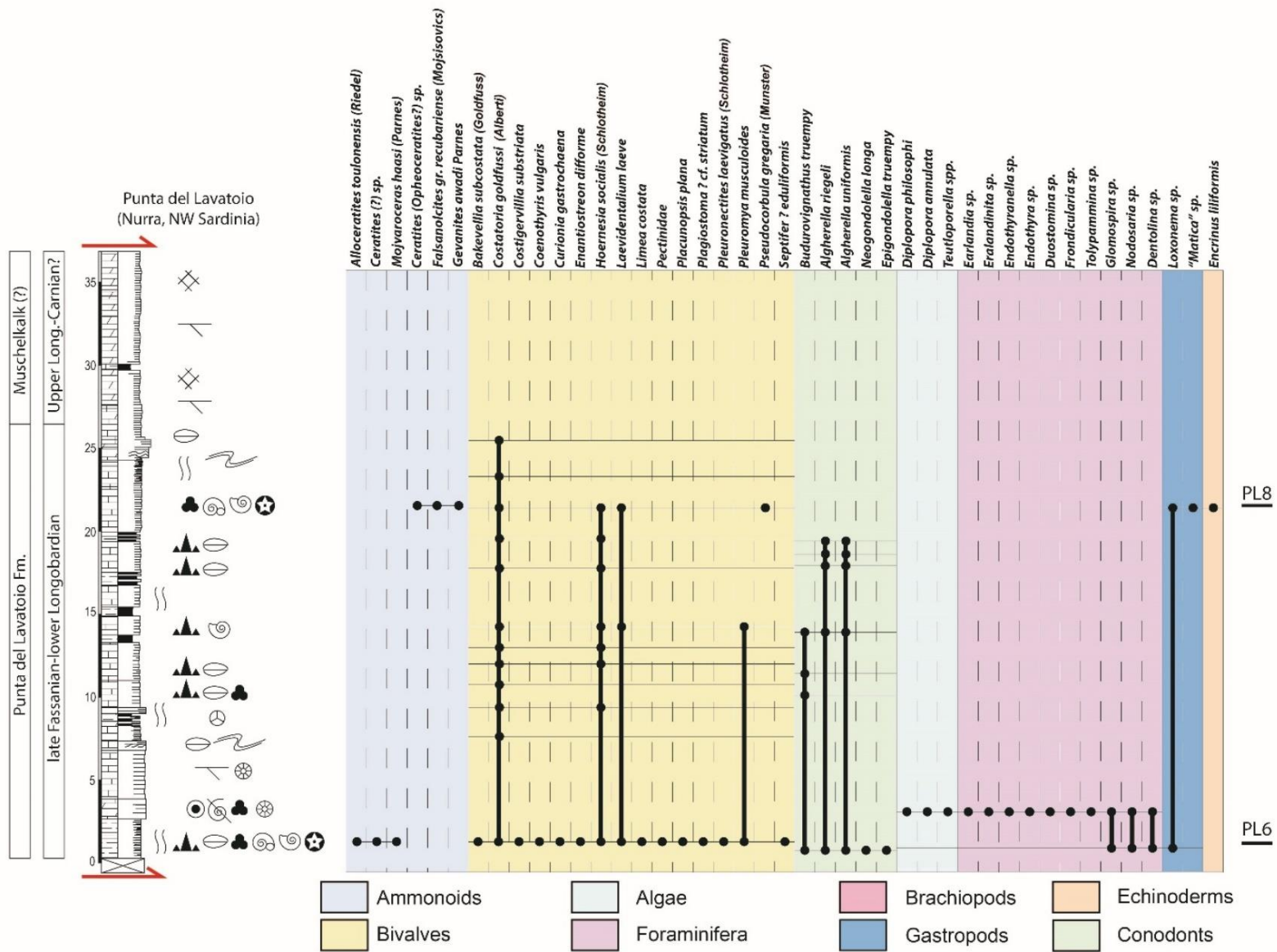


Fig. 5.8. Punta del Lavatoio section (Nurra, NW Sardinia), showing the stratigraphic positions of the most representative fossils.

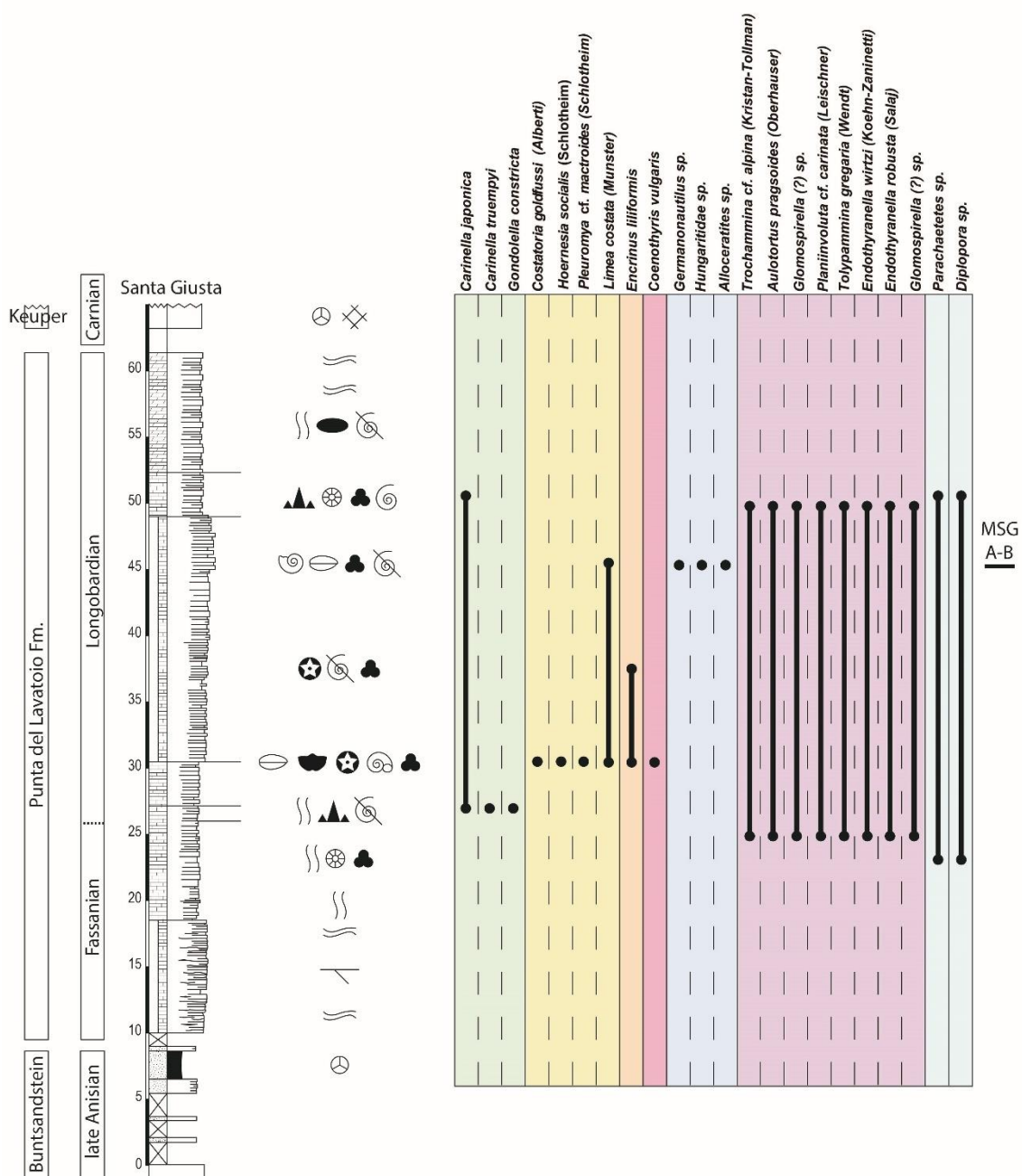


Fig. 5.9. Monte Santa Giusta section (Nurra, NW Sardinia), showing the stratigraphic positions of the most representative fossils.

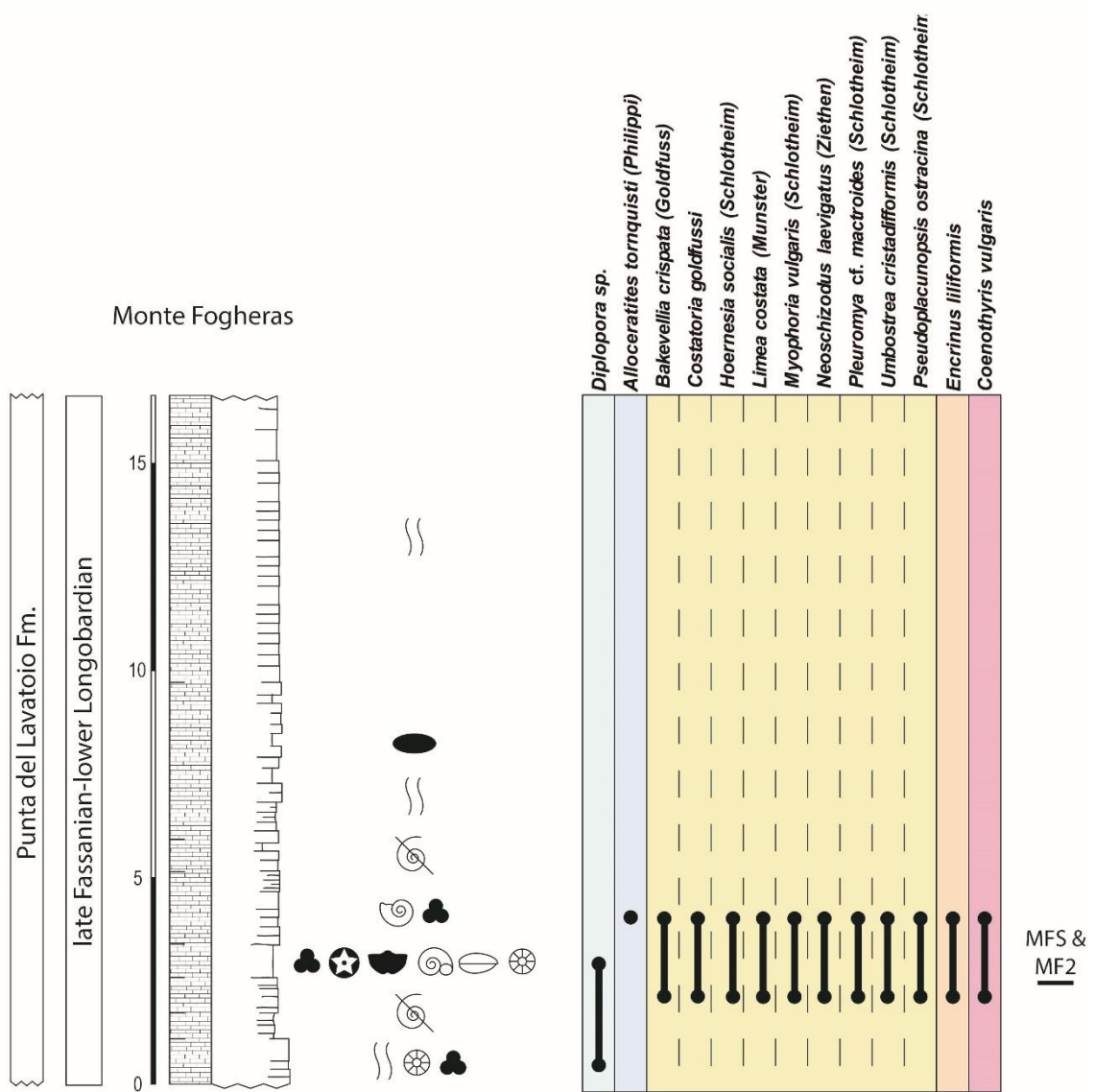


Fig. 5.10. Monte Fogheras section (Nurra, NW Sardinia), showing the stratigraphic positions of the most representative fossils.



Fig. 5.11: A) *Ceratites* (*Opheoceratites*?) sp.: PL8_570. B) *Falsanolcites* gr. *recubariense* (Mojsisovics, 1982): PL8_574. C, D, E) *Gevanites awadi* Parnes, 1975 var. *armata*: 3 PL8_571, 4 PL8_577, 5 PL8_580; F, G) *Gevanites awadi* (Parnes, 1975) var. *expansa*: 5 PL8_572, 6PL8_578. H) *Alloceratites tornquisti* (Philippi, 1901): 7 MF_1. I) *Iberites* near to *I. pradoi* (D'Archiac, 1860): MSG_619.

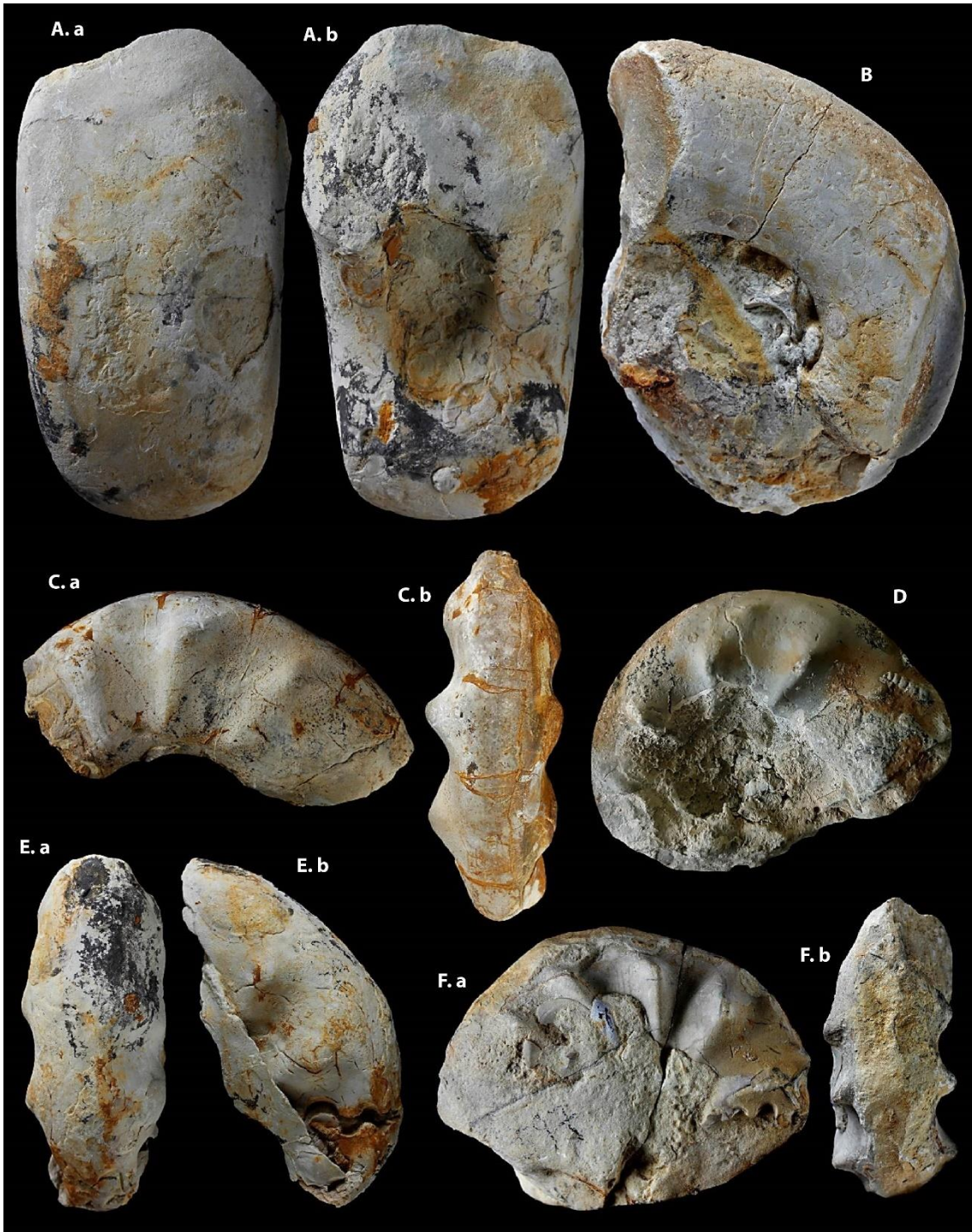


Fig. 5.12. A, B) *Mojsvaroceras haasi* Parnes, 1986: 1 PL6_589, 2 PL6_591. C, D, E, F) *Allocceratites toulonensis* (Riedel, 1916): 3 PL6_592, 4 PL6_595, 5 PL6_596, PL6_599.



Fig. 5.13. Monte Fogheras bivalves assemblage: **A)** *Bakevellia crispata* (Goldfuss). 501MF2; 2-4 m. Left valve, dorsal and posterior view. Note the posterior wing and the commarginal ornamentation of the preserved shell. Bar 10 mm **B)** *Bakevellia crispata* (Goldfuss). 501MF2; 2-4 m. Left valve, anterior and dorsal view. Note the commarginal ornamentation of the preserved shell. Bar 10 mm **C)** *Hoernesia socialis* (Schlotheim).536MFS; 3-5 m. Left valve, lateral and dorsal view. The grow lines of the shell are preserved, mainly in the posterior area. Bar 10 mm **D)** *Limea costata* (Münster). 515MFS; 3-5 m. Right valve. The radial ornamentation of the shell is preserved. Bar 10 mm **E)** *Limea costata* (Münster). 537MF78; 3-5 m. Left valve. The posterior auricle is visible in the umbonal area. In the margin, the radial ornamentation of the shell is preserved. Bar 10 mm **F)** *Umbostrea cristadiformis* (Schlotheim).523MFS a and b; 3-5m. Two right? valves. Showing the xenomorphic area and the divaricate shell ornamentation preserved. Bar 10 mm **G)** *Costatoria goldfussi* (Alberti). 525MF2A; 2-4 m. Left and right valve internal molds. Note the radial ornamentation from umbo to margin. Bar 10 mm **H)** *Encrinus* cf. *liliiformis* Schlotheim. 505MFS; 3-5 m. Calcite columnar fragment. Bar 10 mm **I)** "*Coenothyris*" *vulgaris* (Schlotheim). 516MFS-1; 3-5 m. Upper and lower view valve of an exemplar with part of the shell preserved. Bar 10 mm **J)** "*Coenothyris*" *vulgaris* Schlotheim. 516MFS-2; 3-5 m. Upper and lower valve of two exemplars with the shell preserved. Bar 10 mm **K)** *Costatoria goldfussi* (Alberti), *Hoernesia socialis* (Schlotheim), *Encrinus* cf. *liliiformis* (Schlotheim) and Bivalvia indet. 499MF2; 2-4 m. Fossils accumulation in a hard ground layer. Bar 10 mm **L)** *Umbostrea cristadiformis* (Schlotheim), *Encrinus* cf. *liliiformis* (Schlotheim), *Neoschyzodus laevigatus* (Ziethen) and Bivalvia indet. 514MFS; 2-5 m. Fossils accumulation in a hard ground layer. Bar 10 mm

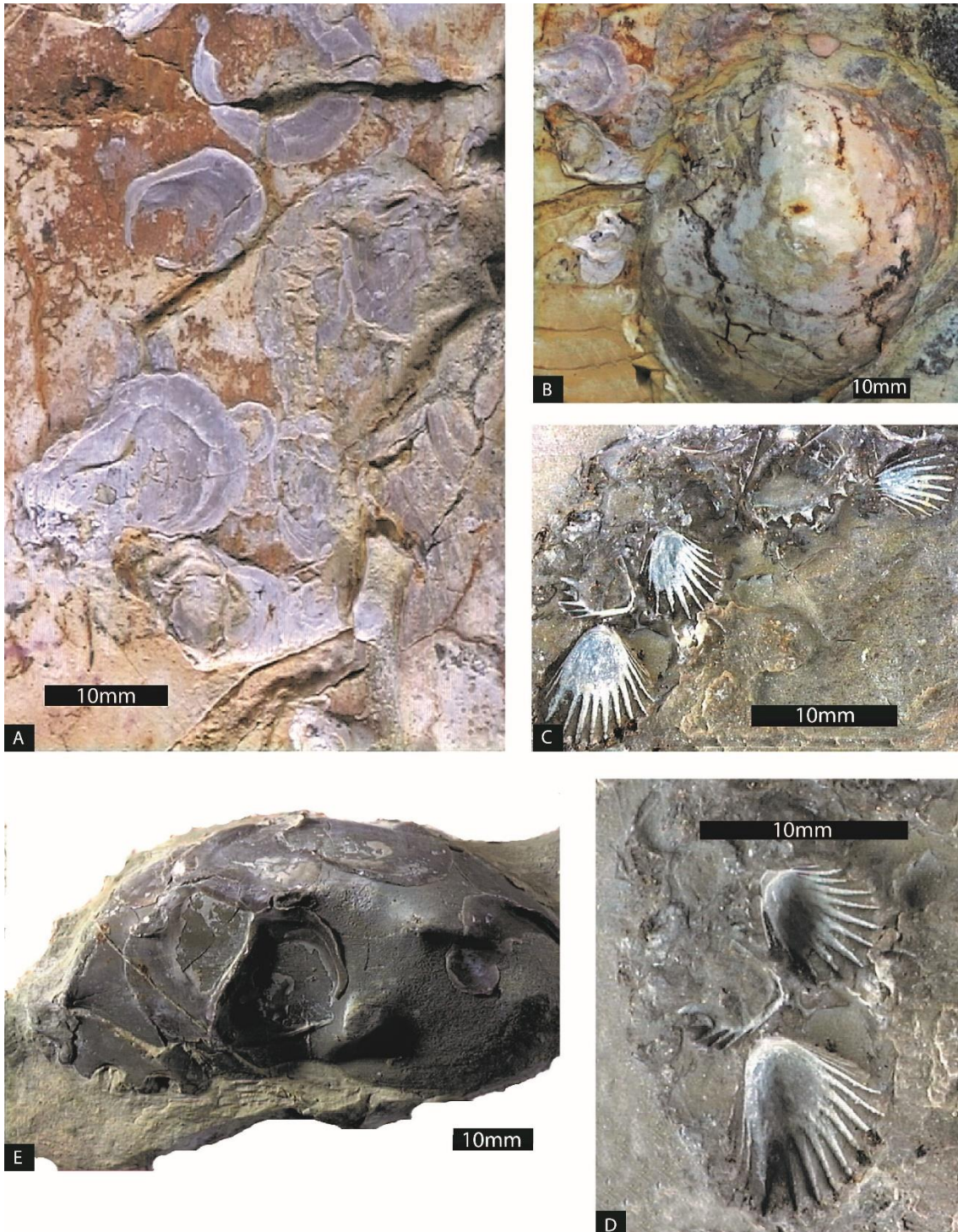


Fig. 5.14. Punta del Lavatoio bivalves assemblage: **A)** *Pseudoplacunopsis ostracina* (Schlotheim). 587PL6; 1-3 m. Interior view of some right valves with the foliar calcite layer preserved. The exemplars were fixed as epizoaria bivalves, in the original aragonitic layer of a Ceratite. Bar 10 mm **B)** *Pleuronectites laevigatus* (Schlotheim). 587PL6; 1-3 m. Left valve Internal mold. Note the two auricles with some visible growth lines. Bar 10 mm **C)** *Costatoria goldfussi* (Alberti). 566PL4; 25-26 m. Two left and one right valves as internal molds. The radial ornamentation is visible. Bar 10 mm **D)** *Costatoria goldfussi* (Alberti). 566PL4; 25-26 m. Two left valves as internal molds. More than ten ribs of the radial ornamentation are visible. Bar 10 mm **E)** *Pseudoplacunopsis ostracina* (Schlotheim). 576PL8; 18-19 m. Interior view of some right valves with the foliar calcite layer preserved. The exemplars were fixed as epizoaria bivalves, in the original aragonitic layer of a Ceratite. Bar 10 mm

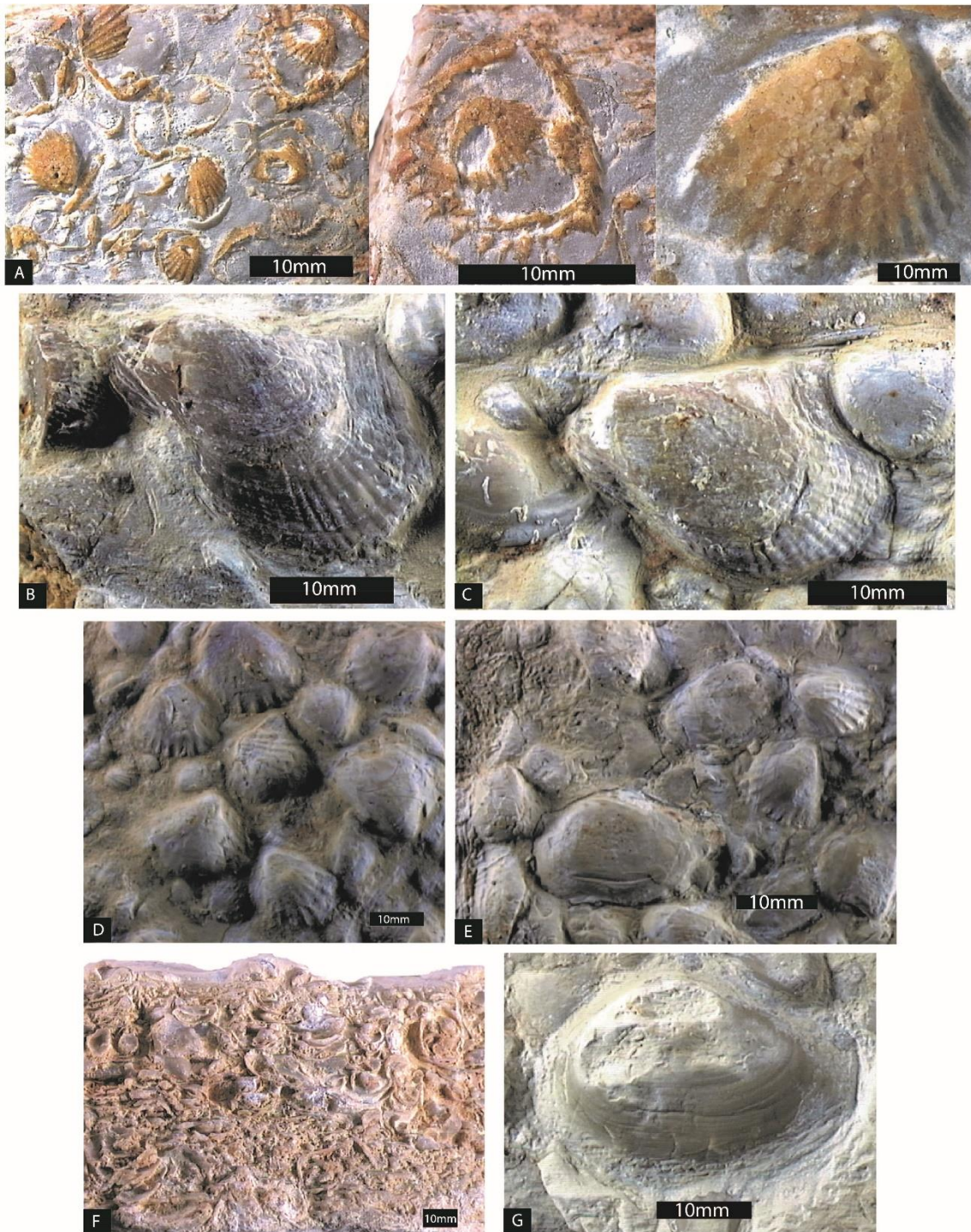


Fig. 5.15. Monte Maggiore bivalves assemblage: **A)** *Costatoria goldfussi* (Alberti). 545MMH; 45-48 m. Bedding plane with many internal molds showing the radial ornamentation of shells. Bar 10 mm. 1a left valve and 2b right valve of two exemplars. Note the diagenetic esparitic layer from an original aragonite one. Bar 5 mm **B)** *Bakevellia subcostata* (Goldfuss). 548aMMI; 54-57 m. Left valve, lateral view. The short anterior and large posterior auricles are visible. The calcite external layer of the shell is preserved. Note the radial ornamentation and the growth lines. Bar 10 mm **C)** *Bakevellia subcostata* (Goldfuss). 548bMMI; 54-57 m. Left valve, lateral view. The short anterior and large posterior auricles are visible. The calcite external layer of the shell is preserved. Note the radial ornamentation and the growth lines. Bar 10 mm **D)** *Costatoria goldfussi* (Alberti). 560MMIa; 54-57 m. Bedding plane with abundant internal molds. Note the bad preserved radial ornamentation of shells. Bar 10 mm **E)** *Pleuromya mactroides* (Schlotheim) and *Costatoria goldfussi* (Alberti). 560MMIb 54-57 m. Bedding plane with abundant internal molds. Bar 5 mm **F)** "Tempestite" Fossil accumulation in cross section with many indeterminate bivalve shells. MMH540. Bar 5 mm **G)** *Pleuromya mactroides* (Schlotheim). MMI560c. Left valve, lateral view of an internal mold with visible growth lines in the ventral area. Bar 10 mm

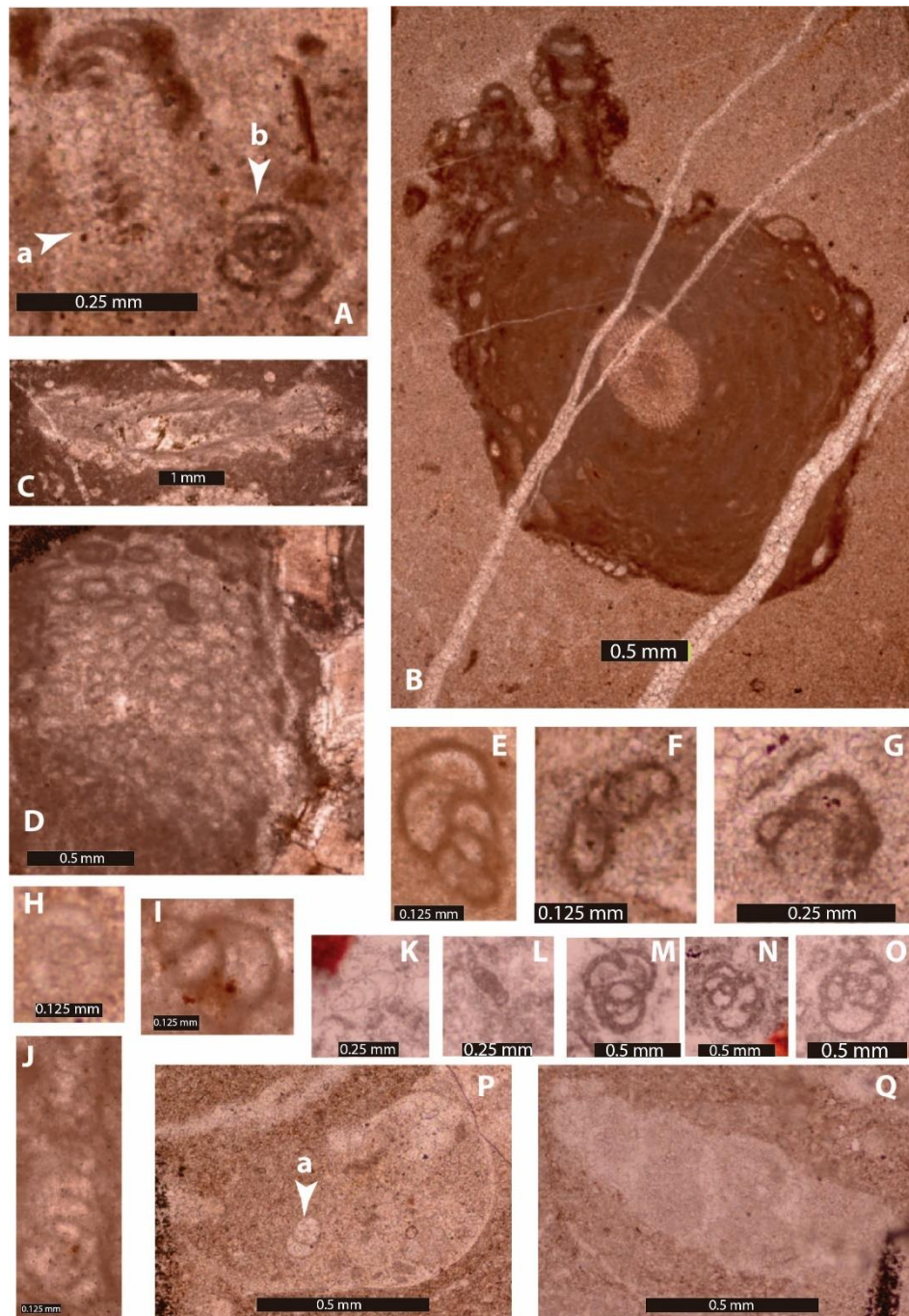


Fig. 5.16. A) a: *Aulotortus pragsoides* (Oberhauser) **b:** *Glomospirella* (?) **B)** *Tolyppammina gregaria* (Wendt). Attached foraminifera that grows on various remains forming voluminous masses, in this case on the radiola of an echinoid. **C)** Terquemidae (?) Bivalve with leaf microstructure. **D)** *Parachaetetes* sp. Solenoporaceous calcareous algae. **E)** *Trochammina* cf. *alpina* (Kristan-Tollmann) **F)** *Planiinvoluta* cf. *carinata* (Leischner) **G)** *Planiinvoluta carinata* (Leischner). Attached foraminifera that grows on various surfaces such as clasts, remains of organisms, algae, etc., therefore it has flat or curved external margins. **H)** *Glomospira* (?) **I)** *Trochammina* cf. *alpina* (Kristan-Tollmann) **J)** *Endothyranella robusta* (Salaj). **K)** *Endothyranella wirtzi* (Koehn-Zaninetti). Fragment of the uniserial part. **L)** *Glomospirella vulgaris* (Ho). **M, N, O)** *Endothyra kueperi* (Oberhauser). **P)** Bakevellidae. Calcitic shell bivalves with prismatic microstructure. **P a)** *Endothyranella wirtzi* (Koehn-Zaninetti). Fragment of the uniserial part. **Q)** *Zigopecten* sp. Gastropod.

5.7 Biochronostratigraphy

Microfloristic associations

From the set of results obtained from the review of previous works, unpublished data and new pollen samples, it has been possible to infer that there has been no palynological dating corresponding to the Early Triassic in Sardinia, in contrast with neighbouring palaeogeographical regions such as the Iberian Peninsula (Diez et al., 2005) and the South of France (Diez, 2000).

Furthermore, sample 1275 collected from the section of Punta del Lavatoio and studied by Pittau Demelia and Flaviani (1982a), within the Punta del Lavatoio Fm., shows only photos of seven taxa and, although the authors initially ascribed it to the Anisian, this age is not consistent. The three species identified have a wide biozone distribution: *Chordasporites singulichorda*, which corresponds from the base of the Anisian to the Longobardian (Eshet, 1990); *Triadispora plicata*, from the Anisian to the Carnian; and *Triadispora suspecta*, from the Pelsonian to the Carnian (Doubinger and Adloff, 1983). Therefore, our dating would be broader, and a Pelsonian-Longobardian interval is proposed for this sample (Fig. 5.17). A later publication by Posenato et al. (2002) studied the same outcrop and, through biostratigraphic analyses of various groups of marine invertebrates, attributed the entire section to the Ladinian. Likewise, palynological data from the same Muschelkalk facies from the Monte di Santa Giusta section to the north of Alghero (Carrillat et al., 1999), are consistent with this latter proposed age.

As regards the rest of the works referred to, it has been possible to verify the presence of *Hexasaccites muelleri*, which indicates that all these levels can be dated as being of the Anisian age (Visscher and Brugman, 1981; Brugman, 1983; Diez 2000; Diez et al., 2005; Kürschner and Hengreen, 2010).

Regarding the Cugiareddu well (Fig. 5.17: 6), although most of the Flaviani (1980) work remains unpublished, the few photos published in Pittau Demelia and Flaviani (1982b) and Pittau and Del Rio (2002) allow to address the following arguments: In the final work of compilation (Pittau and Del Rio, 2002), the authors reevaluated the palynological association, first described by Flaviani (1980) and referred to in Pittau Demelia and Flaviani (1982b), for level 545 (sample 970), and considered it a possible late Scythian or early Anisian due to the impossibility of confirming the identification of *Stellapollentes muelleri* (= *Hexasaccites muelleri*). However, *Voltziaceasporites heteromorpha* made its first appearance in the late

Olenekian, according to Brugman (1986). As said before, the criterion of absence is not acceptable, but since this publication presents photos of three taxa it is possible to infer from the text that they come from level 545. For this reason, it has been possible to confirm the identification of *Triadispora crassa* and *Voltziaceasporites heteromorpha*. Therefore, it is possible to agree that *V. heteromorpha* begins in the upper Scythian, but its biozone extends to the Pelsonian (Visscher and Brugman, 1981; Brugman, 1983, 1986; Diez 2000). Furthermore, the *Triadispora crassa* biozone extends from the Anisian to the base of the Carnian. If added the fact that the association is very poor. Based on the fact that the association is very poor, and considering the above data, it is possible to assume, without much precision, an Anisian age for this association, without extending to the Illyrian (Fig. 5.17: 6).

Following Pittau Demelia and Del Rio (2002), levels 477 (sample 756) and 443 (sample 755) of the Cugiareddu well show *Hexasaccites muelleri*, corresponding with the Anisian, as mentioned above, while *Cristianisporites triangulatus* corresponds to a biozone between the Pelsonian (Anisian) and Fassanian (Ladinian) (Antonescu, 1969; Doubinger and Adloff, 1983; Diez, 2000), which would place these two levels within the Pelsonian-Illyrian interval (late Anisian) (Fig.5.17: 6).

Regarding level 429 (sample 754) of the same well, it is here rejected following the use of the criterion of absence. Moreover, the presence of *Ovalopollis pseudoalatus*, with a photo in Pittau Demelia and Del Rio (2002), does not allow to say that the level is later than the base of the Pelsonian (Doubinger and Böhmann, 1981; Visscher and Brugman, 1981; Brugman, 1983; Diez, 2000).

The outcrops of the Sarcidano-Gerrei region are referred in most of the published works (e.g., Pittau Demelia and Del Rio, 1980; Ronchi, 1997; Costamagna et al., 2000 and Diez, 2000), as well as the new data presented in this thesis. Nevertheless, as already explained in the previous section, the data presented in Pittau Demelia and Del Rio (1980), Ronchi (1997), Costamagna et al. (2000) cannot be used due to the incomplete or non-existent sheets of photographs or the unknown stratigraphic locations (level and section) of each of the photographed and classified taxa. Furthermore, for the reasons mentioned above, it is only possible to attribute all the levels of these sections to the Anisian (Fig. 5.17: 3, 4).

The revised samples from previous works and the new levels obtained here are collected from the sections of Escalaplano SW (Fig. 5.5) and Arcu Is Fronestas (Fig. 5.6). The three samples collected from the Escalaplano SW section have been treated as a single synthetic association (for more details, see the Appendix 1), as they are very similar in their

assemblage's content. If taken into consideration the main Triassic palynostratigraphic works on the Western pery-Tethys domain (Doubinger and Böhmann 1981; Visscher and Brugman, 1981; Brugman 1983; Eshet 1990; Diez et al. 2010), *Enzonasporites vigens*, *Microcachrydites doubingeri*, *Microcachrydites fastidioides*, *Triadispora crassa* and *Triadispora staplinii* are consistent with the Anisian dating provided by *Hexasaccites muelleri*. *Cyclotriletes oligogranifer*, *Illinites chitonoides*, *Triadispora plicata*, and *Triadispora suspecta* show their first appearance in the Pelsonian (Doubinger and Adloff 1983; Eshet 1990), *Punctatisporites triassicus* was usually present until the Pelsonian (Doubinger and Böhmann, 1981) and, finally, *Illinites kosankei* was last recorded in the middle Pelsonian (Doubinger and Adloff 1983) levels of facies, so it is possible to infer that the Buntsandstein facies levels of the Escalaplano SW section were deposited during the lower Pelsonian. Although bad preserved, it also appears a single specimen of *Heliosaccus cf. dimorphus* Mädlar 1964 in sample 3. This species is considered to have its first record in the Anisian-Ladinian transition (Doubinger and Adloff, 1983; Visscher and Brugman, 1981; Brugman, 1983; Kurscher and Herengreen, 2010), and if it is confirmed, the should biozone should be reconsidered (Fig. 5.17: 4).

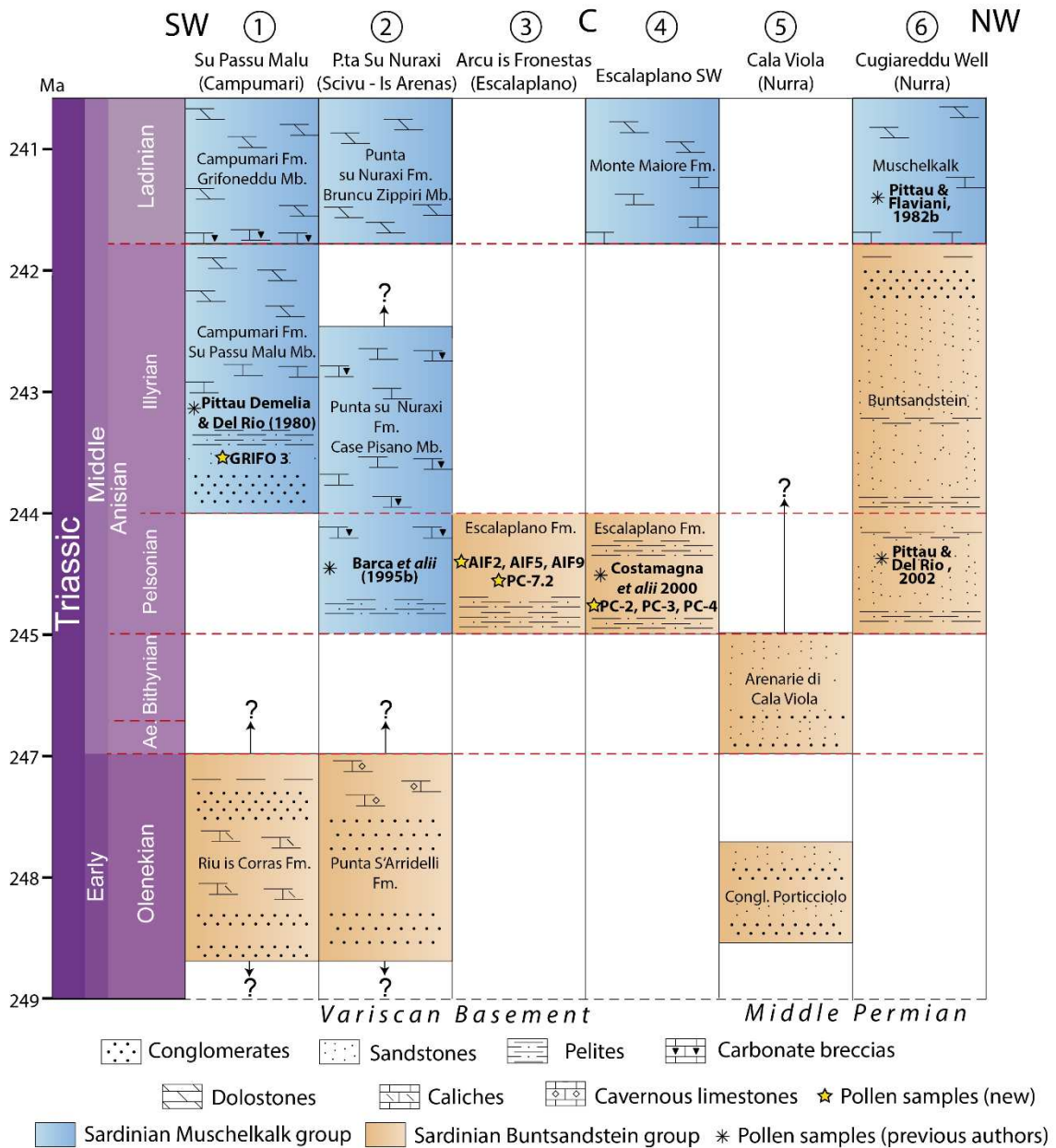
The second section studied in the Escalaplano basin is called Arcu Is Fronestas (Fig. 5.6). Four samples were studied in this section, but as mentioned in the previous section, they have been unified in two synthetic associations (See the complete lists of the samples Appendix 1) due to their similar composition and stratigraphic position. The first corresponds to the lower part of the Escalaplano Fm., associated to the Buntsandstein facies, and composed of samples AIF-2 and AIF-5, and the second to the upper part of this facies and composed of samples PC-7.2 AIF-9. The two synthetic associations present few differences between them; both can be attributed to the early Pelsonian, following the same reasoning used for those of the Escalaplano section, and based on the same taxa sets. The only appreciable difference is the appearance of *Cristianisporites triangulatus* in the upper-part association, which has its first record in the Pelsonian of Central Europe (Doubinger and Adloff, 1983). Its presence does not allow to precise that the age is more modern than samples found at the base, but its relative stratigraphic position could be used as a correlation criterion with the Grifo-3 sample of the Campumari Section, which also presents this taxon (Fig. 5.17: 3).

In the Iglesias region, the first reference is that of Pittau and Del Rio (1980), in which a poor association is described for the Campumari outcrop. Due to the presence of *Hexasaccites muelleri*, the sampled unit can be attributed to Anisian *sensu lato*, as suggested by the authors (Fig. 5.17: 1). It is possible to confirm this attribution thanks to the photo of the taxon. In this region, a new sampling in the Passu Malu section (Fig. 5.7), shows a well-

preserved association containing *Cristianisporites triangulatus*, *Enzonalasporites vigens*, *Illinites chitonoides*, *Triadispora falcata*, *T. plicata* and *T. falcata* together with *Hexasaccites muelleri*, which would indicate a Pelsonian-Illyrian age (Visscher and Brugman, 1981; Brugman, 1983; Doubinger and Adloff, 1983; Diez, 2000).

According to Cirilli (2010) and Mietto et al. (2012), the presence of *Enzonalasporites vigens* and *Duplicisporites granulatus* could indicate a Ladinian age. However, Doubinger and Bühmann (1981) indicate *Enzonalasporites* spp. from the early Anisian, while Doubinger and Adloff (1983) indicate that *Duplicisporites* spp. appear from the Illyrian (late Anisian). Of all the Anisian associations described in Sardinia, this represents the most modern level (Fig. 5.17: 1).

In addition to the data presented in Barca et al. (1995b), new samplings attempted to provide fresh data from the Scivu Is Arenas section, in the Arburese region (Figs. 1, 5), but, unfortunately, they were all unsuccessful due to their data presentation. However, thanks to the partial figuration of above-cited paper, a taxonomic reinterpretation of this section could be done (See also Appendix 1), and, a more precise age for the basal marly levels of the carbonate member of the Punta Su Nuraxi Formation has now been provided. As the authors correctly deduce the presence of *Hexasaccites muelleri* and *Cristianisporites triangulatus*, they consider that the association would include a Pelsonian-Illyrian age (Doubinger and Bühmann, 1981; Doubinger and Adloff, 1980; Visscher and Brugman, 1981; Brugman 1983; Eshet, 1990; Diez 2000; Diez et al., 2010), which would be supported by the coexistence with *Cyclotriletes oligogranifer* and *Triadispora suspecta*. However, reinterpretation of the published photos allows to identify *Punctatisporites triassicus* and *Verrucosisporites thuringiacus*, which, based on their last records, would restrict the dating to the Pelsonian (Doubinger and Bühmann 1981; Doubinger and Adloff, 1980) (Fig. 5.17: 2).



5.17. Chronostratigraphic scheme of the studied succession in SW, C and NW Sardinia.

Ammonoids, bivalves and other fossils

Regarding the ammonoids findings, the stratigraphic positions of samples PL8 and PL6 at the Punta de Lavatoio section, and of MSG.618 and MSG.619 at the Monte Santa Giusta section are as follows (Figs. 5.11 and 5.12): PL8, includes *Gevanites awadi* Parnes, a characteristic species of the early Ladinian (Fassanian) in the Sephardic Province defined by Hirsch (1977), especially for conodont- ammonite- and bivalve associations. This sample belongs to the upper part of the *Curionii* Zone: *Awadi* Subzone in the Betic Cordillera (Pérez-Valera 2005, 2015; Pérez-Valera et al., 2005). In the scope of this province, it may be correlated with the upper part of the *Eoprotrachyceras* Zone in the Negev and Sinai (Parnes 1986; Hirsch 1987). Another palaeobiogeographic area is the *Curionii* Zone - *Awadi* Subzone, which is practically equivalent to the *Curionii* Zone - *Villanovai* Subzone of NE Spain including the Island of Minorca (Goy, 1986, 1995; Escudero-Mozo et al., 2014, 2015).

Somewhat less precise is the correlation with the *Eoprotrachyceras* Zone - *Recubariense* and *Margaritosum* Subzones by Mietto and Manfrin (1995), and with the *Margaritosum* Zone by Balini et al. (2010) in the Province of Tethys. At the moment, its correlation with the Germanic Province is difficult (Urlich, 1997), and with the lower part of Tozer's Poseidon Zone (1994) in British Columbia is imprecise.

The *Ceratites* genus is typical of the Germanic Province but is also present in the Alpine Province. It spans a wide range and does not provide additional details with respect to the above *C. (Opheoceratites?)* sp. If PL8-570 corresponds to the latter subgenus, it would have shown its peak development between the "Trochitenkalk": m1 and the untere *Nodosus* Sch: m2 (Urlich, 1991). This notion is not incompatible with the fact that it can coexist with *G. awadi* and *Falsanolcites* (Rieber and Brack, 2004), nor does it rule out the possibility that *A. tornquisti* from the Monte Fogheras section corresponds to PL6. The association obtained includes *Alloceratites toulonensis* (Riedel, 1916) as the main element. The genus *Alloceratites* shows a Ladinian distribution: late Fassanian - earliest Longobardian, although the species *A. toulonensis* (according to Urlich, 1997, 2016; Urlich and Posenato, 2002) could not have surpassed the late Fassanian in the sense of Balini et al. (2010). The species is known from Provence and the Germanic Basin (Thuringia), among other areas. According to Urlich (2016, p. 32), the migration of *Alloceratites* in the interior of the Germanic Basin probably started from the Peri-Tethys in the Sephardic Province. This author does preclude the idea that they arose from the genus *Israelites* (Parnes, 1962), as suggested by other authors.

As previously mentioned, the carbonatic Middle Triassic of Sardinia has been taxonomically revised in the sections of Punta Lavatoio, Monte Fogheras and Monte Maggiore also according to bivalve data (See Appendix 2). All recognised bivalve taxa show broad biostratigraphic ranges, but their associations indicate relatively well-defined ages and provide relevant palaeobiogeographical information. It should be noted that most specimens belong to the Middle Triassic and are abundant in the Fassanian, which is the only time interval where all of them feature a more lateral distribution, including neighbouring areas of E Iberia. Although these species are characterized by their long temporal ranges, some have been cited throughout the Triassic (Table 1. Appendix 2) and, most importantly, the age of their associations is consistent with ammonoid and conodont ages.

From a palaeogeographic perspective, all the bivalves species mentioned are frequent and common to the Alpine (Tethysian) and Germanic (northern) provinces. These are cosmopolitan elements as defined by Márquez-Aliaga (1985), and no endemic species are present in the studied series. However, we should emphasize that no Sephardic species appear, in contrast with the presence of Sephardic-provenance ammonoid and conodont species.

In palaeoecological terms (Table 2, Appendix 2), bivalves do not appear evenly distributed throughout the studied sections, rather they appear concentrated in some levels, commonly occurring as dense shell-beds typical of shallow-shelf environments and representing a mixed relic of original communities. The modes of life exhibited by the bivalve communities (Table 3, Appendix 2) include an abundance and diversity of shallow burrowers. These species are well adapted to high-energy, near-shore marine environments (Stanley, 1977). Epibyssate bivalves are not common, unlike endobysstates such *Hoernesia socialis*, which is one of the most abundant species. The presence of byssate cemented bivalves suggests the availability of a favourable hard substrate (Szente, 1997) in addition to the soft substrate inhabited by burrower bivalves. In contrast with the great variety shown in the Muschelkalk of the Nurra region (Punta del Lavatoio, Monte Santa Giusta and Monte Fogheras), the low diversity and abundance of the fauna recorded at the Monte Maggiore section could suggest the persistence of extreme environmental conditions during their deposition.

All recorded assemblages of foraminifers in the different area show a low diversity but are consistent with an Anisian-Ladinian age, although they all display a broad temporal and

palaeogeographical distribution. The most common genus is *Nodosaria* corresponding to calcareous benthic foraminifers. The genus *Involutina* is also present in the Alpine domain, and *Glomospirella* has also been reported in the Gres a Voltzia of Vosges, France (Koehn-Zaninetti et al., 1969). *Tolypammina* was recorded in the Letten-Koe (Uppermost Muschelkalk) of Luxembourg (Courel, 1978) and has also been described in the Triassic Levantine-Balearic domain of the Iberian Ranges, E Spain (Escudero-Mozo et al., 2015). With regards to their palaeoecology, the genera *Tolypammina* and *Planinvoluta* are sessile, which is typical of low- to medium energy environments. The rest of the species found are mostly benthic soft-ground dwellers typical of a low-energy environment.

6. Sedimentology and Sequence Stratigraphy

In this chapter a general review of the main sedimentary facies and depositional environments recognized in the Muschelkalk carbonates of Sardinia is presented with the aim of generating a solid basis for reconstructing regional palaeogeography and basin evolution. Also, we present a general approach to the sequence stratigraphy of the Muschelkalk in the considered area.

6.1. Facies and sedimentary environments

The facies analysis has been performed through field observation and petrographic analysis and consider previous approaches to the regional sedimentology (Costamagna, 2000; Costamagna et al., 2000; Posenato et al., 2002; Costamagna and Barca, 2002; Knaust and Costamagna, 2012; among others).

The Muschelkalk of Sardinia can be considered as generated in a broad shallow-water carbonate platform, which has been interpreted as a carbonate ramp (e.g., Costamagna and Barca, 2002). In this thesis, the different depositional environments of that ramp are separated following the “homoclinal” carbonate ramp model of Burchette and Wright (1992), which includes the three main zones: inner, middle and outer ramp. The inner ramp corresponds to the area situated over the fair-weather wave base. In Sardinia, it can be represented by sabkhas, tidal flats, lagoons and shoal-barrier settings. The middle ramp is situated between the storm-wave and the fair-weather-wave base levels, and is characterized by open marine settings, in which storm reworking is frequent and alternate with low-energy conditions over wide areas. Finally, the outer ramp marks the transition to basinal conditions. This area, which is situated under the storm-wave base level, is not clearly represented in the Muschelkalk of Sardinia.

Four main broad sedimentary environments can be differentiated in the Muschelkalk of Sardinia on the basis of facies assemblages (Tables 6.1 to 6.4). These are: 1) sabkha – muddy coastal plain 2) carbonate tidal flat 3) shallow low-energy subtidal (lagoon) 3) calcarenitic shoals and 5) middle ramp environment.

6.1.1 Sabkha – muddy coastal plain

This sedimentary environment has been inferred from the following facies associations (Table 1): S1) Dark brown marls and clayey marls with silt and clays alternation presenting rootlets and halite cubes pseudomorphs (Fig. 6.1: A); S2) Yellowish clayey marls (Fig. 6.1: B); S3) Dark brown clayey marls and dark clays alternation, rich in organic matter, presenting bioturbation (rootlets) and nodular pink satin spar (Fig. 6.1: C); S4) Dark clays and clayey marls alternation, rich in organic matter and lenses of pink satin spar (Fig. 6.1: C); S5) Yellow dolostones and lenticular dark clays horizons rich in organic matter and presenting paedogenetic processes; S6) Thin layered (mm to dm) yellow dolostones occasionally undulated or brecciated, presenting desiccation features; S7) Massive and badly stratified yellow dolostones warped by salt tectonics processes, presenting evaporitic pseudomorphs, quartz and calichified horizons (Fig. 6.1: D); S8) Massive, light yellow to reddish dolostones, brecciated, with evaporitic pseudomorphs and desiccation features (Fig. 6.1: E, F).

Sabkha, muddy coastal plain sedimentary environment					
Facies	Description	Color	Fossil content	Environment	Occurrence
S1	Marls - clayey marls - clay and silt alternation. Halite cubes pseudomorphs, rootlets	Dark brown to dark grey - black	Palynom.	Supralittoral muddy plain to sabkha	BN2, BCS, MN1
S2	Clayey marls	Yellowish - light grey	Palynom.		
S3	Nodular Satin Spar (SP) , clayey marls alternations and dark clays - rich in organic matter - rootlets	Marls: dark brown - brown SP: pink	Palynom.	Sabkha	BN2, BCS2, MN1
S4	Lenticular satin spar, dark clays rich in organic matter, rootlets and clayey marls	Marls: dark brown - brown SP: pink	Palynom.		
S5	Dolostones - lenticular dark clays - rich in organic and matter pedogenized horizons	Dolostones: yellow Clays: dark grey to dark green	Palynom.	Supralittoral coastal plain - hyperaline ponds	BCS2, MCS1
S6	Thin layered dolostones mm to dm occasionally undulated or brecciated with desiccation features	Yellow			
S7	Massive dolostones - warped by salt tectonics. Evaporitic pseudomorphs, quartz and calichified horizons	Light yellow to yellow			
S8	Massive dolostones - brecciated. Evaporitic pseudomorphs, desiccation features	Light yellow to yellow			

Table 6.1. Facies description of the sabkha, muddy plain sedimentary environment, showing the main characteristics of each facies (description, color, fossil content, environment, and occurrence)

Interpretation

The high variety of facies reveals mosaic of sub-environments in a supra-littoral setting, under the influence of variable hydric conditions and high evaporation. The dark clays (S1, S2, and S4) could indicate the persistence of a water table and prevailing reducing conditions, under which microfloristic remaind could be preserved. The marl-gypsum alternation could indicate episodes of periodic evaporitic precipitation and high rates of evaporation (e.g., Kendall, 1981). The dolostones and marly dolostones with evaporitic molds

and desiccation features could be interpreted as deposited in carbonate ponds due to the pronounced carbonatic influence, subject to periodic inundation (e.g., Ortí, 1974; Salvany and Ortí, 1987)

These facies associations and their fossil content are similar to the sabkha-muddy coastal plain systems described by Strohmenger et al. (2011) in the Abu Dhabi coast and Evans (2010) in different areas of the Persian Gulf.

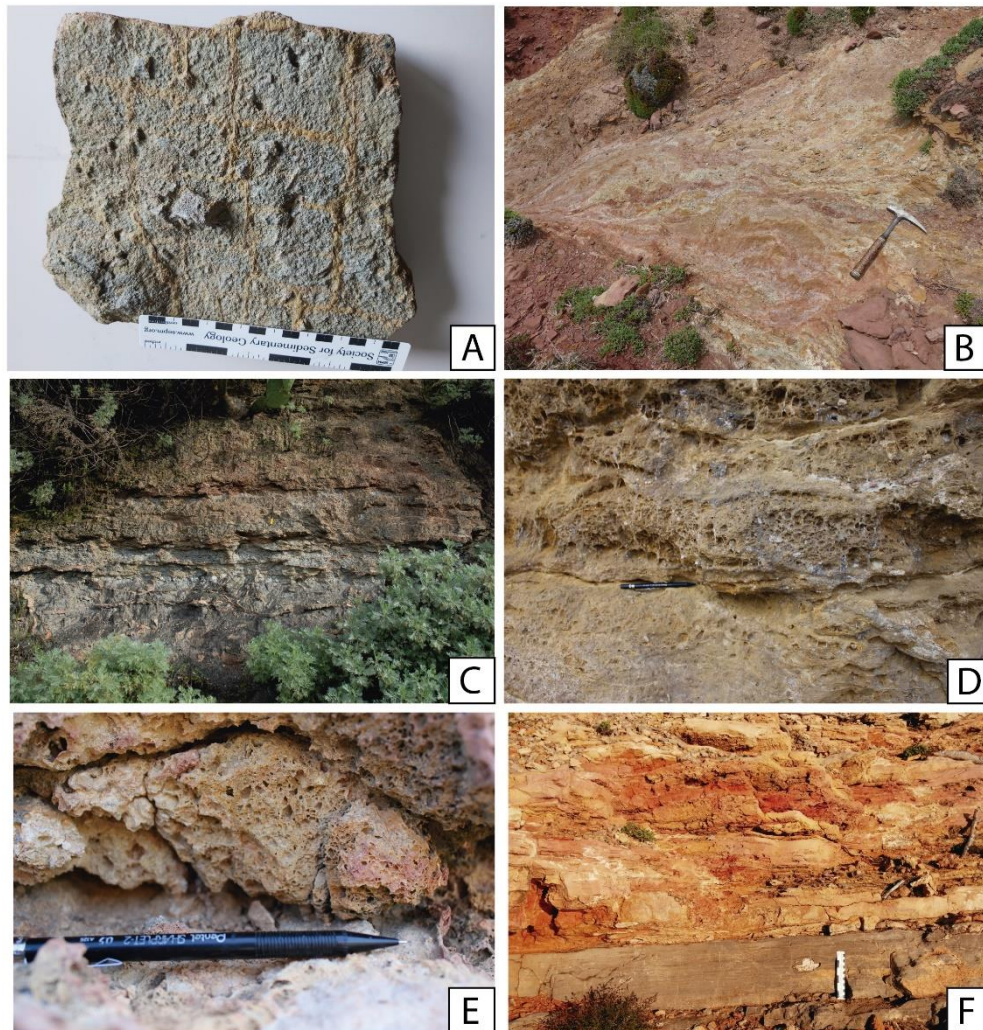


Fig. 6.1. Main characteristics of the sabkha, muddy plain depositional environment (E-F). A) halite pseudomorphs in calcarenitic matrix (Escalaplano Fm.) B) Rot like facies. Yellowish marls and reddish clayey marls located at the top of the Arenarie di Cala Viola Fm. C) Alternation of dark brown marls and grey clayey marls with lenticular and nodular pink satin spar (Escalaplano Fm.) D) Calichified and disrupted yellow dolostones (Punta S'Arridelli Fm.) E) Detail of the yellow dolostones of the Punta S'Arridelli Fm. showing molds of evaporitic minerals F) Yellow-reddish marly dolostones showing desiccation features and tepee structures (Punta Tonnara Fm.)

Location: This sedimentary environment has been defined in the Sarciano and Gerrei areas (CE), particularly in the Escalaplano Fm. (late Anisian), where facies S1 to S4 are predominant.

On the western coast, at the top Mb. of the Punta S'Arridelli Fm. In the Sulcis and Iglesias areas (SE), respectively in the upper part of the Punta Tonnara Fm. and in the Scollieddu Dolostones Fm., and in the lowest part of the Campumari Fm. In the Nurra, at the top of the Arenarie di Cala Viola Fm. and at the bottom of the Keuper. In these areas, the carbonate facies (S5 to S8) are dominant.

Overall, this sedimentary environment can be recognized through all of the island and shows similar features regionally. In a supra-regional level similar depositional systems can be found in Spain: in the "Muschelkalk Medio" and the Miravet Fm. (Keuper) in the Catalan Coastal Range, the Mas Fm. and the lower Keuper in the and Central Iberian Range, and the K1 unit of the Jarafuel Fm. in the Southern and Eastern Iberian Range (Ortí, 1974; Salvany and Ortí, 1987).

6.1.2 Carbonate tidal flats

The definition of this sedimentary environment is based in the following facies (Table 6.2):

Carbonate tidal flat sedimentary environment						
Facies	Description	Color	Fossil content	Microfacies	Environment	Occurrence
T1	Yellowish peloidal bioclastic dolomicrites (original textures: wackestone to packstone), often burrowed, in decimetre scale beds	Yellowish to grey	Scarce to none		High energy subtidal	MN1, MN2, MN6, MCS1, MCS2, MCS6, MCS7
T2	Dolomitic calcarenites. Bioclastic, peloidal or oolitic. Grainstone to packstone original textures, often showing cross-lamination and occasionally bidirectional palaeocurrents	Light grey		Dolomitic calcarenites. Ooids, bioclasts and bioclasts fragments, recrystallization	Intertidal	MN1, MN2, MN6, MCS1, MCS2, MCS6, MCS7
T3	Thin laminated (cm scale) dolomicrites. Faint planar to very low angle, tractive cross lamination	Light grey to yellow		Dolomicrite to dolosparite, porosity, evaporitic molds and scarce quartz fragments	Intertidal	MCS1, MCS2, MN1, MN2
T4	Microbialitic dolomicrites with stromatolitic lamination. Thin, planar lamination - desiccation features, evaporitic molds. Rare bioturbation	Light grey to yellow	Calcareous algae, forams bivalves, echinoderms (fragments)	Dolomicrite - Mudstone - peloids, bioclasts ghosts, low porosity, evaporitic molds, quartz	Intertidal	MN1, MN2, MN6, MCS1, MCS2, MCS6, MCS7
T5	Planar laminated (cm scale) to irregular microbialitic dolomicrites. Thin, planar and lamination - desiccation features, fenestrae, evaporitic molds	Light grey to yellow		Dolomicrite - Mudstone - peloids, bioclasts ghosts, low porosity, evaporitic molds, quartz, brecciated	Intertidal	MN1, MN2, MN6, MCS1, MCS2, MCS6, MCS7
T6	Irregular, laminated microbialitic dolomicrites with stromatolitic lamination. Desiccation features, evaporitic molds, tepee	Light grey to yellow		Dolomicrite - Mudstone - peloids, high porosity, evaporitic molds, quartz, brecciated and recrystallized	Supratidal (sabkha)	MN1, MN2, MN6, MCS1, MCS2, MCS6, MCS7
T7	Intraformational collapse breccias due to evaporites dissolution	Light grey		Brecciated dolomicrites	Supratidal (sabkha)	MN1, MN2, MN6, MCS1, MCS2, MCS6, MCS7
T8	Laminated dolomitic marls and clayey marls showing planar to cross lamination	Dark grey to yellow			Supratidal (sabkha)	MN1, MN2, MN6, MCS1, MCS2, MCS6, MCS7
T9	Thin bioclastic layers with irregular base, positively graded	Light grey	Calcareous algae, forams bivalves, echinoderms	Dolomicrite - Packstone to Grainstone - peloids, bioclasts fragments, ooids	Tempestites	MN1, MN2, MN6, MCS1, MCS2, MCS6, MCS7

Table 6.2. Facies description of the carbonate tidal flat depositional system showing the main characteristics of each facies (description, color, fossil content, environment, and occurrence).

This sedimentary environment has been inferred from the following facies associations: T1) Yellowish peloidal bioclastic dolomicrites (original textures: wackestone to packstone), often burrowed, in decimetre-scale beds (Fig. 6.2: A); T2) dolomitic calcarenites that can be bioclastic, peloidal or oolitic, with grainstone to packstone original textures, which often show cross-lamination. Occasionally bidirectional palaeocurrents can be inferred from cross-lamination (Fig. 6.2: B); T3) Light grey dolomicrites to dolosparites with parallel lamination to low angle cross lamination; T4) Planar to slightly domed, light grey to yellowish microbialitic

dolomicrites with stromatolitic lamination, often showing desiccation features and evaporitic molds. Rare bioturbation (Fig. 6.2: C); T5) Planar to domical or irregular, yellowish microbialitic dolomicrites with stromatolitic lamination showing desiccation features, evaporitic molds and tepee structures (Fig. 6.2: D); T6) Predominantly irregular yellowish microbialitic dolomicrites with stromatolite lamination, often brecciated with thin planar lamination, desiccation features, abundant evaporitic pseudomorphs and tepee structures (Fig. 6.2: E) T7) Intraformational, yellow collapse breccias due to evaporites dissolution (Fig. 6.2: F) T8) Dolomitic marls and clayey marls, dark grey to yellow, showing faint lamination.; T9) Thin bioclastic layers with irregular base, positively graded.

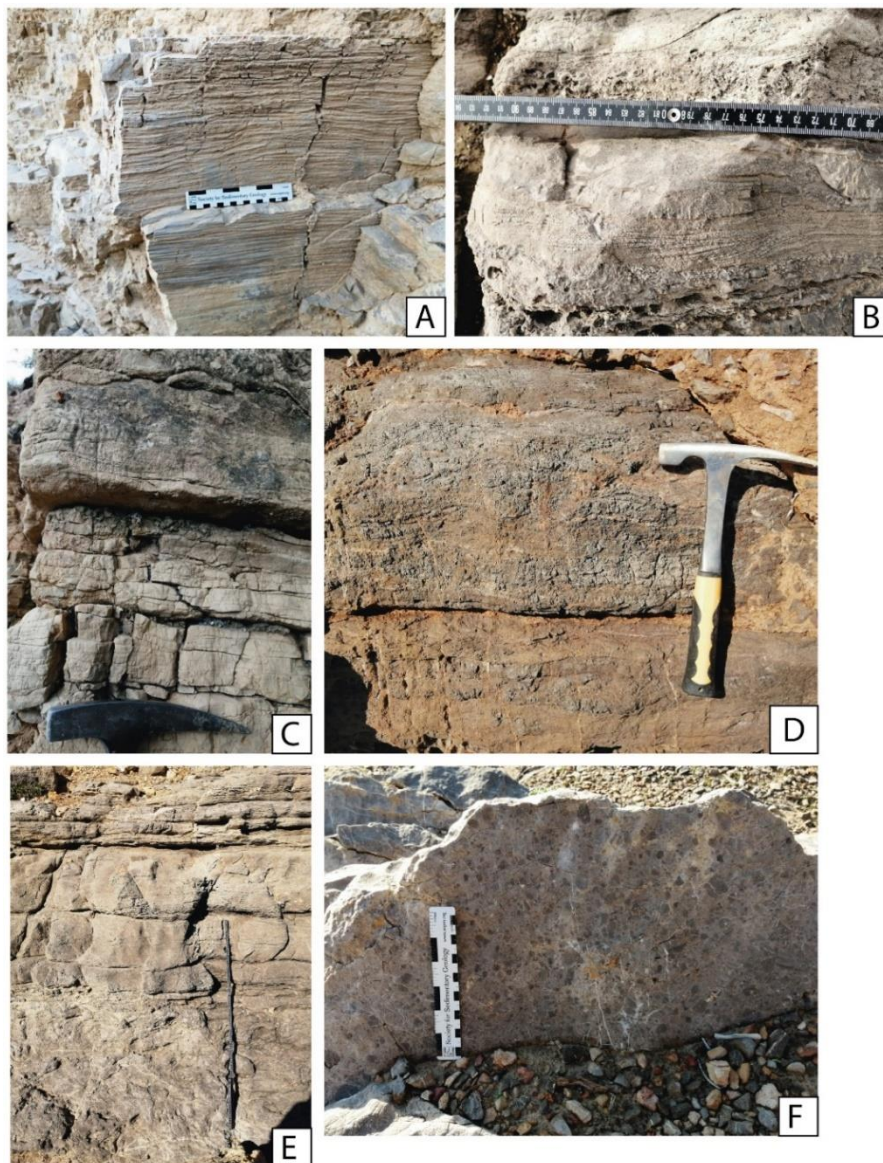


Fig. 6.2. Main characteristics of the carbonate tidal flat depositional environment (A-F). A) yellow, laminated dolostones (low angle cross lamination), (Monte Maggiore Fm.) B) dolo-arenites with ripple marks and positive gradation (Punta del Lavatoio Fm., Cala Bona) C) microbialitic lamination (Monte Maggiore Fm., Escalaplano) D) microbialitic domical lamination showing desiccation features (Punta del Lavatoio Fm., Cala Bona) E) thin layered grey to yellowish dolostones (Punta del Lavatoio Fm., Monte Fogheras) E) collapse breccias (Punta Tonnara Fm.).

Interpretation:

The identified facies association indicates the development of wide carbonate tidal flats, in which subtidal, intertidal, and supratidal settings can be differentiated (following interpretations based on Ren, 1986; James, 1984).

Subtidal conditions are represented dolomicrites and dolo-calcarenites, suggesting conditions dominated by either low and high energy conditions. These shallow subtidal facies are described below within the epigraphs of “lagoon” and “calcarenite shoals”.

Intertidal conditions are dominated by low energy conditions, although small tractive layers can also develop in response to tidal currents (T1 and T2). The main features of the intertidal zone are stromatolitic facies, mainly characterized by planar or slightly undulated laminations. The alternation of calcarenites and dolomicrites (T2) the grey dolostones with planar microbialitic lamination (T3), and irregular lamination (T4, T5) characterize the intertidal zone. These facies and their alternation indicate different moments and different energies within the tidal flat. The presence of calcarenites with current structures (ripples, lamination etc.) (T2) is the result of a more energetic event (tidal flow), and the dolomicrites are the results of a calmer, low energy condition that allows the settling of more fine-grained sediment. The persistence of low energy conditions within the tidal flat, allows the development of algal mats (T4, T5). Facies T6 indicates periodic subaerial exposure of the sediment, that could correspond to a more proximal part of the tidal flat, predominantly characterized by high evaporation rates and less frequent inundation episodes. It is only possible to find some benthic foraminifera, ostracods and bivalve fragments. This low diversity and scarceness indicate a restricted environment, characterized by hypersaline conditions, typical of arid climate.

T7, T8 and T9 are characteristic of a supratidal zone characterized by sabkha conditions. The breccias can be interpreted as the collapse of the evaporites following meteoric water interaction.

Facies of this association are commonly arranged in small shallowing-upwards cycles comparable to the “muddy” and “grainy” peritidal sequences defined by James (1984).

Location:

Tidal flat facies are well represented throughout all the lower part of the Sardinian Muschelkalk Group, but also in some cases it can be found at the top units of the Fms. in transition with the Keuper facies. In the Sulcis Iglesiente region, this facies association is

present in the Campumari Fm. and the P.ta Tonnara Fm. In the Campumari Fm. A similar situation is found in the P.ta Tonnara Fm., where tidal flat facies association are present in the upper part of the P.ta Tonnara outcrop. These deposits are probably related to the upper passage to the Keuper facies. This facies association, characterized by the alternation of centimetric to decimetric, shallow sequences, indicates the cyclicity of intertidal to supratidal conditions, which is typical of the upper units of the Muschelkalk also throughout Europe (Upper Muschelkalk – Catalan Coastal Range – Calvet et al., 1987; Upper Muschelkalk – Fm. Cañete etc.). This sedimentary environment is found as well in the lower and upper units of the Punta del Lavatoio Fm., in the Nurra region. In the Cala Bona outcrop, even if it is interested by a deep tectonization due to a fault zone, in the fault blocks it is possible to identify a well-developed tidal flat facies association (Fig.). This association is present also in the Monte Santa Giusta outcrop, both at the top (contact with the Buntsandstein facies) and at the bottom (proximity with the Keuper facies). The Monte Maggiore Fm. Outcropping in the Sarcidano Gerrei areas, shows similar features. Facies T2 T4 and T5 are predominant and characterize the lower members of this Fm. (Yellow Dolostones Member – Costamagna, 2002; Costamagna and Piro, 2022). It is however also possible to find tempeste layers with bioclasts accumulation (T9) (calcareous algae, Costamagna and Piro, 2022). On the other hand, the Punta Su Nuraxi Fm. lower member (Case Pisano Member – Costamagna, 2002) consists mainly of collapse breccias and massive dolostones with fenestrae and 95vaporate pseudomorphs.

6.1.3 Shallow subtidal low-energy environment (lagoon)

This sedimentary environment is defined by three facies (Table 6.3): I1) Dolostones and marly dolostones, yellow or light grey to dark brown, thinly laminated, with low to moderate degree of bioturbation and low fossiliferous content (Fig. 6.3: A, B); I2) Dolostones and marly dolostones, yellow or light grey to dark brown, thinly bedded (cm layers) nodular, with moderate to high degree of bioturbation and low fossiliferous content (Fig. 6.3: C); I3) Dolostones and marly dolostones, thinly laminated with bioclastic accumulation layers, erosive base, and positive gradation (Fig. 6.3: E F).

Inner carbonatic ramp sedimentary environment						
Facies	Description	Color	Fossil content	Microfacies	Environment	Occurrence
I1	Dolostones and marly dolostones, thinly laminated, with low to moderate degree of bioturbation and low fossiliferous content	yellow to dark brown or light grey to dark grey	Calcareous algae, forams bivalves, gastropods, echinoderms and ammonoids	dolomicrites with low to moderate bioturbation, peloids, bioclasts fragments	Low energy subtidal (lagoon)	MN5, MN6, MCS1, MCS2, MCS3
I2	Dolostones and marly dolostones, thinly laminated, cm banks, nodular, with moderate to high degree of bioturbation and low fossiliferous content			dolomicrites with moderate to high degree bioturbation. Reworked allochems: peloids, bioclasts fragments	Low energy subtidal (lagoon)	MN5, MN6, MCS1, MCS2, MCS3
I3	Dolostones and marly dolostones, thinly laminated, with bio-accumulation layers, erosive base and positive gradation	yellow to dark brown or dark grey		thinly laminated dolomicrites, and marly dolostones, showing bio-accumulation layers, grading upwards packstone to wackestone	Tempestite	MN5, MN6, MCS1, MCS2, MCS3
I4	Thinly laminated dolo-arenites with tractive structures (ripples, cross lamination)	Light grey to brownish grey		thinly laminated dolograinstones - and marly dolostones	High energy subtidal (shoals)	MN4, MCS5

Table 6.3. Facies description of the lagoon sedimentary environment showing the main characteristics of each facies (description, color, fossil content, environment, and occurrence).

Interpretation: The dolostones and marly dolostones with tabular aspect and nodular aspects are interpreted as the result of carbonate mud deposition in a low energy environment. It is possible to find interbedded levels with bioclast accumulations that can be the result of sediment remobilization during storms (tempestite events). This facies is often organized in metric-scale thick successions. Abundant fossils are found in these deposits. It is possible to find beds with bivalves, ammonoids, gastropods, conodonts, calcareous algae etc. The presence of bioturbation (moderate to consistent) indicates that the sediments were well-oxygenated (Savrda and Bottjer, 1986; Martín, 2004). Occasionally, the conditions can be more restricted. In summary this facies association indicates a type of environment characterized by sedimentation of carbonatic muds (peloidal and bioclastic), highly bioturbated and only affected occasionally by higher energy storm events (James, 1984).

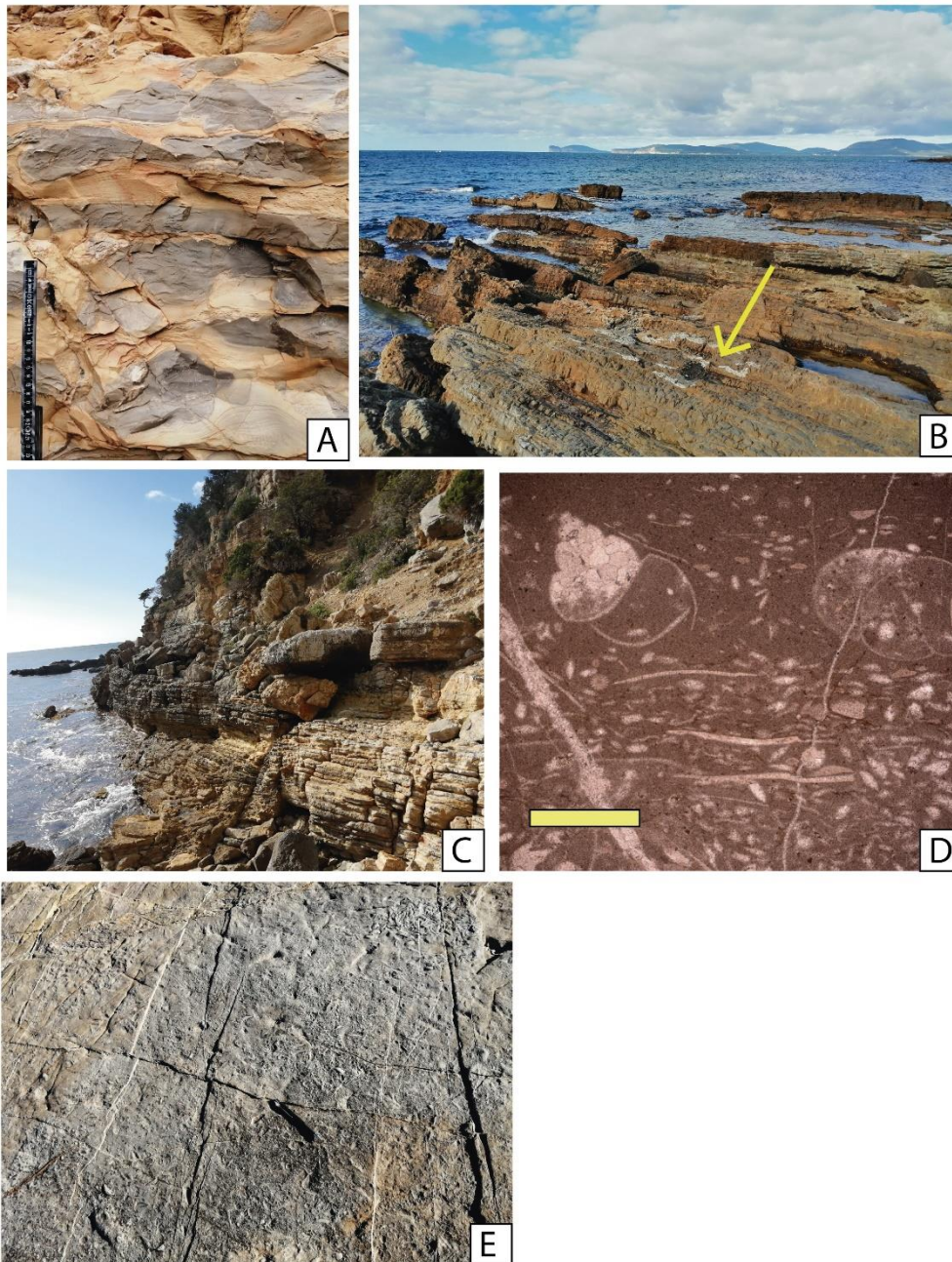


Fig. 6.3 Main characteristics of the low energy, intertidal environment (A-E). A) yellow laminated marls and grey limestones (Punta del Lavatoio Fm., Monte Fogheras). B) Grey dolostones and yellow marl intercalations. Yellow arrow indicates the polarity of the succession, which is overturned. (Punta del Lavatoio Fm., Alghero) C) Grey dolostones and yellow marls intercalations (Punta del Lavatoio Fm., Monte Fogheras) D) wackestone, accumulation of forams, bivalves and gastropods (Punta del Lavatoio Fm., Alghero). Scale bar: 1mm E) surface of bioclastic accumulation (Punta del Lavatoio Fm., Alghero – overturned succession)

Location: It is possible to find these deposits very well represented in Punta del Lavatoio Fm. outcropping in the seaside of Alghero, in the Monte Fogheras outcrop and in the Monte Santa Giusta outcrop, where these deposits form meter-scale shallowing upwards sequences. It is found also in the lowest part of the Punta Tonnara Fm. located in the locality of Porto Pino.

6.1.4 Shallow subtidal high-energy environment (calcarenic shoals)

This environment (Table 6.2) is defined by (dolomitized) calcarenic banks that often show cross stratification at different scales and internal erosive surfaces. Original microfacies can be oolitic or bioclastic. The bioclastic levels are formed mainly by fragments of bivalves, forams and echinoderms (Fig.6.4).

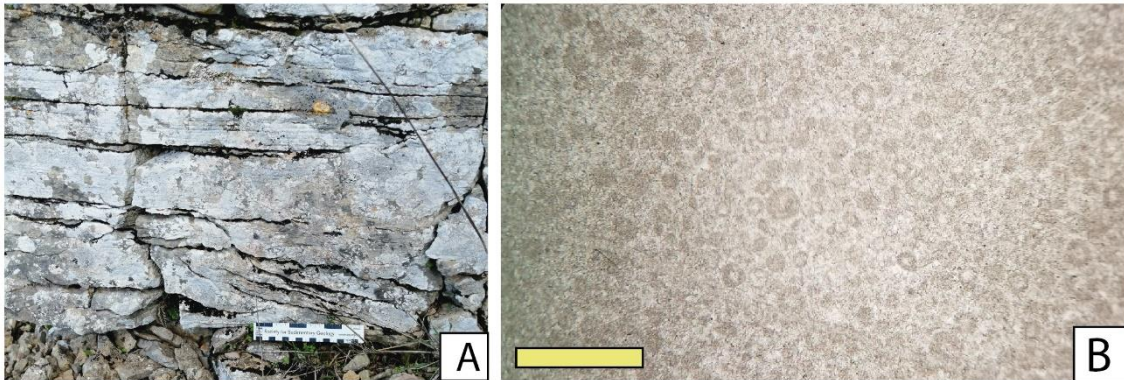


Fig. 6.4 Main characteristics of the carbonate inner ramp depositional environment of high energy (A-D). A) Dolo-arenitic banks showing cross stratification, (Monte Maggiore Fm., Monte Maggiore) B) Oolitic grainstone (Punta del Lavatoio Fm., Monte Santa Giusta). Scale: 1mm.

Interpretation: This facies association is typical of high energy – subtidal environments in the inner ramp, these characterized by the development of calcarenitic shoals, that can act as barriers between the middle ramp and the inner ramp.

Location: These facies are often found in metric banks, such as in the Punta del Lavatoio Fm. and the Punta Tonnara Fm., and in a smaller scale in the uppermost part of the Monte Maggiore Fm. In Spain, these facies are found in the base of the Cañete Fm. in the Iberian Range, in the Middle Muschelkalk of the Southern Catalan Range and the Monte Toro Fm. in Minorca.

6.1.5 Middle ramp sedimentary environment

This sedimentary environment is characterized by deposition of carbonate under low energy conditions (below the fairweather wave base) but punctuated by the remobilization caused by storms (above the stormwave base) that caused tempestite levels often showing cross lamination including HCS (Table 6.4)

Main facies include: M1) Dark brown to dark grey dolostones and marly dolostones, moderately bioturbated (Fig. 6.5: A); M2) Dark brown to dark grey nodular dolostones and marly dolostones, intensely bioturbated, which can show a faint lamination, probably microbialitic (Fig. 6.5: B); M3) Centimetre scale beds consisting of bioclastic dolostones to

marly dolostones, often laminated and showing positive gradation (Fig. 6.5: C) M4) Nodular dark brown to dark grey bioturbated dolomicrites (Fig. 6.5: B, D,E); M5) Bioclastic laminated dolostones that can show wavy bedding or hummocky cross stratification (Fig.6.5: D).

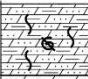


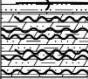

Mid ramp sedimentary environment						
Facies	Description	Color	Fossil content	Microfacies	Environment	Occurrence
M1	 Dolostones and marly dolostones, moderately bioturbated	dark brown - dark grey	Calcareous algae, forams bivalves, gastropods, echinoderms and ammonoids	dolomicrites with low to moderate bioturbation, peloids, bioclasts fragments	Low energy between fairweather wave base and stormwave base	MN2, MN3, MCS4, MCS5
M2	 Dolostones and marly dolostones, intensely bioturbated and nodular, can show microbialitic lamination	dark brown - dark grey		dolomicrites with moderate to high degree bioturbation. Completely reworked allochems: peloids, bioclasts fragments		
M3	 dolostones and marly dolostones, thinly laminated, with bio-accumulation layers	dark brown - light gray to dark grey		thinly laminated dolomicrites, and marly dolostones, showing bio-accumulation layers, grading upwards	Tempestite	
M4	 Nodular dolomicrites, with bioturbation, layers surfaces are difficult to distinguish	dark brown - dark grey		dolomudstone with low fossiliferous content, pellets and faint lamination	Low energy between fairweather wave base and stormwave base	
M5	 Bioclastic laminated dolostones that can show wavy bedding or hummocky cross stratification	dark grey to light grey		thinly laminated dolomicrites and marly dolostones	High energy	

Table 6.4. Facies description of the mid ramp depositional system showing the main characteristics of each facies (description, color, fossil content, environment, and occurrence)

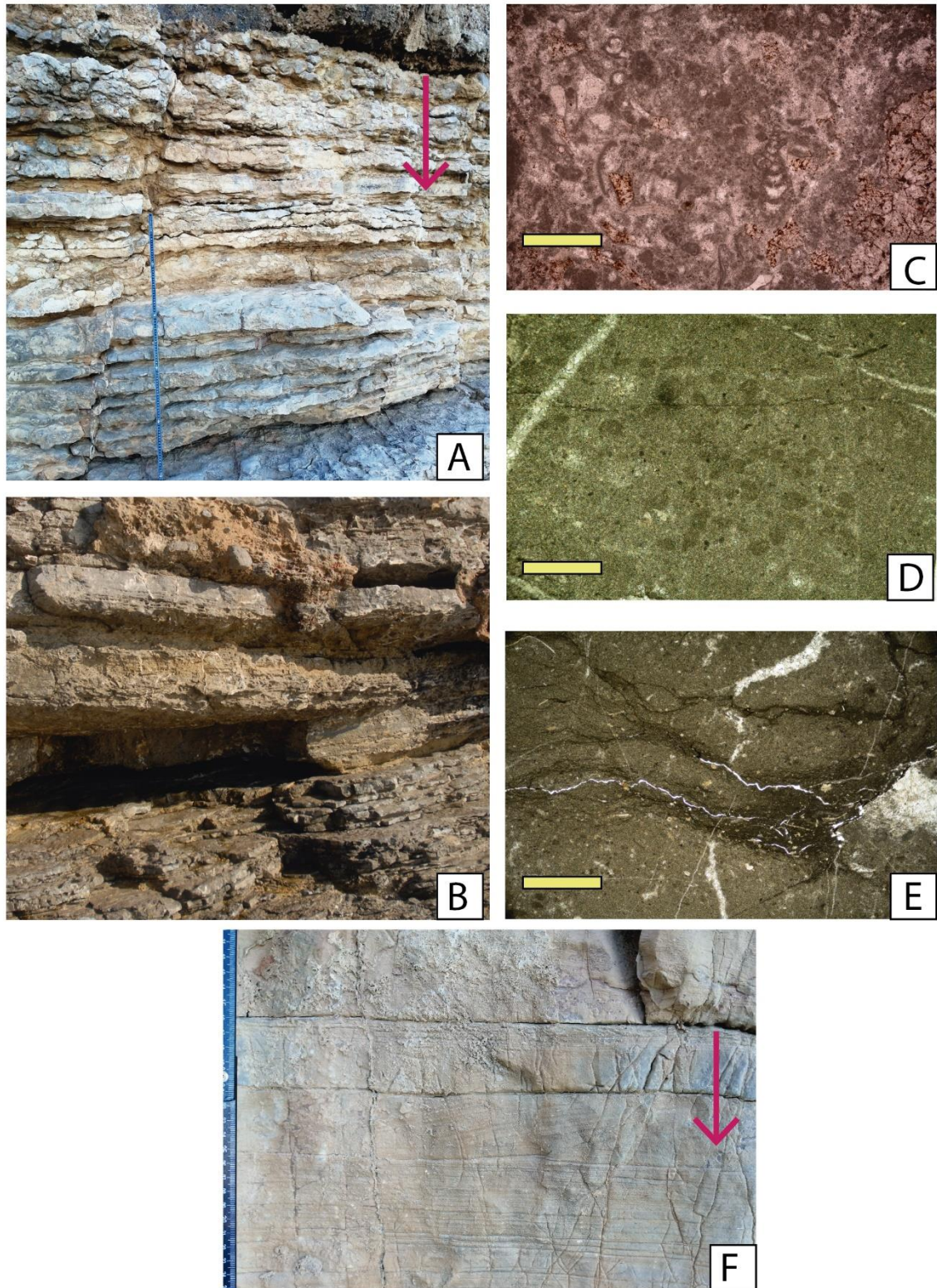


Fig. 6.6. Main characteristics of the carbonate mid ramp depositional environment: A) nodular yellow dolostones and yellow marls intercalations. Red arrow shows the inverse polarity of the succession (Punta del Lavatoio Fm., Alghero); B) Dark brown dolostones and nodular, yellowish dolostones with yellow marls intercalations (Punta Tonnara Fm., Porto Pino); C) bioclastic packstone with dolomitic recrystallization (Punta del Lavatoio Fm., Alghero); D) Peloidal dolomicrite (Punta del Lavatoio Fm., Alghero); E) bioturbated dolomudstone with bioclasts fragments and porosity (Punta Tonnara Fm., Porto Pino); F) Dolo-arenitic banks showing cross lamination (shoals) (Punta del Lavatoio Fm., Alghero). Red arrow shows the inverse polarity of the succession.

Interpretation: The presence of nodular and marly dolostones characterize a low energy environment where the settling of carbonatic mud is the main process. However, the sea bottom become episodically affected by oscillatory and tractive flows, these being interpreted as the result of storm waves and currents. These alternating conditions can be found between the fairweather storm base and the stormwave base. In particular, the presence of faint microbialitic lamination has been described in these types of facies by different authors (Pruss and Bottjer, 2004; Woods, 2009).

Location: These facies association is present in the lowest part of the Punta Tonnara outcrop in the Sulcis Iglesiente region, and in the lowest member (Member A) of Punta del Lavatoio Fm., in the Punta del Lavatoio outcrop.

6.2 Depositional Megasequence

As previously mentioned, the Muschelkalk of Sardinia can be considered as generated in a wide shallow-water carbonate ramp in which sedimentary facies range from sabkha coastal plains to the mid ramp settings. This broad carbonate ramp accumulated during a period of approximately 5-6 million years (late Illyrian to latest Longobardian) and records a major transgressive – regressive cycle (Fig. 6.7), which can be assimilable to a 2nd order cycle in the sense of Vail et al. (1991). This sequence is particularly well developed and continuous in the Nurra Region, especially in the Monte Santa Giusta area, although it has been found in complete stratigraphical continuity only in the subsurface (Cugiareddu Well). The sequence is constituted by the upper part of the Buntsanstein (Röt like facies), the different formations that represent the Muschelkalk (see previous chapters) and the lower part of the Keuper.

The study of the facies associations and the regional evolution of the depositional systems allowed to distinguish three large-scale systems tracts (Fig. 6.7) in the carbonate ramp that forms the Muschelkalk of Sardinia. Following the systems tract nomenclature proposed by Plint and Nummedal (2000) (modified after Posamentier and Vail, 1988) these are: lowstand systems tract, transgressive systems tract, and highstand systems tract.

The lowstand systems tract (LST) corresponds to a rise in accommodation (relative sea level) that allow sedimentary accumulation of continental to coastal plain deposits before the major transgressive episode that marks the onset of the carbonate ramp. It comprises, from north to south the upper part of the: 1) Arenarie di Cala Viola Fm., Punta S'Arridelli Fm., Escalaplano Fm., Riu is Corras Fm. These Fms. belong all to the Sardinian Buntsandstein group and present a Rot like facies.

The transgressive systems tract (TST) corresponds to a rapid sea level rise period during which accommodation rates exceed accumulation. This transgressive episode defines the installation of the carbonate ramp.

Firstly, it led to the development of tidal flat systems, rapidly followed by wide calcarenite shoal complexes (high energy subtidal environments) and, to a lesser extent, protected lagoonal settings. It is possible to observe the first step in the lowest member of the 1) Punta del Lavatoio Fm. (Monte Fogheras, Cala Bona and Monte Santa Giusta outcrops), 2) Monte Maggiore Fm., 3) Punta su Nuraxi Fm., 4) Campumari Fm. In particular, in the Punta del Lavatoio Fm. It is clearly possible to observe the expression of this transgressive pulse, especially in the Alghero outcrop and in the Monte Santa Giusta outcrop. There, the tidal flat facies are directly overlain by middle ramp facies.

The highstand system tract (HST) is defined by a normal regression outlined by a progressive shallowing upwards trend observable in the upper – middle part of the Muschelkalk elsewhere in Sardina. The middle ramp systems pass upwards to inner ramp environments. This passage is marked by few meters of shoals, progressively passing upwards to a more protected lagoonal environment and then into tidal flats. Finally, these tidal flat systems gradually change into coastal sabkhas that marks the transition from the Muschelkalk to the Keuper facies.

The HST is clearly represented in the upper Mb. of the Punta del Lavatoio Fm. and the lower part of the Keuper of the Nurra, the Punta Tonnara Fm., the uppermost part of the Monte Maggiore Fm. and the Punta su Nuraxi Fm.

The upper limit of this sequence is difficult to locate, but it is possible to hypothesize its presence in a slumped level located in the Alghero outcrop, and in the upper part of the Monte Santa Giusta outcrop, and somewhere in the Monte Fogheras outcrop, which presents different erosional surfaces (Fig. 6.7).

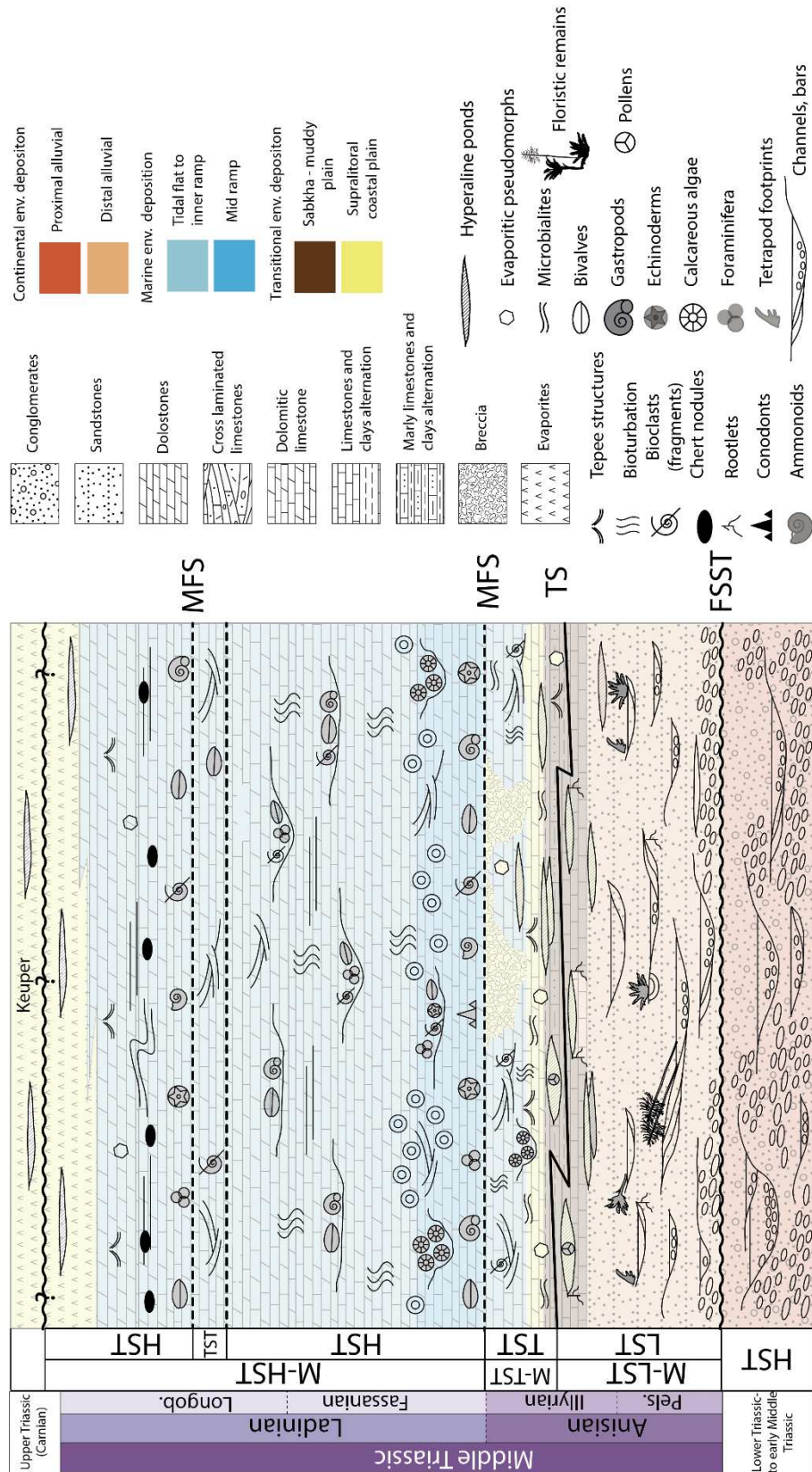


Fig. 6.7. Sequence stratigraphy scheme showing the main system tracts identified in the study. M-LST: Mega Lowstand System tract. M-TST: Mega Transgressive System Tract. M-HST: Mega Highstand System Tract. HST: Highstand System Tract. LST: Lowstand System Tract. TST: Transgressive System Tract. FSST: Falling Stage System Tract. MFS: Maximum Flooding surface. TS: Transgressive Surface.

6.2.1 3rd order Depositional Sequences

Within the identified depositional megasequence, it has been possible to differentiate five main III^o order depositional sequences: DSI, DSII, DSIII and DS IV (Figs. 6.8 and 6.9).

Depositional Sequence I (DS-I)

This sequence corresponds to a progradational stacking pattern and a progressive increase in marine influence.

Sarcidano – Gerrei

Towards the south of Escalaplano village (Fig. 6.10: A), the association mainly consists of Röt-like facies consisting of dark clays (dark grey to dark brown) with brownish marls intercalations (with rootles traces), and lenses / disrupted layers of pink satin spar – gypsum. The dark clays could indicate the persistence of a water table, in which the main process is the settling of pelites. The dark color of the clays could also indicate reducing conditions, and the marls - gypsum intercalation episodes of periodic carbonate inputs and high rates of evaporation – precipitation of salts.

Towards the north of Escalaplano village (Arcu is Fronestas section), it is possible to observe a very similar facies association. Dark clays (dark grey to reddish grey) and yellowish marls – calcarenites intercalations. In this locality, the satin – spar lenses are not found, instead it is possible to observe the presence of halite cubes in the marls – calcarenites intercalations.

These facies associations within the Escalaplano Fm. could indicate a mud flat sabkha – middle to distal coastal plain, with local interdigitation of shallow lagoon environment extending towards the inner plain.

Nurra

It is possible to observe a thin, in place horizon at the top of the Buntsandstein facies, in the Cala Bona outcrop (Fig. 6.11.: A), as alternation of thin grey-yellowish marls and grey-greenish clays. As mentioned, a more developed and complete succession has been described and studied through the Cugiareddu Well. Here at the top of the Buntsandstein, a facies association consisting of dark clays and dolomitic marls has been found bearing microfloristic associations.

Arburese

The top of the Punta S'Arridelli Fm. consists of yellow to reddish massive, brecciated dolostones, with disrupted and calichified horizons and evaporitic pseudomorphs. It is not possible to distinguish a clear stratification. This facies association can be interpreted as evaporitic ponds, within a sabkha environment.

Depositional Sequence II (DS-II)

This sequence corresponds to the instauration of the first, ephemeral carbonate ramp on the island after a transgressive pulse that can be identified at the base of the Muschelkalk group Fms. This sequence also marks the beginning of the M-TST. Overall, this sequence does not hold a various fossiliferous content, but, where present, it is possible to ascribe it to an upper Anisian (Illyrian).

Nurra

In the Cala Bona outcrop, it is possible to identify a well-developed tidal flat facies association (Fig.), which overlains the Rot-like deposits and marks the first transgressive pulse TST.II. This facies association is present also in the Monte Santa Giusta outcrop and has been studied at the base of the Muschelkalk in the subsurface of the Cugiareddu Well. The presence of calcarenites and oolitic grainstones with ripples with a positive gradation, and their association with disrupted and brecciated microbialitic dolomicrites with desiccation features, and bioturbation traces, testifies the onset of the TST.II, and the gradual passage to a progradational to aggradational pattern of the sequence leading to less energetic conditions.

Iglesiente.

Here it is possible to find the association of yellow, thinly laminated dolostones with dark clays intercalations, followed by thinly laminated yellow dolostones warped and disrupted by evaporite tectonics. The dark color of the clays indicates a reducing environment, and the preservation and presence of microfloristic association, and a persistence of thin water table where the settling of pelites is the main process. The dolostones and marly dolostones show evaporitic molds and desiccation features, this could be interpreted as ponds within a distal coastal plain, due to the pronounced carbonatic influence, subject to periodic inundation.

Sarcidano-Gerrei.

The Monte Maggiore Fm. The lower members of this Fm. (Yellow Dolostones Member.) shows tempestitic layers with bioclasts accumulation (calcareous algae, Costamagna and Piros,

2022) which could be correlated with a high energy setting of the carbonate platform and the mfs of the TST.II.

Arburese

In the Punta Su Nuraxi Fm. lower member (Case Pisano member – Costamagna, 2002) consists mainly of collapse breccias and massive dolostones with fenestrae and evaporitic pseudomorphs. It is difficult to identify the boundaries of the sequence here due to the massive presence (about 20m) of collapse breccias. In any case, the presence of a depositional sequence which marks the TST.II transgression event, is testified by a sharp contact between the upper member of the Punta S'Arridelli Fm.

Depositional Sequence III (DS-III)

This sequence starts with a rapid, second transgressive pulse that can be well observed through the Island and brings to the setting of a more open carbonate platform environment. The related maximum flooding surface at the top of this transgressive pulse marks the start of the MHST. By means of fossiliferous associations, this depositional sequence is dated Ladinian.

Nurra.

In the Punta del Lavatoio Fm. (Fig. 6.11: B) It is clearly possible to observe the expression of this transgressive pulse, especially in the Alghero outcrop and in the Monte Santa Giusta outcrop. There, the tidal flat facies are sharply overlain by a middle ramp facies, marking the mfs of the TST.III, which passes upwards to an inner ramp environment. This passage is marked by few meters of shoals, progressively passing upwards to a more protected lagoonal environment characterized by peritidal cycles (Lithofacies C – Punta del Lavatoio Fm.).

Arburese

In the Punta su Nuraxi Fm. The passage to the upper member is marked by the setting of more open carbonate platform environment. The mfs of the TST.III could be in correspondence of the first bioclastic and laminated levels at the bottom of the Bruncu Zippiri Mb.

Sarcidano-Gerrei

In the Monte Maggiore Fm., at the bottom of the Blue Limestones Fm. it is uncertain the precise position of the mfs related to the TST.III, but it could be placed in correspondence of the first bioclastic layers and laminated dolostones. Moving upwards, the highstand develops within different peritidal cycles that progressively mark a shallowing sequence and corresponds to the upper part of the DS-III.

Depositional Sequence IV

This sequence is found within the MHST and consists on its topmost part, following a second, brief transgressive pulse. It represents the passage to a very quickly progradation highstand setting, passing from inner ramp carbonate platform to evaporitic environment settings.

Nurra

The base of the TST.IV and the position of its relative mfs could be located within the oolitic shoals outcropping at the top of the Mt. Santa Giusta section. In the Punta del Lavatoio section (Fig. 6.11: D), it could be located in correspondence to the last consistent bioaccumulation levels, between MN5 and MN6. At Monte Fogheras (Fig. 6.11: C), this moment could be identified in the bioclastic accumulations at the bottom part of the section, where ammonoids, bivalves, gastropods and calcareous algae have been found.

Sulcis

In the Punta Tonnara section (Fig. 6.10: B), the shoal banks showing cross lamination, bioclasts accumulation marks a transgressive episode that could correspond to the TST.IV. In few meters, it is possible to observe upwards a very rapid passage to a proximal inner ramp.

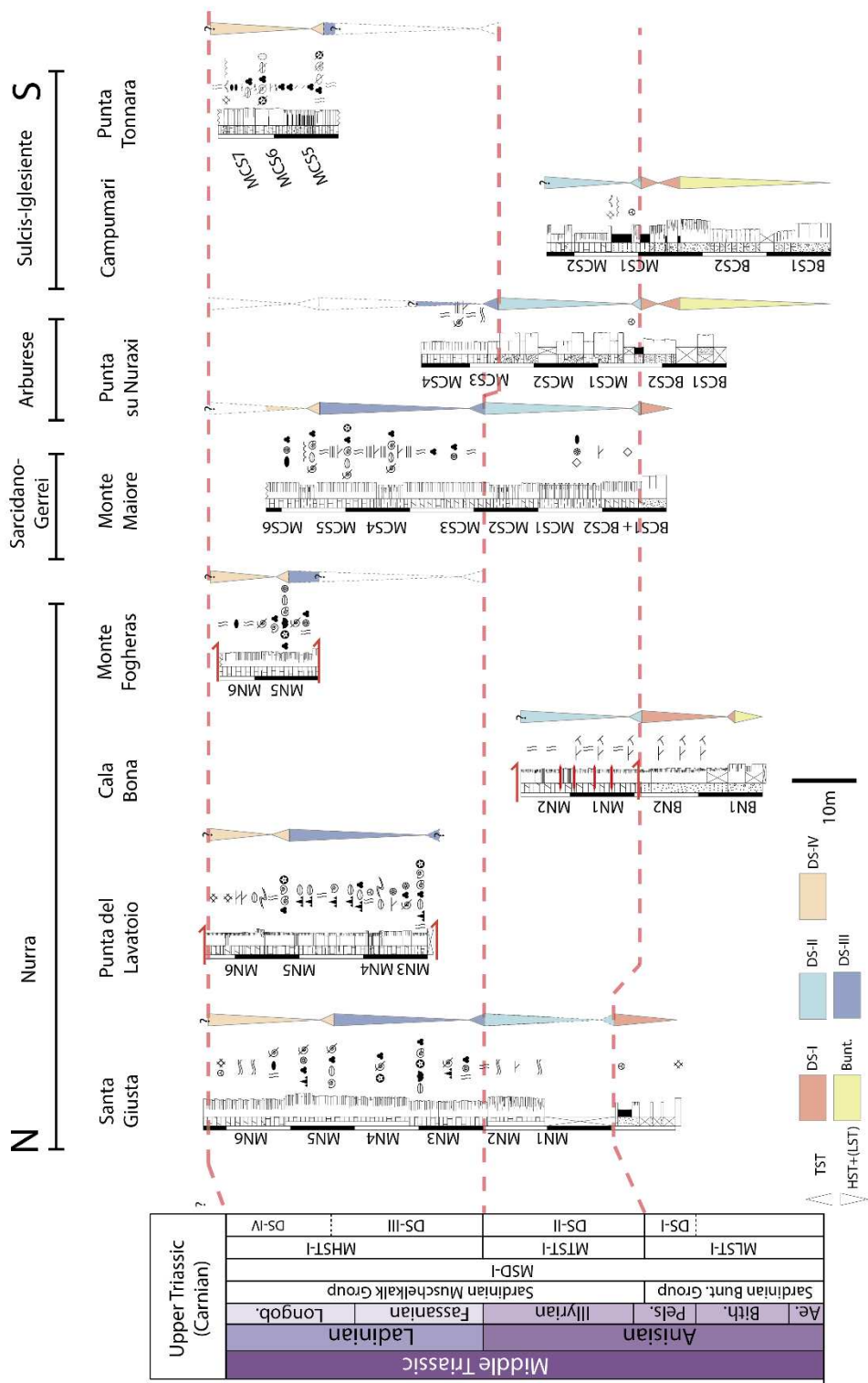


Fig. 6.8. Depositional sequences and interpretation of the depositional Megasequence.

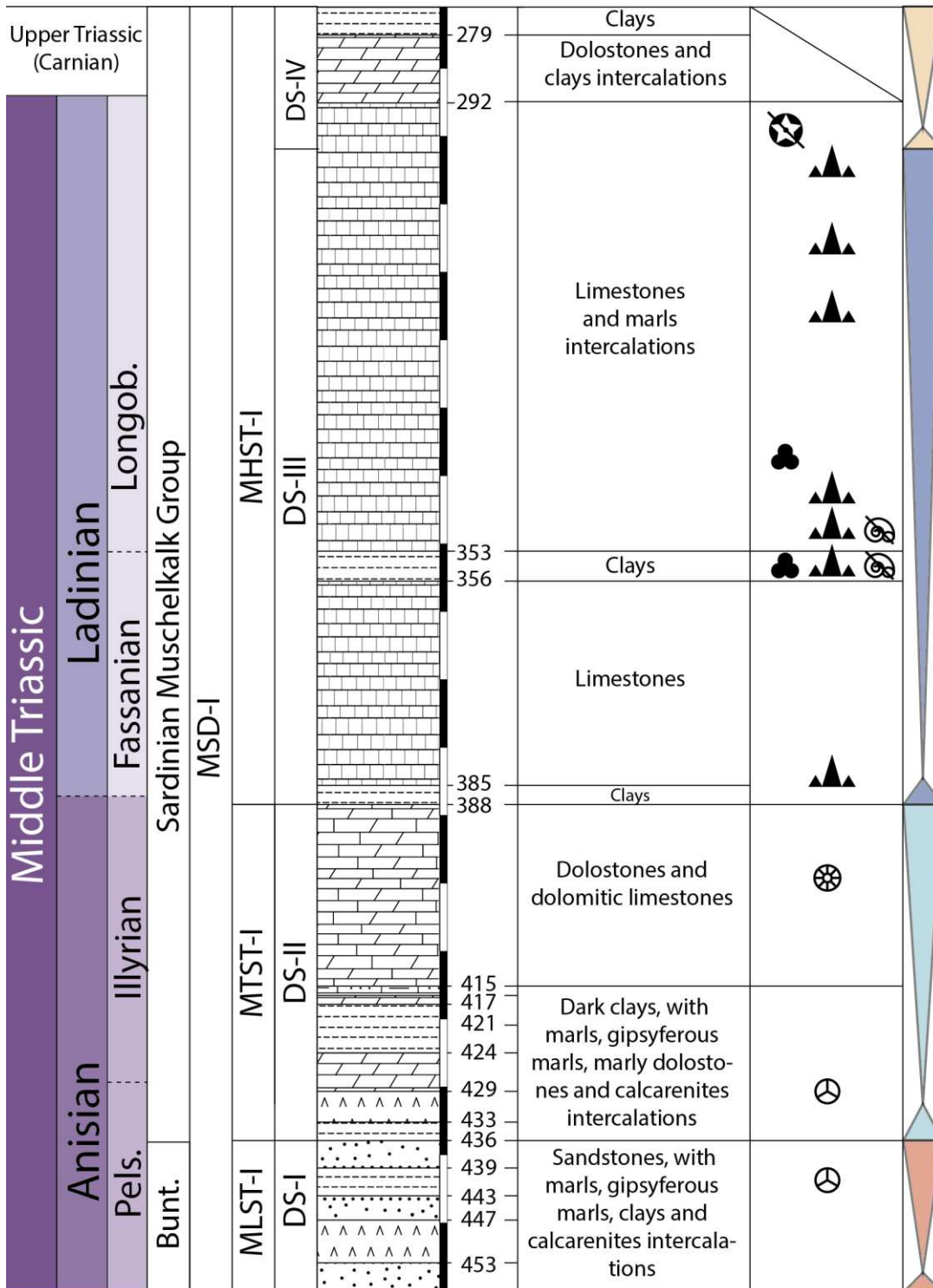


Fig. 6.9: Cugiarreddu well log (modified after Cherchi and Schroeder, 1985)

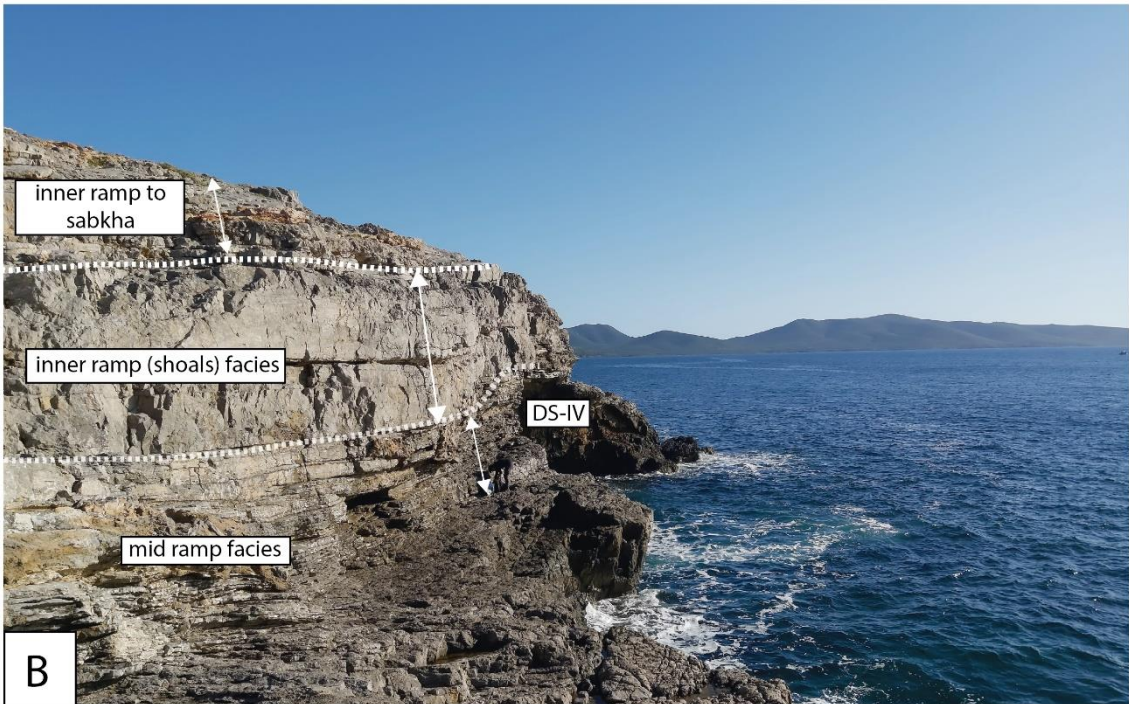


Fig. 6.10.: A) boundary between the Escalaplano Fm. and the Monte Maiore Fm. (Sarcidano area) B) Punta Tonnara outcrop (Punta Tonnara Fm., Sulcis).

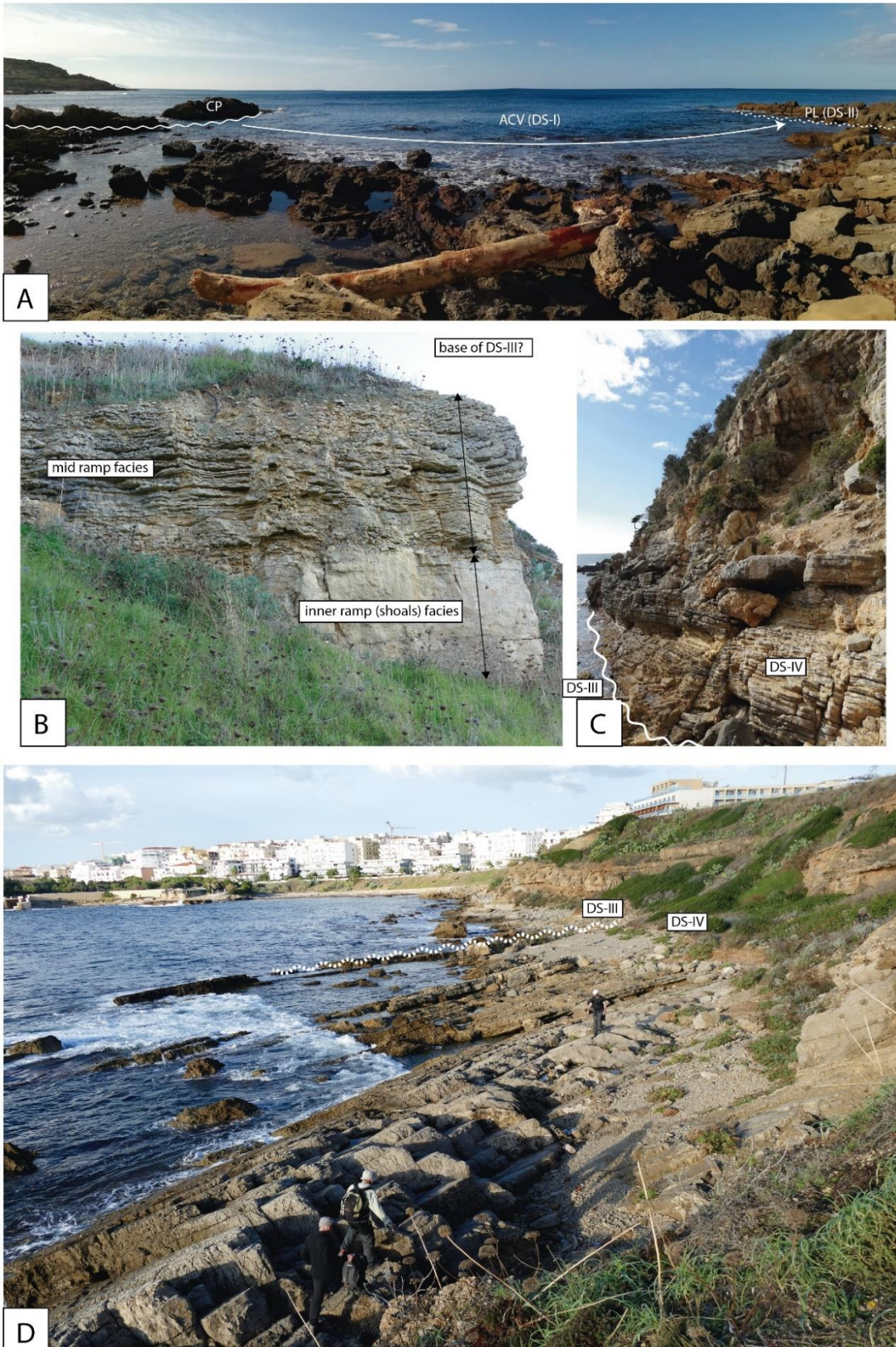


Fig. 6.11. Nurra outcrops showing the main boundaries of the discussed sequences in the text. A) Cala Bona outcrop B) base of the Punta del Lavatoio outcrop C) Monte Fogheras outcrop D) top part of the Punta del Lavatoio outcrop

6.3 Correlation with Western Peri-Tethys areas (Iberian Ranges and Minorca)

Interregionally, the 2nd order depositional sequence of the Sardinian Muschelkalk finds its equivalence in different basins of Spain (Mega-Depositional Sequence-II of Escudero-Mozo, 2015 and equivalents) (Fig. 6.12). The large-scale transgressive-regressive pattern is well-defined in these basins. In the Iberian Range, the MSD-II has a variable thickness, increasing towards E, and can reach a maximum thickness of 120m in the Mediterranean and Levantine-Balearic domain. It is represented by the upper part of the Mas Fm., the Cañete Fm. and the first unit (Jarafuel Fm) of the Keuper facies. In the Catalan Coastal Ranges, it is represented by the upper part of the “Middle Muschelkalk” unit, the “Upper Muschelkalk” and the lower part of the Keuper facies, while in Minorca it is represented by the Röt facies, the Monte Toro Fm. and the Arenal d’en Castell Fm. It should be noted that, unlike the Iberian Range – Coastal Catalan range, Levantine balearic Domain and Menorca – Castellon areas, the outer ramp – distal middle ramp systems do not appear in Sardinia.

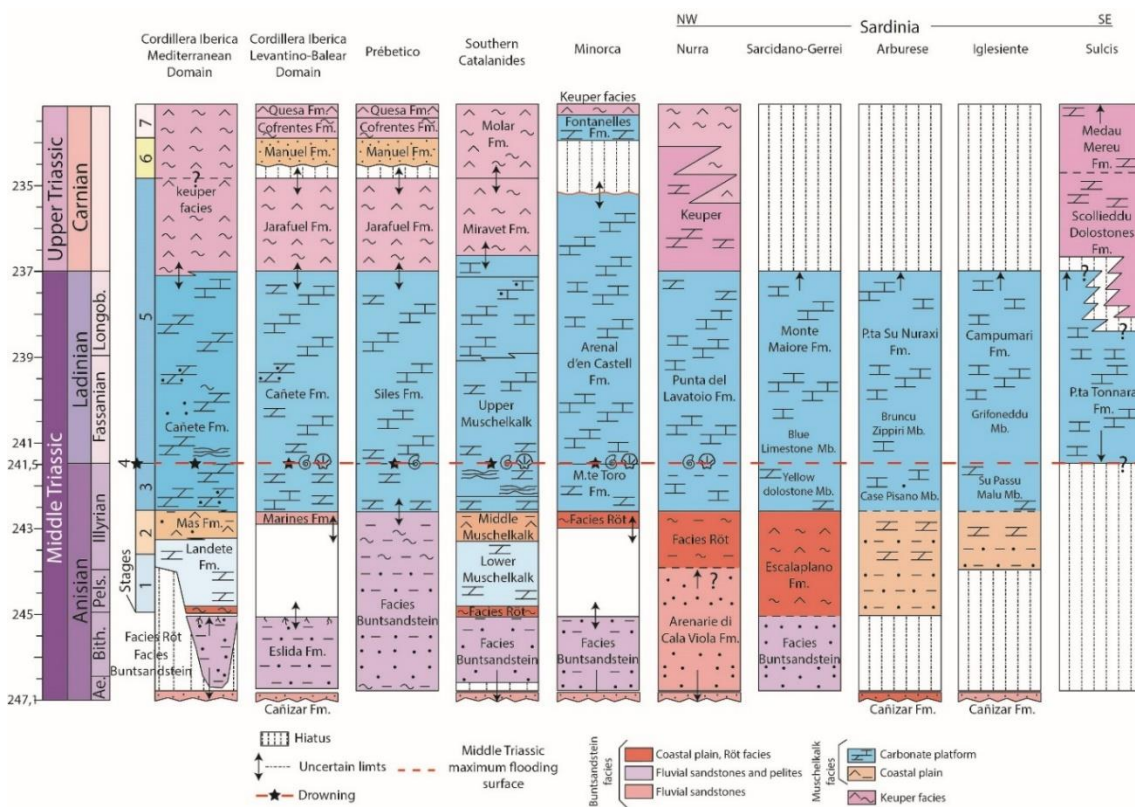


Fig. 6.12 Stratigraphic correlation of the different units of the Middle and Upper Triassic and of the main stages identified in the Muschelkalk facies along the basins that made up the western and northwest of Tethys Modified from (Escudero-Mozo, PhD thesis 2015). Betics (Pérez-Valera, 2005; Pérez-Valera and Pérez-López, 2008); correlation between different facies of the Keuper (Salvany and Ortí, 1987; Pérez-López et al., 1996; Arche and López-Gómez, 2014). Sardinia (Knaust and Costamagna, 2012; Costamagna, 2002).

It should be noted however that the Muschelkalk facies in some parts of the Iberian Ranges includes older units (late Bithynian to early Illyrian) that do not exist in Sardinia nor in some regions of Spain such as the Castellón Area and the Minorca Island (Escudero Mozo, 2015). These areas constituted topographical highs until the late Illyrian, as probably the area of Sardinia did. These older carbonates in Spain define another 2nd order transgressive-regressive sequence (Mega-Depositional Sequence – II of Escudero-Mozo, 2015).

7. Geochemistry

7.1 Introduction

The aim of this chapter is to present the first stable oxygen and carbon isotope records of the Muschelkalk carbonates in Sardinia. For this, five columns with good outcrop conditions and good stratigraphic control were chosen. For this study, 4 different columns have been analyzed through C, O and Sr. Two are found in the Nurra region and belongs to the Punta del Lavatoio Fm. and are the Punta del Lavatoio outcrop (seaside of Alghero city) and Monte St. Giusta, in the Northern part of the Nurra. One section is found in the Sarcidano-Gerrei area, in the Nureci village area, and belongs to the Monte Maggiore Fm. The fourth analyzed section is found in the seaside promontory of Punta Tonnara, in the locality of Porto Pino (Sulcis).

It is intended that the isotopic records included in this Thesis form a first chemostratigraphic approximation that could serve as a basis for future work on the sedimentary and diagenetic evolution of the Muschelkalk carbonate platforms of Sardinia. It should be noted, however, that the interpretations set out below are somewhat preliminary and have a significant component of uncertainty. To reduce this uncertainty, additional petrological and geochemical studies are required that are clearly outside the initial objectives (and the real possibilities) of this Thesis.

7.2 Materials and methods

In the selected columns a high frequency sampling has been performed. We selected samples from those sections that showed an original wackestone or mudstone texture and sampled the micritic matrix with the help of a microdrill system coupled to a binocular lens. Drill bits of 0.5 mm in diameter were used to obtain about 65 micrograms for each analysis.

A total of 143 carbonate samples were taken for oxygen isotope analysis. Samples were run in an IRMS Thermo Scientific MAT 253 coupled to Kiel device at the Institute of Geosciences (CSIC-UCM) in Madrid (Spain). Isotopic ratios were calibrated against the NBS-19 and NBS-18 and own lab standards and are reported with the delta notation ($\delta^{18}\text{O}\text{‰}$ and $\delta^{13}\text{C}\text{‰}$) relative to the Vienna Pee Dee Belemnite (VPDB) standard. The analytical error of the instrument was better than $\pm 0.02\text{‰}$.

7.3 C and O isotopes

C and O stable isotopes analysis in carbonates gives important information on their formation processes. They are widely used in the study of marine strata and fossils, since they provide an effective tool to understand the conditions of the water column from which they precipitate and form (Tanner, 2010). The study of their trend in the geological record can give important insights on large-scale environmental processes. The change of environmental parameters in fact regulate the relative abundance of C and O isotopes and the way they fraction in carbonates. Both C and O depend primarily on the composition of the fluid they precipitate from. Oxygen isotopes ratios are related to the temperature, salinity, and evaporation rates while Carbon is more related to the biological processes (Hoefs, 2009).

The carbon finds one of the widest uses in isotopic studies and can be measured in different ways: from inorganic and organic carbon and from carbonates carbon, both whole rock and fossil material (Tanner, 2010). As previously mentioned, the main factors determining the ^{13}C and ^{12}C partitioning between the different reservoirs (inorganic and organic) are biological processes (Kump and Arthur, 1999). $\delta^{13}\text{C}$ usefulness resides in the fact that C in carbonates it is presumed to be quite resistant to diagenetic processes of low temperature (Banner and Hanson, 1990). Hence, if compared and proved that carbonate carbon trend is parallel to the organic matter trend, diagenetic processes influences can be excluded (Kump and Arthur, 1999).

The O isotope fractioning is more sensitive to different factors than the C, related to its high susceptibility to temperature changes (e.g. diagenesis) and to the parent fluid composition. However, this susceptibility can be used to understand the changes in temperature of the fluids from which carbonates precipitate. This parameter can be achieved through empirical functions formulated by O'Neill et al. (1969), Hais and Grossman (1991). Different assumptions and considerations must be made for O data interpretation. In particular 1) the mentioned influence of temperature in isotopic partitioning, since d^{18}O values tend to be progressively lighter with the increasing of temperature 2) the variation of the water chemistry while the sediment was forming (Tucker and Wright, 1990; Warren, 2000) 3) since the dolomicrites analyzed are assumed to be penecontemporaneous, following Fritz and Schmidt fractioning (1970) formula for dolostones precipitated in the range 25-79°C, Muschelkalk dolomicrites have to be 2‰ heavier than the calcites precipitating from the same water.

The covariance of $\delta^{13}\text{C}$ and $\delta^{18}\text{O}$ is a great tool to understand and identify diagenetic processes influencing the isotopic composition of carbonates and their equilibration with the diagenetic fluids (Marshall, 1992).

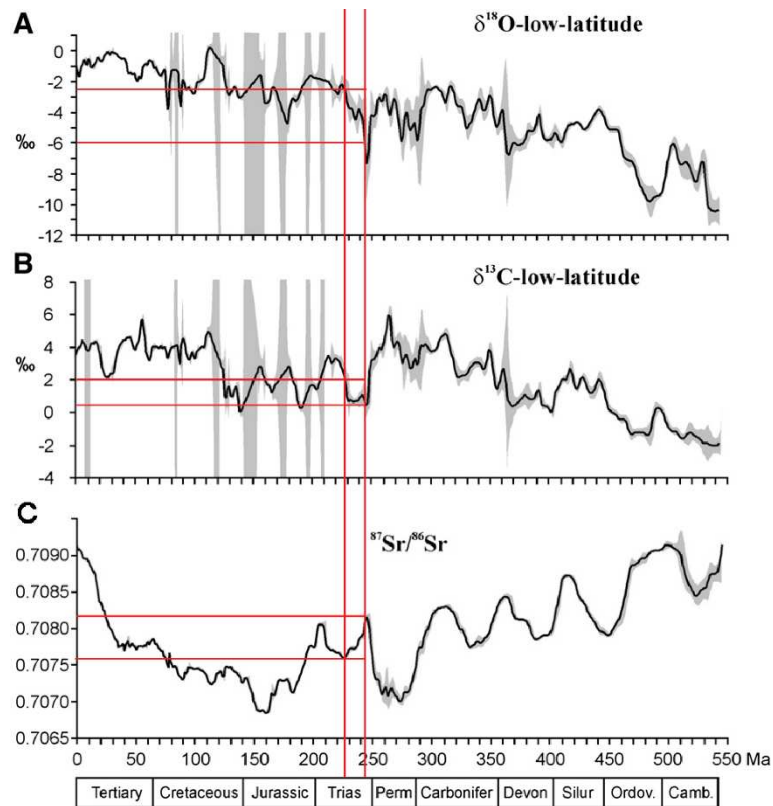


Fig. 7.1. Curves showing the variation of the isotopic composition of carbonates throughout the Phanerozoic. The red lines mark the isotopic composition of the carbonates for the Middle Triassic (modified from Escudero-Mozo, 2015 and Prokoph et al., 2008).

7.4 C and O isotopes analysis and result

7.4.1 Punta del Lavatoio section

The values of the isotopic relationship between the $\delta^{13}\text{C}$ and $\delta^{18}\text{O}$ are displayed in Figs 7.2. The analyzed samples of this series are mainly micrites and dolomicrites, with exception to the upper part of the column, where dolosparites are found. At the bottom of the section, the micrites and dolomicrites are predominantly fine to medium grained, some with abundant bioaccumulation and lamination (packstone to wackestone), while towards the top of the section it is possible to observe a shift towards coarser granulometries and a decrease in the abundance of the fossiliferous content, other than the presence of dolosparites with dolomitization processes. The carbon isotopic composition of the micrites and dolomicrites of the Punta del Lavatoio section varies from a minimum of -7.89‰ and a maximum of 2.62‰ . It is possible to observe a slight increase in the value of C towards the top of the section. These values are similar to other Middle Triassic carbonates, as shown in Fig. 7.1 (Prokoph et al., 2008).

The $\delta^{18}\text{O}$ values vary from -1.21‰ and -7.42‰ . These values are consistent with the Middle Triassic carbonates, whose range is approximately of 0‰ and -4‰ (Prokoph et al., 2008). Considering the Fritz and Schmith (1979) formula, a dolostone is approximately 2% heavier than the calcite that precipitates from the same water at the same temperature. Considering the dolostones of this series penecontemporaneous, the $\delta^{18}\text{O}$ data for the analysed samples fall in the range. The vertical distribution shows a trend going from more-negative values, setting towards $5\pm 2\text{‰}$, to less-negative values, setting towards $2\pm 0.5\text{‰}$ (Fig.). Four main trends can be identified (Fig. 7.2) 1) a first shift towards more negative values 2) a more homogeneous distribution with no apparent trend, settings towards $\delta^{18}\text{O}$ values of approximately -3.5‰ 3) a second shift towards more negative values, with greater variability 4) a second, more homogeneous distribution with no apparent trend setting between -3‰ and -2‰ , following a great shift towards heavier values. The enrichment in heavier ^{18}O isotope of the dolomicrites lying at top of the section mean that the water from which they have precipitated were heavier and more depleted of ^{16}O than the water from which dolomicrites at the bottom of the series precipitated.

Punta del Lavatoio

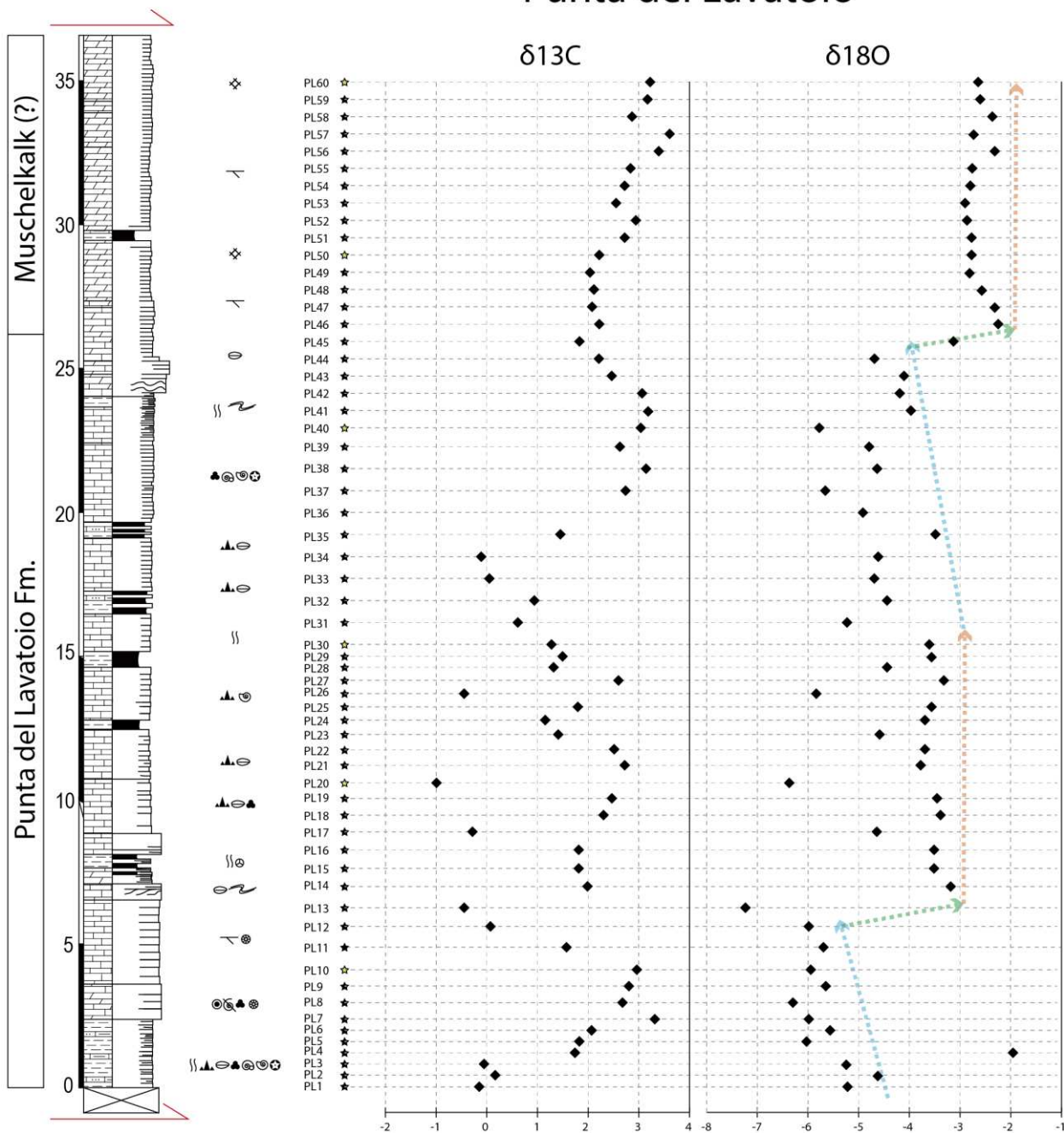


Fig. 7.2. C, O isotopic composition of the Punta del Lavatoio column. Vertical distribution of $\delta^{13}C$, of $\delta^{18}O$.

7.4.2 Monte Santa Giusta

The values of the isotopic relationship between the $\delta^{13}\text{C}/\delta^{12}\text{C}$ and $\delta^{18}\text{O}/\delta^{16}\text{O}$ are displayed in Figs. 7.3. The bottom of the succession is represented mainly by medium grain dolostones with algal lamination, passing upwards to micrites, biomicrites, dolomicrites and oo-bio-grainstones with a medium-high fossiliferous content. To top of the succession is made of fine micrites and dolomicrites with lamination and a scarce fossiliferous content. The top of the succession, although poorly outcropping and tectonized, is also in stratigraphic continuity with the Keuper facies.

The $\delta^{13}\text{C}$ varies between 3.07‰ and -4.43‰. The range is broader than the range of the $\delta^{13}\text{C}$ of the Middle Triassic, which varies approximately between 0.5‰ and 2‰ (Prokoph et al., 2008). The microfacies that best fits the Middle Triassic values is the 3: having a range that varies from a minimum of 0.2‰ and 1.79‰. These values fall into the range of marine carbonates (0‰ -4‰). It is not clearly possible to identify a trend of the curve, and not a correlation between the facies/microfacies.

The $\delta^{18}\text{O}$ varies from a minimum of -7.42‰ to a maximum of -1.21‰. These values are consistent with the Middle Triassic carbonates, whose range is approximately of 0‰ and -4‰ (Prokoph et al., 2008). Considering the Fritz and Schmith (1979) formula, a dolostone is approximately 2‰ heavier than the calcite that precipitates from the same water at the same temperature. Considering the dolostones of this penecontemporaneous series, the $\delta^{18}\text{O}$ data for the analyzed samples fall in the range. Lithofacies 1 at bottom of the series presents dolostones with algal lamination and dessication features. Upwards, the lithofacies tend to be predominantly fossiliferous, up to the top part of the series, where the fossiliferous content decreases.

The $\delta^{18}\text{O}$ shows no clear trend up until the top of the section, where the mean value shifts from more negative values to less negative and heavier values. There is in fact a broad variation between the $\delta^{18}\text{O}$ values. The heavier values of the top of the section could be due to the proximity to the keuper facies, meaning that the system was going towards hyperaline conditions and closed lagoon environment, where the evaporation rates dominated the fractioning between ^{18}O and ^{16}O .

Santa Giusta

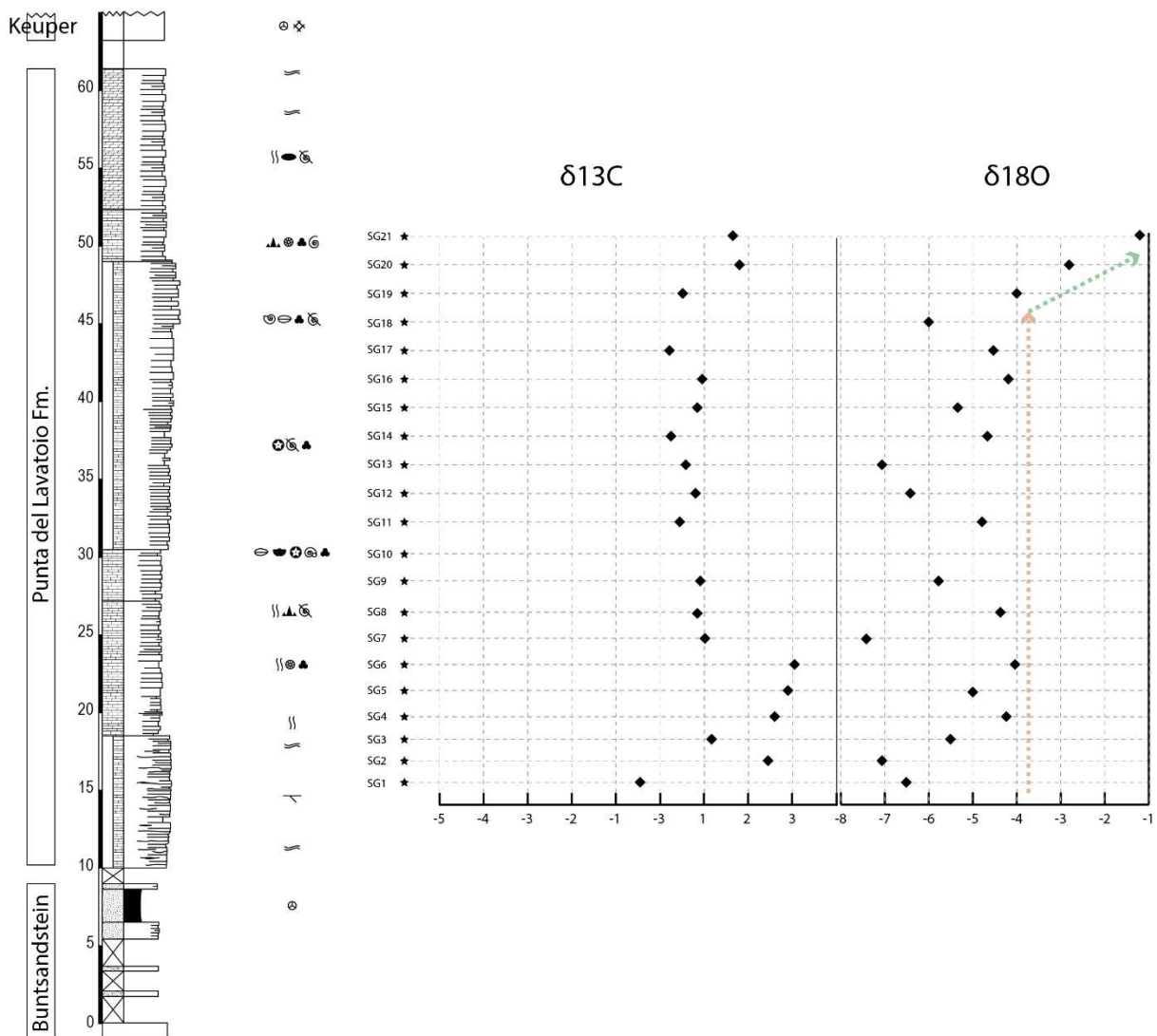


Fig. 7.3. C, O isotopic composition of the Monte Santa Giusta column. Vertical distribution of $\delta^{13}\text{C}$, of $\delta^{18}\text{O}$.

7.4.3 Monte Maggiore – Orroli

The values of the isotopic relationship between the $\delta^{13}\text{C}/\delta^{12}\text{C}$ and $18\text{O}/16\text{O}$ are displayed Figs. 7.4 and 7.5.

The Orroli outcrop is a composite column, consisting of a few meters thick wall exposed along the SP65 street (Bruncu su Para), and a quarry wall about 200m E from the first outcrop. It comprises the lowest part of the Monte Maggiore Fm., it consists of a tidal flat facies association and its lower part is in direct contact with the upper part of the Escalaplano Fm.

The section is mainly composed by dolomicrites medium to fine, with little to no fossiliferous content, high pellet content, and it is possible to find quartz fragments among the allochems. In the bottom part of the section it is possible to notice a high porosity.

The $\delta^{13}\text{C}$ varies between 0,052‰ and -3.04‰. The trend goes towards higher positive values however there is one notable shift towards negative values. The $\delta^{18}\text{O}$ instead goes from a minimum value of -3.11‰ and a maximum value of -0.33‰. There is no clear trend, but it is possible to notice a wide shift towards more negative values in the middle-upper portion of the section.

The Monte Maggiore outcrop comprises the entirety of the Monte Maggiore Fm., and it is a composite of two outcrops. The first one is about 10m thick and located at the base of a quarry located south of the Nureci village. This lower part comprises the base of the Monte Maggiore Fm. lying directly on top of the basement. The top of the studied column is about 15m thick. This outcrop located at the top of the Monte Maggiore hill, and it comprises the top part of the Fm.

The bottom part of the section is composed mainly by pel-dolomicrites, with a high pellet content, porosity and it is possible to notice a high content of sulphates, especially evident at the macro scale as altered pyrite. The top part of the column instead mainly consists of fine grained micritic mudstones and biomicrites (wackestones to packstones), with algal lamination, bioaccumulation levels, stylolites and chert nodules.

The $\delta^{13}\text{C}$ ranges from a minimum of 0.13‰ and a maximum of 2.14‰. There seems to be no clear trend in the vertical distribution of the values. The $\delta^{18}\text{O}$ ranges from a minimum of -7.28‰ to a maximum of -1.98‰. The bottom of the section shows less negative values with an average of -2.24‰, while the top of the section has more negative values, with an average of -5.28‰. The values of the top part of the Monte Maggiore Fm. are consistent with the Middle Triassic carbonates, whose range is approximately of 0‰ and -4‰ (Prokoph et al.,

2008). Considering the Fritz and Schmith (1979) formula, a dolostone is approximately 2% heavier than the calcite that precipitates from the same water at the same temperature. Considering that the dolostones of this series are penecontemporaneous in origin, the $\delta^{18}\text{O}$ data for the analysed samples fall in the range.

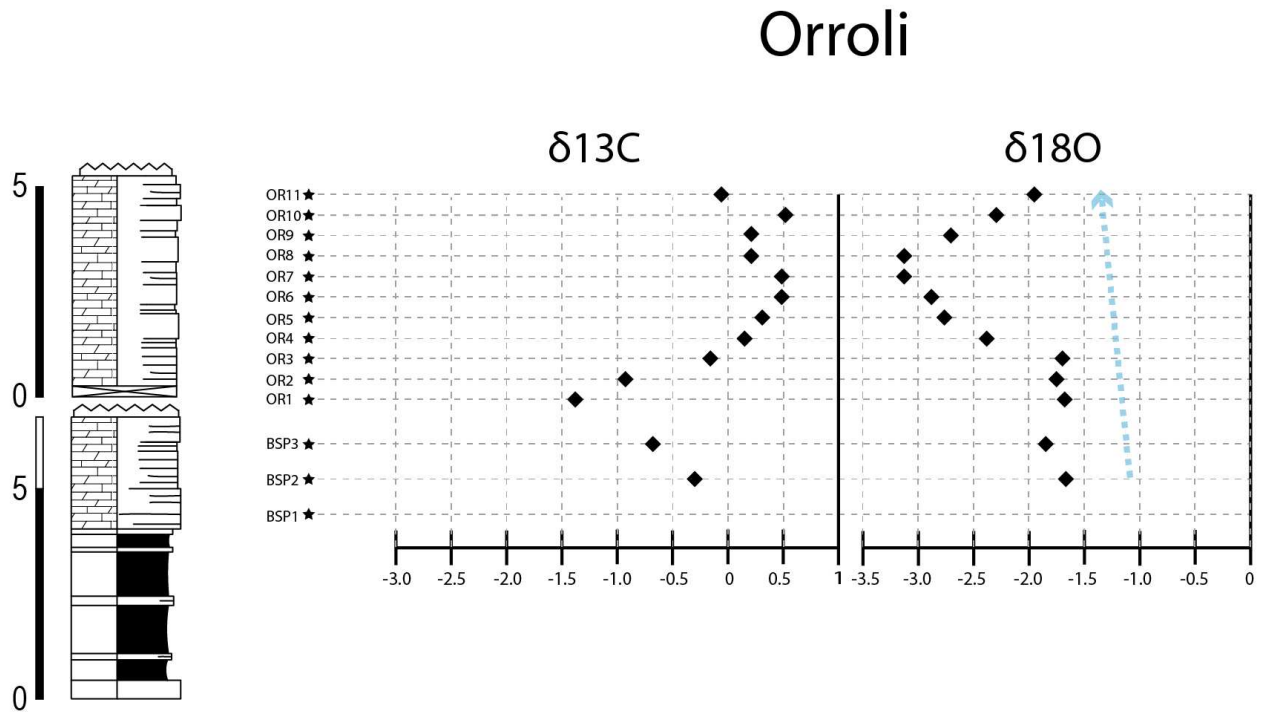


Fig. 7.4. C, O isotopic composition of the Orroli column. Vertical distribution of $\delta^{13}\text{C}$, of $\delta^{18}\text{O}$.

Monte Maggiore

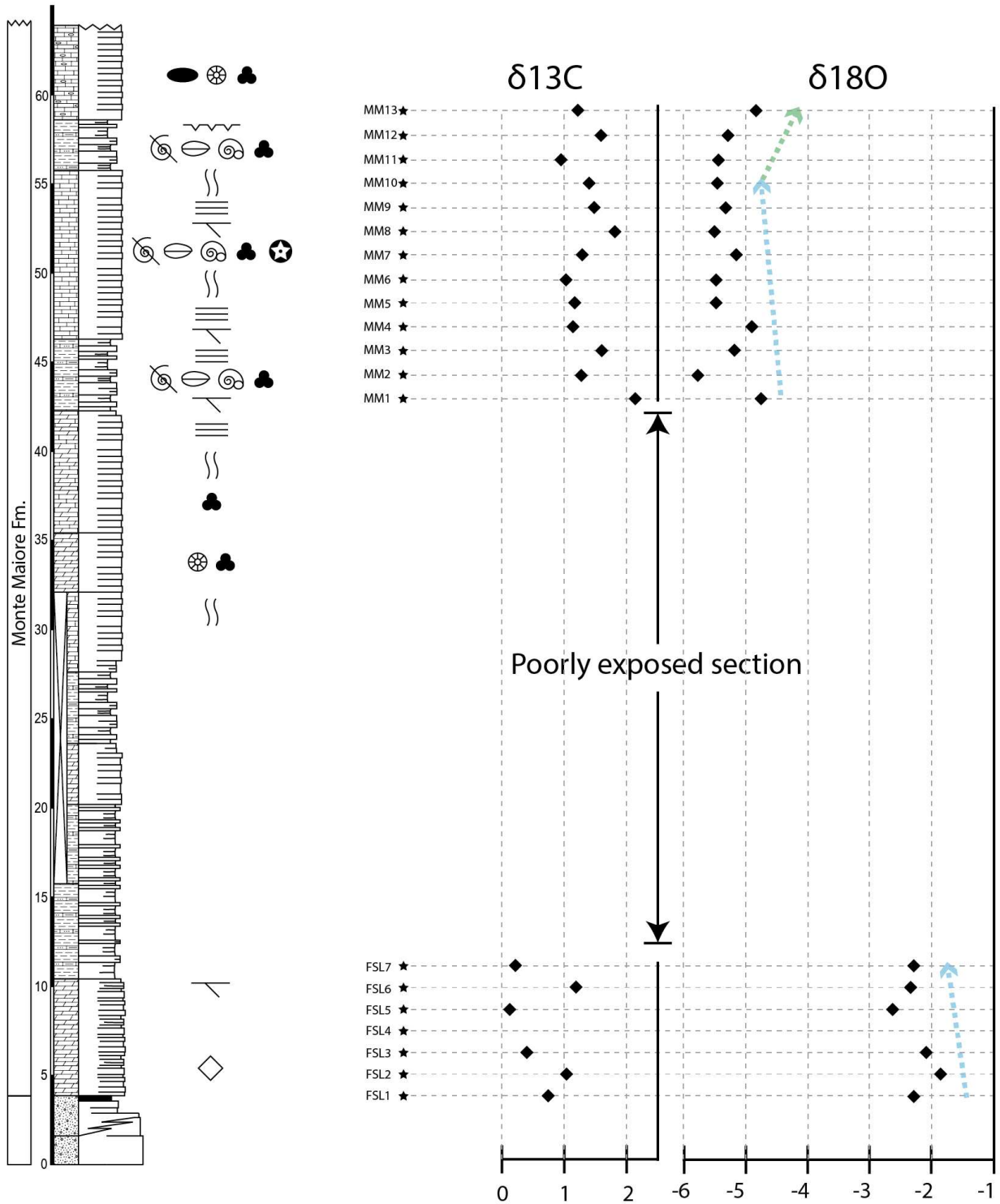


Fig. 7.5. C, O isotopic composition of the Monte Maggiore section. Vertical distribution of $\delta^{13}\text{C}$, of $\delta^{18}\text{O}$.

7.4.4 Punta Tonnara

The values of the isotopic relationship between the $\delta^{13}\text{C}$ and $\delta^{18}\text{O}$ are displayed in Fig. 7.6.

The Punta Tonnara section is composed mainly by dolomicrites, very fine to medium, with different degrees of alteration due to the pervasive presence of calcite veins and stylolites, especially at the bottom of the section, and different degree of bioturbation (very high at the bottom) and fossiliferous content.

The Punta Tonnara section is mainly composed by very fine micrites (bio-micrites to mudstones) occasionally interested by dolomitization processes, pervasively bioturbated especially in the first meters of the section. It is possible to notice a high presence of bioclasts, even if they present a very low variety, as well as pervasive fracturation testified by the dense network of calcitic veins. In the last meters of the section, where the environment passes from shallow marine to extreme proximal sabkha it is possible to observe chert nodules, desiccation features like tepee structures and evaporitic pseudomorphs.

The $\delta^{13}\text{C}$ varies from a minimum of -7.18‰ to a maximum of 2.87‰ . Excluding the top values (PT22 and PT23) and the more negative values, that show an important negative peak of $\delta^{13}\text{C}$, the other values average at 2‰ , which is in the range of the Middle Triassic carbonates $\delta^{13}\text{C}$ (0.5‰ - 2‰), and in any case fall in the range of marine carbonates (0‰ - 4‰). The variance of the $\delta^{13}\text{C}$ values is low (6.2‰), and there is no clear trend in the vertical distribution.

On the other side, the $\delta^{18}\text{O}$ vertical distribution in this section shows a more pronounced trend, that goes from less negative values to more negative values. The $\delta^{18}\text{O}$ values go from a minimum of -6.94‰ to a maximum of -3.49‰ . These values are consistent with the Middle Triassic carbonates, whose range is approximately of 0‰ and -4‰ (Prokoph et al., 2008). Considering the Fritz and Schmith (1979) formula, a dolostone is approximately 2% heavier than the calcite that precipitates from the same water at the same temperature. The general upwards trend towards more negative $\delta^{18}\text{O}$ values is not regular, in fact it is possible to observe different well-defined shifts towards less negative values.

Punta Tonnara

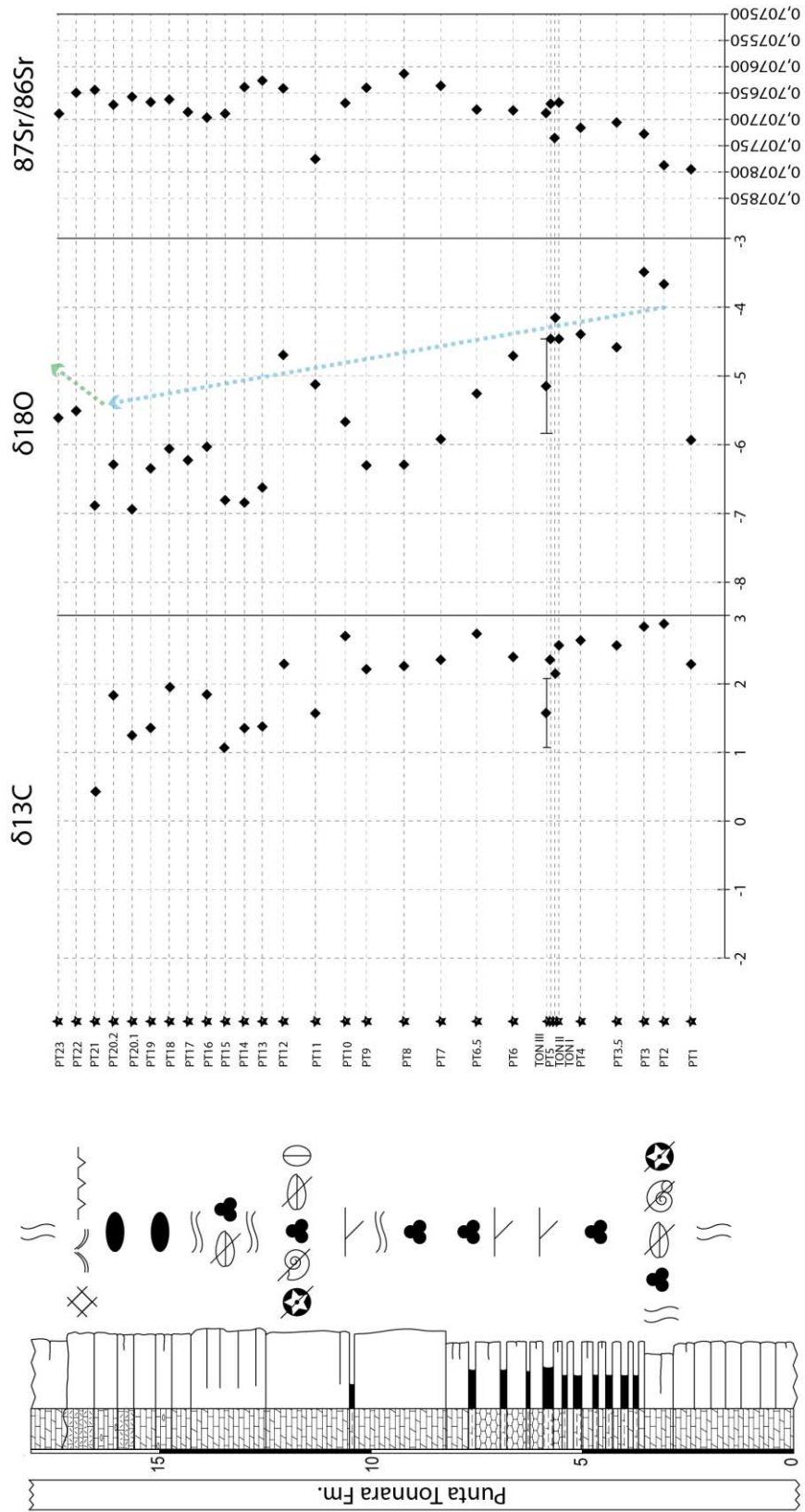


Fig. 7.6. C, O isotopic composition of the Punta Tonnara column. Vertical distribution of $\delta^{13}\text{C}$, of δ^{180}

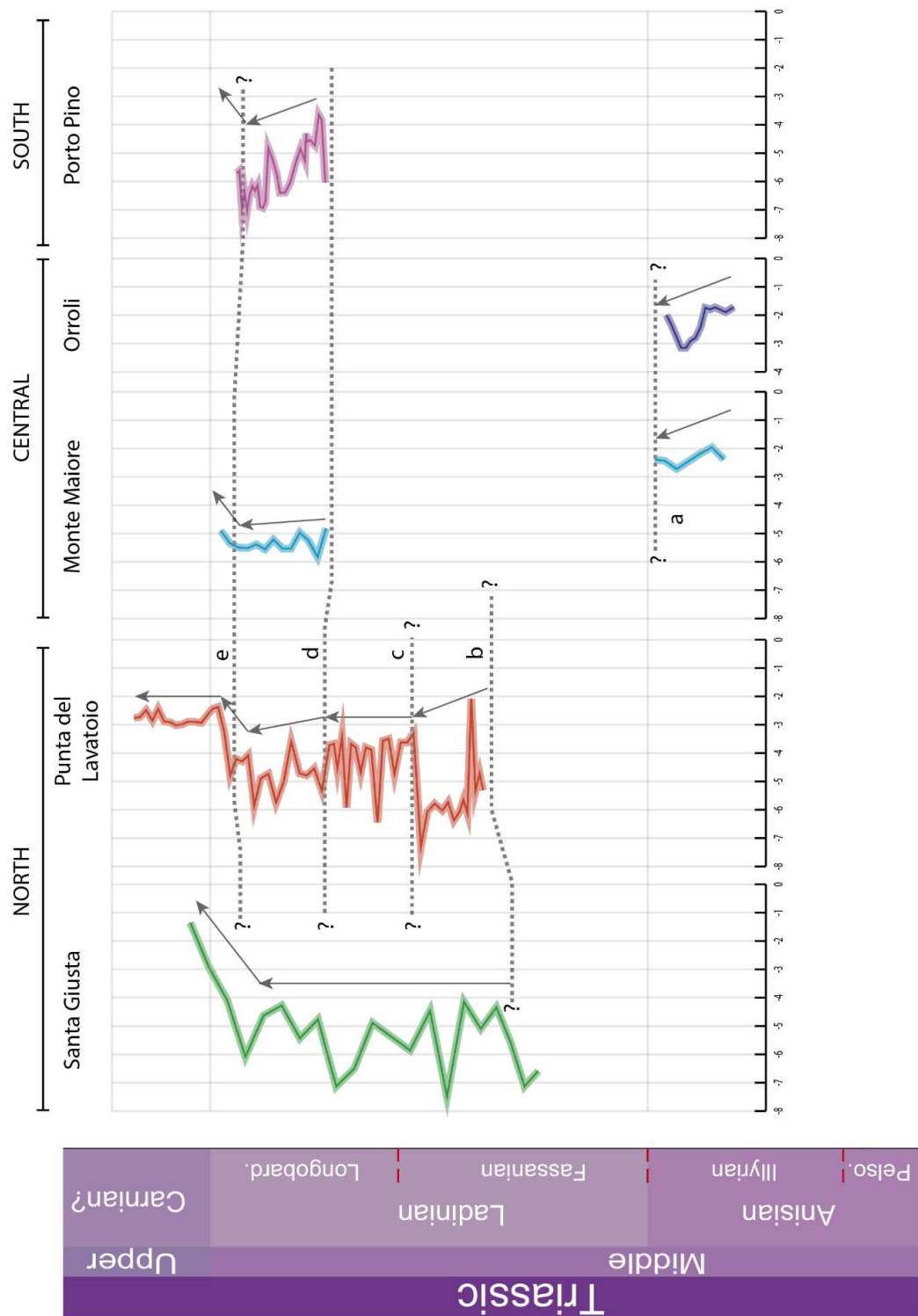


Fig. 7.7. Correlation of the $\delta^{18}O$ curves of the different studied section.

sample	weight (ug)	$\delta^{13}\text{C}$	$\pm (1\text{ s})$	$\delta^{18}\text{O}$	$\pm (1\text{ s})$	$^{87}\text{Sr}/^{86}\text{Sr}$	$\pm\text{StdErr}\cdot 10^{06}$	Microfacies	Microfacies code	n°
Orroli										
BSP-1	61	-3,04	0,01	-0,33	0,01			dolomicrite vf - dark + ox + qz	1	1
BSP-2	52	-0,30	0,01	-1,65	0,01			dolomicrite mf	6	2
BSP-3	56	-0,67	0,01	-1,83	0,01			dolomicrite mg + qz sc.	6	3
OR-01	54	-1,36	0,01	-1,67	0,02			pel-dolomicrite m - high porosity + qz	10	4
OR-02	61	-0,92	0,01	-1,73	0,01			pel-dolomicrite m - high porosity + qz	10	5
OR-03	66	-0,15	0,02	-1,68	0,01			dolomicrite mf	6	6
OR-04	59	0,16	0,02	-2,37	0,01			dolomicrite mf	6	7
OR-05	60	0,31	0,01	-2,75	0,01			dolomicrite mf	6	8
OR-06	57	0,48	0,01	-2,86	0,01			dolomicrite mf + pellet sc.	6	9
OR-07	54	0,48	0,01	-3,11	0,01			dolomicrite mf	6	10
OR-08	61	0,22	0,01	-3,11	0,01			dolomicrite mf - pellet - slightly laminat.	6	11
OR-09	55	0,22	0,01	-2,68	0,01			dolomicrite mf - pellet - slightly laminat.	6	12
OR-10	55	0,52	0,01	-2,28	0,01			dolomicrite mf + pellet sc.	6	13
OR-11	59	-0,05	0,01	-1,94	0,02			dolomicrite mf + pellet + mud clasts + chert + qz	4	14
Monte Maggiore										
FSL-01	58	0,74	0,01	-2,28	0,01			pel-dolomicrite mf + sulph	10	1
FSL-02	56	1,03	0,01	-1,85	0,01			pel-dolomicrite mf + sulph	10	2
FSL-03	65	0,40	0,01	-2,08	0,01			pel-dolomicrite mf + sulph	10	3
FSL-05	59	0,13	0,01	-2,60	0,00			pel-dolomicrite mf + sulph	10	4
FSL-06	52	1,19	0,01	-2,34	0,02			dolomicrite f	3	5
FSL-07	64	0,22	0,01	-2,28	0,01			dolomicrite f + pellets	3	6
MM-01	54	2,14	0,01	-4,75	0,01			dolomicrite f	3	7
MM-02	57	1,27	0,01	-5,77	0,01			dolomicrite f	3	8
MM-03	57	1,60	0,01	-5,20	0,01			dolomicrite f + bioclasts sc.	3	9
MM-04	55	1,14	0,01	-4,90	0,01			dolomicrite f + bioclasts sc.	3	10
MM-05	57	1,17	0,01	-5,47	0,02			dolomicrite f	3	11
MM-06	55	1,03	0,01	-5,49	0,01			dolomicrite f + lamination sc. + stilolites + dolomitiz. In pores	1	12
MM-07	53	1,29	0,01	-5,15	0,02			dolomicrite f - mud clasts f + dolomitized cement	1	13
MM-08	54	1,81	0,01	-5,50	0,01			dolomicrite f + lamination sc.	3	14
MM-09	57	1,48	0,01	-5,33	0,01			dolomicrite f	3	15
MM-10	50	1,40	0,01	-5,46	0,01			dolomicrite f + algal lamination - pores + bioclasts	1	16
MM-11	52	0,95	0,02	-5,44	0,01			dolomicrite f + lamination sc.	3	17
MM-12	52	1,59	0,01	-5,28	0,01			dolomicrite f + bioclasts sc. + mud clasts f.	1	18
MM-13	51	1,22	0,00	-4,83	0,01			dolomicrite f + bioclasts sc. + mud clasts f.	1	19
Punta del Lavatoio										
PL-01	52	-1,13	0,02	-5,26	0,01			Dolomicrite medio fine biocl ossidi stilo vene	4	1
PL-02	60	-0,43	0,00	-4,66	0,01			Dolomicrite medio fine biocl ossidi stilo vene	4	2
PL-03	57	-1,05	0,01	-5,28	0,01			Dolomicrite medio fine biocl ossidi stilo vene	4	3
PL-04	64	0,74	0,01	-1,98	0,01			Dolomicrite medio fine biocl ossidi stilo vene	4	4
PL-05	54	0,83	0,01	-6,06	0,01			Dolomicrite medio fine biocl ossidi stilo vene	4	5
PL-06	58	1,05	0,01	-5,59	0,01			Dolomicrite medio fine omogenea	6	6
PL-07	56	2,33	0,02	-6,02	0,02			Dolomicrite medio fine omogenea	6	7
PL-08	52	1,68	0,01	-6,33	0,01			Dolomicrite medio fine omogenea	6	8
PL-09	53	1,82	0,01	-5,69	0,00			Dolomicrite medio fine omogenea	6	9
PL-10	64	1,97	0,01	-5,97	0,01			Dolomicrite medio fine omogenea	6	10
PL-11	57	0,58	0,02	-5,73	0,01			Dolomicrite medio fine omogenea	6	11
PL-12	53	-0,92	0,00	-6,00	0,01			Dolomicrite medio fine omogenea	6	12
PL-13	51	-1,44	0,01	-7,28	0,01			Dolomicrite medio fine omogenea	6	13
PL-14	56	0,99	0,02	-3,21	0,01			Dolomicrite fine omogenea pellet	3	14
PL-15	55	0,83	0,01	-3,54	0,01			Dolomicrite fine omogenea	3	15
PL-16	64	0,82	0,01	-3,53	0,01			Dolomicrite fine omogenea	3	16
PL-17	54	-1,28	0,01	-4,67	0,01			Dolomicrite fine laminazione	2	17
PL-18	52	1,31	0,01	-3,42	0,01			Dolomicrite fine laminazione bioclasti sc.	2	18
PL-19	59	1,48	0,01	-3,48	0,01			Dolomicrite fine laminazione bioclasti abb.	2	19
PL-20	57	-2,00	0,02	-6,41	0,02			Dolomicrite fine laminazione	2	20
PL-21	51	1,72	0,01	-3,80	0,01			Dolomicrite fine laminazione bioclasti sc.	2	21
PL-22	46	1,52	0,01	-3,72	0,02			Dolomicrite fine laminazione bioclasti	2	22
PL-23	57	0,43	0,01	-4,62	0,02			Dolomicrite fine laminazione bioclasti	2	23
PL-24	51	0,17	0,01	-3,72	0,01			Dolomicrite fine laminazione	2	24
PL-25	50	0,80	0,01	-3,59	0,00			Dolomicrite fine laminazione bioclasti	2	25
PL-26	51	-1,44	0,01	-5,87	0,01			Dolomicrite medio fine omogenea	6	26
PL-27	57	1,57	0,01	-3,35	0,01			Dolomicrite medio fine laminazione ooliti	5	27
PL-28	50	0,33	0,01	-4,47	0,02			Dolomicrite medio fine laminazione ooliti	5	28
PL-29	62	0,58	0,01	-3,60	0,02			Dolomicrite medio fine laminazione ooliti	5	29
PL-30	53	0,28	0,01	-3,64	0,01			Dolomicrite medio fine laminazione ossidi	5	30
PL-31	51	-0,38	0,01	-5,27	0,01			Dolomicrite medio fine laminazione bioclasti	5	31
PL-32	61	-0,06	0,02	-4,46	0,02			Dolomicrite medio fine laminazione bioclasti	5	32
PL-33	53	-0,95	0,01	-4,72	0,01			Dolomicrite fine vene abb.	1	33
PL-34	51	-1,11	0,01	-4,64	0,00			Dolomicrite media laminazione ossidi	7	34
PL-35	54	0,45	0,01	-3,52	0,01			Dolomicrite fine laminazione bioclasti abb.	2	35
PL-36	52	-7,89	0,01	-4,96	0,01			Dolomicrite grana medio fine omogenea porosità	6	36
PL-37	54	1,74	0,01	-5,70	0,01			Dolomicrite grana medio fine omogenea	6	37

PL-38	59	2,14	0,01	-4,66	0,01		Dolomicrite grana medio fine omogenea	6	38
PL-39	52	1,64	0,01	-4,85	0,01		Dolomicrite grana medio fine laminazione	5	39
PL-40	51	2,04	0,01	-5,81	0,01		Dolomicrite grana media laminazione	5	40
PL-41	50	2,20	0,01	-4,01	0,01		Dolomicrite grana medio fine laminazione dolomit.	5	41
PL-42	54	2,06	0,01	-4,22	0,01		Dolomicrite grana medio fine laminazione dolomit.	5	42
PL-43	53	1,47	0,02	-4,14	0,01		Dolomicrite grana fine omogenea	3	43
PL-44	52	1,21	0,01	-4,72	0,01		Dolomicrite grana fine omogenea dolomit.	3	44
PL-45	53	0,84	0,01	-3,16	0,01		Dolomicrite grana fine omogenea	3	45
PL-46	50	1,20	0,01	-2,27	0,02		Dolomia grana media omogenea	8	46
PL-47	56	1,08	0,01	-2,34	0,01		Dolomia grana media omogenea	8	47
PL-48	53	1,12	0,01	-2,60	0,01		Dolomia grana media omogenea	8	48
PL-49	53	1,05	0,01	-2,84	0,00		Dolomia grana media omogenea	8	49
PL-50	55	1,23	0,01	-2,80	0,02		Dolomia grana media omogenea	8	50
PL-51	51	1,73	0,02	-2,79	0,01		Dolomia grana media laminata deb.	8	51
PL-52	52	1,95	0,01	-2,90	0,01		Dolomia grana media laminata deb.	8	52
PL-53	51	1,58	0,01	-2,93	0,01		Dolomia grana media omogenea	8	53
PL-54	53	1,73	0,01	-2,82	0,02		Dolomia grana media omogenea	8	54
PL-55	50	1,84	0,02	-2,78	0,02		Dolomia grana media omogenea	8	55
PL-56	64	2,40	0,01	-2,35	0,01		Dolomia grana media omogenea	8	56
PL-57	58	2,62	0,02	-2,76	0,01		Dolomia grana media omogenea	8	57
PL-58	55	1,87	0,01	-2,39	0,01		Dolomia grana media omogenea	8	58
PL-59	58	2,18	0,01	-2,63	0,01		Dolomia grana media omogenea	8	59
PL-60	60	2,23	0,01	-2,67	0,01		Dolomia grana media omogenea	8	60
Monte Santa Giusta									
S4-01	83	-0,47	0,01	-6,50	0,02		dolomicrite f + ooids sc. + foram sc. + recrystallized dolostone c	1	1
S4-02	60	2,45	0,01	-7,06	0,01		dolomicrite f + ooids sc. + foram sc. + recrystallized dolostone c	1	2
S4-03	54	1,17	0,01	-5,59	0,00		dolo-bio-grainstone mf - foram + pellets + bivalves fr. + algae	9	3
S4-04	58	2,61	0,02	-4,23	0,01		dolomicrite mf	6	4
S4-05	72	2,94	0,00	-4,97	0,01		dolostone m - pores - ferruginous dolostone	8	5
S4-06	53	3,07	0,01	-4,04	0,02		dolostone m - pores - ferruginous dolostone	8	6
S4-07	59	2,26	0,01	-7,42	0,01		dolostone m - ooids	8	7
S4-08	54	0,83	0,01	-4,37	0,01		dolostone mf - porosity + ooids sc.	6	8
S4-09	53	0,90	0,01	-5,77	0,02		dolomicrite f + bioclasts sc. + forams	3	9
S4-11	56	0,47	0,01	-4,79	0,02		dolograinstone ooids + dolograinstones bioclasts	9	10
S4-12	58	0,78	0,01	-6,41	0,01		dolomicrite vf - bioclasts sc.	3	11
S4-13	57	0,59	0,01	-7,06	0,01		dolomicrite mf - ooids ab. + bioclast f.	4	12
S4-14	55	0,27	0,02	-4,67	0,01		dolomicrite f - lamination sc.	3	13
S4-15	59	0,87	0,01	-5,33	0,01		dolomicrite f - lamination sc. + forams sc.	3	14
S4-16	51	0,95	0,01	-4,19	0,01		dolomicrite f - lamination sc. + forams sc.	3	15
S4-17	59	0,21	0,01	-4,52	0,01		dolomicrite f - scarce bivalves (L)	3	16
S4-18	69	-4,43	0,01	-5,97	0,01		dolostone mf - ox	6	17
S4-19	52	0,54	0,01	-4,00	0,01		dolomicrite f	3	18
S4-20	54	1,79	0,01	-2,80	0,00		dolomicrite f - lamination sc.	3	19
S4-21	62	1,68	0,01	-1,21	0,01		dolostone mf	6	20
Punta Tonnara									
PT-01	55	2,27	0,02	-5,93	0,02	0,707689	dolomicrite vf - algal lamination - bioclasts - peloids - stylolites	2	1
PT-02	53	2,87	0,01	-3,67	0,01	0,707650	dolomicrite vf - algal lamination - bioclasts - peloids - stylolites	2	2
PT-03	50	2,84	0,01	-3,49	0,02	0,707644	dolomicrite vf - algal lamination - bioclasts - peloids - stylolites	2	3
PT-03.5	52	2,55	0,00	-4,58	0,01	0,707674	dolomicrite vf - algal lamination - bioclasts - peloids - stylolites	2	4
PT-04	58	2,63	0,01	-4,39	0,01	0,707657	dolomicrite f - veins	1	5
TON-I	51	2,58	0,02	-4,46	0,02	0,707662	dolomicrite vf - algal lamination - bioclasts - peloids - stylolites	2	6
TON-II	48	2,11	0,01	-4,16	0,01	0,707686	dolomicrite f - lamination - bioclasts - peloids - stylolites	2	7
PT-05	50	2,35	0,01	-4,46	0,01	0,707668	dolomicrite vf - algal lamination - bioclasts - peloids - stylolites	2	8
TON-III.1	48	1,09	0,01	-5,84	0,01	0,707697	dolomicrite vf - algal lamination - bioclasts - peloids - stylolites	2	9
TON-III.2	49	2,03	0,01	-4,48	0,01	0,707689	dolomicrite vf - algal lamination - bioclasts - peloids - stylolites	2	10
PT-06	49	2,38	0,00	-4,71	0,02	0,707639	dolomicrite vf - algal lamination - bioclasts - peloids - stylolites	2	11
PT-06.5	50	2,73	0,00	-5,25	0,02	0,707627	dolomicrite mf - heterogeneous - vein with recryst.	4	12
PT-07	53	2,32	0,01	-5,92	0,02	0,707640	dolomicrite vf - algal lamination - bioclasts - peloids - stylolites	2	13
PT-08	50	2,25	0,01	-6,29	0,02	0,707776	dolomicrite vf - algal lamination - bioclasts - peloids - stylolites	2	14
PT-09	57	2,19	0,01	-6,30	0,02	0,707669	dolomicrite vf - algal lamination - bioclasts - peloids - stylolites	2	15
PT-10	53	2,69	0,01	-5,67	0,01	0,707639	dolomicrite mf - bioclasts	6	16
PT-11	50	1,56	0,01	-5,12	0,02	0,707613	dolomicrite mf - veins recryst.	4	17
PT-12	58	2,29	0,00	-4,70	0,01	0,707636	dolomicrite mf - veins recryst.	4	18
PT-13	57	1,37	0,00	-6,63	0,02	0,707682	dolomicrite vf - algal lamination - bioclasts - peloids - stylolites	2	19
PT-14	52	1,31	0,01	-6,84	0,01	0,707683	dolomicrite mf - bioclasts	6	20
PT-15	52	1,07	0,01	-6,80	0,02	0,707695	dolomicrite vf - algal lamination - bioclasts - peloids - stylolites	2	21
PT-16	49	1,83	0,02	-6,04	0,01	0,707681	dolomicrite vf - algal lamination - bioclasts - peloids - stylolites	2	22
PT-17	51	-3,41	0,00	-6,23	0,01	0,707736	dolomicrite vf - algal lamination - bioclasts - peloids - stylolites	2	23
PT-18	53	1,94	0,01	-6,06	0,01	0,707668	dolomicrite f - algal lamination - bioclasts - peloids - stylolites	2	24
PT-19	49	1,36	0,01	-6,35	0,02	0,707670	dolomicrite mf - pellet - lamination - bioclasts ab.	5	25
PT-20.1	54	1,24	0,01	-6,94	0,02	0,707716	dolomicrite f - lamination - bioclasts - chalcidony	2	26
PT-20.2	51	1,82	0,01	-6,29	0,02	0,707706	dolomicrite f - lamination - bioclasts - chalcidony	2	27
PT-21	55	0,41	0,01	-6,88	0,01	0,707728	dolomicrite mf - lamination - peloids	4	28
PT-22	51	-6,90	0,01	-5,51	0,02	0,707787	dolomicrite mf	5	29

8. Palaeogeography

The Anisian-Ladinian interval was a crucial period of evolution of the westernmost Tethys. The northward drift of Cimmeria is key to understanding the development of carbonate platforms, fauna migration routes and basin evolution in the western Tethys realm during this time interval. These profound changes in the configuration of Pangaea's terrains were mainly related to the opening of the Neotethys to the south, and contemporary closure of the Palaeotethys towards the north, but also linked to microplate reorganization (e.g., Apulia and Adria), and the opening of back-arc basins in the active European margin, such as Meliata and Maliak, both involving sea-floor spreading (Robertson, 2002; Stampfli and Borel, 2004) up until the early Late Triassic. Over time, the forces playing a role in this process led to the collapse of the Variscan belt (McCann et al., 2006) and dismemberment of the Cimmeria micro-continent, which was drifting from Gondwana towards Laurasia (Ziegler and Stampfli, 2001). The rapid evolving of this palaeogeographic configuration resulted in the consecutive closing and opening of seaways that connected different bioprovinces and through which the Tethys reached its westernmost domain during the Anisian. Four different bioprovinces can be distinguished in this domain: 1) Germanic, related to the Germanic Basin (N); 2) Tethyan (E), 3) Alpine (E-NE), and 4) Sefardi (S) (Hirsch, 1972, 1975, 1977).

During the Bythinian (early Anisian p.p.), the westernmost sector of the Tethys (e.g., E Iberia, Majorca, SE France) was controlled by continental sedimentation (Bourquin et al. 2011). As the consequence of the accelerated roll-back of the Palaeotethys, seafloor spreading caused readjustments in eastern Iberia and the Balearic Islands and Sardinian basins during the late Anisian (Anadón et al., 1979; Sanz et al., 2012; Escudero-Mozo et al., 2014) (Fig. 8.1) along with active differential subsidence in the Dolomites (Posenato, 2019). The first transgressive-regressive episode occurred in the east of the Iberian basin and the Catalan basin during the Pelsonian to early Illirian interval (e.g., Landete Formation and “lower Muschelkalk” respectively, Calvet et al., 1990; Escudero-Mozo et al. 2014, 2015). These first carbonate, shallow marine units are the expression of not yet fully developed marine corridors and recorded scarce but significant fossil assemblages (López-Gómez et al., 1998; Escudero-Mozo, 2015). In particular, the Alpine and Germanic influence in the fossil record suggests an open connection towards the north and Palaeotethys domain. No record of this first transgressive early Pelsonian pulse is present in Sardinia, Minorca or the Castellón area, which were still emerged at that time (López-Gómez et al., 1998; Escudero-Mozo et al., 2015) and likely formed a topographical high and an important geographical barrier separating the neighbouring palaeobioprovinces (Escudero-Mozo et al., 2015; Stori et al., 2022).

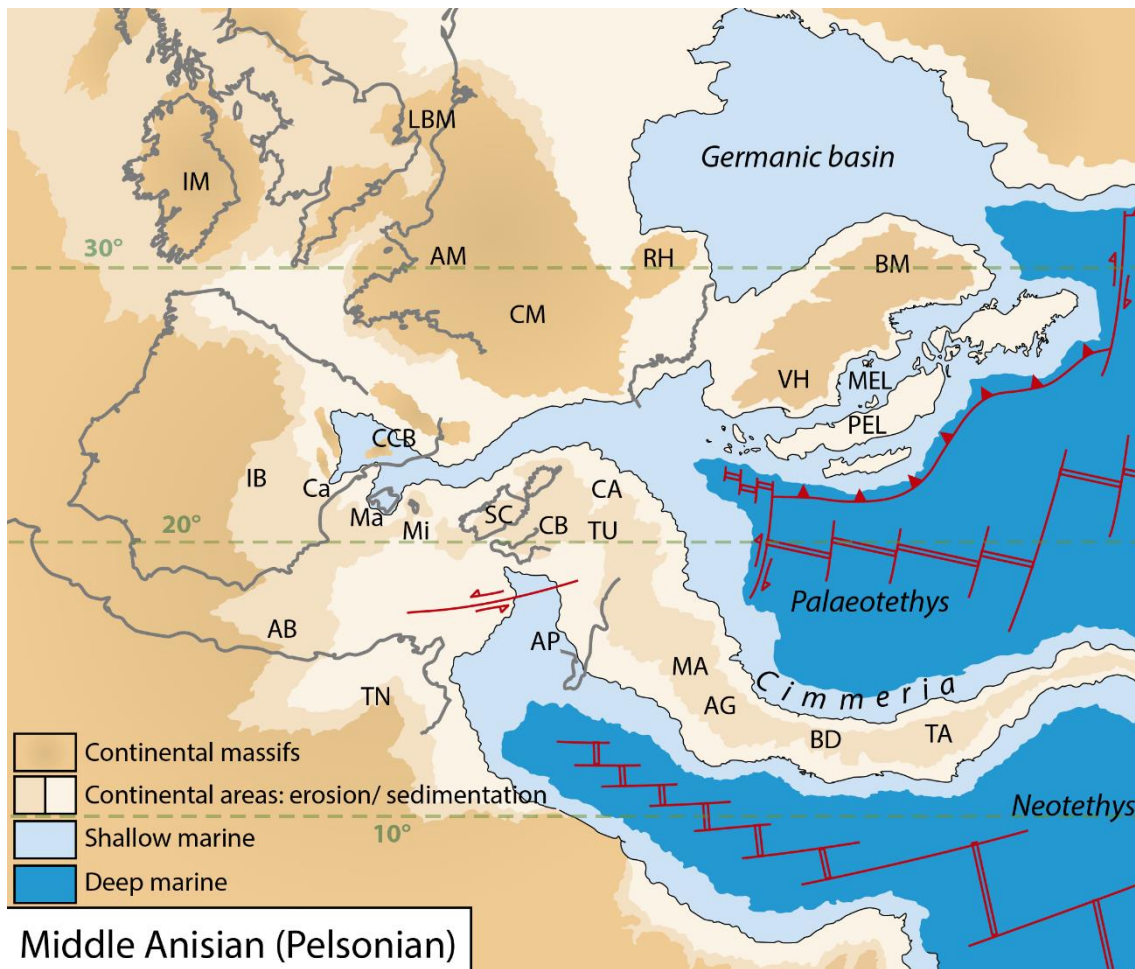


Fig. 8.1. Palaeogeographic reconstruction of the western Tethys realm for the Middle Triassic (middle Anisian). AM Armorica; AB Alboràn; AG Authoctonus Greece; AP Apulia; BA Balearic; BD Bey-Daglari; BM Bohemian Massif; CA Carnic; CB Calabria; CM Central Massif; IB Iberian Massif; IM Irish Massif; LBM London-Brabant Massif; MA Mani; MEL Meliata; PEL Pelagonia; SC Sardinia-Corsica; TA Taurus; TN Tunisia; TU Tuscan; RH Rhenish Massif; VH Vindelician High; Mi Minorca; Ma Majorca; CCB Catalan Coastal Basin; Ca Castellón. Image modified from Escudero-Mozo et al. (2015), Ziegler and Stampfli (2001), Stampfli and Borel (2002) and Muttoni et al. (2009).

The subsequent transgressive-regressive pulse took place during the middle-late Illyrian, and has been recorded throughout the Tethys domain including the Balearic Islands, central-eastern Iberia, Betic External Zone and Southern Europe (Fig 8.2 and 8.3) (Gianolla and Jaquin, 1998; Ziegler, 1999; Sanz De Galdeano et al., 2001; Martín-Algarra and Vera, 2004; Pérez-López and Pérez-Valera, 2007; Martín-Rojas et al., 2009; Mercedes-Martín et al., 2013; Escudero-Mozo et al., 2015; Ortí et al., 2020; Pérez-Valera et al., 2023). In Sardinia, the beginning of this stage is marked by the presence of transitional and Röt-like facies, dated by means of palynological associations as late Pelsonian-Illyrian (Stori et al., 2022). The first carbonate platform of regional significance that developed in Muschelkalk facies was related to a shallow marine origin and designated a first cycle by Costamagna (2002). In the lower parts of the Punta Su Nuraxi, Campumari and Monte Maggiore Formations in the central and SW areas of the island, this sedimentary record contains scarce or null fossils, and shows only

dasycladacean algae associations of Illyrian age (Costamagna and Piros, 2022) in the Monte Maggiore area (Sarcidano-Gerrei) in the lower part of the Monte Maggiore Formation. However, a more consistent diverse fossil record was found in the upper part of the Monte Maggiore Formation and the Punta del Lavatoio Formation (Nurra). The data derived from associations of the different fossil groups and their diversity relative to that of the lower parts of these same units suggest: i) that the transgression progressively reached the island in the late Anisian giving rise to a restricted shallow marine environment and, ii) the progressively increasing influence of the neighbouring palaeobioprovinces of the island. Hence, greater and more developed seaway connections to the different Tethyan realms seems likely. In the Punta del Lavatoio Formation (Nurra), which harbours the richest and most diverse fossiliferous associations of the Muschelkalk of Sardinia, and the upper part of the Monte Maggiore Formation, bivalve associations show a strong link to the Tethys province (Alpine domain) and the Germanic Basin. This supports the hypothesis of a seaway open towards the north during the late Fasnian - early Longobardian allowing fauna migration. The same situation appears in Minorca and the Catalan basin, where all bivalve associations show Tethyan affinities.

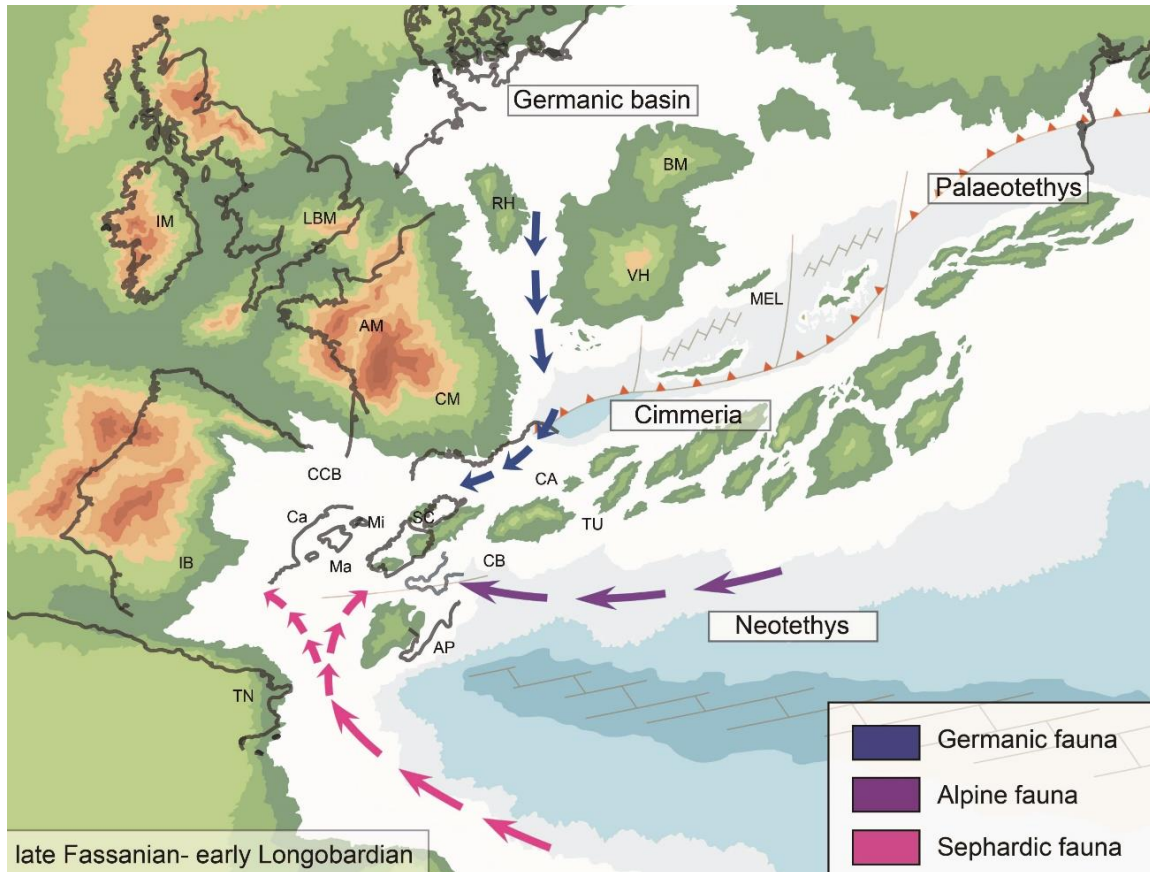


Fig. 8.2: Palaeogeographic reconstruction of the W Tethys realm for the Middle Triassic (late Fasnian-early Longobardian). AM Armorica; AB Alboràn; AG Autochthonous Greece; AP Apulia; BA Balearic; BD Bey-Daglari; BM Bohemian Massif; CA Carnic; CB Calabria; CM Central Massif; IB Iberian Massif; IM Irish Massif; LBM London-Brabant Massif; MA Mani; MEL Meliata; PEL Pelagonia; SC Sardinia-Corsica; TA Taurus; TN Tunisia; TU Tuscan; RH Rhenish Massif; VH Vindelic High; Mi Minorca; Ma Majorca; CCB Catalan Coastal Basin; Ca Castellón. Image modified from Escudero-Mozo et al. (2015) Ziegler and Stampfli (2001), Stampfli and Borel (2002) and Muttoni et al. (2009)

A mixed influence appears in the ammonite association of the Punta del Lavatoio Formation studied in Alghero and Monte Santa Giusta which shows strong affinity with the Sephardic province and the peri-Tethys domain, with the presence of *Gevanites awadi* Parnes (lower Fasnian) and *Alloceratites tornquisti* Philippi, but also of elements that point to a Germanic and Tethyan influence, with the presence of *Ceratites* sp. A similar influence can be seen in the Arenal d'en Castell Formation in Minorca (Escudero-Mozo et al., 2015). The Ladinian conodont assemblages found in the Punta del Lavatoio Formation by Bagnoli et al. (1985a, b) show a Sephardic influence, supporting a more open marine connection. The new palaeogeographic conditions that arose from these tectonic pulses and sea-level changes during the Ladinian means that the boundaries of the bioprovinces are less well-defined (Escudero-Mozo et al., 2014; Stori et al., 2022).

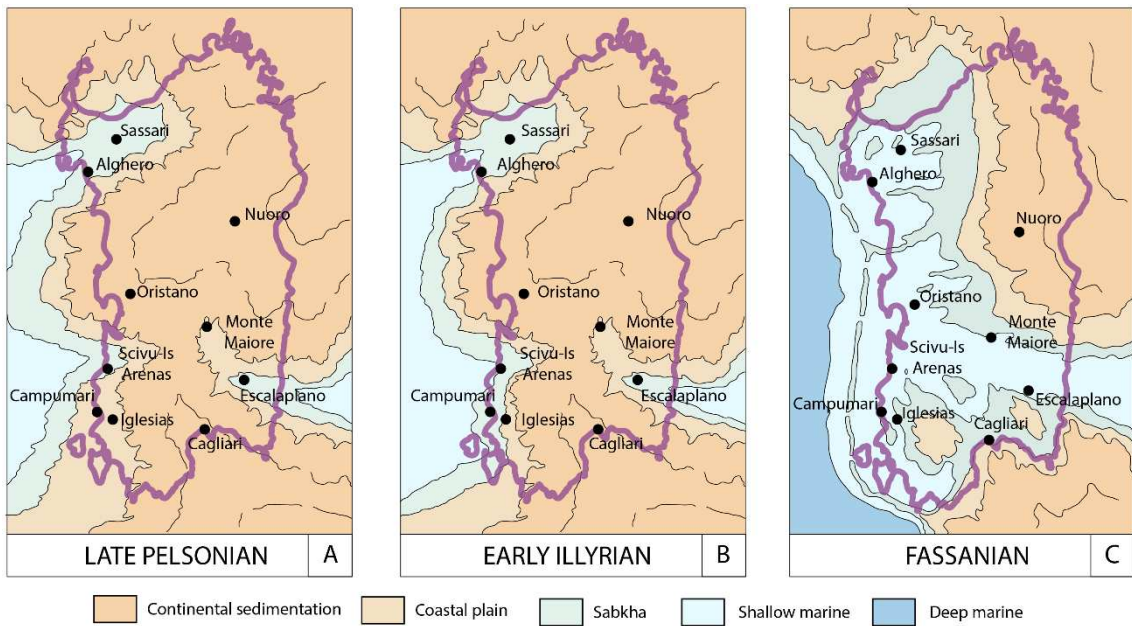


Fig. 8.3. Three stages of palaeogeographic evolution in Sardinia during the Middle Triassic, modified from Costamagna e Barca, 2002.

9. Conclusions

This thesis consists of an integrated and multidisciplinary study of the Middle Triassic facies of Sardinia, with particular focus on the continental to transitional Buntsandstein facies, and the shallow marine Sardinian Muschelkalk group Fms. It allowed a better framing and understanding of their stratigraphical, sedimentological, palaeontological, geochemical and sequence stratigraphy aspects. Moreover, the integration of these data with those obtained from other sectors of Sardinia and Western Europe make it possible to evaluate the palaeogeographical evolution of the Western Tethys realm during the late Anisian- Ladinian with greater precision.

From this study, the main conclusions can be summarized as follows:

1-The palynostratigraphical associations analyzed provided precise data on the age of the studied sections. It was possible to attribute the Escalaplano Formation to the Pelsonian, thanks to the data obtained from the Escalaplano SW and Arcu is Fronestas sections. As regards the Campumari succession, the sample from Su Pasu Malu Member (Campumari Formation) gave an Illyrian age-constraint. No indications of Early Triassic or lower Anisian associations were identified.

2- Where present, the fossiliferous content is scarce in the lower units of all the Sardinian Muschelkalk facies. This could be due to extreme environmental conditions. In contrast, all the upper units show a relatively great abundance of fossiliferous content. In particular, it is higher and more diverse in the Muschelkalk of the Nurra region (Punta del Lavatoio Fm), whereas in the Central and South sectors of the Island is less abundant.

3- The analysis of the fossiliferous content provenance shows that Sardinia records a mixed influence from the neighbouring Sephardic, Alpine and Germanic bioprovinces. This fact, associated with the progressive increase of fossiliferous content and diversity towards the upper units of the Muschelkalk facies, proves a more open connection between the different palaeobiogeographic domains. The key location of Sardinia during the Ladinian allowed to record this moment of regional transgression.

4- The concomitant presence of fauna with Palaeotethys (Germanic and Alpine) and Neotethys (Sephardic) affinity is related to different groups. Ammonoids show a mixed influence from both Palaeotethys and Neotethys domains. Bivalves show affinity only to the Palaeotethys domain, while the conodonts are exclusively Sephardic (Neotethys). This differences in diversity could be due to the way of migration and the different mobility of these species.

5-These data allow to define with greater accuracy the Tethys Sea incursion towards its westernmost domains during the Middle Triassic, as well as the different stages of the transgression in Sardinia during the late Anisian-early Ladinian.

6- Four main broad sedimentary environments can be differentiated in the Muschelkalk of Sardinia on the basis of facies. These are: 1) sabkha – muddy coastal plain 2) carbonate tidal flat 3) shallow low-energy subtidal (lagoon) 3) calcarenitic shoals and 5) middle ramp environment.

7- The study of the facies associations and the regional evolution of the depositional systems allowed to distinguish three large-scale systems tracts in the carbonate ramp that forms the Muschelkalk of Sardinia. These are: lowstand systems tract, transgressive systems tract, and highstand systems tract. Within the identified depositional megasequence, it has been possible to differentiate four main III° order depositional sequences: DSI, DSII, DSIII and DS IV.

8 - In Sardinia, the Muschelkalk facies does not appear until the late Illyrian. A similar situation is recorded in Minorca, Prebetic domain and the Levantino-Balear Domain. This could be due to the fact that, until that time, these areas constituted topographical highs that somehow were not affected by marine sedimentation, but only continental to transitional one. Indeed, the Sardinian Muschelkalk records only the later of the two transgressive–regressive cycles of the Tethys Sea, which is represented by the late Illyrian–Longobardian one.

9-Sardinia, together with Minorca and the eastern area of Castellón (easternmost Iberia), constituted a topographical high area until the middle-late Illyrian (late Anisian), when an important change in the configuration of the Western Tethys realm occurred. Up until that point, the Sardinia-Minorca block had played a key role by acting as a barrier between the realms of the Palaeotethys and Neotethys seas.

10- From the late Illyrian to the early Fassanian, the new transgression of the Tethys Sea progressively covered Sardinia with shallow marine deposits that also reached the neighbouring easternmost Iberia and Minorca areas. During this stage of the Tethys transgression, almost all the elevated areas of the Western Tethys domain were finally covered by the Tethys.

10. References

- Advokaat Eldert L., Douwe J.J. van Hinsbergen, Marco Maffionea, Cor G. Langereis, Reinoud L.M. Vissers, Antonietta Cherchi, Rolf Schroeder, Haroen Madani, Stefano Columbu, 2014. Eocene rotation of Sardinia, and the paleogeography of the western Mediterranean region. *Earth and Planetary Science Letters* 401, 183–195
- Algeo, T.J., Chen, Z., Frasier, M., Twitchett, R.J., 2011. Terrestrial–marine teleconnections in the collapse and rebuilding of Early Triassic marine ecosystems. *Palaeogeography, Palaeoclimatology, Palaeoecology* 308, 1–11.
- Anadón, P., Colombo, F., Esteban, M., Marzo, M., Orozco, S. R., Santanach, P., & Sugrañés, L. S., 1979. Evolución Tectonoestratigráfica De Los Catalánides. *Acta Geológica Hispánica* 14, 242-270.
- Angiolini L., Crippa G., Muttoni G., Pignatti J (2013) Guadalupian (Middle Permian) paleobiogeography of the Neotethys Ocean. *Gondwana Research* 24: 173–184
- Antonescu, E., (1969) Deux nouveaux types de spores dans les depots du Trias Moyen des Environs De Cristian (Roumanie). *Rev. Micropaleontol.; Fra;* 1969(6), Vol. 12, Num. 0001, P. 9 A 15
- Barca S., Costamagna L.G. & Del Rio M. (1995a). La successione triassica di Scivu-Is Arenas (Sardegna sud-occidentale). *Nuovi dati stratigrafici e sedimentologici. Atti Soc. Tosc. Sci. Nat., Mem., Serie A*, 102, 5-15.
- Barca S., Costamagna L.G. & Del Rio M., 1995b. Affioramenti permo-carboniferi e mesotriassici fra Porto Piscinas e Punta Acqua Durci (Arburese, Sardegna SW). *Bollettino della Società Sarda di Scienze Naturali* 30, 1-11
- Barca S. & Costamagna L.G. (1997b) – The Triassic succession of Campumari and Scivu-Is Arenas (SW Sardinia, Italy): analogues, correlations and some remarks. 18° IAS Meeting, Heidelberg, September 1997, Abstracts Book: 60, Heidelberg.
- Barca S. & Costamagna L.G., 2003. Analisi di facies e stratigrafia della successione permo?-triassica di Campumari-Coremò (Iglesiente, Sardegna SW). *Bollettino della Società Paleontologica Italiana* 122, 25-45.
- Barca S., Del Rio M & Pittau P., (2004). The Middle Triassic deposits of Escalaplano. In BARCA S. & Cherchi A. (eds), *Sardinian Paleozoic Basement and its Meso- Cainozoic covers*, Field Trip Guide Book, XXXII IGC Firenze 2004, APAT
- Bagnoli G., Gandin A. & Perri C., 1985a. Ladinian conodont apparatuses from northwestern Sardinia, Italy: *Bollettino della Società Paleontologica Italiana* 23(2), 311-232.
- Bagnoli G., Barattolo F., Fois E., Murru M., Perri C. & Pittau P., 1985b, Site B.1 – Middle Triassic of Punta del Lavatoio (Alghero). In Cherchi, A. (Ed.), *Guidebook of the “19th European Micropaleontological Colloquium”, Sardinia Oct. 1-10 1985*, 135-296.
- Balini, M., Lucas, S.G., Jenks, J.F., Spielmann, J.A., 2010. Triassic ammonoid biostratigraphy. *Geological Society, London, Specials Publications*, 334, 221-262.
- Banner, J. L., & Hanson, G. N. (1990). Calculation of simultaneous isotopic and trace element variations during water-rock interaction with applications to carbonate diagenesis. *Geochimica et Cosmochimica Acta*, 54(11), 3123-3137.

- Bartusch, M., 1985. Geologie des Monte Santa Giusta (Nurra, NW Sardinien). Thesis, University of Frankfurt, Frankfurt, 203 pp.
- Baud, A., Mégard-Galli, J., Gandin, A., & Amaudric du Chaffaut, S., 1977. Le Trias de Corse et de Sardaigne, tentative de corrélation avec le Trias d'Europe sud-occidentale. *Comptes Rendus de l'Académie des Sciences de Paris, Série D*, 284.
- Benton, M. J., & Newell, A. J., 2014. Impacts of global warming on Permo-Triassic terrestrial ecosystems. *Gondwana Research* 25(4), 1308-1337.
- Bond, D.P.G., Wignall, P.B., 2014. Large igneous provinces and mass extinctions: an update. *Geological Society of America Special Papers* 505, 29–55.
- Bornemann, G., 1881: Sul Trias della parte meridionale dell'isola di Sardegna. *Bollettino del R. Comitato geologico d'Italia* 12, 267–275, Roma.
- Bourquin S., Durand M., Diez J.B., Broutin J. & Fluteau F. (2007) - The Permian-Triassic boundary and Early Triassic sedimentation in Western European basins: An overview. *J. Iber. Geol.*, 33, 221-236.
- Borrueal-Abadía V., Barrenechea J.F., Galán-Abellán A.B., De La Horra R., López-Gómez J., Ronchi A., Luque F.J., Alonso-Azcárate J., Marzo M., (2019). Could acidity be the reason behind the Early Triassic biotic crisis on land?, *Chemical Geology*, Volume 515, Pages 77-86, ISSN 0009-2541.
- Broutin J., Cassinis G., Cortesogno L., Gaggero L., Ronchi A. & Sarria E. (1996) - Research in progress on the Permian deposits of Sardinia (Italy). *Permophiles*, a Newsletter of SPS, 28, 45-48.
- Brugman, W.A., (1983). Permian-Triassic Palynology. Lab. of Palaeobotany and Palynology. State university of Utrecht, The Netherlands, 121 p.
- Brugman, W.A., (1986). A Palynological Characterization of the Upper Scythian and Anisian of the Transdanubian Central Range (Hungary) and the Vincentinian Alps (Italy). PhD Thesis. Univ. de Utrecht, 95 p.
- Calvet, F., March, M., Pedrosa, A., 1987. Estratigrafía, sedimentología y diagénesis del Muschelkalk superior de los Catalánides. *Cuadernos de Geología Ibérica*, 11: 171-197.
- Carmignani L., Coccozza T., Ghezzi C., Pertusati P.C. & Ricci C.A. (1986) - Guide-book to the excursion on the Paleozoic Basement of Sardinia. I.G.C.P., N. 5, Newsletter, Special Issue, Cagliari, pp 102.
- Carmignani L., Franceschelli M., Pertusati P.C., Memmi I. & Ricci C.A. (1979) - Evoluzione tettono-metamorfica del basamento ercinico della Nurra (Sardegna NW). *Mem. Soc. Geol. It.*, 20, 57-84.
- Carmignani L., Ghezzi C., Marcello A., Pertusati P.C., Pretti S., Ricci C.A. & Salvadori I. (1994) - Petrology, geology and ore deposits of the Paleozoic basement of Sardinia. Guide book to the field excursion – B3. 16th General Meeting of the International Mineralogical Association. Pisa, September 10-15, pp 91.
- Carmignani, L., Oggiano, G., Barca, S., Conti, P., Salvadori, I., Eltrudis, A., Funedda, A. & Pasci, S. (2001) - Geologia della Sardegna. Note illustrative della Carta Geologica della Sardegna a scala 1:200.000. *Memorie descrittive della Carta Geologica d'Italia*, 60, 283 pp.

- Carosi R., Cruciani G., Franceschelli M., Montomoli C., 2014. The Variscan Basement in Sardinia. Field guide to the excursion of the 29th Himalaya-Karakoram-Tibet Workshop, Lucca 5-8 September 2014.
- Carrillat A., Martini R., Zaninetti L., Cirilli S., Gandin A. & Vrielynck B. (1999). The Muschelkalk (Middle to Upper Triassic) of the Monte di Santa Giusta (NW Sardinia): Sedimentology and biostratigraphy. *Eclogae geol. Helv*, 92, 81-97.
- Carrillat, A., Martini, R., Zaninetti, L., Cirilli, S., Gandin, A. and Vrielynck, B., 1999a. The Muschelkalk (Middle to Upper Triassic) of the Monte di Santa Giusta (NW Sardinia): sedimentology and biostratigraphy. *Eclogae Geologicae Helveticae* 92, 81–97.
- Carrillat, A., Gandin, A., Martini, R. and Oggiano, G., 1999b. Stratigraphic reconstruction and tectonic structure of the Triassic sequence of Monte Santa Giusta (Nurra) NW Sardinia, Italy. In: International Congress on the Continental Permian of the Southern Alps and Sardinia (Italy). (Ed. G. Cassinis) Regional reports and general correlations, 15–25 Sept. 1999, Abstracts book, pp. 88–89. Earth Science Department of the Pavia University, Brescia.
- Casula, G., Cherchi, A., Montadert, L., Murru, M., & Sarria, E., 2001. The Cenozoic graben system of Sardinia (Italy): geodynamic evolution from new seismic and field data. *Marine and petroleum geology* 18(7), 863-888.
- Cassinis G. & Ronchi A., 2002. - The (late-) Post-Variscan continental succession of Sardinia. *Rendiconti della Società Paleontologica Italiana* 1, 77-92.
- Cassinis, G., Cortesogno, L., Gaggero, L., Ronchi, A. & Valloni, R., 1996. Stratigraphic and petrographic investigations into the Permo-Triassic continental sequences of Nurra (NW Sardinia): *Cuad. Geol. Iberica, spec. issue*, 21: 149-169.
- Cassinis, G., Durand, M., Ronchi, A., 2002. The Permian and Triassic continental framework of Nurra (NW Sardinia). *Rendiconti della Società Paleontologica Italiana* 1, 297-305.
- Cassinis G., Durand M. & Ronchi A., 2003. Permian-Triassic continental sequences of Northwest Sardinia and South Provence: stratigraphic correlations and palaeogeographical implications. *Bollettino della Società Geologica Italiana* 2, 119-129.
- Casula, G., Cherchi, A., Montadert, L., Murru, M., & Sarria, E., 2001. The Cenozoic graben system of Sardinia (Italy): geodynamic evolution from new seismic and field data. *Marine and petroleum geology* 18(7), 863-888.
- Catuneanu, O., 2006. *Principles of Sequence Stratigraphy*. Elsevier, Amsterdam, 375 p.
- Cherchi A., Schroeder R., 1985. Mesozoic of NW Sardinia. Stratigraphy. In: Cherchi A. (Ed.), 19th European Colloquy on Micropaleontology, Sardinia, Oct. 1985 – Guidebook, pp. 44-56.
- Cirilli S. (2010) Upper Triassic-lowermost Jurassic palynology and palynostratigraphy: A review. *Geological Society, London, Special Publications* 2010; v. 334; p. 285-314
- Citton P., Ronchi A., Nicosia U., Sacchi E., Maganuco S., Cipriani A., Innamorati G., Zuccari C., Manucci F. & Romano M., Tetrapod tracks from the Middle Triassic of NW Sardinia (Nurra region, Italy), *Ital. J. Geosci.*, Vol. 139 No. 2 (2020), pp. 309-320, 6 figs. (<https://doi.org/10.3301/IJG.2020.07>) © Società Geologica Italiana, Roma 2020
- Cocozza T. & Gandin A. (1976) - Età e significato ambientale delle facies detritico-carbonatiche dell'altopiano di Campumari (Sardegna sud-occidentale). *Boll. Soc. Geol. It.*, 95, 1521-1540.
- Coe, A.L. (Ed.), 2003. *The Sedimentary Record of Sea-Level Change*. Cambridge University Press, New York, 287 p.

- Costamagna L.G., Barca S., Del Rio M. & Pittau P. (2000) - Stratigrafia, paleogeografia ed analisi di facies deposizionale del Trias del Sarcidano-Gerrei (Sardegna SE). *Boll. Soc. Geol. It.*, 119, 473-496.
- Costamagna, L.G., Barca, S., Del Rio, M. & Pittau, P., 2000. Stratigrafia, paleogeografia ed analisi di facies deposizionale del Trias del Sarcidano-Gerrei (Sardegna SE). *Bollettino della Societa Geologica Italiana* 119, 473–496.
- Costamagna, L. G., Barca, S., 2002. The «Germanic» Triassic of Sardinia (Italy): a stratigraphic, depositional and paleogeographic review. *Rivista Italiana di Paleontologia e Stratigrafia* 108 (1), 67-100.
- Costamagna L.G., Barca S. & Lecca L. (2007) - The Bajocian-Kimmeridgian Jurassic sedimentary cycle of eastern Sardinia: Stratigraphic, depositional and sequence interpretation of the new «Baunei Group». *C.R. Geoscience*, 339 (9), 601-612.
- Costamagna L. G. (2011) Alluvial, aeolian and tidal deposits in the Lower to Middle Triassic “Buntsandstein” of NW Sardinia (Italy): a new interpretation of the Neo-Tethys transgression. *Z. dt. Ges. Geowiss.*, 163/2, p. 165–183, 18 figs., 2 tables Article Stuttgart, June 2012
- Costamagna L. G. (2012) Facies analysis, stratigraphy and petrographic data from the Permian-Middle Triassic Cala Bona – Il Cantaro rock sections (Alghero, NW Sardinia, Italy): contribution to the post-Variscan Nurra basin evolution
- Costamagna L. G. (2016) - Middle Jurassic continental to marine transition in an extensional tectonics context: the Genna Selole Fm depositional system in the Tacchi area (central Sardinia, Italy). *Geol. J.* 51: 722–736 (2016).
- Costamagna, L. (2019). The carbonates of the post-Variscan basins of Sardinia: The evolution from Carboniferous–Permian humid-persistent to Permian arid-ephemeral lakes in a morphotectonic framework. *Geological Magazine*, 156(11), 1892-1914. doi:10.1017/S0016756819000232
- Costamagna, L. G., Barca, S., 2002. The «Germanic» Triassic of Sardinia (Italy): a stratigraphic, depositional and paleogeographic review. *Riv. Ital. Paleont. Strat.* 108 (1), 67-100.
- Courel, L., 1978. Presence De Polypamma Dervillei Schneider, Foraminifere, Dans La Lettenkohle De La Region De Bettendorf (Luxembourg).
- D’Archiac, A., 1860. Histoire des progrès de la Géologie de 1834-1849. Société Géologique de France, Paris, 8, 1-680.
- Damiani A.V. & Gandin A. (1973a) - L’affioramento triassico del Monte Maggiore di Nureci (Sardegna centrale). Nota I. *Boll. Soc. Geol. It.*, 92, 355-362.
- Damiani A.V. & Gandin A. (1973b) - Geologia ed ambiente di sedimentazione della successione triassica di M. Maggiore (Sardegna centrale). Nota II. *Boll. Soc. Geol. It.*, 92 (Suppl.), 41-83.
- Damiani, A.V. and Gandin, A. (1973c). Il Muschelkalk della Sardegna centro meridionale. *Boll. Serv. Geol. It.* 94, 81–116.
- Deninger, K., 1906. Einige neue Tabulaten und Hydrozoen aus mesozoischen Ablagerungen. *Neues Jahrbuch für Mineralogie, Geologie und Paläontologie* 1, 61-70.
- Deninger, K., 1907. Die mesozoischen Formationen auf Sardinien. *Neues Jahrbuch für Mineralogie, Geologie und Paläontologie* 23, 435-473.

Dieni I., Fischer J.C., Massari F., Salard-Cheboldaeff M. & Vozenin- Serra C. (1983) - La succession de Genna Selole (Baunei) dans le cadre de la paléogéographie mésojurassique de la Sardaigne orientale. Mem. Sci. Geol., Padova, 36, 117-148.

Diez J.B., (2000). Geología y Palaeobotánica de la Facies Buntsandstein en la Rama Aragonesa de la Cordillera Ibérica. Implicaciones bioestratigráficas en el Peritethys Occidental. Ph.D. thesis, Universidad de Zaragoza/Université Paris VI.

Diez J.B., Broutin J. & Ferrer J. (2005) - Difficulties encountered in defining the Permian-Triassic in Buntsandstein facies of the western Peritethyan based on palynological data. Palaeogeogr., Palaeoclimatol., Palaeoecol., 229, 40-53.

Dockter J., Puff P. Seidel, G. & Kozur H., (1980). Zur Trias Gliederung und Symbolgebung in der D.D.R. Z. geol. Wiss., 8: 951-963.

Dorn P., (1940) - Keuper in germanischer Fazies in Ostsardinien, Zentralbl. Mineral. Geol. Paleontol., Abt. B, Stuttgart.

Doubinger J. & Adloff M.C., (1983). Triassic palynomorphs of the Mediterranean Area. C.N.R.S. Rapport Centre de Sédimentologie et Géochimie de la Surface, Strasbourg, France, 26 p.

Durand M. (2006) - The problem of the transition from the Permian to the Triassic Series in southeastern France: comparison with other Peritethyan regions. In: Lucas S.G., Cassinis G. & Schneider J.W. (eds.). Non-Marine Permian Biostratigraphy and Biochronology. Geol. Soc., London, Spec. Publ., 265, 281-296.

Durand M. (2008) - Permian to Triassic continental successions in southern Provence (France): an overview. Boll. Soc. Geol. Ital., 127, 697-716.

Edel, J. B., Casini, L., Oggiano, G., Rossi, P., & Schulmann, K., 2014. Early Permian 90° clockwise rotation of the Maures–Estérel–Corsica–Sardinia block confirmed by new palaeomagnetic data and followed by a Triassic 60° clockwise rotation. Geological Society, London, Special Publications 405(1), 333-361.

Emery, D., Myers, K. J., 1996. Sequence Stratigraphy. Blackwell Science, 297 p.

Enos, P., 1983. Shelf environments. En: Scholle, P.A., Bebout, D.G., Moore, C.H. (Ed.), Carbonate depositional environments, American Association of Petroleum Geologist Memoir, 33: 268-295.

Erwin, D.H., 1993. The Great Paleozoic Crisis, Life and Death in the Permian. Columbia University Press, New York. (327 pp.).

Erwin, D.H., 1996. Recoveries and radiations: gastropods after the Permo-Triassic mass-extinction. In: Hart, M.B. (Ed.), Biotic Recovery from Mass-Extinction Events. Geological Society Special Publications 102, pp. 223–229.

Erwin, D.H., 2001. Lessons from the past: biotic recoveries from mass extinctions. Proceedings of the National Academy of Sciences, U.S.A 98, 5399-5403.

Escudero-Mozo, M.J., Martín-Chivelet, J., Goy, A., López-Gómez, J., 2014. Middle-Upper Triassic carbonate platforms in Minorca (Balearic Islands): implications for Western Tethys correlations. Sedimentary Geology 310, 41–58.

Escudero-Mozo, 2015. the Triassic carbonate platforms (Muschelkalk facies) of Eastern Iberia and Minorca: implications for the paleogeographic evolution of the Western Tethys. Thesis.

- Eshet Y., (1990). Paleozoic-Mesozoic palynology of Israel. 1. Palynological Aspects of the Permo-Triassic Succession in the Subsurface of Israel. Geological Survey of Israel. 81, p. 1-57.
- Fazzini P., Gasperi G. & Gelmini R. (1974) - Ricerche sul Verrucano. 2. Le successioni basali dei Tacchi tra Escalaplano e Jerzu (Sardegna sud-orientale). Boll. Soc. Geol. It., 93, 221-243.
- Fernández-López, S.R., 1985. El Bajociense en la Cordillera Ibérica. Departamento de Paleontología, Universidad Complutense de Madrid, pp. 1-850.
- Ferrandini M., Ginsburg L., Ferrandini M. & Rossi Ph. (2000) - Présence de *Pomelomeryx boulangerii* (Artiodactyla, Mammalia) dans l'Oligocène supérieur de la région d'Ajaccio (Corse): étude paléontologique et conséquences. C. R. Acad. Sci. Paris, 331, 675-681.
- Flaviani A. (1980). Palinologia e stratigrafia del Trias del sondaggio Cugiareddu: Sardegna nord occidentale. Thesis, unpublished. Cagliari University.
- Flügel, E. (Ed.), 2004. Microfacies of Carbonate Rocks: Analysis, Interpretation and Application. Springer, 972 p.
- Fontana, D., Gelmini, R. and Lombardi, G. (1982). Le successioni sedimentarie e vulcaniche carbonifere e permo-Triassiche della Sardegna. In Guida alla Geologia del Paleozoico sardo. Guide Geologiche Regionali, Boll. Soc. Geol. It. 183-192.
- Fontana D., Neri C., Ronchi A. & Stefani C. (2001) – Stratigraphic architecture and composition of the Permian and Triassic siliciclastic succession of Nurra (north-western Sardinia). In Cassinis G. (Ed.): The Continental Permian of the Southern Alps and Sardinia (Italy). Regional reports and general correlations, 25, 149-161.
- Frechengues M., Peybernes B., Fournier-Vinas C. & Lucas C., (1993). Palynologic assemblages within the depositional sequences from the middle to Late Triassic series of the Spanish and French Pyrenees. Rev. Esp. Paleo., 25 (3), p. 91-105.
- Fritz, P., Smith, D.G.W., 1970. The isotopic composition of secondary dolomites. *Geochimica et Cosmochimica Acta*, 34: 1161-1173.
- Gaillot, J., & Vachard, D., 2007. The Khuff Formation (Middle East) and time-equivalents in Turkey and South China: biostratigraphy from Capitanian to Changhsingian times (Permian), new foraminiferal taxa, and palaeogeographical implications/La Formación Khuff (Oriente Medio) y sus equivalentes cronológicos de Turquía y China del Sur: bioestratigrafía, nuevos taxones de foraminíferos e implicaciones paleogeográficas del Capitanense al Changhsingense (Pérmico Medio-Superior). *Coloquios de Paleontología*, 57, 37.
- Gandin, A., 1978. Il Trias medio di Punta del Lavatoio (Alghero, Sardegna NW). *Memorie della Società Geologica Italiana* 18, 3–13.
- Gandin, A., Tongiorgi, M., Rau, A., & Virgili, C., 1982. Some examples of the Middle-Triassic marine transgression in south-western Mediterranean Europe. *Geologische Rundschau* 71(3), 881-894.
- Gandin, A., Martini, R., & Zaninetti, L., 1987. Microfaunal diversity and diagenesis in the Muschelkalk facies. *Cuadernos Geologia Ibérica* 11, 827-835.
- Gaggero L., Grotter N., Langone A. & Ronchi A., 2017. U-Pb geochronology and geochemistry of late Palaeozoic volcanism in Sardinia (southern Variscides). *Geoscience Frontiers* 8(6), 1-22.
- Gattacceca J., Deino A., Rizzo R., D.S. Jones D.S., Henry B., Beaudoin B., Vadeboin F., 2007. Miocene rotation of Sardinia: New paleomagnetic and geochronological constraints and geodynamic implications. *Earth and Planetary Science Letters* 258 (2007) 359–377.

- Gianolla, P., 2010. The changing climate framework and depositional dynamics of Triassic carbonate platforms from the Dolomites. *Palaeogeography, Palaeoclimatology, Palaeoecology* 290, 43-57.
- Gianolla P. & Jaquin, T. (1998) - Triassic sequences stratigraphic framework of western European basins. In: DE Graciansky P.C., Hardenbol J., Jaquin T. & Vail P. (Eds.), *Mesozoic and Cenozoic Sequences Stratigraphy of European Basins*. Society for Sedimentary Geology, Special Publication 60: 643-650.
- Goy, A., 1986. Ammonoideos del Triásico de España. Universidad Complutense de Madrid, pp. 1-28.
- Goy, A., 1995. Ammonoideos del Triásico Medio de España: Bioestratigrafía y Correlaciones. *Cuadernos de Geología Ibérica* 19, 21-60
- Hayashi, S., 1968. The Permian conodonts in chert of the Aoyama Formation, Ashio mountains, central Japan. *Earth Science* 22(2), 63-77.
- Hays and Grossman, 1991 P.D. Hays, E.L. Grossman Oxygen isotopes in meteoric calcite cements as indicators of continental paleoclimate *Geology*, 19 (5) (1991), pp. 441-444.
- Hips, K., 1998. Lower Triassic storm-dominated ramp sequence in northern Hungary: an example of evolution from homoclinal through distally steepened ramp to Middle Triassic flat-topped platform. En: Wright, V.P., Burchette, T.P. (Eds.), *Carbonate Ramps*, The Geological Society, special publication, 149: 315-338.
- Hirsch, F., 1971. Conodontes nouvelles du Trias méditerranéen. *Compte Rendu des Seances de la Société de Physique et d'Historie Naturelle de Genève* 6, 65-69.
- Hirsch F., 1975. Lower Triassic Conodonts from Israel. *Geological Survey of Israel Bulletin* 66, 39-48.
- Hirsch, F. (1972). Middle Triassic conodonts from Israel, southern France and Spain. *Mitteilungen der Gesellschaft der Geologie-und Bergbaustudenten* 21, 811-828.
- Hirsch, F., 1977. Essai de corrélation biostratigraphique des niveaux Meso et Neotriassic de facies "Muschelkalk" du Domaine Sepharade. *Cuadernos de Geología Ibérica* 4, 511-525.
- Hirsch, F., 1987. Bio-stratigraphy and correlation of the marine Triassic of the Sepharadic Province. *Cuadernos de Geología Ibérica* 11, 815-826.
- Hoefs, J., 2009. *Stable isotope Geochemistry*. Springer, Berlín, 285 p.
- James, N.P., 1984. Shallowing upwards sequences in Carbonates. En: Walker, R.G. (Ed.), *Facies Models*. Geosciences Canada Reprint Series, 1: 213-228.
- Kendall, A.C., Harwood, G.M., 1996. Marine evaporites: arid shorelines and basins. En: Reading, H.G. (Ed.), *Sedimentary Environments: Processes, Facies and Stratigraphy*. Blackwell Science. Oxford, 281-324.
- Knaust D. & Costamagna L.G., 2012. Ichnology and sedimentology of the Triassic carbonates of North-west Sardinia, Italy. *Sedimentology* (2012) 59, 1190-1207
- Krystyn, L., 1983. Das Epidaurus-Profil (Griechenland)—ein Beitrag zur Conodonten-Standardzonierung des tethyalen Ladin und Unterkarn
- Koehn-Zaninetti, L., Bronnimann, P., & Gall, J. C., 1969. Description de quelques Foraminifères du grès à Voltzia (Buntsandstein supérieur) des Vosges (France). *Sciences Géologiques, bulletins et mémoires* 22(2), 121-130.

- Kovács, S., & Kozur, H., 1980. Stratigraphische Reichweite der wichtigsten Conodonten (ohne Zahnreihenconodonten) der Mittel-und Obertrias.
- Kozur, H., Krainer, K., & Mostler, H., 1994. Middle Triassic conodonts from the Southern Karawanken Mountains (Southern Alps) and their stratigraphic importance. *Geologisch-Paläontologische Mitteilungen Innsbruck* 19, 165-200.
- Kump, L. R., & Arthur, M. A. (1999). Interpreting carbon-isotope excursions: carbonates and organic matter. *Chemical Geology*, 161(1-3), 181-198.
- Kürschner W. & Waldemaar Herengreen G.F., 2010. Triassic palynology of central and northwestern Europe: a review of palynofloral diversity patterns and biostratigraphic subdivisions, in: LUCAS S.G. (Eds.), *Triassic Timescale*. Geological Society of London, London, United Kingdom; Special Publications 334, 263-283.
- Lamarmora A., 1826. *Voyage en Sardaigne de 1819 à 1825 ou Description Statistique, Physique et Politique de cette Île, avec des Recherches sur ses Productions Naturelles et ses Antiquités*. Paris, Delaforest, pp. 1-802
- Liu, D., Huang, C., Ogg, J. G., Kemp, D. B., Li, M., Yu, M., & Foster, W. J., 2021. Astronomically forced changes in chemical weathering and redox during the Anisian (Middle Triassic): Implications for marine ecosystem recovery following the end-Permian mass extinction. *Palaeogeography, Palaeoclimatology, Palaeoecology* 569, 110355.
- López-Gómez, J., Mas, R., 1991. Middle Triassic (Muschelkalk) carbonate platforms of the Iberian Ranges, East Spain: Sedimentary evolution and its diagenetic implication. En: *Dolomieu Conference on Carbonate Platforms and Dolomitization*. Libro de Abstract, Ortisei/St. Ulrich, Italia.
- López-Gómez, J., Más, R., Arche, A., 1993: The evolution of the Middle Triassic (Muschelkalk) carbonate ramp in the SE Iberian Ranges, Eastern Spain: sequence stratigraphy, dolomitization processes and dynamic controls. *Sedimentary Geology*, 87: 165-193.
- López-Gómez, J., Arche, A., Calvet, F., Goy, A., 1998. Epicontinental marine carbonate sediments of the Middle and Upper Triassic in the westernmost part of the Tethys Sea, Iberian Peninsula. *Zentralblatt für Geologie und Paläontologie*, 9-10, 1033-1084.
- Lovisato D., 1884. Nota sopra il Permiano ed il Triassico della Nurra in Sardegna. *Bollettino del R. Comitato Geologico d'Italia* 15, 305-324, Roma.
- Martin, K.D., 2004. A re-evaluation of the relationship between trace fossils and dysoxia. En: McIlroy, D. (Ed.), *The application of Ichnology to Palaeoenvironmental and Stratigraphic Analysis*. Geological Society, London, Special Publications, 228: 141-156.
- Martini, R., Amieux, P. D. G., Gandin, A., & Zaninetti, L., 1987. Triassic foraminifers from Punta Tonnara (SW Sardinia) observed in cathodoluminescence. *Revue de Paléobiologie* 6, 23-27.
- Martín-Algarra A, & Vera J.A. (2004) - La Cordillera Bética y las Baleares en el contexto del Mediterráneo POccidental. In: Vera, J.A. (Ed.), *Geología de España*. Sociedad Geológica de España. Instituto Geológico y Minero de España, Madrid, 352-354.
- Martín-Rojas I., Somma R., Delgado F., Estévez A., Iannace A., Perrone V., (2009) - Triassic continental rifting of Pangaea: direct evidence from the Alpujarride carbonates, Betic Cordillera, SE Spain. *Journal of Geological Society, London* 166: 447-458.

- Martín-Chivelet, J., 2005. Estratigrafía secuencial y acomodación: Claves para la interpretación genética del relleno sedimentario. *Boletín de la Real Sociedad Española de Historia Natural*, 100(1-4): 55-75.
- Márquez-Aliaga, A., 1985. Bivalvos del Triásico Medio del Sector Meridional de la Cordillera Ibérica y de los Catalánides. Editorial Universidad Complutense de Madrid 40, 429 pp.
- Márquez-Aliaga, A., Gandin, A., Goy, A., Plasencia, P., 2000. Nuevas aportaciones paleontológicas del Triásico Medio de Cerdeña (Italia). I Congreso Ibérico de Paleontología / XVI Jornadas de la Sociedad Española de Paleontología, Evora (Portugal), Libro de Abstrac, 103-104.
- Marshall, J. D. (1992). Climatic and oceanographic isotopic signals from the carbonate rock record and their preservation. *Geological magazine*, 129(2), 143-160.
- Mas, R., Benito, M.I., Alonso, A., 2010. La sedimentación carbonática en mares someros: las plataformas carbonáticas. En: Arche, A. (Ed.), *Sedimentología: del proceso físico a la cuenca sedimentaria*, Consejo Superior de Investigaciones Científicas, 639-917.
- McCann, T., Pascal, C., Timmerman, M. J., Krzywiec, P., López-Gómez, J., Wetzel, L., ... & Lamarche, J., 2006. Post-Variscan (end Carboniferous-Early Permian) basin evolution in western and central Europe. *Geological Society, London, Memoirs* 32(1), 355-388.
- McGhee Jr, G. R., Clapham, M. E., Sheehan, P. M., Bottjer, D. J., & Droser, M. L., 2013. A new ecological-severity ranking of major Phanerozoic biodiversity crises. *Palaeogeography, Palaeoclimatology, Palaeoecology* 370, 260-270.
- Mercedes-Martín R., Salas R., & Arenas C. (2013) – Microbial-dominated carbonate platforms during the Ladinian rifting: sequence stratigraphy and evolution of accommodation in a fault-controlled setting (Catalan Coastal Ranges, NE Spain). *Basin Research* 25: 1-28.
- Mietto, P., Manfrin, S., Preto, N., Rigo, M., Roghi, G., Furin, S., Gianolla, P., Posenato, R., Muttoni, G., Nicora, A., Buratti, N., Cirilli, S., Spötl, C., Ramezani, J., Bowring, S.A., (2012). The Global Boundary Stratotype Section and Point (GSSP) of the Carnian Stage (Late Triassic) at Prati di Stuares/Stuares Wiesen Section (Southern Alps, NE Italy). *Episodes* 35 (3), 414–420.
- Muttoni G., Gaetani M., Kent D.V., Sciunnach D., Angiolini L., Berra F., Garzanti E., Mattei M. and Zanchi A. (2009). Opening of the Neo-Tethys Ocean and the Pangea B to Pangea A transformation during the Permian. *GeoArabia*, v. 14, no. 4, 2009, p. 17-48 Neo-Tethys opening and Pangea transformation. Gulf PetroLink, Bahrain
- Mojsisovics, E. Von, 1882. Die Cephalopoden der mediterranean Triasprovinz. *Abhandlung der Kaiserlich Königlichen Geologischen Reichsanstalt, Wien* 10, 1-322.
- Moore R.C. (1962) - *Treatise of Invertebrate Paleontology*, Vol. W, *Miscellanea*. Geol. Soc. America, University of Kansas Press, Boulder, Colorado, and Lawrence, Kansas.
- Mosher, L. C., & Clark, D. L., 1965. Middle Triassic conodonts from the Prida Formation of northwestern Nevada. *Journal of Paleontology*, 551-565.
- Nichols, G., 2009. *Sedimentology and Stratigraphy*. Oxford, U. K., Wiley-Blackwell, 419 p.
- Nicora, A., & Brack, P., 1995. The Anisian/Ladinian boundary interval at Bagolino (Southern Alps, Italy): II. The distribution of Conodonts. *Albertiana* 15, 57-65.
- Novarese V. (1914) – Il rilevamento geologico delle tavolette Iglesias e Nebida. *Boll. R. Com. Geol. Italiano*: 44, 29-59, Roma.

- Oosterbaan A. M., 1936. Étude géologique et paléontologique de la Nurra avec quelques notes sur le Permien et le Trias de la Sardaigne meridionale. University Utrecht, 130 pp.
- Ortí, F., 1974. El Keuper del Levante Español. *Estudios geológicos*, 30: 7-46.
- Ortí F., J.Guimerà J., Götz A.E., 2020. Middle-Upper Triassic stratigraphy and structure of the Alt Palància (eastern Iberian Chain): A multidisciplinary approach, *Geologica Acta*, 18.4, 1-25. DOI: 10.1344/GeologicaActa2020.18.4
- Park, R.K., 2011. The impact of sea-level change on ramp margin deposition: lessons from the Holocene sabkhas of Abu Dhabi, United Arab Emirates. En: Kendall, C.G.St.C. y Alsharhan, A.S. (Eds.), *Quaternary carbonate and evaporate sedimentary facies and their ancient analogues*, International Association of Sedimentologist, Special publication, 43: 89-131.
- Parnes, A., 1962. Triassic Ammonites from Israel. *Geological Survey of Israel Bulletin* 33, 1-78.
- Parnes, A., 1975. Middle Triassic ammonite biostratigraphy in Israel. *Geological Survey of Israel Bulletin*, 66, 1-35.
- Parnes, A., 1986. Middle Triassic Cephalopods from the Negev (Israel) and Sinai (Egypt). *Geological Survey of Israel Bulletin* 79, 1-59.
- Pastor-Galán D., Groenewegen T., Brouwer D., Krijgsman W., Dekkers M.J. (2015) One or two oroclines in the Variscan orogen of Iberia ? Implications for Pangea amalgamation. *Geology* 43: 527–530.
- Payne JL & Kump LR (2007) Evidence for recurrent Early Triassic massive volcanism from quantitative interpretation of carbon isotope fluctuations. *Earth and Planetary Science Letters* 256: 264–277
- Pecorini G. (1974) - Nuove osservazioni sul Permo-Trias di Escalaplano (Sardegna sud-orientale). *Boll. Soc. Geol. It.*, 93, 991-999.
- Pérez-López, A. & Pérez-Valera, F. (2007)- Palaeogeography, facies and nomenclature of the Triassic units in the different domains of the Betic Cordillera (SE Spain). *Palaeogeography, Palaeoclimatology, Palaeoecology* 254: 606-626.
- Pérez-Valera, J.A., 2005. Ammonoideos y bioestratigrafía del Triásico Medio (Anisiense superior-Ladiniense) en la sección de Calasparra, sector oriental de la Cordillera Bética, Murcia, España). *Coloquios de Paleontología* 55, 125-161.
- Pérez-Valera, J.A., 2015. Ammonoideos y Bioestratigrafía del Triásico Medio (Ladiniense) del sector oriental de la Cordillera Bética. Tesis Doctoral, Universidad Complutense de Madrid, XXII, 489 pp.
- Pérez-Valera, J.A., Pérez-Valera, F., Goy, A., 2005. Bioestratigrafía del Ladiniense Inferior en la región de Calasparra (Murcia, España). *Geo-Temas* 8, 211-2015.
- Pérez-Valera, J.A., Pérez-López, F., Götz, A.E., Ros-Franch, S., Márquez-Aliaga, A., Baeza-Carratalá, J.F., Pérez-Valera, J.A., 2023. First record of Anisian deposits in the Betic External Zone of southern Spain and its paleogeographical implications. *Sedimentary Geology*. <https://doi.org/10.1016/j.sedgeo.2023.106374>
- Pertusati P.C., Sarria E., Cherchi G.P., Carmignani L., Barca S., Benedetti M., Chighine G., Cincotti F., Oggiano G., Ulzega A., Orru P. & Pintus C. (2002a) - Note illustrative della Carta Geologica d'Italia alla scala 1:50.000 - Foglio 541 Jerzu. Servizio Geologico Nazionale - Regione Autonoma Sardegna, 168 pp.

Pertusati P.C., Sarria E., Cherchi G.P., Carmignani L., Barca S., Benedetti M., Chighine G., Cincotti F., Oggiano G., Ulzega A., Orru P. & Pintus C. (2002b) - Foglio 541 Jerzu – Carta Geologica d'Italia alla scala 1:50.000. Servizio Geologico Nazionale. Regione Autonoma Sardegna.

Philippi E., 1901b. Die Ceratiten des oberen deutschen Muschelkalkes. Paläontologische Abhandlungen, NF 4, 8, 347-458.

Pittau Demelia P. & Del Rio M. (1980) - Pollini e spore del Trias medio e del Trias superiore negli affioramenti di Campumari e di Ghisciera Mala (Sardegna). Boll. Soc. Paleont. It., 19, 241-249, Modena.

Pittau Demelia, P. and Flaviani, A. (1982a). Palinostratigrafia della serie Triassica di Punta del Lavatoio (Sardegna nord-occidentale). Riv. It. Paleont. Strat. 88, 401-416, Milano.

Pittau Demelia, P. and Flaviani, A. (1982b). Aspect of the palynostratigraphy of the Triassic Sardinia sequences (Preliminary report). Rev. Palaeobot. and Palyn. 37, 377-380, Amsterdam.

Pittau, P., 1999. The Triassic succession of Northwest Sardinia: data from the subsurface. Cassinis G., Cortesogno L., Gaggero L., Pittau P., Ronchi A. & Sarria E. (Coordinators) (2000): Late Palaeozoic continental basins of Sardinia. Field trip guidebook, 15-18.

Pittau P. & Del Rio M. (2002). Palynofloral biostratigraphy of the Permian and Triassic sequences of Sardinia. Rend. Soc. Paleont. It., 1, 93-109.

Pittau P., Del Rio M. & Funedda A. (2008). Plant communities characterization and basin formation in the Carboniferous-Permian of Sardinia. Boll. Soc. Geol. It. (Ital.J.Geosci.), Vol. 127, No. 3 (2008), pp. 637-653.

Plint, A. G., Nummedal, D., 2000. The falling stage systems tract: recognition and importance in sequence stratigraphic analysis. En: Hunt, D., Gawthorpe, R.L. (Eds.), Sedimentary Response to Forced Regression. Geological Society of London Special Publication, 172: 1-17.

Pomesano Cherchi A., 1967. I conodonti del Muschelkalk della Nurra (Sardegna nord-occidentale). Rivista Italiana di Paleontologia e Stratigrafia 73(1), 205-272.

Pomesano Cherchi A., 1968. Studio biostratigrafico del sondaggio Cugiareddu nel Trias e Permico della Nurra nord - occ. Università di Cagliari, Istituto di Geologia e Paleontologia, 61.

Posamentier, H.W., Vail, P.R., 1988. Eustatic controls on clastic deposition II—sequence and systems tract models. En: Wilgus, C. K., Hastings, B. S., Posamentier, J.V., Van Wagoner, J., Ross, C. A., Kendall, C.G.St.C. (Eds.), Sea Level Changes-An Integrated Approach. SEPM Special Publication, 42: 125–154.

Posenato, R., 2002a. The Triassic of the Nurra region (Northwestern Sardinia, Italy). Rend. Soc. Paleontol. Ital., 1, 111–118. Posenato, R. (2002b) Bivalves and other macrobenthic fauna from the Ladinian “Muschelkalk” of Punta del Lavatoio (Alghero, SW Sardinia). Rendiconti della Società Paleontologica Italiana 1, 185–196.

Posenato, R., 2002b. Bivalves and other macrobenthic fauna from the Ladinian “Muschelkalk” of Punta del Lavatoio (Alghero, SW Sardinia). Rendiconti della Società Paleontologica Italiana, 1, 185–196.

Posenato R., Simone L., Urlichs M. & Ibba A. (2002). The Ladinian Muschelkalk of Punta del Lavatoio (Alghero, NW Sardinia). Rend. Soc. Paleont. Ital., 1, 283-291

- Prokoph, A., Shields, G.A., Veizer, J., 2008. Compilation and time-series analysis of a marine carbonate $\delta^{18}\text{O}$, $\delta^{13}\text{C}$, $87\text{Sr}/86\text{Sr}$ and $\delta^{34}\text{S}$ database through Earth history. *Earth-Science Reviews*, 87: 113-133.
- Rieber, H. & Brack, P., 2004. Taxonomy and stratigraphic significance of *Falsanolcites* gen. nov., Anolcites-like Middle triassic ammonioidea from the Alps and Greece. *Mitteilungen aus dem Geologisch-Paläontologischen Institut (GPI) der Universität Hamburg* 88, 157-178.
- Riedel, A., 1916. Beiträge zur Paläontologie und Stratigraphie der Ceratiten des deutschen Oberen Muschelkalks. *Jahrbuch der Königlich Preussischen geologischen Landesanstalt zu Berlin*, 37, 1/1, , 1-116.
- Robertson, A. H., 2002. Overview of the genesis and emplacement of Mesozoic ophiolites in the Eastern Mediterranean Tethyan region. *Lithos* 65(1-2), 1-67.
- Ronchi A. (1997). I prodotti sedimentari e vulcanici dei bacini permiani di Escalaplano e Perdasdefogu nella Sardegna sudorientale: stratigrafia e loro inquadramento nell'evoluzione tardo-paleozoica del settore sudeuropeo. PhD Thesis, Univ. Parma, 231 pp.
- Ronchi A., Sarria E., Broutin J., (2008). The «Autuniano Sardo»: basic features for a correlation through the Western Mediterranean and Paleoeurope. *Boll. Soc. Geol. It.* 127 (3): 655-681.
- Ronchi A., Sacchi E., Nicosia U. & Romano M., 2008. Ritrovamento di un vertebrato di grandi dimensioni nei depositi continentali permiani della Nurra (Sardegna NO). *Istituto Lombardo (Rendiconti Scienze) B*, 142, 291-306. 84° Congresso Nazionale della Società Geologica Italiana - Sassari, 2008. Volume 3 (1)/2011. Pp. 1-43. DOI: <https://doi.org/10.3301/GFT.2011.01>
- Ronchi A., Sacchi E., Romano M. & Nicosia U., 2011. A huge caseid pelycosaur from north-western Sardinia and its bearing on European Permian stratigraphy and palaeobiogeography. *Acta Palaeontologica Polonica* 56(4), 723-738.
- Ronchi A., Cassinis G., Durand M., Fontana D., Oggiano G. & Stefani C, 2011. Stratigrafia e analisi di facies della successione continentale permiana e triassica della Nurra: confronti con la Provenza e ricostruzione paleogeografica.
- Salvany , J.M., Ortí, F., 1987. El Keuper de los Catalánides. *Cuadernos de Geología Ibérica*, 11: 215-236.
- Sanz, T., Lago, M., Gil, A., Galé, C., Ramajo, J., Ubide, T., ... & Larrea, P., 2013. The Upper Triassic alkaline magmatism in the NW Iberian Chain (Spain). *Journal of Iberian Geology* 39(2), 203-222.
- Sanz De Galdeano C., Andreo B., García-Tortosa F.J. & López-Garrido A.C. (2001) - The Triassic palaeogeographic transition between the Alpujarride and Malaguide complexes, Betic Rift Internal Zone (S Spain, N Marocco). *Palaeogeography, Palaeoclimatology, Palaeoecology* 167: 157-173.
- Sartori, R. (2001). Corsica—Sardinia block and the Tyrrhenian Sea. In: Vai, G.B., Martini, I.P. (eds) *Anatomy of an Orogen: the Apennines and Adjacent Mediterranean Basins*. Springer, Dordrecht. https://doi.org/10.1007/978-94-015-9829-3_21
- Savrda, C., Bottjer, D., 1986. Trace fossil model for reconstruction of paleo-oxygenation in bottom waters. *Geology*, 14: 3-6.
- Seilacher A. (1982) - Distinctive features of sandy tempestites. In: Einsele G. & Seilacher A. (Eds.): *Cyclic and Event Stratification*. Springer, Berlin, Heidelberg, 333-349.

Scotese CR, Schettino A, 2017, Late Permian-Early Jurassic Paleogeography of Western Tethys and the World, Permo-Triassic salt provinces of Europe, North Africa and the Atlantic margins, 57-95

Shinn, E.A., 1983. Tidal Falt Environemnts. En: Scholle, P.A., Bebout, D.G., Moore, C.H. (Eds.), Carbonate depositional environments, American Association of Petroleum Geologist Memoir, 33: 172-210.

Sinisi, R., Mongelli, G., Mameli, P., Oggiano, G., 2014. Did the Variscan relief influence the Permian climate of mesoeurope? Insights from geochemical and mineralogical proxies from Sardinia (Italy). *Palaeogeogr. Palaeoclimatol. Palaeoecol.* 396.

Speranza, F., Villa, I. M., Sagnotti, L., Florindo, F., Cosentino, D., Cipollari, P., & Mattei, M., 2002. Age of the Corsica–Sardinia rotation and Liguro–Provençal Basin spreading: new paleomagnetic and Ar/Ar evidence. *Tectonophysics* 347(4), 231-251.

Stampfli GM, Borel GD (2002) A plate tectonic model for the Paleozoic and Mesozoic constrained by dynamic plate boundaries and restored synthetic oceanic isochrones. *Earth and Planetary Science Letters* 196: 17–33

Stampfli, G. M., & G. D. Borel., 2004. The TRANSMED transects in space and time: constraints on the paleotectonic evolution of the Mediterranean domain. In W. Cavazza, F. Roure, W. Spakman, G. M. Stampfli, P. A. Ziegler, eds., *The TRANSMED Atlas. The Mediterranean Region from Crust to Mantle*. Mediterranean Consortium for the 32nd International Geological Congress. p. 53–80 Stefani, M., Furin, S.,

Stampfli GM, Hochard C, Vérard C, Wilhem C, Von Raumer J (2013) The formation of Pangea. *Tectonophysics* 593: 1–19.

Stanley, S. M., 1977. Coadaptation in the Trigoniidae, a remarkable family of burrowing bivalves. *Palaeontology* 20(4), 869-899.

Stordal, F., Svensen, H. H., Aarnes, I., Roscher & M., 2017. Global temperature response to century-scale degassing from the Siberian Traps Large igneous province. *Palaeogeography, Palaeoclimatology, Palaeoecology*, 471. 96-107 doi:10.1016/j.palaeo.2017.01.045 Sun, Y., Joachimski, M.M., Wignall, P.B., Yan,

Stori, L., Diez, J.B., Juncal, M., De la Horra, R., Borrueal- Abadía, V., Martín- Chivelet, J., López-Gómez, J., Barrenechea, J.F. & Ronchi, A., 2022. The Anisian continental-marine transition in Sardinia (Italy): state of the art, new palynological data and regional chronostratigraphic correlation. *Journal of Iberian Geology*, 1-28.

Strohmenger, C.J., Shelb, H., Al-Mansoori, A., Al-Mehsin, K., Al-Jeelani, O., Al-Hosani, I., Al-Shamry, A., Al-Baker, S., 2011. Facies stacking patterns in a modern arid environment: a case study of the Abu Dhabi sabkha in the vicinity of Al-Qanatir Island, United Arab Emirates. En:

Sun Y D, Joachimski M M, Wignall P B, Chunbo Ch, Haishui J, Lina W, Xulo L (2012) Lethally hot temperatures during the Early Triassic greenhouse. *Science* 338: 366–370

Svensen H., Planke S., Polozov AG, Schmidbauer N, Corfu F., Podladchikov Y.Y., Jamtveit B., 2009, Siberian gas venting and the end-Permian environmental crisis, *Earth and Planetary Science Letters* 277 (2009) 490–500

Szente, I., 1997. Bivalve assemblages from the Middle Triassic Muschelkalk of the Mecsek Mts, South Hungary: An overview. *Acta Geologica Hungarica* 40(4), 411-424.

Taricco M. (1928) – Il Cambriano del Sulcis (Sardegna) Res. Ass. Min. Sarda: 33, 10-29, Iglesias.

Tanner L., 2010. The Triassic isotope record. Geological Society, London, Special Publications. Volume 334. Pages 103 – 118. <https://doi.org/10.1144/SP334.5>

Tornquist A. (1902) - Die Gliederung und Fossiliführung der ausseralpinen Trias auf Sardinien. Sitz. K. Preuss, Akad. Wiss., 38, 1098-1117, Berlin.

Tornquist, A., 1904. De Gliederung und Fossilführung der ausseralpinen Trias auf Sardinien. Sitzungsberg. Sitzungsberichte der Königlich Preussischen Akademie der Wissenschaften zu Berlin Proceedings 38, 1098-1117.

Török, A., 1998. Controls on development of Mid-Triassic ramps: examples from southern Hungary. En: Wright, V.P., Burchette, T.P. (Eds.), Carbonate Ramps, The Geological Society, special publication, 149: 339-367.

Tozer, E.T., 1994. Canadian Triassic ammonoid faunas. Geological Survey of Canada Bulletin 463, 1-663

Tucker, M., Wright, V.P., 1990. Carbonate sedimentology. Blackwell Science. Oxford, 482 p.

Urlichs, M., 1993. Zur Gliederung des Oberen Muschelkalks in Baden-Württemberg mit Ceratiten. Muschelkalk Schöntaler Symposium 1991 (H. Hagdorn & A. Seilacher Ed.), Goldschneck-Verlag Werner K. Weider, Stuttgart, 153-156.

Urlichs, M., 1997. Die Gattung Ceratites (Ammonoidea) aus dem Muschelkalk der Provence (Mitteltrias, Südost-Frankreich). Stuttgarter Beiträge zur Naturkunde., B, 252, 1-12.

Urlichs, M., 2000. Zur Entwicklungsreihe Germanonautilus bidorsatus-G. suevicus aus dem Germanischen Oberen Muschelkalk (Nautiloidea, Mitteltrias). Stuttgarter Beiträge zur Naturkunde B, 292, 1-16.

Urlichs, M., 2016. Phyletic relationships among Alloceratites species from the upper Erfurt Formation of Thuringia (Late Ladinian, Germany) and from the Early Ladinian of Recoaro (Italy) and Toulon (France). Neues Jahrbuch Paläontologie Geologie Paläontologische Abhandlung 282/1, 27-35.

Urlichs, M., Mudlos, R., 1987. Revision der gattung Ceratites De Haan 1825 (Ammonoidea, Mitteltrias). I. Stuttgarter Beiträge zur Naturkunde, B, 128, 1-36.

Urlichs, M. & Posenato, R., 2002. Ammonoids from the Ladinian "Muschelkalk" of Punta del Lavatoio (Alghero, NW Sardinia). Rendiconti della Società Paleontologica Italiana 1, 197-2001.

Vail, P.R., Audemard, F., Bowman, S.A., Eisner, P.N., Perez-Cruz, C., 1991. The stratigraphic signatures of tectonics, eustasy and sedimentology—an overview. En: Einsele, G., Ricken, W., Seilacher, A. (Eds.), Cycles and Events in Stratigraphy. Berlin, Springer-Verlag, 617–659

Van Wagoner, J.C., Mitchum, R.M.Jr., Campion, K.M., Rahmanian, V.D., 1990. Siliciclastic sequence stratigraphy in well logs, core, and outcrops: concepts for high-resolution correlation of time and facies. American Association of Petroleum Geologists Methods in Exploration Series 7, 55 p.

Vardabasso S., 1956. La fase sarda dell'orogenesi caledonica in Sardegna. In : Geotektonisches Symposium zu Ehren von H. Stille

Vilas, F., Bernabéu, A., Rubio, B., Rey, D., 2010. Estuarios, rías y llanuras intermareales. En: Arche, A. (Ed.), Sedimentología: del proceso físico a la cuenca sedimentaria, Consejo Superior de Investigaciones Científicas, 619-673.

Visscher H., Brugman W.A., 1981. Ranges of selected palynomorphs in the Alpine Triassic of Europe. *Review of Palaeobotany and Palynology* 34 (1), 115-128.

Vrielynck, B., 1987. Conodontes du Trias périméditerranéen. systématique, stratigraphie. *Travaux et Documents des Laboratoires de Géologie de Lyon* 97(1), 3-306.

Warren, J., 2000. Dolomite: occurrence, evolution and economically important associations. *Earth-Sciences Re-views*, 52: 1-81.

Wei H., Shen J., D. Schoepfer S., Krystyn L., Richoz S., J. Algeo T., 2015. Environmental controls on marine ecosystem recovery following mass extinctions, with an example from the Early Triassic, *Earth-Science Reviews*, Volume 149, 2015, Pages 108-135, ISSN 0012-8252, <https://doi.org/10.1016/j.earscirev.2014.10.007>.

Wignall P B. The End-Permian mass extinction— How bad did it get? *Geobiology*, 2007, 5: 303–309

Wilson, J.L., Jordan, C., 1983. Middle Shelf Environments. En: Scholle, P.A., Bebout, D.G., Moore, C.H. (Ed.), *Carbonate Depositional Environments*, American Association of Petroleum Geologist Memoir, 33: 298-343.

Wood G.D., Gabriel A.M., & Lawson J.C. 1996. Palynological techniques – processing and microscopy. In: Jansonius J. & McGregor D.C. (eds.) *Palynology: principles and applications*, American Association of Stratigraphic Palynologists Foundation, 1, 29-50.

Wright, V.P., Burchette, T. P., 1996. Shallow-water carbonate environments. En: Reading, H. G., (Ed.), *Sedimentary Environments: processes, facies, and stratigraphy*. Blackwell Science, Oxford, 325-394.

Ziegler, P.A., 1990. Geological atlas of western and central Europe. Shell Internationale Petroleum Maatschappij B.V. Geological Society of London, (239 pp.).

Ziegler, P.A., 1999. Evolution of the Arctic-North Atlantic and the Western Tethys AAPG. *Bulletin* 43, 164–196.

Ziegler, P.A., Stampfli, G.M., 2001. Late Paleozoic–Early Mesozoic plate boundary reorganization: collapse of the Variscan orogen and opening of Neotethys. *Natura Bresciana. Ann. Mus. Civ. Sc. Nat. Bresci.* 25, 17–34.

Appendix 1

Table of Palynomorphs referenced in the Study.

Plates 1, 2 Escalaplano Assemblage (PC-2, PC-3, PC-4)

Plates 3, 4 Lower Arcu Is Fronestas Assemblage (AIF-2, AIF-5) Plates 5, 6 Upper Arcu Is Fronestas Assemblage (AIF-9, PC-7.2) Plates 7, 8 Su Passu Malu Assemblage (Grifo-3)

The photomicrographs were taken using a Leica DM 2000 LED microscope with a Leica ICC50 W camera using a magnification of x1000.

Palynomorph labelling is as follow: PC-3_B_03_K234. PC-3 means the sample, B_03 means the number of slides within the sample and K234 means the location within the slide calculated with an England Finder slide.

TABLE OF PALYNOMORPHS REFERENCED IN THE STUDY

	PREVIOUS WORKS										THIS WORK				
	Pitau, Demelia and De Rui (1980)	Flavianni (1980)	Pitau, Demelia and Flavianni (1982)	Pitau, Demelia and Flavianni (1982)	Pitau, Demelia and Flavianni (1982)	Pitau, Demelia and Flavianni (1982)	Pitau, Demelia and Flavianni (1982)	Pitau, Demelia and Flavianni (1982)	Pitau, Demelia and Flavianni (1982)	Pitau, Demelia and Flavianni (1982)	Pitau, Demelia and Flavianni (1982)	Restubled Diez (2000)	Field trip 1996	New samples	Field trip 2018-19
<i>Alisporites grunowii</i> Klaus 1964															
<i>Alisporites opii</i> Daugherty 1945															
<i>Alisporites magnus</i> Jain 1968															
<i>Alisporites microreticulatus</i> Reinhardt 1964															
<i>Alisporites thomasi</i> (Couper) Nilsson 1958															
<i>Alisporites</i> sp.															
<i>Alisporites</i> complex															
<i>Argastisulites gortii</i> Visscher 1966															
<i>Argastisulites grandis</i> (Freudenthal) Visscher 1966															
<i>Argastisulites klausii</i> Freudenthal 1964															
<i>Argastisulites</i> sp.															
<i>Amulapora</i> sp.															
<i>Aratrisporites bulloides</i> Pitau Demelia in Flavianni 1980															
<i>Aratrisporites distalirgulatus</i> Pitau Demelia in Flavianni 1980															
<i>Aratrisporites fisheri</i> (Klaus) Playford & Detmann 1965															
<i>Aratrisporites cf. granulatus</i>															
<i>Aratrisporites parapsinosus</i> Klaus 1960															
<i>Aratrisporites</i> sp.															
<i>Rozansporites</i> sp.															
<i>Bruchisaccus microsaccus</i> Mädlar 1964															
<i>Bruchisaccus neomundanus</i> Leschik 1955															
<i>Bruchisaccus ovalis</i> Mädlar 1964															
<i>Bruchisaccus</i> sp.															
<i>Calanospora tener</i> (Leschik) Mädlar 1964															
<i>Calanospora</i> sp.															
<i>Callisporites dampieri</i> (Balme) Suk Dev 1964															
<i>Comarozonosporites cf. rudis</i> (Leschik) Klaus 1960															
<i>Comarozonosporites</i> sp.															
<i>Ceratosporites mesozoicus</i> Nilsson 1950															
<i>Chamatosporites</i> sp.															
<i>Chorasporites stigulichorda</i> Klaus 1964															
<i>Chorasporites</i> sp.															
<i>Convolvigera</i> sp.															
<i>Cosporites albigranis</i> Visscher 1966															
<i>Cosporites</i> sp.															
<i>Coverzanosporites major</i> Pitau Demelia in Flavianni 1980															
<i>Lurakella</i> sp.															
<i>Uristanisporites triangularis</i> Antonescu 1969															
<i>Luncoisporites radialis</i> Leschik 1955															
<i>Luncoisporites</i> sp.															
<i>Cycadites subgracilissus</i> (Couper) Dharwadaj & Singh 1964															
<i>Cycadites</i> sp.															
<i>Cyclogranisporites granulatus</i> Mädlar 1964															
<i>Cyclogranisporites</i> sp.															
<i>Cyclotriletes oligogranifer</i> Mädlar 1964															
<i>Cyclotriletes margaritatus</i> Mädlar 1964															
<i>Melanospora</i> sp.															
<i>Densosporites neburgii</i> (Schulz) Balme 1970															
<i>Densosporites</i> sp.															
<i>Densosporites variomarginatus</i> Playford 1962															
<i>Densosporites</i> sp.															
<i>Dicryopylites moronti</i> (De Jersey) Playford & Detmann 1965															
<i>Diodonipora filamentosa</i> Scherwag 1970															
<i>Diplicisporites granulatus</i> (Leschik) Scherwag 1970															
<i>Diplicisporites viciiformis</i> Bruggen 1983															
<i>Elioporettoporites plebeus</i> Klaus 1960															
<i>Enzanosporites leschiki</i> Mädlar 1964															
<i>Enzanosporites tenuis</i> Leschik 1955															
<i>Enzanosporites vigena</i> Leschik 1955															
<i>cf. Falcisporites stabilis</i> Balme 1970															
<i>Falcisporites amplexus</i> Visscher 1966															
<i>Foveosporites missouri</i> (De Jersey and Hamilton) 1967															
<i>Foveosporites vischeri</i> Van Erve 1975															
<i>Foveosporites</i> sp.															
<i>cf. Gardenosporites</i> sp.															
<i>Gigiospora escalaplanis</i> Pitau Demelia in Flavianni 1980															
<i>Guttatisporites elegans</i> Visscher 1966															
<i>Heliosaccus dimorphus</i> Mädlar 1964															
<i>Heliosaccus cf. dimorphus</i> Mädlar 1964															
<i>Hexasaccus muelleri</i> (Reinhardt & Schmitz) Adloff & Doubringer 1968															
<i>Illites chitonoides</i> Klaus 1964															
<i>Illites kosankei</i> Klaus 1964															
<i>Illites</i> aff. <i>kosankei-chitonoides</i>															
<i>Illites</i> sp.															
<i>Jugosporites delavansi</i> (Rittner & Klaus) Leschik 1956															
<i>Klausipollenites schubertzi</i> (Patonie & Klaus) Janzonius 1962															
<i>Klausipollenites</i> sp.															
<i>Kraeuselisporites cuspidus</i> Balme 1963															
<i>Kraeuselisporites</i> sp.															
<i>Lapposporites lapposus</i> Visscher 1966															
<i>Lapposporites</i> sp.															
<i>Leptolepidites</i> sp.															

Plate 1. Escalaplano assemblage, Plate 1:

1. *Alisporites magnus* Jain 1968. PC-3_B_03_K234.
2. *Alisporites opii* Daugherty, 1941. PC-3_B_03_S292.
3. *Alisporites grauvogeli* Klaus, 1964. PC-3_B_02_P333.
4. *Alisporites* sp. PC-4_B_03_K380.
5. *Angustisulcites klausii* (Freudenthal) Visscher, 1966. PC-4_B_01_M324.
6. *Illinites kosankei* Klaus, 1964. PC-3_B_01_P293.
7. *Illinites chitonoides* Klaus, 1964. PC-3_01_G364.
8. *Illinites chitonoides* Klaus, 1964. PC-3_B_03_E300.
9. *Angustisulcites grandis* (Freudenthal) Visscher, 1966. PC-2_B_01_V350.
10. *Triadispora falcata* Klaus, 1964. PC-04_B_03_O400.
11. *Triadispora staplinii* (Jansonius) Klaus, 1964. PC-3_B_02_E270.
12. *Triadispora crassa* Klaus, 1964. PC-3_02_O414.
13. *Triadispora plicata* Klaus, 1964. PC-3_B_03_P404.
14. *Triadispora suspecta* Scheuring, 1970. PC-3_B_01_D274.
15. *Triadispora* sp.1. PC-2_B_02_F432.
16. *Klausipollenites schaubergeri* (Potonié and Klaus) Jansonius, 1962. PC-3_B_01_J202.
17. *Triadispora* sp. (Three-saccated anomalous form). PC-3_01_U434.
18. *Triadispora* sp. (asymmetric tetrad). PC-3_01_K320.
19. *Triadispora* sp. (symmetric tetrad). PC-4_B_03_T480.
20. *Microcachrydites fastidioides* (Jansonius) Klaus, 1964. PC-3_B_02_Q421.
21. *Lunatisporites acutus* Leschik, 1955. PC-4_B_03_X480.
22. *Lunatisporites noviaulensis* (Leschik) de Jersey, 1979. PC-4_B_02_U313.
23. *Lunatisporites* cf. *puntii* Visscher, 1966. PC-3_01_O313.
24. *Microcachrydites doubingeri* Klaus, 1964. PC-3_B_02_G482.
25. *Platysaccus papilionis* Potonié and Klaus, 1954. PC-3_B_03_M352.
26. *Platysaccus* sp. PC-2_B_03_J470.
27. *Chordasporites singulichorda* Klaus, 1960. PC-2_B_01_H402.

Plate 1. Escalaplano assemblage.

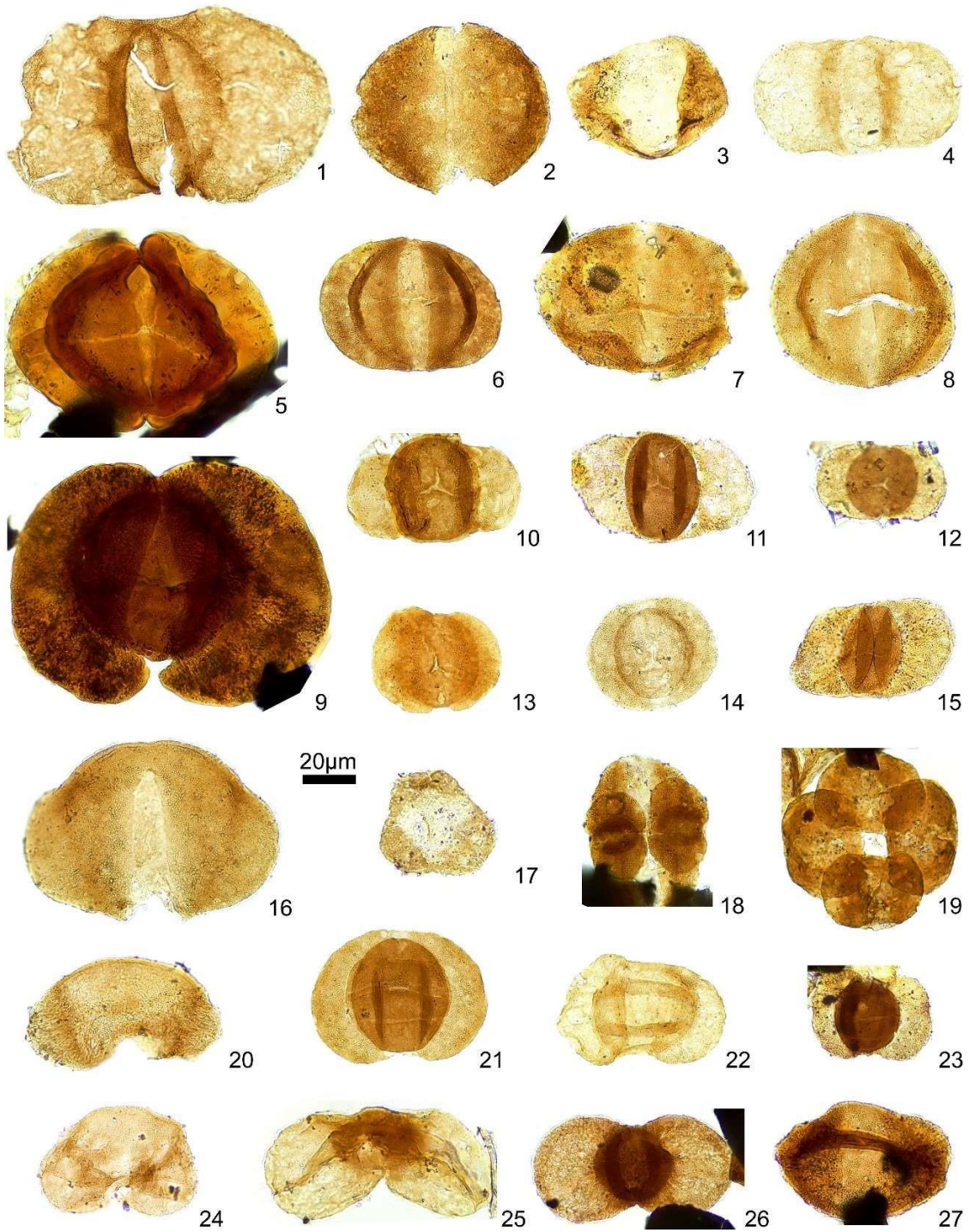


Plate 2. Escalaplano assemblage:

1. *Hexasaccites muelleri* (Reinhardt and Schmitz) Adloff and Doubinger, 1969 (= *Stellapollenites thiergartii* (Mädler) Clement-Westerhof et al. 1974). (Equatorial view). PC-4_B_02_S360.
2. *Hexasaccites muelleri* (Reinhardt and Schmitz) Adloff and Doubinger, 1969. (Immature form). PC-3_B_01_Q411.
3. *Hexasaccites muelleri* (Reinhardt and Schmitz) Adloff and Doubinger, 1969. PC-3_B_03_M464.
4. *Hexasaccites muelleri* (Reinhardt and Schmitz) Adloff and Doubinger, 1969. PC-2_B_04_W351.
5. *Hexasaccites muelleri* (Reinhardt and Schmitz) Adloff and Doubinger, 1969. PC-3_03_R431.
6. *Hexasaccites muelleri* (Reinhardt and Schmitz) Adloff and Doubinger, 1969. PC-3_B_01_M233.
7. *Hexasaccites muelleri* (Reinhardt and Schmitz) Adloff and Doubinger, 1969. PC-3_01_M233.
8. *Enzonalasporites vigens* Leschik, 1955 (Tetrad). PC-3_01_O222.
9. *Enzonalasporites vigens* Leschik, 1955. PC-3_B_03_N404.
10. *Striatopodocarpidites cancellatus* (Balme and Hennelly) Hart, 1963. PC-3_B_01_U232.
11. *Striatoabieites aytugii* (Visscher) Scheuring, 1978. PC-4_B_03_X400.
12. *Heliosaccus dimorphus*. Mädler, 1964. PC-4_B_02_Q411.
13. *Strotersporites jansonii* Klaus, 1963. PC-3_B_02_T340.
14. *Rewanispora vermiculata* Antonescu and Taugourdeau-Lantz, 1973. PC-2_B_04_W343.
15. *Rewanispora* sp. PC-3_B_01_T342.
16. *Limbosporites* sp. PC-2_B_03_Q274.
17. *Uvaesporites* sp. PC-3_B_03_L291.
18. *Aratrisporites* sp. PC-3_01_F300.
19. *Cerebropollenites mesozoicus* Nilsson, 1958. PC-3_B_02_H310.
20. *Calamospora tener* (Leschik) Mädler, 1964. PC-4_B_02_E343.
21. *Calamospora* sp. PC-2_B_01_M520.
22. *Cyclotriletes oligogranifer* Mädler, 1964. PC-3_B_02_H270.
23. *Cyclotriletes granulatus* Mädler, 1964. PC-3_B_03_R452.
24. *Microreticulatisporites gallii* Adloff and Doubinger, 1969. PC-4_B_02_K250.
25. *Kraeuselisporites* sp. PC-3_B_03_K294.
26. *Punctatisporites fungosus* Balme, 1963. PC-3_B_01_P414.
27. *Punctatisporites triassicus* Schulz, 1964. PC-3_B_03_N281.
28. Unidentified spore 1. PC-4_B_02_S310.
29. *Paleospongisporis europaeus* Schulz, 1965. PC-2_B_01_E472.
30. Unidentified spore 2. PC-4_B_01_Q292.
31. *Verrucosisporites* sp.1. PC-4_B_01_M320.
32. *Chasmatosporites* sp. PC-2_B_03_P262.

Plate 1. Escalaplano assemblage.

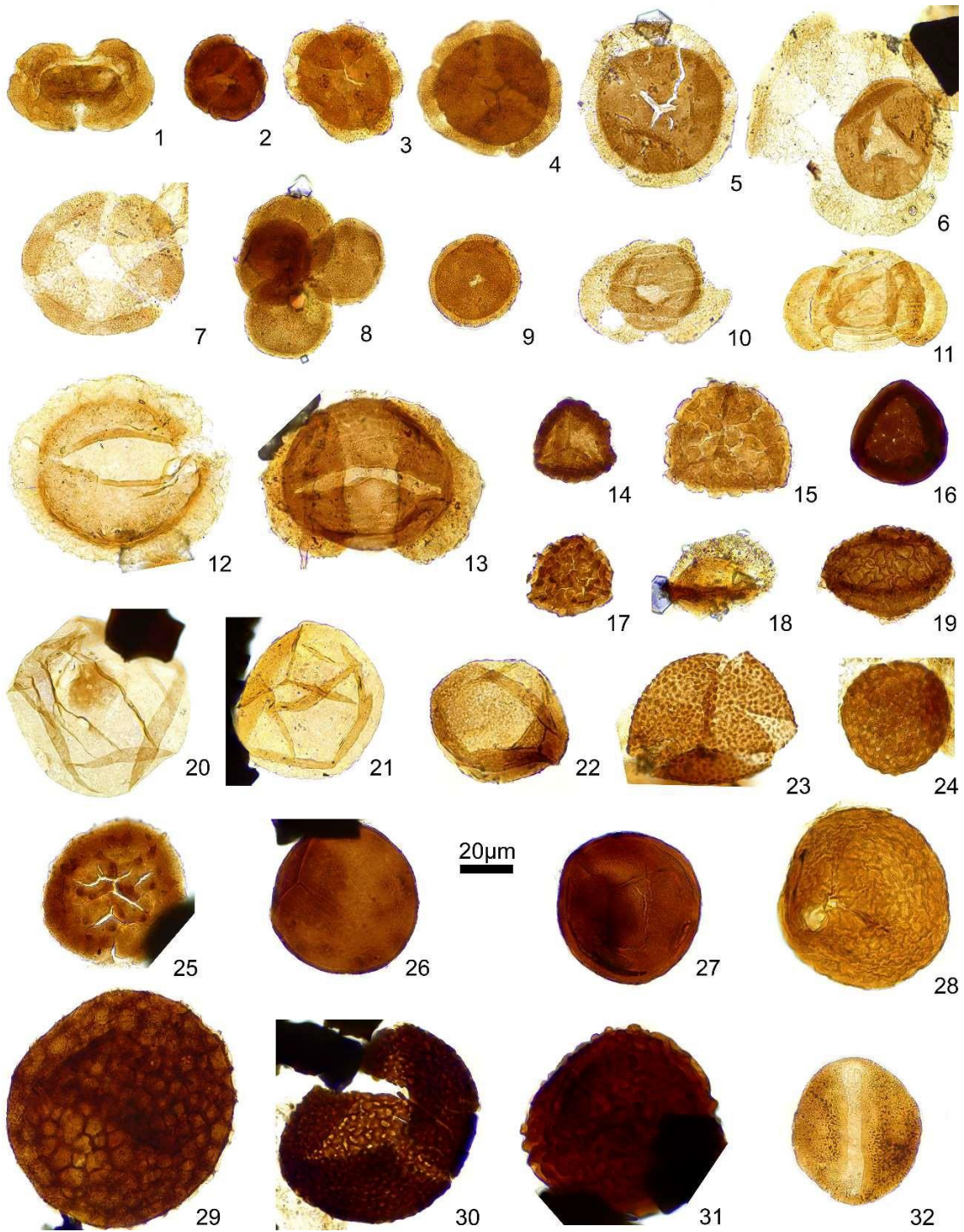


Plate 3. Lower Fronestras assemblage:

1. *Alisporites grauvogeli* Klaus, 1964. AIF-5_04_N151.
2. *Alisporites opii* Daugherty, 1941. AIF-2_01_N140.
3. *Alisporites magnus* Jain 1968. AIF-5_01_F191.
4. *Alisporites* sp. AIF-5_02_Q170.
5. *Brachisaccus neomundanus* (Leschik) Mádler, 1964. AIF-5_01_E200.
6. *Illinites chitonoides* Klaus, 1964. AIF-5_04_L211.
7. *Illinites kosankei* Klaus, 1964. AIF-5_01_R370.
8. *Illinites* sp. AIF-5_01_N221.
9. *Angustisulcites gorpil* Visscher, 1966. AIF-5_02_H193.
10. *Angustisulcites klausii* (Freudenthal) Visscher, 1966. AIF-2_01_Q343.
11. *Angustisulcites* sp. AIF-2_01_R193.
12. *Chordasporites singulichorda* Klaus, 1960. AIF-2_01_H493.
13. *Lunatisporites noviaulensis* (Leschik 1956) de Jersey, 1979. AIF-2_02_G231.
14. *Lunatisporites noviaulensis* (Leschik 1956) de Jersey, 1979. AIF-2_01_J220.
15. *Microcachrydites doubingeri* Klaus, 1964. AIF-5_01_D351.
16. *Microcachrydites fastidioides* (Jansonius) Klaus, 1964. AIF-5_01_S192.
17. *Microcachrydites* sp. AIF-2_02_D404.
18. *Platysaccus* sp. AIF-5_01_L191.
19. *Platysaccus leschikii* Hart, 1960. AIF-2_01_S273.
20. *Klausipollenites* sp. AIF-5_01_M480.
21. *Vitreisporites* sp. AIF-5_04_M040.

Plate 3. Lower Fronestras assemblage:

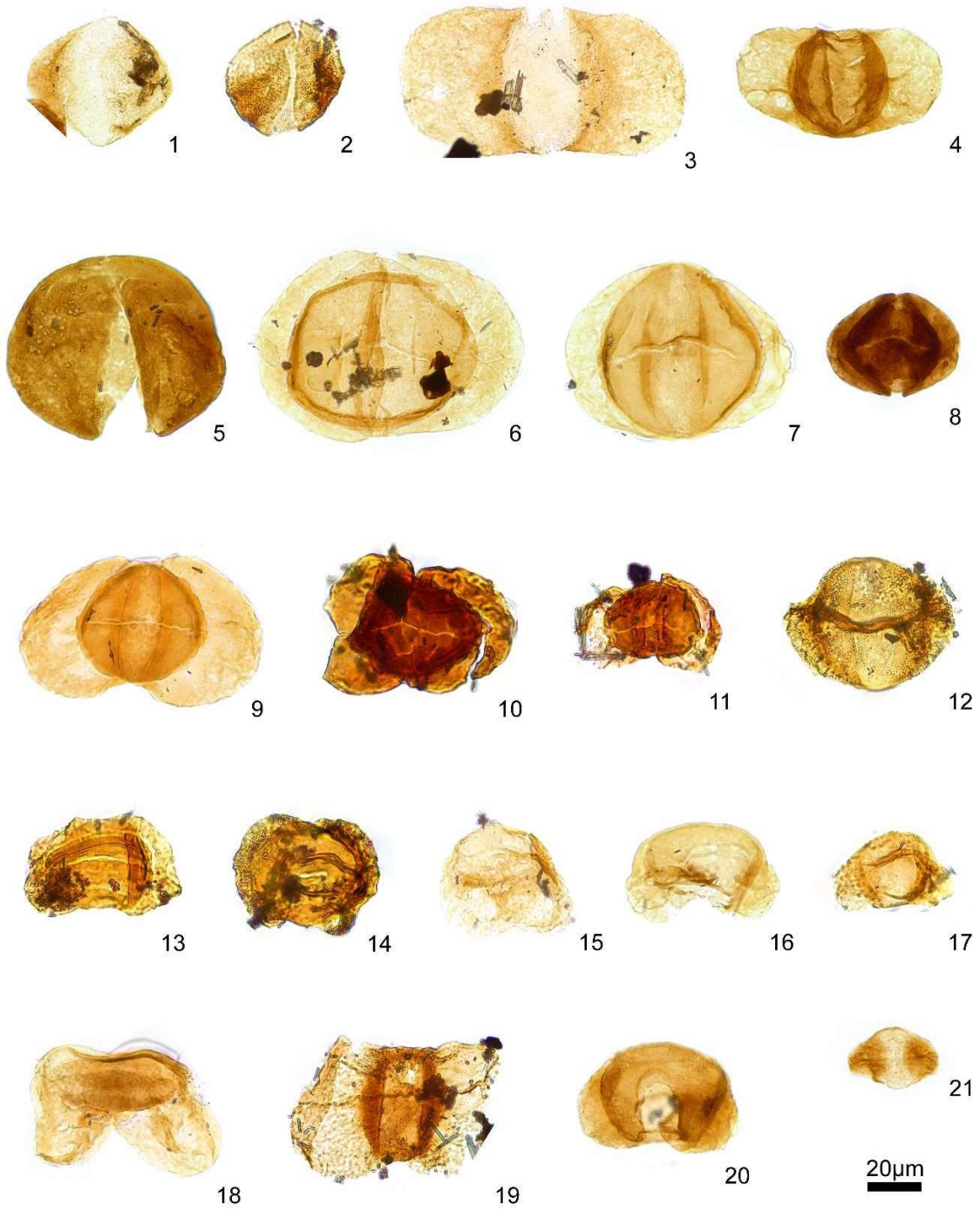


Plate 4. Lower Fronestras assemblage:

1. *Hexasaccites muelleri* (Reinhardt and Schmitz) Adloff and Doubinger, 1969. AIF-5_01_U133.
2. *Hexasaccites muelleri* (Reinhardt and Schmitz) Adloff and Doubinger, 1969. AIF-5_01_Q144.
3. *Hexasaccites muelleri* (Reinhardt and Schmitz) Adloff and Doubinger, 1969. AIF-2_01_J333.
4. *Cristianisporites triangulatus* Antonescu, 1969. AIF-5_01_J264.
5. *Cristianisporites triangulatus* Antonescu, 1969. AIF-5_02_R500.
6. *Triadispora crassa* Klaus, 1964. AIF-5_02_R464.
7. *Triadispora plicata* Klaus, 1964. AIF-5_02_L363.
8. *Triadispora staplinii* (Jansonius) Klaus, 1964. AIF-5_01_G291.
9. *Triadispora suspecta* Scheuring, 1970. AIF-5_01_G230.
10. *Triadispora* sp. AIF-5_02_G050.
11. *Triadispora* sp. (Tetrad). AIF-5_03_Q410.
12. *Enzonasporites vigens* Leschik, 1955. AIF-5_01_P394.
13. *Paracirculina* sp. (Tetrad). AIF-5_03_H190.
14. *Paracirculina* sp. AIF-2_01_N061.
15. *Cycadopites* sp. AIF-5_01_M443.
16. *Aratrisporites* cf. *granulatus* (Klaus) Playford and Dettmann, 1965. AIF-5_02_O301.
17. *Aratrisporites* sp. AIF-5_01_O094.
18. *Chasmatosporites* sp. AIF-5_01_H324.
19. *Chasmatosporites* sp. AIF-5_03_H401.
20. *Punctatisporites fungosus* Balme, 1963. AIF-5_01_U124.
21. *Kraeuselisporites* sp. AIF-5_03_F133.
22. *Rewanispora vermiculata* Antonescu and Taugourdeau-Lantz, 1973. AIF-5_02_S261.
23. *Uvaesporites* sp. AIF-5_01_M383.
24. *Densoisporites nejburgii* (Schulz) Balme, 1970. AIF-5_03_C430.
25. *Camarozonosporites* sp. AIF-5_04_J353.
26. Unidentified spore 3. AIF-5_01_E220.
27. *Rewanispora vermiculata* Antonescu and Taugourdeau-Lantz, 1973. (Tetrad). AIF-5_01_U342.

Plate 4. Lower Fronestras assemblage:

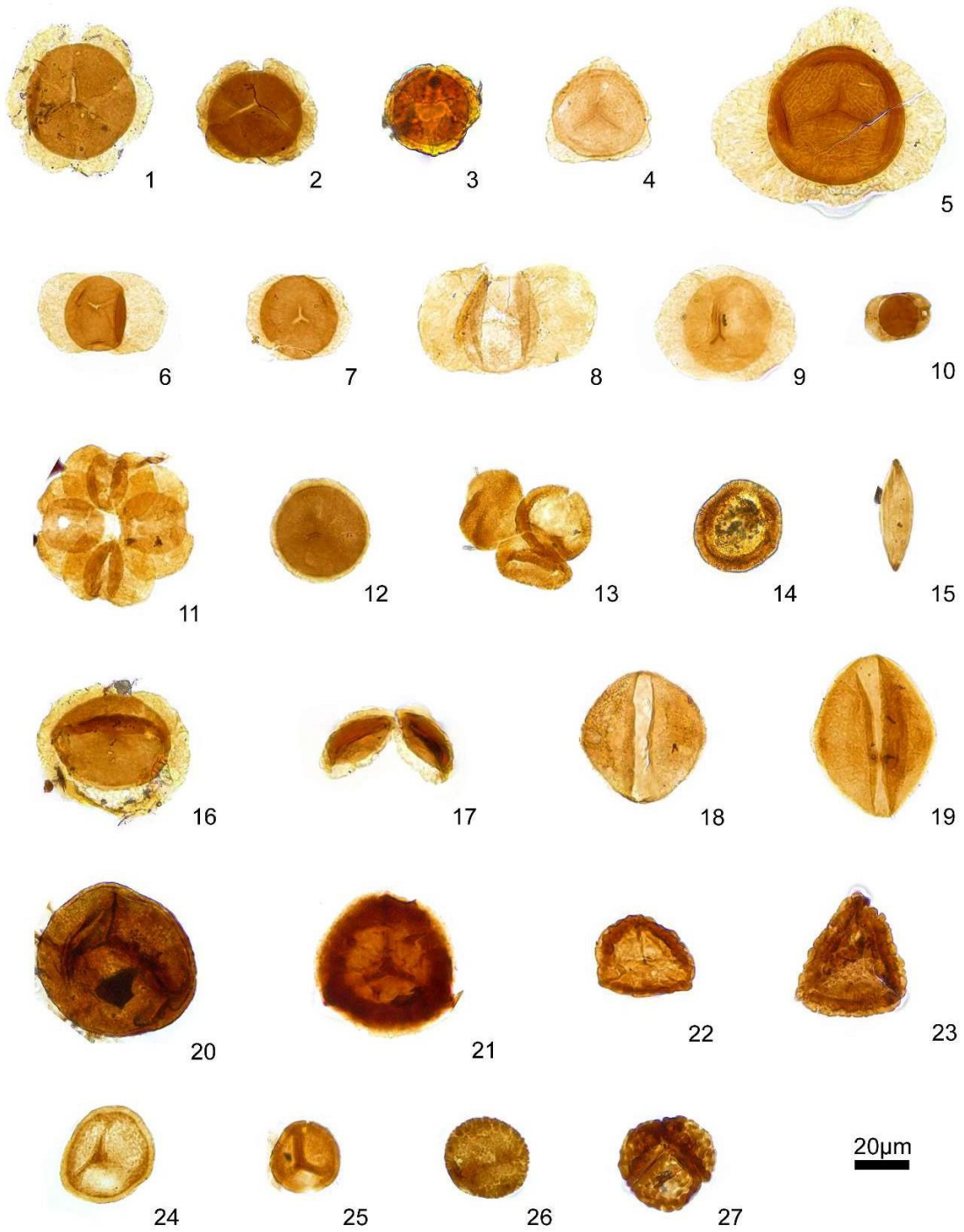


Plate 5. Upper Fronestras assemblage:

1. *Alisporites grauvogeli* Klaus, 1964. AIF-9_01_E412.
2. *Alisporites opii* Daugherty, 1941. PC7.2_01_U424.
3. *Alisporites* sp. PC7.2_01_E272.
4. *Chordasporites singulichorda* Klaus, 1960. PC7.2_01_K242.
5. *Angustisulcites klausii* (Freudenthal) Visscher, 1966. AIF-9_03_O402.
6. *Angustisulcites* sp. AIF-9_02_D474.
7. *Illinites kosankei* Klaus, 1964. PC7.2_01_D263.
8. *Illinites chitonoides* Klaus, 1964. PC7.2_03_O291.
9. *Microcachryidites doubingeri* Klaus, 1964. AIF-9_01-T372.
10. *Microcachryidites fastidioides* (Jansonius) Klaus, 1964. PC7.2_01_E312.
11. *Microcachryidites sittleri* Klaus, 1964. PC7.2_01_X352.
12. *Microcachryidites* sp.1. AIF-9_01_F101.
13. *Platysaccus papilionis* Potonié and Klaus, 1954. AIF-9_02_O300.
14. *Lunatisporites acutus* Leschik, 1955. AIF-9_03_C393.
15. *Lunatisporites* sp. pc7.2_01_v234.
16. *Striatoabieites aytugii* (Visscher) Scheuring, 1978. PC7.2_02_D382.
17. *Striatoabieites aytugii* (Visscher) Scheuring, 1978. PC7.2_02_D393.
18. *Striatoabieites* sp. PC7.2_01_H372.
19. *Strotersporites jansonii* Klaus, 1963. AIF-9_03_L183.
20. *Strotersporites jansonii* Klaus, 1963. PC7.2_01_K290.
21. *Hexasaccites muelleri* (Reinhardt and Schmitz) Adloff and Doubinger, 1969. AIF-9_01_G452.
22. *Hexasaccites muelleri* (Reinhardt and Schmitz) Adloff and Doubinger, 1969. AIF-9_02_Q180.
23. *Hexasaccites muelleri* (Reinhardt and Schmitz) Adloff and Doubinger, 1969. AIF-9_03_R462.
24. *Cristianisporites triangulatus* Antonescu, 1969. PC7.2_03_M393.

Plate 5. Upper Fronestras assemblage:

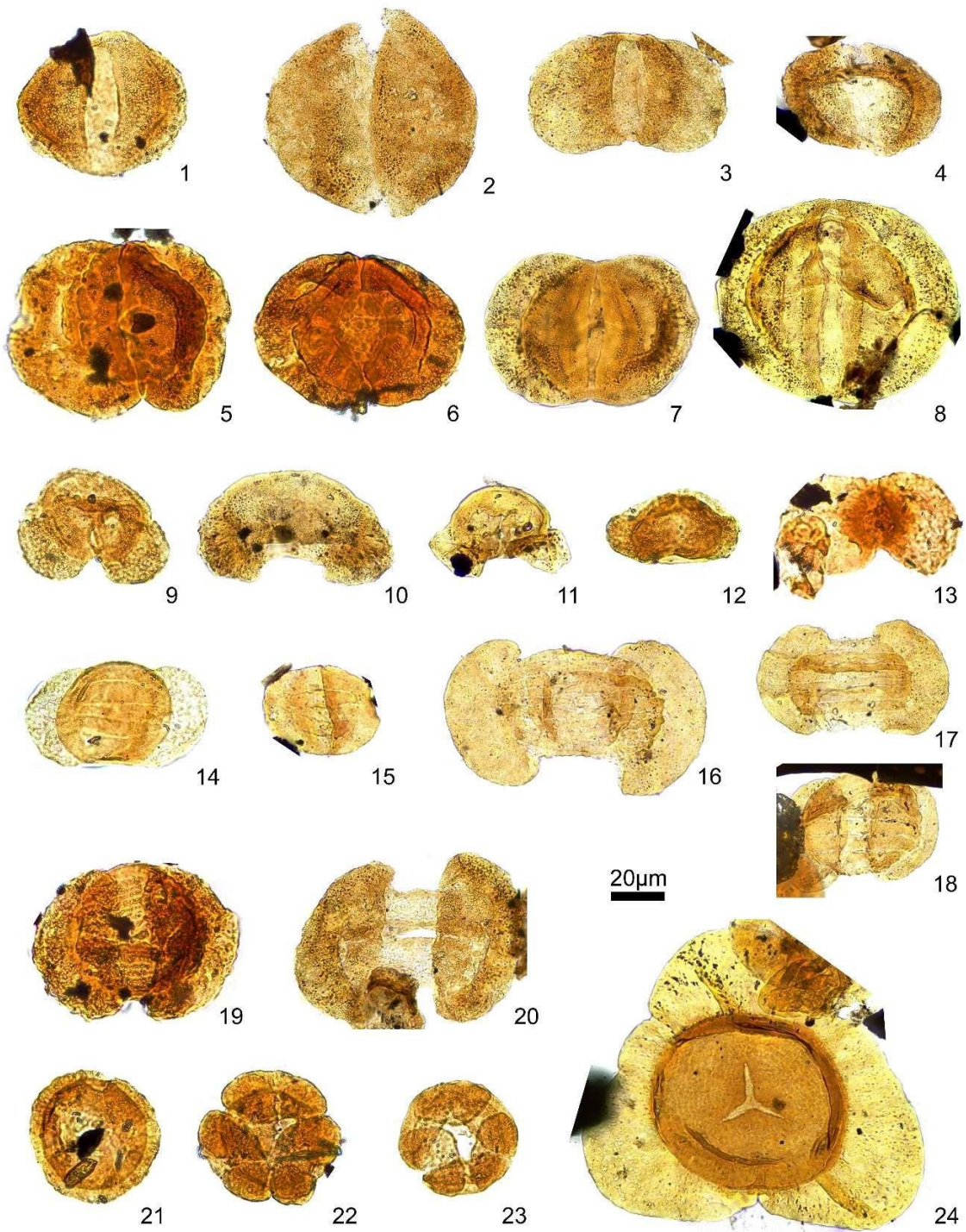


Plate 6. Upper Fronestras assemblage:

1. *Triadispora crassa* Klaus, 1964. PC7.2_01_L431.
2. *Triadispora falcata* Klaus, 1964. PC7.2_02_E404.
3. *Triadispora plicata* Klaus, 1964. PC7.2_01_D304.
4. *Triadispora staplinii* (Jansonius) Klaus, 1964. PC7.2_02_F360.
5. *Triadispora suspecta* Scheuring, 1970. AIF-9_01_L100.
6. *Triadispora* sp. (Tetrad). AIF-9_01_E173.
7. *Triadispora* sp.2. PC7.2_01_F400.
8. *Triadispora* sp. (Three-saccate form). PC7.2_01_M481.
9. *Enzonalasporites vigens* Leschik, 1955 (Tetrad). PC7.2_01_X311.
10. *Enzonalasporites vigens* Leschik, 1955. AIF-9_01_G472.
11. *Paracirculina* sp. AIF-9_04_C173.
12. *Cerebropollenites mesozoicus* Nilsson, 1958. PC7.2_01_W362.
13. *Cycadopites* sp. AIF-9_01_Q110.
14. *Calamospora tener* (Leschik) Mädler, 1964. AIF-9_03_H353.
15. *Calamospora* sp. AIF-9_04_F071.
16. *Rewanispora vermiculata* Antonescu and Taugourdeau-Lantz, 1973. PC7.2_02_O520.
17. *Kraeuselisporites* sp. PC7.2_03_Q373.
18. *Cyclotriletes oligogranifer* Madler, 1964. PC7.2_01_U302.
19. *Reticulatisporites* sp. PC7.2_01_R410.
20. *Uvaesporites* sp. PC7.2_02_U512.
21. *Densosporites* sp. PC7.2_01_W391.
22. *Punctatisporites triassicus* Schulz, 1964. PC7.2_01_Q381.
23. *Cyclogranisporites* sp. PC7.2_01_O364.
24. *Verrucosisporites thuringiacus* Mädler, 1964. PC7.2_02_U432.

Plate 6. Upper Fronestras assemblage:

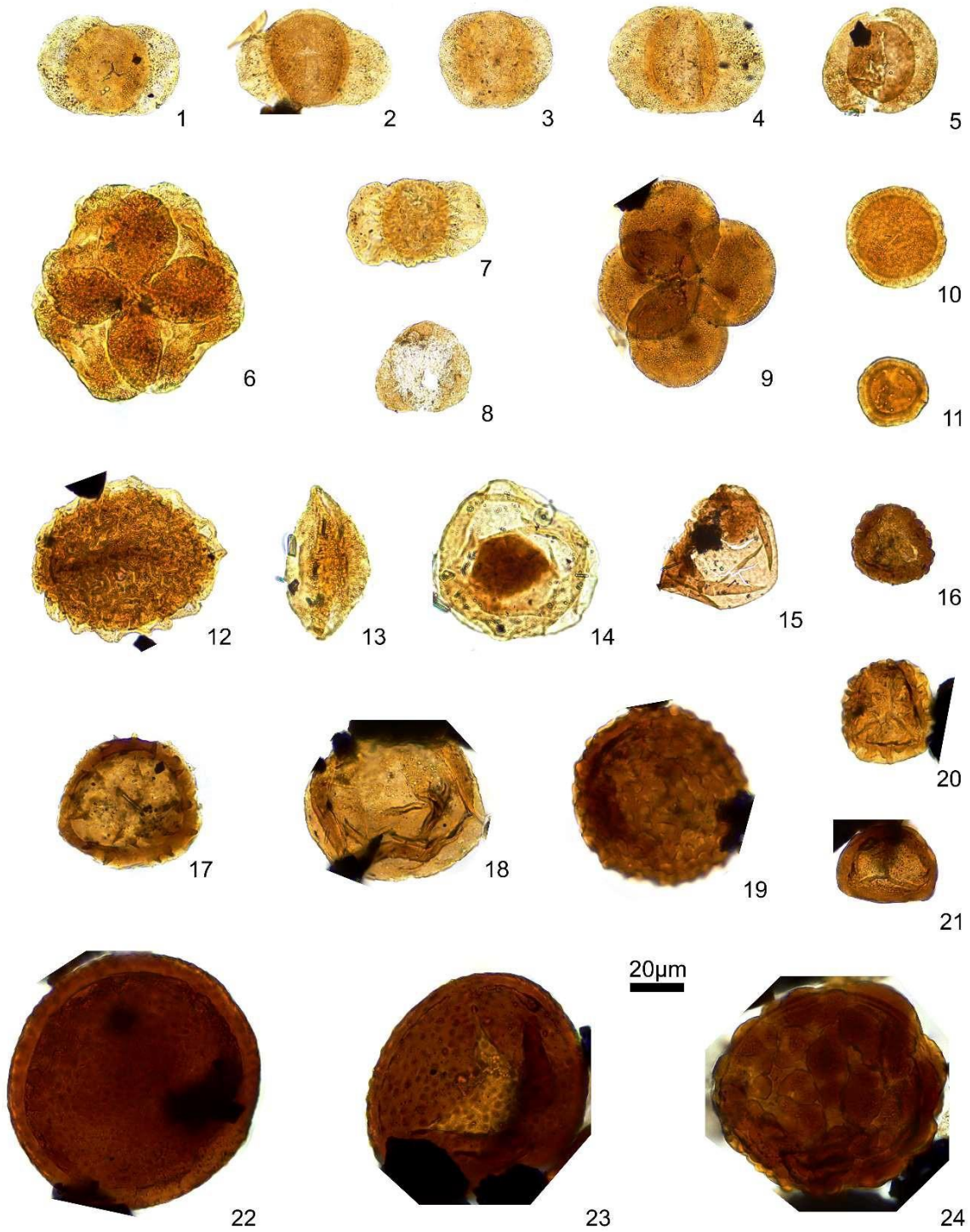
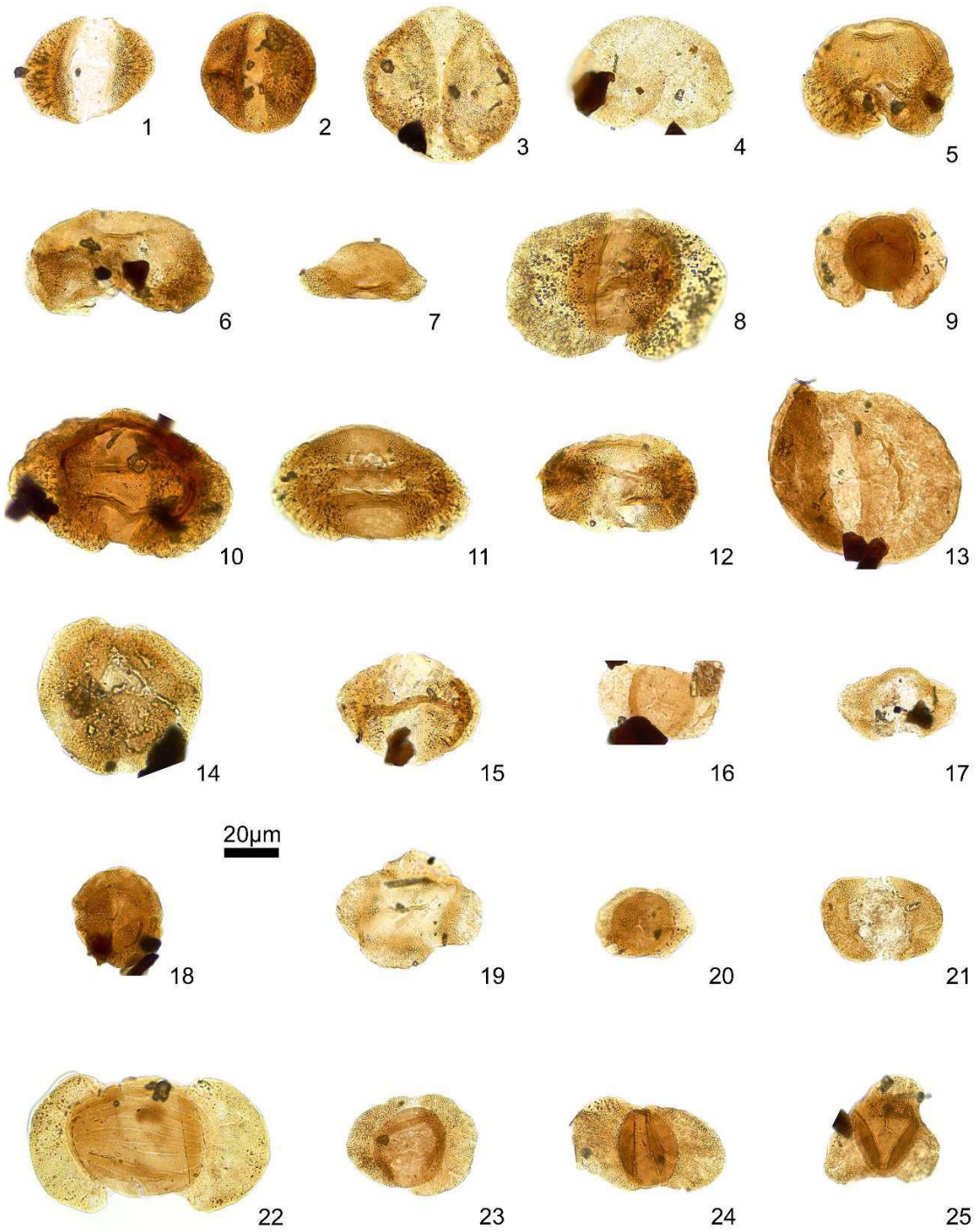


Fig. 8. Upper Fronestras assemblage, Plate 2.

Plate 7. Su Passu Malu Assemblage:

1. *Alisporites grauvogeli* Klaus, 1964. GRIFO3_01_H404.
2. *Alisporites opii* Daugherty, 1941. GRIFO3_01_E123.
3. *Brachisaccus neomundanus* (Leschik) Mádler, 1964. GRIFO3_01_D332.
4. *Brachisaccus neomundanus* (Leschik) Mádler, 1964. GRIFO3_02_G200.
5. *Microcachryidites doubingeri* Klaus, 1964. GRIFO3_03_N163.
6. *Microcachryidites fastidioides* (Jansonius) Klaus, 1964. GRIFO3_04_P081.
7. *Microcachryidites* sp.1. GRIFO3_01_R180.
8. *Angustisulcites gorpil* Visscher, 1966. GRIFO3_01_D043.
9. *Angustisulcites* sp. GRIFO3_01_J052.
10. *Lunatisporites noviaulensis* (Leschik) de Jersey, 1979. GRIFO3_01_G152.
11. *Lunatisporites noviaulensis* (Leschik) de Jersey, 1979. GRIFO3_02_M451.
12. *Lunatisporites* sp. GRIFO3_01_D164.
13. *Illinites chitonoides* Klaus, 1964. GRIFO3_01_M372.
14. *Hexasaccites muelleri* (Reinhardt and Schmitz) Adloff and Doubinger, 1969. GRIFO3_04_Q382.
15. *Chordasporites singulichorda* Klaus, 1960. GRIFO3_02_K042.
16. *Triadispora crassa* Klaus, 1964. GRIFO3_01_T231.
17. *Triadispora falcata* Klaus, 1964. GRIFO3_01_H214.
18. *Hexasaccites muelleri* (Reinhardt and Schmitz) Adloff and Doubinger, 1969. GRIFO3_04_K374.
19. *Bascanisporites* sp. GRIFO3_02_E154.
20. *Triadispora plicata*. Klaus, 1964. GRIFO3_01_J284.
21. *Triadispora staplinii* (Jansonius) Klaus, 1964 GRIFO3_01_K493.
22. *Striatoabieites aytugii* (Visscher) Scheuring, 1978. GRIFO3_01_L411.
23. *Triadispora suspecta* Scheuring, 1970. GRIFO3_01_L412
24. *Triadispora* sp.1. GRIFO3_01_L150.
25. *Triadispora* sp. (three-saccated form). GRIFO3_01_M270.

Plate 7. Su Passu Malu Assemblage:



1. *Cristianisporites triangulatus* Antonescu, 1969. GRIFO3_01_R110.
2. *Paleospongisporis europaeus* Schulz, 1965. GRIFO3_02_V163.
3. *Paleospongisporis europaeus* Schulz, 1965. GRIFO3_03_E302.
4. *Chasmatosporites* sp. GRIFO3_01_J262.
5. *Cerebropollenites mesozoicus* Nilsson, 1958. GRIFO3_02_W482.
6. *Enzonasporites vigenis* Leschik, 1955. GRIFO3_01_M181.
7. *Enzonasporites vigenis* Leschik, 1955. GRIFO3_01_G371.
8. *Paracirculina* sp. GRIFO3_01_M170.
9. Cf. *Cordaitina* sp. GRIFO3_02_F123.
10. *Duplicisporites granulatus* (Leschik) Scheuring, 1970. GRIFO3_04_K353.
11. *Ovalipollis ovalis* (Kruttsch) Scheuring, 1970. GRIFO3_01_E052.
12. *Rewanispora vermiculata* Antonescu and Taugourdeau-Lantz, 1973. GRIFO3_02_E433.
13. *Rewanispora* sp. GRIFO3_03_P374.
14. *Uvaesporites* sp. GRIFO3_03_S062.
15. *Calamospora tener* (Leschik) Mädler, 1964. GRIFO3_01_J481.
16. *Calamospora* sp. GRIFO3_04_N143.
17. *Cyclogranisporites granulatus* Mädler, 1964. GRIFO3_04_G101.
18. *Dictyophyllidites mortonii* (de Jersey) Playford and Dettmann, 1965. GRIFO3_01_M420.
19. *Annulispora* sp. GRIFO3_02_J401.
20. *Aratrisporites* cf. *granulatus* (Klaus) Playford and Dettmann 1965. GRIFO3_01_S294.
21. *Kraeuselisporites* sp. GRIFO3_02_j260
22. *Kraeuselisporites* sp. GRIFO3_01_n344.
23. *Deltoidospora* sp. GRIFO3_01_u174.
24. *Deltoidospora* sp. GRIFO3_01_K262.
25. *Verrucosisporites* sp.2. GRIFO3_02_U261.
26. *Verrucosisporites thuringiacus* Mädler, 1964. GRIFO3_03_M293.
27. *Verrucosisporites thuringiacus* Mädler, 1964. GRIFO3_01_P360.

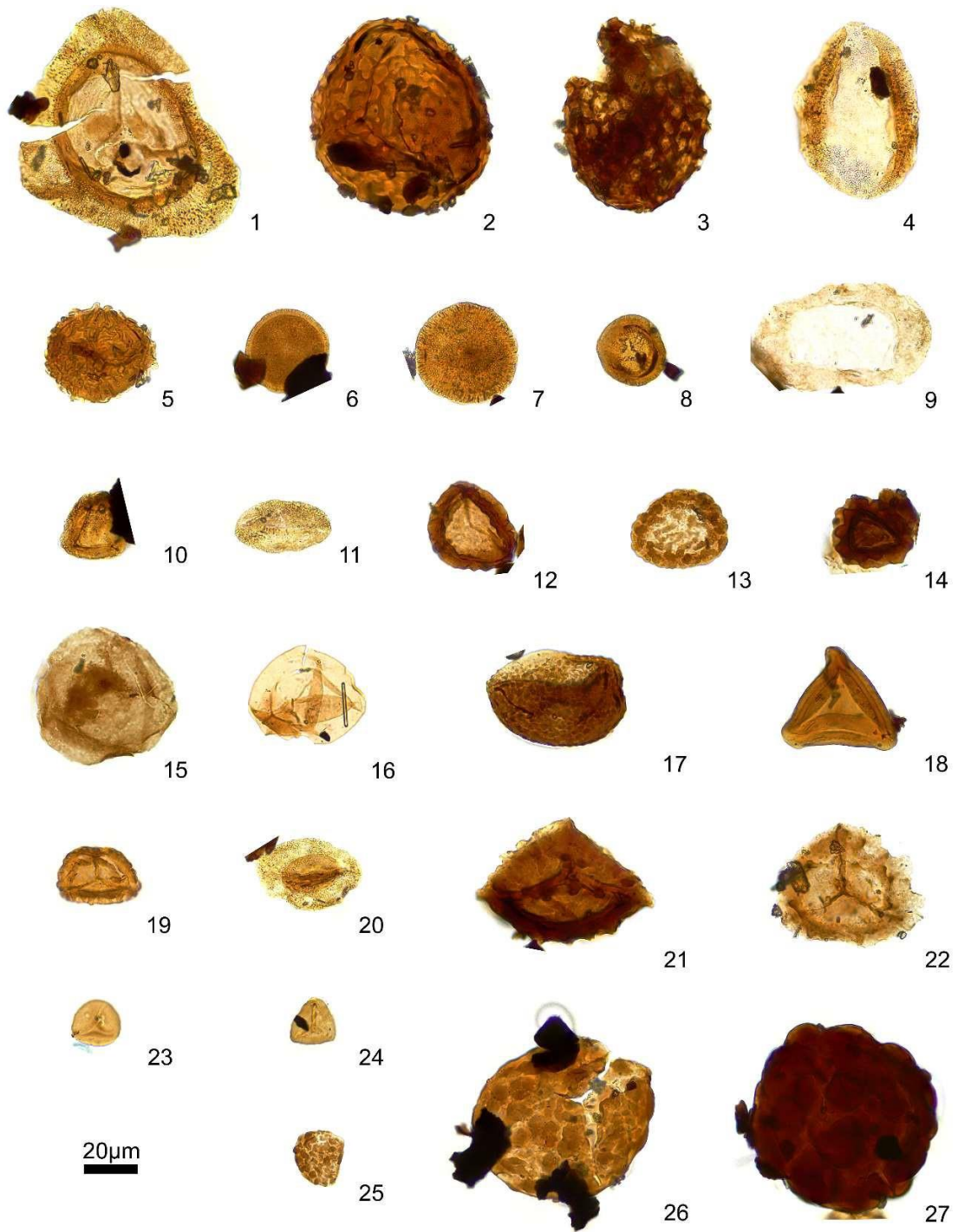


Fig 4. Grifo 3 assemblage, plate 2.

Appendix 2

T	Anisian	Ladinian		Carnian	Norian
Age/Range Localities		Fassanian	Longobardian		
<i>Bakevella subcostata</i> (GOLDFUSS)	Germany (1)	Germany (2,3), Italy (Sardinia, 4) , Spain (5)	Spain (Calanda, 6; Ibérica y Menorca; 5,7), Italy (Sardinia, 8), Germany (2,3)	Spain (Cádiz, 7)	
<i>Bakevella crispata</i> (GOLDFUSS)		Spain (5)	Germany (9), Spain (Calanda, 5, 7, 10)		
<i>Costatoria goldfussi</i> (ALBERTI)	Hungary (11), Germany (12), Alpin-Tethys (12), Spain (5), Jordan (13), China (14)	Germany (12), Alpin-Tethys (12), Italy (Sardinia, 8), Hungary (11), Swiss Pre-Alps (15), Spain (Costero-Catalana Range, 5)	Spain (Alicante, 7, 12, 16; Costero-Catalana Range, 5), Germany (12), Alpin-Tethys (12); Italy (Sardinia, 8); Japan (17)	Italy (Lombardia; 18), Spain (Betic range, 12, 19, 20), Germany (12), Alpin-Tethys (12, 21), Japan (17, 22)	Japan (22)
<i>Hoernesia socialis</i> (SCHLOTHEIM)	Hungary (11), Bulgaria (23), Poland (24, 25), Germany (1, 26, 27, 28), Spain (Valencia, 5)	Germany (29), China (30), Italy (31)	Italy (8)		
<i>Limea costata</i> (MÜNSTER)	Poland (32, 33), Jordan (13)	Spain (5)	Spain (5, 7, 16)	S. Alps (34)	Bulgaria (35), USA (Nevada, 36)
<i>Elegantinia elegans</i> (DUNKER)	China (37), Hungary (11), Spain (5, 23, 38); Germany (39); Romania (40); Egypt (41), Israel (42), S. Alpen (43)	Germany (44,45), Afghanistan (46), Spain (23, 38, 47, 48, 49)			

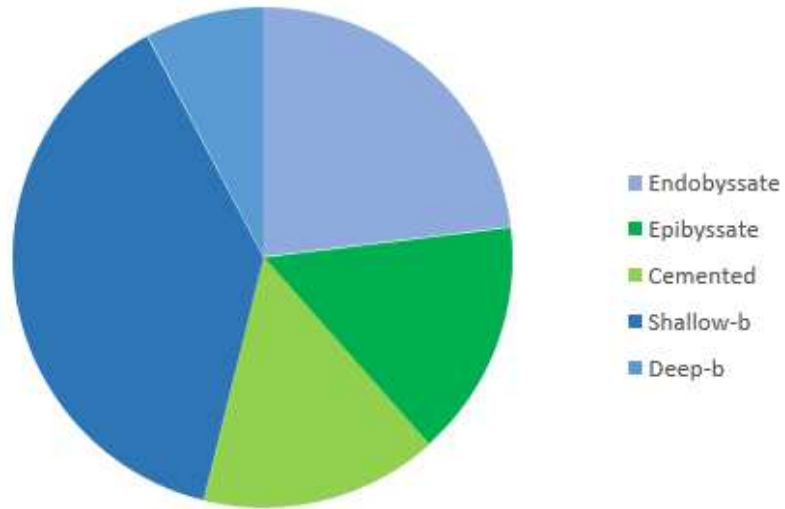
<i>Myophoria vulgaris</i> SCHLOTHEIM	Spain (5, 23), Netherlands (50), Israel (42), Poland (24), Hungary (11), Germany (51)	Germany (51), Spain (5)	Spain (5, 16, 49)		
<i>Neoschizodus laevigatus</i> (ZIETHEN)	China (30, 57), Spain (5), Israel (42)	Germany (53), Spain (5), Israel (42)	Hungary (11), Spain (5)	Spain (12)	Japan (58, 59)
<i>Pseudocorbula gregaria</i> MÜNSTER	Hungary (11, 52), Spain (5), Germany (53, 54),	Spain (5,47), Hungary (11)	Spain (5,23,47,55)	Spain (12, 56)	
<i>Pleuromya cf. mactroides</i> (SCHLOTHEIM)			Spain (55)		
<i>Pleuronectites laevigatus</i> (SCHLOTHEIM)	Hungary (33), Spain (5), Germany (60)	Germany (60, 61), Spain (5)	Italy (Sardinia, 8)		
<i>Pseudoplacunopsis ostracina</i> (SCHLOTHEIM)	Poland (11), Hungary (11)	Germany (62, 63)	Spain (16, 48), France (64)	Spain (20)	
<i>Umbostrea cristadiformis</i> (SCHLOTHEIM)	Poland (52), Jordan (13), S. China (37), Germany (65), Bulgaria (66), Hungary (11)	Spain (5); Israel (42), Germany (65)	Spain (5), Germany (65), Italy (Sardinia, 8, 65, 67)		

Table 1 Temporal and geographic distribution of bivalve species recorded in the Sardinia sections during Middle and Upper Triassic. The numbers indicate the bibliography from which the data has been extracted: 1, Philippi (1898); 2, Goldfuss (1838); 3, Geyer et al. (2005); 4, Urlichs & Posenato (2002); 5, Escudero et al. (2014); 6, Márquez-Aliaga et al. (1987); 7, Márquez-Aliaga & Martínez (1996); 8, Posenato (2002); 9, Goldfuss (1863); 10, Márquez-Aliaga et al. (2002); 11, Szente (1997); 12, Freneix (1999); 13, Cox (1924); 14, Chen (1980); 15, Baudet et al. (2016); 16, López-Gómez et al. (1994); 17, Hayami (1975); 18, Allasinaz (1966); 19, Márquez-Aliaga & García-Gil (1991); 20, Martín-Algarra, et al. (1995); 21, Bittner (1895); 22, Onoue & Tanaka (2005); 23, Márquez-Aliaga (1985); 24, Senkowiczowa (1985); 25, Kaim (1997); 26, Roemer (1851); 27, Hagdorn (1978); 28, Busse & Horn (1978); 29, Urlichs (1978); 30, Lu & Chen (1986); 31, Posenato et al. (2002); 32, Assmann (1915); 33, Szente & Vörös (2003); 34, Fürsich & Wendt (1977); 35, Benatov (2001); 36, Tackett & Bottjer (2016); 37, Komatsu et al. (2004); 38, Virgili (1958); 39, Friesenbichler et al. (2021); 40, Forel & Gradinaru (2018); 41, Awad (1945); 42, Lerman (1960); 43, Posenato (2008); 44, Dunker (1849); 45, Hagdorn (2015); 46, Farsan (1972); 47, Schmidt (1935); 48, Martínez & Márquez-Aliaga (1994); 49, Márquez-Aliaga & Molina (2019); 50, Eldijk et al. (2019); 51, Klug et al. (2005); 52, Foster & Sebe (2017); 53, Urlichs (1992); 54, Walther (1927); 55, Wurm (1911); 56, Martín-Algarra et al. (1993); 57, Ling (1988); 58, Tamura (1990); 59, Tamura (1996); 60, Hautmann (2010); 61, Hagdorn (1995); 62, Bachmann (1979); 63, Bachmann (2002); 64, Hölder (1961); 65, Márquez-Aliaga et al. (2005); 66, Budurov et al. (1993); 67, Márquez-Aliaga et al. (2000).

Triassic Sardinia	Species / Sections	M. S. Giusta	Punta Lavatoio	Punta Lavatoio	Punta Lavatoio	Monte Folgheras	Monte Folgheras Strada	Monte Maiore	Monte Maiore	Punta Tonnara	BIVALVE LIFE STYLE	
		Sections North to South		North 1	North 2			North 3		South		
		MSG A- B	Sector 3	Sector 2	Sector 1	MFS	MF2A	Sector H	Sector I			
BIVALVES	<i>Bakevella subcostata</i> (GOLDFUSS)		2	6					2		ENDOBYSSATE	
	<i>Bakevella crispata</i> (GOLDFUSS)					1	2				ENDOBYSSATE	
	<i>Costatoria goldfussi</i> (ALBERTI)	15	11	7	12	4	3	10	2		SHALLOW BURROWER	
	<i>Hoernesia socialis</i> (SCHLOTHEIM)	1	30	2	4	12	2				ENDOBYSSATE	
	<i>Limea costata</i> (MÜNSTER)	1	3	1		2	7			1	EPIBYSSATE	
	<i>Elegantinia elegans</i> (DUNKER)		1									SHALLOW BURROWER
	<i>Myophoria vulgaris</i> (SCHLOTHEIM)						1					SHALLOW BURROWER
	<i>Neoschizodus laevigatus</i> (ZIETHEN)		1	2	1		1					SHALLOW BURROWER
	<i>Pseudocorbula gregaria</i> MÜNSTER			2					10	3		SHALLOW BURROWER
	<i>Pleuromya cf. mactroides</i> (SCHLOTHEIM)	1				2	3	1	1			DEEP BURROWER
	<i>Pleuronectites laevigatus</i> (SCHLOTHEIM)		1	2	1							EPIBYSSATE
	<i>Pseudoplacunopsis ostracina</i> (SCHLOT.)		1	3	5	1	2					CEMENTED
<i>Umbostrea cristadiformis</i> (SCHLOTH.)						6					CEMENTED	
Bivalvia indet.			20		20	10	10	10		10		

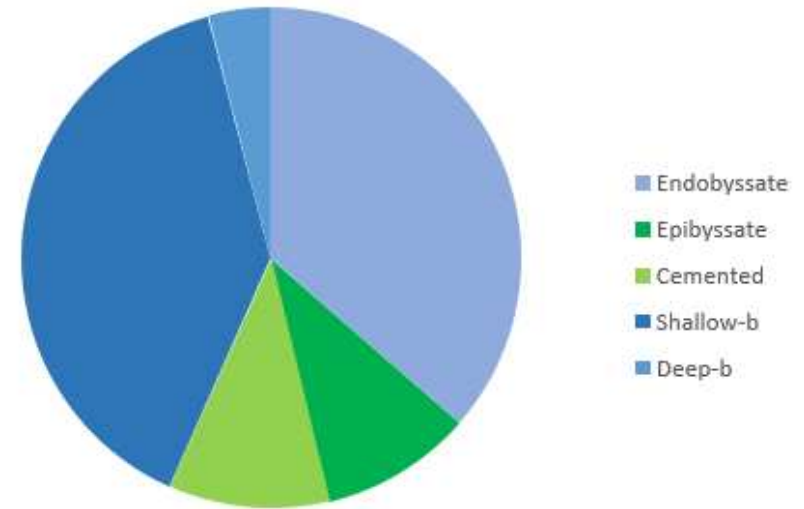
Table 2 Data abundance of bivalve species recorded at M. S. Giusta, Punta Lavatoio, Monte Folgheras, Monte Maiore y Punta Tonnara sections with indication of life habits of species. Bivalve life habits adopted: Epifaunalattached(epibyssate), Epifaunalattached(cemented), Semi-infaunal attached(endobysate), Infaunal shallow-burrower, Infaunal deep-burrower. Allspecies are suspension feeders.

Bivalve diversity



Life habit percentage composition of some Triassic bivalve assemblages from Sardinia. **Diversity** data from Punta del Lavatoio, Monte Fogheras and Monte Maiore sections. Bivalve life habits: Epifaunal attached (epibyssate), Epifaunal attached (cemented), Semi-infaunal attached (endobyssate), Infaunal shallow-burrower, Infaunal deep-burrower. All species are suspension feeders.

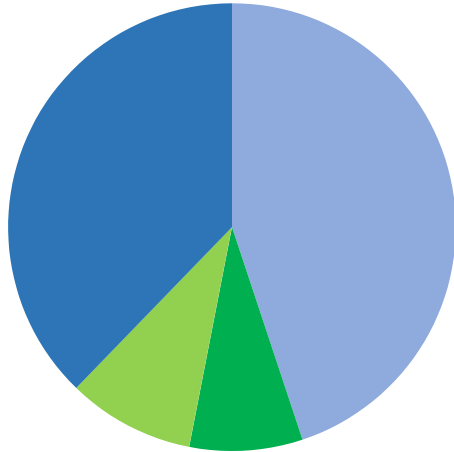
Bivalve abundance



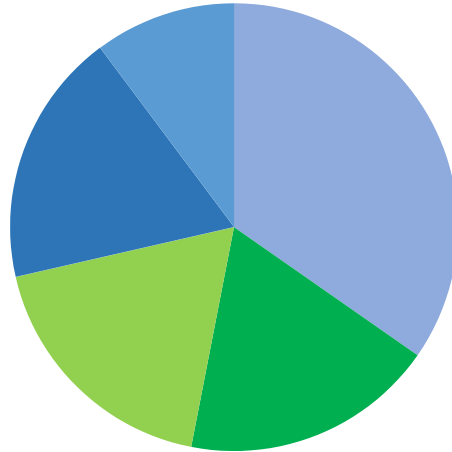
Life habit percentage composition of some Triassic bivalve assemblages from Sardinia. **Abundance** data from Punta del Lavatoio, Monte Fogheras and Monte Maiore sections. Bivalve life habits: Epifaunal attached (epibyssate), Epifaunal attached (cemented), Semi-infaunal attached (endobyssate), Infaunal shallow-burrower, Infaunal deep-burrower. All species are suspension feeders.

(1)

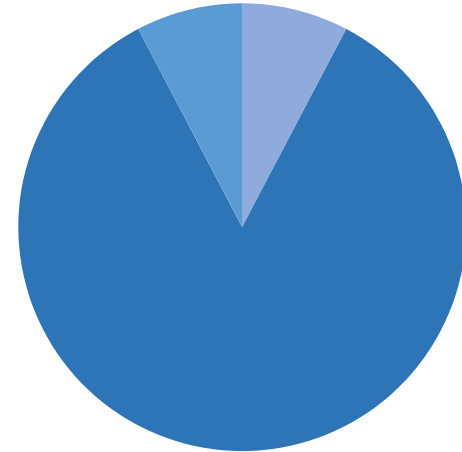
Punta del Lavatoio



Monte Fogheras



Monte Maggiore



(2)

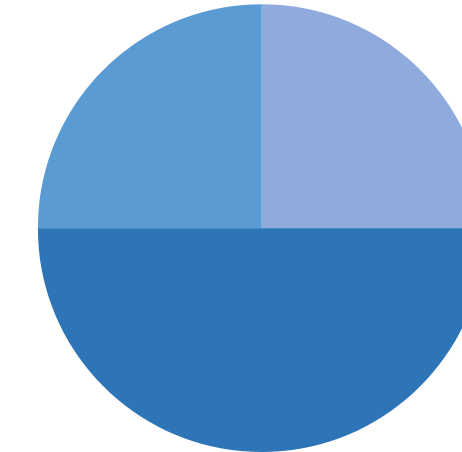
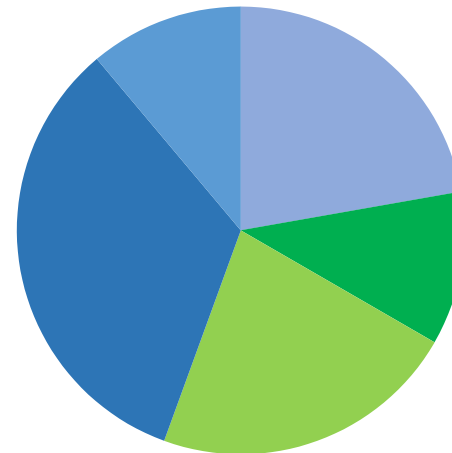
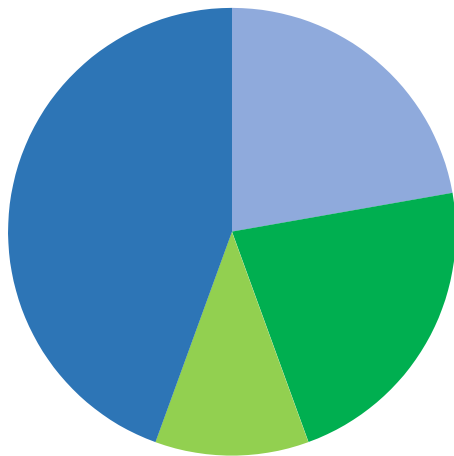


Table 4. Life habit percentage composition of some Triassic bivalve assemblages from Sardinia. Bivalve **abundance (1)** and **diversity (2)** data from Punta Lavatoio, Monte Fogheras and Monte Maggiore sections. Bivalve life habits: Epifaunal attached (epibysate), Epifaunal attached (cemented), Semi- infaunal attached (endobysate), Infaunal shallow-burrower (Shallow-b), Infaunal deep-burrower (Deep-b). All species are suspension feeders.

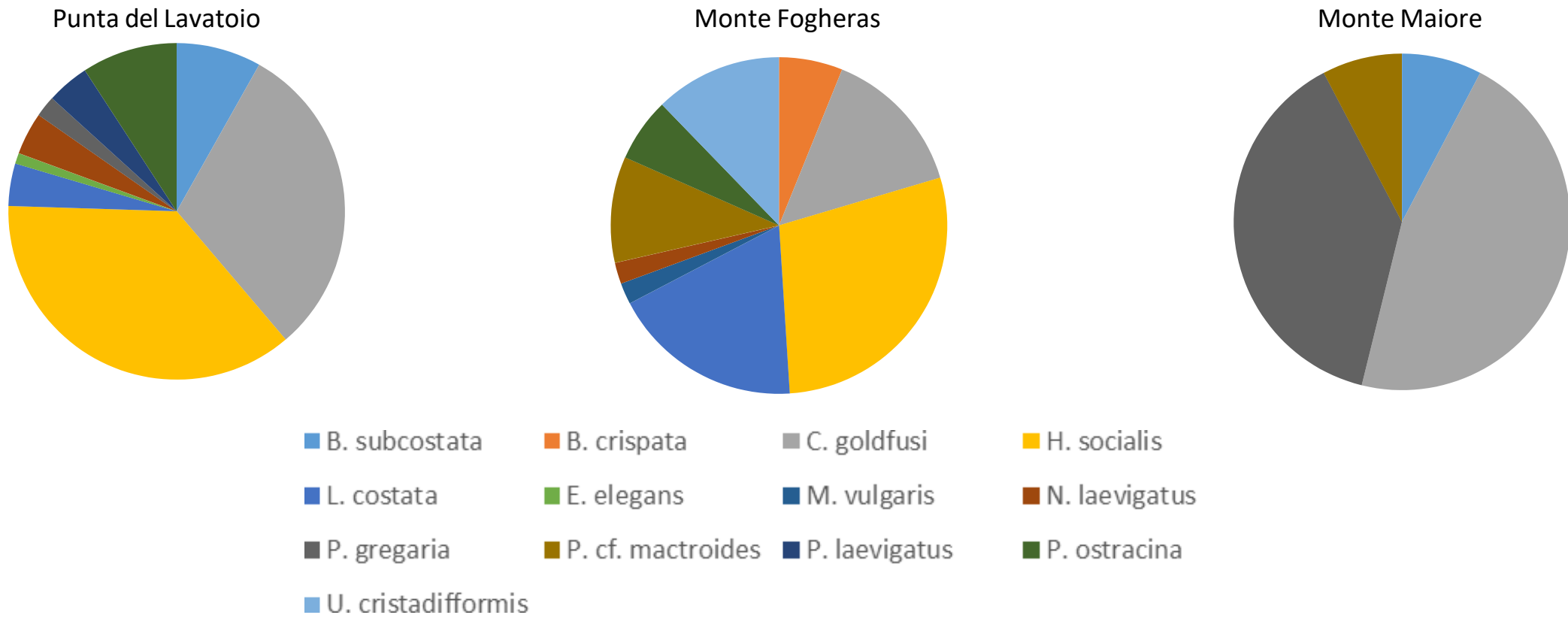


Table 5. Specific percentage composition of some Triassic bivalve assemblages from Sardinia. Diversity data from Punta del Lavatoio, Monte Fogheras and Monte Maggiore sections. Complete nomination of species in Table 1 and 2.